AOAD

ESCWA

EDS

IHP

IAEA

IDA

UNDP

UNEP

UNESCO

WHO/EMRO

WSTA 4th Gulf
Water
Conference

February 13-17, 1999
State of Bahrain

Water in the Gulf, Challenges of the 21st Century

Ministry of
Electricity and
Water

Secretariat General
of the Gulf
Cooperation
Council (GCC)

Arabian
Gulf University
Bahrain

Bahrain Center
for Studies
and Research
Bahrain

Edited by
DR. WALEED K. AL-ZUBARI

RDC PAPERS

TABLE OF CONTENTS

(RDC PAPERS—ABSTRACTS*)

SESSION 1
KEYNOTES ON WATER RESOURCES PLANNING AND MANAGEMENT

SESSION 2A
GROUNDWATER RESOURCES

SESSION 2B
WATER DESALINATION

SESSION 3A
WASTEWATER

SESSION 3B
SURFACE WATER

SESSION 3C
MUNICIPAL WATER SUPPLY

SESSION 3D
AGRICULTURAL WATER

SESSION 3E
DRINKING WATER

SESSION 4A
WATER RESOURCES PLANNING AND MANAGEMENT

TABLE OF CONTENTS

VOLUME 1

WATER RESOURCES PLANNING AND MANAGEMENT SESSION

GROUNDWATER RESOURCES

SURFACE WATER

TABLE OF CONTENTS

VOLUME 2

WATER DESALINATION SESSION

DRINKING WATER

WASTEWATER

AGRICULTURAL WATER

RDC PAPERS
ABSTRACTS

Degradation Study of Cellulose Triacetate Hollow Fine Fiber SWRO Membranes

A. Mohammed Farooque and Ahamed Al-Amoudi

The Fourth Gulf Water Conference
Water in the Gulf, Challenges of the 21st Century
State of Bahrain (13-17 February, 1999)

DEGRADATION STUDY OF CELLULOSE TRIACETATE HOLLOW FINE FIBER SWRO MEMBRANES

A. Mohammed Farooque and Ahamed Al-Amoudi
Research and Development Center
Saline Water Conversion Cooperation
P.O. Box # 8328
Al-Jubail 31951
Kingdom of Saudi Arabia.

K. Numata
Japan International Cooperation Agency (JICA)
Japan

ABSTRACT

Cellulose acetate (CA) membranes are liable to chemical attack mainly by operation at improper pH or by chlorine and other oxidizing agents. The chemical attack could lead either to hydrolysis of the pendant acetyl group or to oxidation of polymer backbone leading to chain scission. Hydrolysis can be detected by determining the degree of polymer acetylation, whereas oxidation can be detected by changes in polymer molecular weight as measured directly, for example by the intrinsic viscosity measurement, and/or indirectly by determining polymer tensile strength. In the present study degree of acetylation, intrinsic viscosity and tensile strength measurements, were used for identifying the causes of the poor performance of two cellulose triacetate hollow fine fiber membranes obtained from a commercial SWRO plant after being in operation for five and two years, respectively. To establish causes of degradation in the commercial samples, analyses were also performed on fresh virgin fiber, on a second sample exposed to high concentration of chlorine, and a third sample exposed to high pH. By comparison to the virgin sample, it was established that fiber exposure to high concentration of chlorine and to high pH induced decrease in polymer chain molecular weight and in degree of acetylation, respectively. Both the commercial SWRO membranes were found to have undergone both hydrolysis as well as oxidation. However, polymer chain oxidation was established as the major cause for the degradation in performance of the commercial sample which was in operation for nearly five years, while hydrolysis of the pendant acetyl group was established as the major cause for the degradation in performance of the second commercial membrane sample which was in operation for two years. The paper describes the detail of the measurements made and results obtained.

KEYWORDS: Cellulose acetate, RO membranes, chemical degradation, degree of acetylation, intrinsic viscosity and tensile strength.

A New Approach to Membrane and Thermal Seawater Desalination Process Using Nanofiltration Membranes (Part 2)

A.M. Hassan, M. AK. Al-Sofi, A.S. Al-Amoudi,
A.T.M. Jamaluddin, A.M. Farooque, A. Rowaili,
A.G.I. Dalvi, N.M. Kither, G.M. Mustafa and I.A.R. Al-Tisan

The Fourth Gulf Water Conference
Water in the Gulf, Challenges of the 21st Century
State of Bahrain (13-17 February, 1999)

A NEW APPROACH TO MEMBRANE AND THERMAL SEAWATER DESALINATION PROCESSES USING NANOFILTRATION MEMBRANES (PART 2)

A. M. Hassan, M. AK. Al-Sofi, A. S. Al-Amoudi,
A. T. M. Jamaluddin, A. M. Farooque, A. Rowaili, A. G. I. Dalvi,
N. M. Kither, G. M. Mustafa and I. A. R. Al-Tisan
Research and Development Center
Saline Water Conversion Corporation (SWCC)
P.O. Box 8328, Al-Jubail 31951, Kingdom of Saudi Arabia

ABSTRACT

In earlier publications it was reported that for the first time ever, a new approach to seawater desalination processes by integrating the nanofiltration (NF) membrane pretreatment process with one of the conventional desalination processes to form, for example, an NF-SWRO or NF-MSF or a combination thereof, such as NF-SWRO$_{\text{reject}}$-MSF, was developed at Saline Water Conversion Corporation (SWCC), R & D Center, and was successfully applied to those cases on a pilot plant scale with remarkable results. The seawater treatment first with the NF membrane removed from it turbidity and microorganism, caused significant rejection of the scale forming hardness ions, e.g., $SO_4^=$ by up to 98%, reduced TDS in Gulf Seawater by up to 65 %, and produced a new, partially desalinated seawater product, considerably different and superior to seawater in qualities and without the problems normally associated with seawater of high concentration of scale forming ions, high TDS, high turbidity and high bacteria count. The said desalination arrangements led to a significant improvement in the seawater desalination processes, for example by doubling the SMRO product water output and recovery ratio and the production of high purity permeate (TDS < 200 ppm) from one single stage SWRO. It also allowed for the successful operation at high recovery of the MSF as part of a NF-MSF unit or as part of a trihybrid NF-SWRO$_{\text{reject}}$-MSF desalination system, where the reject from SWRO constituted the make-up to the MSF unit, at top brine temperature of 120 °C, without the addition to the MSF make-up of acid or antiscalant or antifoam and its operation under those conditions without scale formation. Moreover, by this tri-hybrid process, up to 90% of the NF permeate was converted to potable water. The paper describes the effect of long term operation on the performance of those seawater hybrid desalination processes.

Evaluation of Ultra-Violet Radiation Disinfection on the Bacterial Growth in the SWRO Pilot Plant, Al-Jubail

Hassan Ahmed Munshi, N. Sasikumar,
A.T. Jamaluddin and Kither Mohammed

EVALUATION OF ULTRA-VIOLET RADIATION DISINFECTION ON THE BACTERIAL GROWTH IN THE SWRO PILOT PLANT, AL-JUBAIL

Hassan Ahmed Munshi, N. Sasikumar,
A.T. Jamaluddin, and Kither Mohammed
Research and Development Center
Saline Water Conversion Corporation,
P.O. Box 8328, Al-Jubail 31951,
Kingdom Of Saudi Arabia

ABSTRACT

The present study summarizes findings of an experiment on the evaluation of UV- treatment for bacterial disinfection at SWRO pilot plant at Al-Jubail. Two UV-generation units were installed along the pretreatment line. One before the dual media filter and the second before the micron cartridge filter. The study was carried out at three seawater flow rates: the regular flow operation and two other flow rates below the normal flow. The investigation was carried out at five locations in the plant: raw seawater (RSW), after UV-unit (AUV), after media filter (AMF), after cartridge filter post the second UV-unit (ACF) and the brine (BR). The study showed 90-99% reduction in bacterial counts after UV- treatment as compared to raw seawater at the three flow rates suggesting relatively good performance of the first UV-sterilizing unit. However, an increase in bacterial count was noticed at AMF and ACF. Presumably, the second UV-sterilizing unit has not reduced the bacterial counts in the feed water at this site. Laboratory studies also showed that, incubation of UV-treated samples for 24h resulted in bacterial recovery and aftergrowth. AMF and ACF also registered reduced Total Organic Carbon (TOC), nitrite and phosphate levels in the feed water indicating the presence of a nutrient trap before CF. A decline in phosphate, nitrite and TOC levels were also found in 24h incubated samples indicating that bacteria had used these nutrients. The study suggests that while UV-treatment considerably reduced bacterial counts in the SWRO plant, stagnant condition of the feed water before CF has presumably led to bacterial recovery.

KEY WORDS: Ultra-Violet Radiation, Bacterial After Growth, Reverse Osmosis, Micronutrients

Effect of Various Forms of Iron in Recycle Brine on Performance of Scale Control Additives in MSF Desalination Plants

Abdul Ghani I. Dalvi, M.N. Kither Mohammad,
Saad Al-Sulami, K. Sahul and Radwan Al-Rasheed

EFFECT OF VARIOUS FORMS OF IRON IN RECYCLE BRINE ON PERFORMANCE OF SCALE CONTROL ADDITIVES IN MSF DESALINATION PLANTS

Abdul Ghani I. Dalvi, M. N. Kither Mohammad,
Saad Al-Sulami, K. Sahul and Radwan Al-Rasheed
Research and Development Center
Saline Water Conversion Corporation
P. O. Box # 8328, Al-Jubail 31951
Kingdom of Saudi Arabia

ABSTRACT

Scale control additives (SCA) or antiscalants are used in multistage flash desalination plant to prevent fouling problems. Effective dose rates of some of these SCA are found to vary from plant to plant. Efficiency of antiscalants could be influenced by its chemical nature, plant configuration and design, heat transfer rate and its surface and antiscalant reaction with brine constituents. To understand the variation in concentration of SCA and effect of brine constituents on efficiency of SCA, some bench top experiments at 95 °C with brine were conducted using the threshold effect technique. Two SCA, a polyphosphonate based (PPN) and polymaleic acid based (PMA) were used for these evaluations. The effect of Fe^{3+}, Fe^{2+}, Fe_2O_3, $Fe(OH)_3$, and rust on efficiency of SCA was determined.

The threshold effect method which measures the total alkalinity and calcium content of supernant to evaluate efficiency of SCA was found to be an effective technique. Recycled brine constituents and corrosion products, especially Fe and its various chemical forms affect the efficiency of SCA at 2 ppm concentration and at 95 °C in 1.4 times concentrated seawater brine. Various chemical hydrated and hydroxylated forms of Fe present in brine, viz., $Fe^{3+}(H_2O)_6$, $Fe(OH)_3$, Fe^{2+}, Fe_2O_3, rust, etc., all showed detrimental effect on efficiency of SCA. Among all the species of iron, $Fe(OH)_3$, reduced the efficiency of SCA by maximum of 40%.

Among the two antiscalants, PPN showed 10-12% better efficiency in the presence of various iron species compared to PMA under similar bench top experimental conditions. The effect of brine constituents on PMA was more pronounced compared to PPN perhaps due to better complexing ability of the former.

KEY WORDS: Antiscalant, Polyphosphonate, Polymaleic acid, Scales, MSF, Iron, Brine

The Performance of Different Antiscalants in Mutli-Stage Flash Distillers

Osman A. Hamed, Mohammad AK. Al-Sofi,
Ghulam M. Mustafa and Abdul Ghani Dalvi

The Fourth Gulf Water Conference
Water in the Gulf, Challenges of the 21st Century
State of Bahrain (13-17 February, 1999)

THE PERFORMANCE OF DIFFERENT ANTISCALANTS IN MULTI-STAGE FLASH DISTILLERS

Osman A. Hamed, Mohammad AK. Al-Sofi,
Ghulam M. Mustafa, and Abdul Ghani Dalvi
Research & Development Center
P. O. Box- 8328, Al-Jubail, SWCC
Saudi Arabia

ABSTRACT

The Saline Water Conversion Corporation (SWCC) is an internationally recognized authority on scale control in multi-stage flash (MSF) distillers. This international recognition came about as a result of many years of work on this topic. There are publications of SWCC on MSF scaling phenomena over the past couple of decades. During the last decade, there was a monumental growth in SWCC's installed MSF plant capacities. The majority of SWCC MSF distillers were designed to operate with additive scale control method rather than the previously predominant method of carbonate depletion through chemical reaction with acid, e.g., sulfuric or hydrochloric.

The Research and Development Center (RDC) in Al-Jubail has been involved during the last three years in the evaluation of available commercial scale inhibitors. A total of eight tests have been carried out at RDC MSF pilot plant, Jeddah Phases III & IV and Al-Jubail Phase II to evaluate the effectiveness of three antiscalants. These tests by antiscalant types and places are (i) polycarboxylates in Al-Jubail II, RDC pilot plant and Jeddah IV, (ii) polymaleic acid in Jeddah IV and RDC pilot plant and (iii) polyphosphonate in Jeddah III and RDC pilot plant. Moreover, a run of acid operation carried out in the pilot plant is included for comparison.

This paper presents qualitative and quantitative performance results of three different antiscalants as well as acid dosing tests for scale control. The threshold effect of these antiscalants was tested on laboratory scale. On pilot and commercial plants the variation of the fouling factor with time is examined and quantified. The evaluation tests conducted on the commercial plants revealed that all the examined antiscalants were successful in inhibiting alkaline scale formation and improving plant performance at top brine temperature ranging between 105 and 110°C and with respective dosing rates of 1.5 and 3.0 ppm.

KEYWORDS: Desalination, Multistage flash, Alkaline scale, Antiscalants and Fouling Factor.

Investigating Intake System Effectiveness with Emphasis on Self-Jetting Well-Point (SJWP) Beachwell System

A.M. Hassan, A.T.M. Jamaluddin and Ali Rowaili,
Ellen Abart and Robert Lovo

INVESTIGATING INTAKE SYSTEM EFFECTIVENESS WITH EMPHASIS ON SELF-JETTING WELL-POINT (SJWP) BEACHWELL SYSTEM

A. M. Hassan, A.T.M. Jamaluddin and Ali Rowaili
Research and Development Center
Saline Water Conversion Corporation (SWCC)
Al Jubail, Saudi Arabia

Ellen Abart and Robert Lovo
United States Bureau of Reclamation (USBR)
Denver, U.S.A.

ABSTRACT

A well-designed subsurface SWRO intake not only yields good quality feed that requires none or minimum of pretreatment, but also when used instead of surface type intake results in a significant saving in plant capital investment and in cost of plant O&M. An SJWP subsurface intake system was tested at SWCC Al-Jubail site, onshore, at high-tide seawater line and mid-tide point at depths of 3.5 m, 3.5 m, and 4.5 m, respectively. The project objective is to investigate the suitability of this relatively new subsurface SJWP as an intake for some SWRO plants. The best SDI values with an average of $SDI_{ave} = 2.9$, which compares reasonably well with $SDI_{ave} = 2.6 \pm 0.2$ for conventionally pretreated surface seawater feed, were obtained when the well-points were fixed at sea mid-tide point at depth of 4.5 m. The filtrate TDS, total hardness and pH values were lesser than those of seawater indicating mixing of seawater with underground or surface water. At zero incubation time, bacteria count was in the range of $5\text{x}10^2$ to $4\text{x}10^3$ colony forming units (CFU), but high aftergrowth rates and short bacteria generation time were observed in the SJWP feed after 24 and 72 hours of incubation. Based on SDI measurements, as well as on other physical and chemical measurements, a good quality SWRO feed can be derived from subsurface well-point beachwells located on a clean non-polluted site, which is expected to diminish the high aftergrowth rate and short generation time of bacteria found in the present case. Accurate

information on this point can be established by testing the effect on SWRO membrane performance of feed derived from SJWP beachwell located on a clean non-polluted site which is to be conducted under Part 2 of this program.

Corrosion Behavior of Steels in Gulf Seawater Environment

Anees U. Malik, Shahreer Ahmad, Ismaeel Andijani and Saleh Al-Fouzan

CORROSION BEHAVIOR OF STEELS IN GULF SEAWATER ENVIRONMENT

Anees U. Malik, Shahreer Ahmad and Ismaeel Andijani
SWCC, R&D Center, Al-Jubail

Saleh Al-Fouzan
Al-Jubail Desalination Plant

ABSTRACT

Due to the aggressive environment prevailing in and around the Gulf seacoast, the materials of construction are subjected to corrosion of varying degree. There are many factors influencing the initiation of one or several corrosion processes. These factors include nature of material, surface finish, temperature, humidity, wind directions, rainfall, etc. Steels are the predominant constructional materials in seashore structures including desalination plants which are subjected to general or localized corrosion of varying degree. A complete systematic information regarding corrosivity of materials in Gulf seawater is lacking. Keeping in view the importance of the corrosion data of materials particularly steels in Gulf seawater, a systematic study on this subject had been initiated in 1990 and was completed in 1996. This paper provides the results of this study concerning the corrosion behavior of steels, in Gulf seawater. The steels include carbon steels, stainless steels and super stainless steels (austenitic, ferritic and duplex). The study encompasses the factors influencing general, pitting and crevice corrosion of materials. The effects of TDS in general and chloride concentration in particular and degree of chlorination have been discussed in detail. The role of dominant alloy addition on the corrosion behavior of steels has been emphasized.

Weight loss and electrochemical techniques have been employed in determining the corrosion rates of materials. Potentiodynamic polarisation technique has been used to evaluate parameters related to localized corrosion. Both exposure and accelerated tests have been carried out to study crevice corrosion attack. Effect of surface finish on crevice attack has been investigated in detail. Rank orders of corrosion rates of steels under different conditions have been presented and their importance concerning materials selection in desalination plants is discussed.

KEYWORDS: Pitting, Crevice Corrosion, Stainless Steel, Breakdown Potential, Pitting Potential, PRE_N and Chlorination

Vapor-Side Corrosion Monitoring in Al-Khafji Desalination Plant

*Nausha Asrar, Anees U. Malik, Shahreer Ahmed,
Madeeh Al-Khalidi and Khalid Al-Moaili*

VAPOR-SIDE CORROSION MONITORING IN AL-KHAFJI DESALINATION PLANT

Nausha Asrar, Anees U. Malik and Shahreer Ahmed
R&D Center, SWCC, P.O. Box: 8328
Al-Jubail - 31951, Saudi Arabia

Madeeh Al-Khalidi and Khalid Al-Moaili
Al-Khafji Desalination Plant, SWCC
Al-Khafji, Saudi Arabia

ABSTRACT

The corrosion problem in vapor side is aggravated due to uncertainties in concentrations of oxygen, carbondioxide and other non-condensable gases. In such a situation, vapor-side corrosion could be a limiting factor in a MSF plant life, if not studied properly. This paper presents the results of a vapor-side corrosion monitoring study carried out at Al-Khafji desalination plant. Corrosion behavior of 70/30 Cu-Ni alloy, carbon steel and AISI-316 have been studied in vents and in the vapor-side of evaporator for about 9000 hours. Corrosion rates have been determined by weight loss method. The corrosion products have been analyzed by Energy Dispersive X-ray Analyzer (EDAX).

Analyses of the experimental data indicate that in addition to O_2, H_2S evolved during flashing of seawater has reacted more with Cu-Ni alloy as compared to carbon- and Stainless steels. Contrary to other reported works, ammonia and bromine, have not been found in corrosion products. Explanations for comparatively higher corrosion of alloys exposed to the vapors of early (1-3) and middle (11-13) stages of MSF plant have been given with experimental results. Stainless steel 316L has been found as the most resistant alloy to vapor-side corrosion in all stages of distiller.

KEYWORDS : Vapor-side Corrosion, Non-condensable Gases, MSF Plant, Seawater, Oxygen Ingress.

Studies on the Stress Corrosion Cracking Behavior of Few Alloys Used in the Desalination Plants

T.L. Prackash and A.U. Malik

The Fourth Gulf Water Conference
Water in the Gulf, Challenges of the 21st Century
State of Bahrain (13-17 February, 1999)

STUDIES ON THE STRESS CORROSION CRACKING BEHAVIOR OF FEW ALLOYS USED IN THE DESALINATION PLANTS

T.L. Prakash and A.U. Malik
SWCC, Research Center,
P.O. Box 8328, Al-Jubail - 31951
Kingdom of Saudi Arabia

ABSTRACT

This paper describes a study on the Stress Corrosion Cracking (SCC) behavior of alloys resulting from the synergistic action of corrodents such as chlorides, oxidants and H_2S. In the this study, the threshold stresses for SCC have been determined for few generic alloys namely, mild steel, 316L, 317L, 430 and Monel 400 used in the desalination plants. The standard Proof Rings and U-Bend samples in NACE and SHELL solutions containing H_2S are used for the purpose. Electrochemical polarization measurements were performed on these alloys in the specified environments to study the effect of electrochemical potential on the intergranular SCC. Structural analysis were conducted by Scanning Electron Microscopy supplemented by Energy Dispersive Spectroscopy. The test results showed that the intergranular and intragranular SCC fracture of mild steel and alloy 430 in H_2S environment occurs only in the limited potential environment, whereas, the alloys viz, 316L and 317L are immune to SCC under the condition of test performed. The alloy Monel 400 was found however susceptible to SCC in presence of H_2S which may be present in some part of desalination plants due to pollution of seawater.

KEYWORDS: Stress Corrosion Cracking; Threshold Stress; Electrochemical Polarization: Sulfide Ion; Passive Film.

Studies on Corrosion of Carbon Steel in Deaerated Saline Solutions in Presence of Scale Inhibitor

Ismaeel Andijani and S. Turgoose

The Fourth Gulf Water Conference
Water in the Gulf, Challenges of the 21st Century
State of Bahrain (13-17 February, 1999)

STUDIES ON CORROSION OF CARBON STEEL IN DEAERATED SALINE SOLUTIONS IN PRESENCE OF SCALE INHIBITOR

Ismaeel Andijani[1] and S. Turgoose[2]
[1] SWCC, RDC
P.O. Box 8134, Al-Jubail 31951
[2] Corrosion Protection Centre, UMIST
Manchester, M60 1QD
UK

ABSTRACT

An investigation has been carried out to evaluate the corrosion behaviour of carbon steel in deaerated 1.0 M NaCl solutions and artificial seawater at pH ranges of 3 to 8.5 and temperatures up to 80°C under static conditions, using the polarization resistance technique. The effect of scale inhibitor addition on the corrosion rates has also been studied.

It has been found that the polarization resistance of carbon steel in deaerated solutions is generally high. With increasing pH, the polarization resistance increases, and is highest at 25°C and lowest at 80°C.

In long-run measurements, for 50°C at pH 8.5 the corrosion rates gave lower values compared to short-run measurements under the same conditions. This reduction in the corrosion rate is due to the formation of a protective hydroxide film on the metal surface, which restrict access of H_2O to the surface.

The results obtained with addition of 20 ppm phosphonobutanetricarboxylic-acid scale-inhibitor at 50°C at pH 8.5, showed that there was no effect on the R_P values.

KEY WORDS: Carbon Steel, Desalination, Dissolve oxygen, Corrosion rate, Inhibitor, Polarization,

Optimum Utilization of Resources

Mohammad Abdul-Kareem Al-Sofi

The Fourth Gulf Water Conference
Water in the Gulf, Challenges of the 21st Century
State of Bahrain (13-17 February, 1999)

OPTIMUM UTILIZATION OF RESOURCES

Mohammad Abdul-Kareem Al-Sofi[1]

ABSTRACT

This paper is divided into three parts covering three vital aspects of water resources. The first being current conditions of a large number of countries in various parts and levels of industrialization in the world. Second aspect proposes an escalating water tariff for domestic consumption. This concept is said to be applicable in other water and energy sectors. Third and last calls for restructuring of all water and energy authorities in such a way that conflicts of interest are avoided in the future.

In reviewing current conditions of supply and demand the selected countries were put into three main groups: A, B & C. In group A countries of very healthy water balances are shown to consume between 0.48% in Norway of the annual renewable water resources to 19.71% in Japan. In group B annual consumption are shown to be from 23.46% of renewable resources in Syria to 95.21% in Egypt. Group C lists countries facing water deficit from 11% in Iraq (and upwards) of consumption compared to renewable resources. Where are the Tigris and the Euphrates!

In part two four primary inputs for four primary human activities and four inseparable outputs are considered to encompass the entire domain of life. This part starts by stressing the fact that certain regions of the world have accomplished monumental developments through recent decades. While achieving such paramount goals, organizational and administrative growth was so rapid. The organizational background of both private and public sector set ups led in many cases to overlaps and undesired inter-mingled relationships.

In reviewing current status, points of weaknesses were focused on in order to identify obstacles which could hamper further advancement into the twenty first century. The aim of this review is to first pinpoint existing

---

[1] Correspondence through: Water Science and Technology Association, Telephone 973-826512 and Fax: 973-826513 P.O. Box 20018, Manama, State of Bahrain.

and potential obstacles and then to find a way out by suggesting possible solutions that would, indeed, resolve any conflict.

In part three an escalating water tariff in proposed. This proposal calls for setting up a stepwise rising water charge for domestic consumption. In this respect household consumption is broken down into 12 tiers of increasing quantities and charges. Against these quantities and charges where users are placed into 9 categories where by starting with first category (A) for a household consuming only at a modest level of ten kilo liter per month this category is to be exempted from charges. Then only four tiers is to applied to each one of the remaining 8 categories as shown in Table 1 by check versus cross-mark. The applied four tiers will be raised one step when moving from one category to the next. In other words tiers 2 to 12 are applied to categories B to I, at increasing capacities starting form 10 to 170 liter except the last tier (12) which is of open capacity at 900 Bf/kl applicable only to consumers in category I.

Table 1 : Escalating domestic water tariff

Nature of → USE ↓				Sustenance			Necessities			Prosperous		
	Tiers	**Tariff Bf/kl**	**Categories →** **Capacity ↓ (kl/ m-hh)**	**A**	**B**	**C**	**D**	**E**	**F**	**G**	**H**	**I**
SU	1	**Zero**	**10**	✔	✖	✖	✖	✖	✖	✖	✖	✖
ST	2	5	10	✖	✔	✖	✖	✖	✖	✖	✖	✖
EN	3	15	20	✖	✔	✔	✖	✖	✖	✖	✖	✖
AN	4	25	30	✖	✔	✔	✔	✖	✖	✖	✖	✖
CE	5	50	40	✖	✔	✔	✔	✔	✖	✖	✖	✖
	6	100	50	✖	✖	✔	✔	✔	✔	✖	✖	✖
NECE	7	200	70	✖	✖	✖	✔	✔	✔	✔	✖	✖
SSI	8	300	90	✖	✖	✖	✖	✔	✔	✔	✔	✖
TIES	9	400	110	✖	✖	✖	✖	✖	✔	✔	✔	✔
PROS	10	500	140	✖	✖	✖	✖	✖	✖	✔	✔	✔
PER	11	700	170	✖	✖	✖	✖	✖	✖	✖	✔	✔
OUS	**12**	**900**	**Open**	✖	✖	✖	✖	✖	✖	✖	✖	✔

✔ = denotes valid & applicable ✖ = denotes invalid & inapplicable

For the purpose of clarity a graphical presentation is felt to be of value. The following Figure-1 illustrates the concept.

Figure 1 Optimum Utilization of Resources

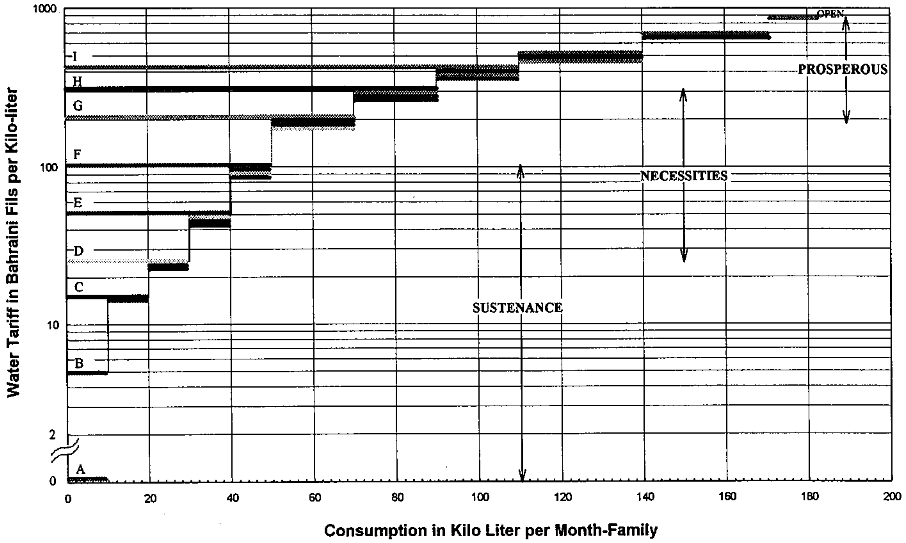

It is to be noted that the above figure is plotted on a semi-log scale. In this figure, there are couple of discontinuities along the logarithmic vertical axis in order to show the zero charge for category A and along the linear horizontal axis to denote that Tier 12 has a starting quantity but is open on the upper side. Moreover, it is to be noted that consumption tiers as well as categories are also placed into groups based on the nature of water usage. These are water for sustenance, necessities and prosperous uses.

The above thoughts could give way to upgrading services and utilities through improved relations and tariff structure. Careful analysis also indicates that removal of overlaps could lead to administrative productive roles, thus precluding any conflict of interest and hence allowing the society to achieve prosperity through:

Optimum Utilization of Resources

RDC
PAPERS

Degradation Study of Cellulose Triacetate Hollow Fine Fiber SWRO Membranes

A. Mohammed Farooque and Ahamed Al-Amoudi

DEGRADATION STUDY OF CELLULOSE TRIACETATE HOLLOW FINE FIBER SWRO MEMBRANES

A. Mohammed Farooque and Ahamed Al-Amoudi
Research and Development Center
Saline Water Conversion Cooperation
P.O. Box # 8328, Al-Jubail 31951
Kingdom of Saudi Arabia.

K. Numata
Japan International Cooperation Agency (JICA)
Japan

ABSTRACT

Cellulose acetate (CA) membranes are liable to chemical attack mainly by operation at improper pH or by chlorine and other oxidizing agents. The chemical attack could lead either to hydrolysis of the pendant acetyl group or to oxidation of polymer backbone leading to chain scission. Hydrolysis can be detected by determining the degree of polymer acetylation, whereas oxidation can be detected by changes in polymer molecular weight as measured directly, for example by the intrinsic viscosity measurement, and/or indirectly by determining polymer tensile strength. In the present study degree of acetylation, intrinsic viscosity and tensile strength measurements, were used for identifying the causes of the poor performance of two cellulose triacetate hollow fine fiber membranes obtained from a commercial SWRO plant after being in operation for five and two years, respectively. To establish causes of degradation in the commercial samples, analyses were also performed on fresh virgin fiber, on a second sample exposed to high concentration of chlorine, and a third sample exposed to high pH. By comparison to the virgin sample, it was established that fiber exposure to high concentration of chlorine and to high pH induced decrease in polymer chain molecular weight and in degree of acetylation, respectively. Both the commercial SWRO membranes were found to have undergone both hydrolysis as well as oxidation. However, polymer chain oxidation was established as the major cause for the degradation in performance of the commercial sample which was in operation for nearly five years, while hydrolysis of the pendant acetyl group was established as the major cause for the degradation in performance of the second commercial membrane sample which was in operation for two years. The paper describes the detail of the measurements made and results obtained.

KEYWORDS: cellulose acetate, RO membranes, chemical degradation, degree of acetylation, intrinsic viscosity and tensile strength.

INTRODUCTION

Cellulose acetate (CA) membranes are widely used in RO desalination industries because of the overall advantages of their properties, cost and ease of use. One of the most outstanding features of CA membrane is their claimed resistance to Cl_2. However, occasionally the CA membranes exhibited reversible and irreversible deterioration in their performance. Reversible decline, which is usually caused by fouling due to accumulation of scale, suspended solids or microbiological growth, can be restored to some extent by chemical cleaning. However, in case of irreversible decline, the performance could not be restored and in such cases membrane replacement was required. The irreversible decline is induced either by physical or by chemical membrane damage. Physical damage is caused either by compaction due to creeping, or by scratching or by mechanical causes such as vibration. The major chemical processes of CA membrane deterioration are hydrolysis and/or oxidation. Both hydrolysis and oxidation will lead to poor membrane performance.

CA membranes are most stable at pH 4.7 and the extreme pH, less or above this value, will accelerate the process of hydrolysis of acetyl group, pendant to the polymer chain. It is reported that deacetylation of cellulose acetate is caused by chlorine at pH 7, in presence of metal salts. In this study [Murphy, 1991] revealed that deacetylation was more effective in presence of cobalt and ruthenium, moderately in presence of iron, nickel, rhodium, palladium and silver, and slightly in presence of copper and gold salts. Hydrolysis leads to reduction in degree of acetylation which in tum leads to loss of salt rejection capacity of the RO membranes.

Another major cause for the chemical degradation of CA is oxidation. Oxidation is accelerated at high concentration of oxidizing agents such as chlorine (Cl_2), which is used in RO process as disinfectant [Motomura and Taniguchi, 1981]. Studies [Fujiwara et al., 1994; Kumano et al., 1994] indicated that chlorine in presence of heavy metals lead to oxidation as well as some times to hydrolysis of CA membranes. Cobalt and copper have a remarkable effect on the deterioration of the CA membranes while iron, manganese and nickel affect membrane performance but to a lesser extent. Also, temperature, pH and chlorine concentration have an influence on CA membrane performance. The effect of oxidation is mainly through the scission of membrane polymer chain, thus reducing both its molecular weight as well as mechanical strength, resulting in a decline in salt rejection and to an increase in permeate flux of RO membrane. The oxidation can be detected by either mechanical strength measurement and/or by molecular weight determination. Several methods are used in determination of molecular weight of polymer including intrinsic viscosity which is directly proportional to the polymer molecular weight.

In this study, because of its simplicity and availability the intrinsic viscosity, the tensile strength measurements and determination of acetyl content were employed, to establish the causes of the observed poor performance of two commercial SWRO cellulose triacetate (CTA) hollow fine fiber (HFF) membranes. For comparison reasons, the performance of a fresh virgin membrane, a known oxidized membrane and a hydrolyzed membrane, each of CTA HFF origin were also examined by the same three methods.

EXPERIMENTAL

Materials

Membranes

The two commercial SWRO CTA HFF membranes with poor performance are brine side membrane elements. After about 5 years in operation, the first one (Mem#1) had permeate conductivity of 13,480 μS/cm. The second one (Mem#2) after about 2 years in operation, it had permeate conductivity of 3,920 μS/cm. Virgin membrane fibers and oxidized membrane fibers were obtained from membrane manufacturer as well as a new membrane module which was used for the hydrolysis. Both the commercial membranes and the hydrolyzed membrane were autopsied and samples were collected from inner, middle and outer portions for detailed analysis.

Hydrolyzed CTA membrane was prepared by continuously operating a new SWRO CTA HFF membrane element (size 5" x 20") for about 375 hours in recirculation mode using non chlorinated raw seawater feed with SDI $\approx$ 4.5. The pH of the feed was maintained at about 9.5 by adding NaOH as and when required. The membrane performance (flow and conductivity) were continuously monitored until the performance of the membrane was remarkably reduced. At the end of the experiment, the membrane was removed and autopsied, and samples were collected for further analyses. Before carrying out any analysis all the membranes cut were thoroughly cleaned with distilled water for about 15 hours.

Degree of Acetylation

Acetylation degree of membranes, which is normally expressed as percent of acetyl group in the polymer, was determined using standard ASTM procedure with slight modification [ASTM, 1983]. In this method, a known amount of membrane sample (0.7 g) was first added to 70 ml of acetone in an Erlenmeyer flask and kept stirring using a magnetic stirrer, for 1 hour followed by addition of 5 ml of methanol. After 30 minutes of additional stirring, IN NaOH was added in excess (15 ml), to the highly swollen (not completely soluble) membrane sample solution and kept stirring for another 1 hour. After adding hot (60°C) distilled water for washing down the sides of the flask and continuing stirring for another 10 minutes, the unreacted excess amount of NaOH was titrated against standard sulfuric acid (0.5 N) using phenolphthalein indicator. When the pink color disappeared completely, an excess (0.2 - 0.3ml) of sulfuric acid was added and retitrated with 0.1 N NaOH. For each sample, a duplicate was also carried out as well as two blank analyses. The acetylation degree was then calculated as the percentage weight of combined acetic acid formed to the total weight of membrane polymer during hydrolysis by the excess NaOH.

Stress Strain Measurements

Instron Series IX automated Materials Testing System, Series 4200 Interface, was used to measure the tensile properties. Hollow fine fibers samples of length 7 to 8 cm were soaked in distilled water prior to the tensile measurement. To prevent the fibers from drying, distilled water was sprayed on to the fiber while running the test. The test conditions were as follows :

Number of test specimens	10
Sample length between the grips	2 cm
Cross head speed	2 cm/min.

Percentage elongation and tensile strength at break were automatically calculated by the computerized Instron for each of the fibers.

Intrinsic viscosity measurement

The intrinsic viscosity [η], which is related to the polymer molecular weight, was determined following the standard procedure [Avlonitis et al., 1992]. Ubbelohde type capillary viscometer was used at constant temperature of 30 ± 1°C. After determining the efflux time (t_0) for the solvent methylene chloride/ methanol (9/1) mixture, the same (t_i) was determined for the known concentration of the sample. For each concentration of sample, five measurements were made and average of three measurements were taken after discarding both the lowest and highest readings. The measurements were made at different concentrations for each sample by successive dilution using the above solvent. The intrinsic viscosity $[\eta]$ was then obtained as intercept of the plot of η_{sp}/c against c, where c is concentration (g/dl) of membrane sample and η_{sp} is specific viscosity. The specific viscosity can be obtained from relative viscosity (η_{rel}) as $\eta_{rel}-1$. The η_{rel} can be determined from the efflux time of solvent t_o and sample t_i as $\eta_{rel} = t_i / t_o$.

RESULTS & DISCUSSION

Degree of Acetylation

The degree of acetylation for all the tested membrane samples, i.e., virgin, oxidized, hydrolyzed, and two commercial samples with poor performance, are shown in Figure 1. For all the membrane samples analyzed, the difference between different portions (i.e., inner, middle and outer) of membrane was found to be not significant as can be seen from the figure. It is very clear from the figure that the hydrolyzed membrane is definitely having lower degree of acetylation (acetyl content) than that of the virgin or the oxidized membranes, where no hydrolysis is supposed to take place. The commercial membrane (Mem#1) which was in operation for nearly 5 years showed only a slight loss (about 1.4%) in degree of acetylation, whereas the Mem#2, which was in operation for about 2 years, showed a remarkable loss in degree of acetylation (about 5%), indicating a severe degree of the membrane polymer hydrolysis. So, it can be said that the hydrolysis was the main reason for the poor performance of Mem#2 and the observed slight hydrolysis of Mem#1 have contributed somewhat to its poor performance.

Tensile Strength

The membranes tensile strength and percentage elongation at break are shown in Figures 2 & 3. Both the percentage elongation and tensile strength show the same trend in that a reduction in the membrane polymer molecular weight, resulting from polymer chain scission by oxidation is noticed for the Mem#1 and Mem#2 samples but not for the virgin or hydrolyzed membrane fibers. The tensile strength of the oxidized fibers could not be evaluated as the fibers were too brittle for the measurement, indicating that the membrane polymer is highly oxidized. A maximum value of tensile strength and percent elongation at break are noticed, as expected, for the virgin membrane fibers, and with comparable values for the hydrolyzed membrane. Thus proves that the latter membrane did not undergo any sort of oxidation leading to membrane polymer scission. Hydrolysis removes the pendant acetyl group and is not expected to affect the chain backbone which is responsible for the polymer strength. By comparison to virgin membrane, the tensile strength and percent elongation of Mem#2 were 48% and 60%, respectively, of that for the virgin fibers, indicating membrane polymer oxidation. Whereas the tensile strength and percent elongation of Mem#l were found to be too much lower than those of Mem#2, i. e., only 24% and 1 0% respectively of that of the virgin fibers (see Figures 2 & 3). So, it can be said that both the commercial membranes have undergone oxidation, and the Mem#1 which was in operation for nearly 5 years was highly oxidized and more so than Mem#2.

Intrinsic Viscosity

Intrinsic viscosity measurement results support the tensile strength (see Figure. 4). As expected, virgin membrane was found to have the maximum value of intrinsic viscosity (1.24 dl/g) and the oxidized membrane had the lowest value (0.30 dl/g). For hydrolyzed membrane, the intrinsic viscosity was found to be about 1.24 dl/g indicating that the membrane did no undergo any oxidation, thus confirming the results obtained by tensile measurement. Intrinsic viscosity of Mem#2 could not be measured because the fibers were not soluble in the solvent (methylene chloride / methanol mixture). This was obvious, because it is known that the solubility of cellulose acetate polymers in a particular solvent is strongly influenced by the degree of acetylation [Encycl. of Polym. Sci. & Eng., 1985]. Degree of acetylation measurement results indicated that Mem#2 had lower degree of acetylation compared to all the other membranes analyzed, thus making it insoluble in the solvent by altering the solubility property of the polymer. The Mem#l sample showed a remarkable reduction in intrinsic viscosity (0.72 dl/g) indicating that membrane polymer molecular weight was decreased by polymer chain scission due oxidation, thus supporting the tensile study that the membrane was oxidized.

CONCLUSION

By comparison to virgin sample, it was established that same CTA HFF membrane exposure to high concentration of chlorine and to high pH induced decreases in Polymer chain molecular weight and in degree of acetylation, respectively. It was found that both the commercial membranes, Mem#1 and Mem#2 which were in operation for 5 years and 2 years, respectively, have undergone both oxidation as well as hydrolysis. However, polymer chain oxidation was the main cause for the degradation in performance of the commercial sample Mem#1. Whereas, hydrolysis of the pendant acetyl group was established as the major cause for the degradation in performance of commercial membrane sample Mem#2.

ACKNOWLEDGEMENT

The authors wish to thank Dr. Ata M. Hassan for his continuos support and encouragement, during the course of this work.

REFERENCES

ASTM, 1983, Standard Methods of Testing Cellulose Acetate Propionate and Cellulose Acetate Butyrate, Designation: D 817 - 72 (Reapproved 1983).

Avlonitis, S., W.T. Hanbury, and T. Hodgkiess, 1992, Chlorine Degradation of Aromatic Polyamides. Desalination, 85, pp. 321-334.

Encyclopedia of Polymer Science and Engineering, 1985, Vol. 3, second Edn., Eds. Mark, H.F., Bikales, N.M., Overberger, C.G., Menges, G., and Kroschwitz, J.I., John Wiley & Sons, NewYork.

Fujiwara, N., K. Numata, A. Kumano, V. Ogino, M. Nagai, and H. Iwahashi, 1994, The effect of heavy metal ions on the oxidation of cellulose triacetate membranes. Desalination, 96, pp. 431-439.

Kumano, A., Y. Matsui, K. Numata, N. Fujiwara, H. Iwahashi, and M. Nagai, 1994, Performance change formula of cellulose triacetate hollow fiber RO membrane due to oxidation and hydrolysis. Desalination, 96, pp. 451-457.

Motomura, H., and Y. Taniguchi, 1981, Durability study of cellulose acetate reverse osmosis membrane under adverse circumstances for desalting, Synthetic Membranes : Vol. 1 Desalination, Ed. A.F. Turbak, ACS Symposium Series 153, American Chemical Society, Washington, D.C.

Murphy, A.P., Accelerated deacetylation of cellulose acetate by metal salts with aqueous chlorine, 1991, Research Journal WPCF, 63, pp. 177-180.

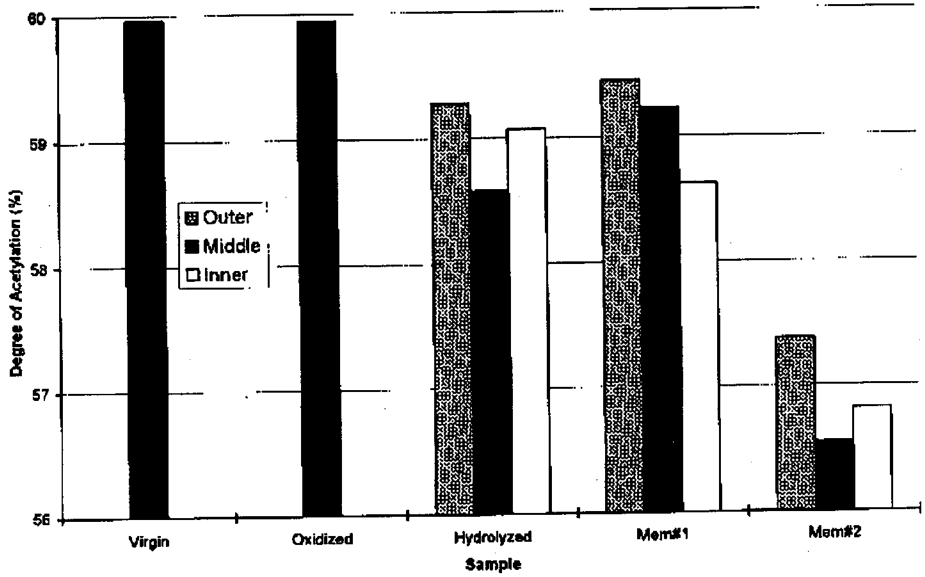

Figure 1: Degree of Acetylation of Various Membrane Samples

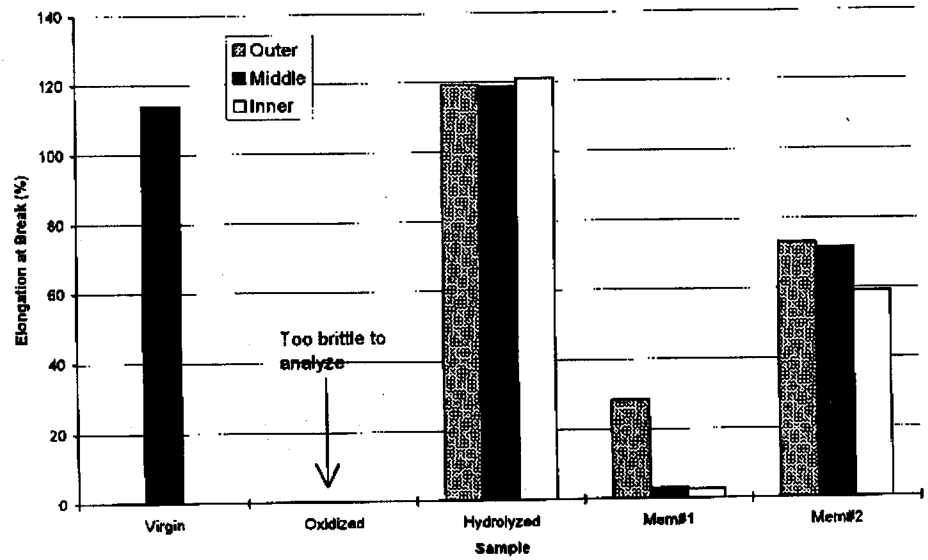

Figure 2: Percentage Elongation at Break for Various Membrane Samples

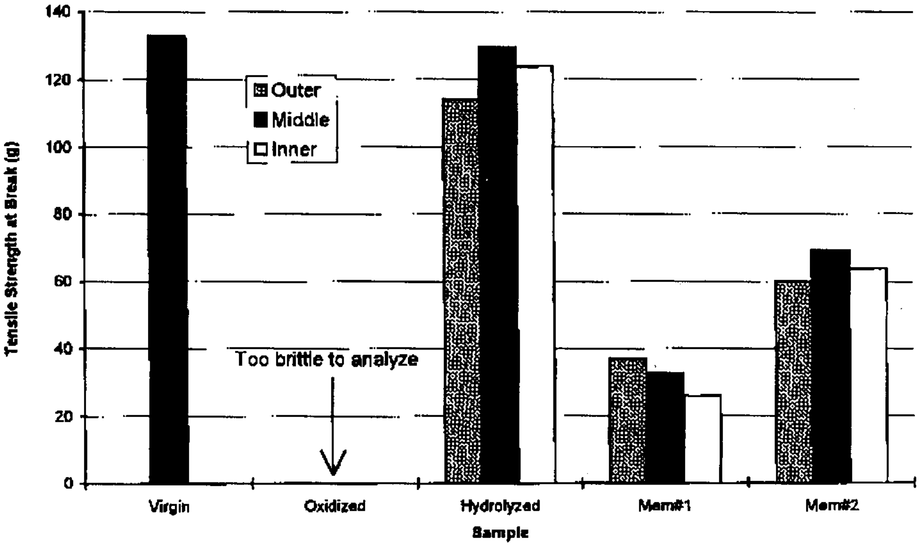

Figure 3 : Tensile Strength at Break of Various Membrane Samples

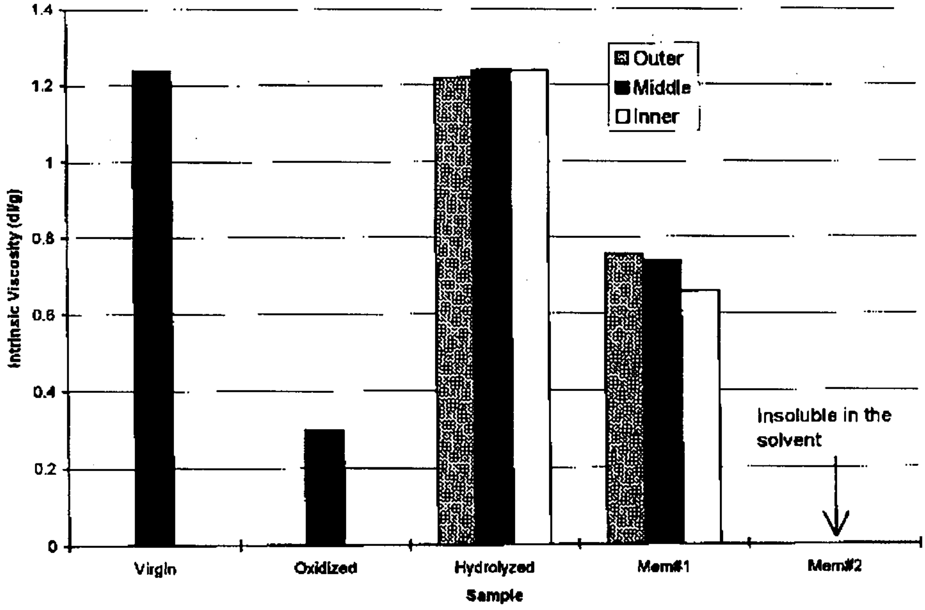

Figure 4: Intrinsic Viscosity of Various Membrane Samples

A New Approach to Membrane and Thermal Seawater Desalination Process Using Nanofiltration Membranes (Part 2)

A.M. Hassan, M. AK. Al-Sofi, A.S. Al-Amoudi,
A.T.M. Jamaluddin, A.M. Farooque, A. Rowaili,
A.G.I. Dalvi, N.M. Kither, G.M. Mustafa and I.A.R. Al-Tisan

A NEW APPROACH TO MEMBRANE AND THERMAL SEAWATER DESALINATION PROCESSES USING NANOFILTRATION MEMBRANES (PART 2)

A. M. Hassan, M. AK. Al-Sofi, A. S. Al-Amoudi,
A. T. M. Jamaluddin, A. M. Farooque, A. Rowaili, A. G. I. Dalvi,
N. M. Kither, G. M. Mustafa and I. A. R. Al-Tisan
Research and Development Center
Saline Water Conversion Corporation (SWCC)
P.O. Box 8328, Al-Jubail 31951
Kingdom of Saudi Arabia

ABSTRACT

In earlier publications it was reported that for the first time ever, a new approach to seawater desalination processes by integrating the nanofiltration (NF) membrane pretreatment process with one of the conventional desalination processes to form, for example, an NF-SWRO or NF-MSF or a combination thereof, such as NF-SWRO$_{reject}$-MSF, was developed at Saline Water Conversion Corporation (SWCC), R & D Center, and was successfully applied to those cases on a pilot plant scale with remarkable results. The seawater treatment first with the NF membrane removed from it turbidity and microorganism, caused significant rejection of the scale forming hardness ions, e.g., $SO_4^=$ by up to 98%, reduced TDS in Gulf Seawater by up to 65 %, and produced a new, partially desalinated seawater product, considerably different and superior to seawater in qualities and without the problems normally associated with seawater of high concentration of scale forming ions, high TDS, high turbidity and high bacteria count. The said desalination arrangements led to a significant improvement in the seawater desalination processes, for example by doubling the SMRO product water output and recovery ratio and the production of high purity permeate (TDS < 200 ppm) from one single stage SWRO. It also allowed for the successful operation at high recovery of the MSF as part of a NF-MSF unit or as part of a trihybrid NF-SWRO$_{reject}$-MSF desalination system, where the reject from SWRO constituted the make-up to the MSF unit, at top brine temperature of 120 °C, without the addition to the MSF make-up of acid or antiscalant or antifoam and its operation under those conditions without scale formation. Moreover, by this tri-hybrid process, up to 90% of the NF permeate was converted to potable water. The paper describes the effect of long term operation on the performance of those seawater hybrid desalination processes.

Key Words: NF-SWRO, NF-MSF, $SWRO_{reject}$-MSF, hybrid desalination process, NF-pretreatment of seawater

INTRODUCTION

In earlier publications [1-4] the application of "A New Approach to Membrane and Thermal Seawater Desalination Using Nanofiltration Membranes", which was developed at SWCC, was described. Use of the NF membrane as part of feed pretreatment eliminated the main problems encountered in conventional seawater desalination by removal of turbidity, microorganisms as well as removal of hardness scale forming ions, e.g., $SO_4^=$ ions by up to 98% and Ca^{++} ions by up to 90%, and overall reduction of feed TDS by up to 65%. By the removal of hardness ions and by lowering of feed TDS, the NF feed pretreatment also has performed a significant part of the desalination process. Prior to its NF pretreatment the nonchlorinated seawater feed was filtered through dual media filtration followed by cartridge filtration without adding the coagulant chemicals which are normally employed in SMRO feed pretreatment. Moreover, the NF pretreatment allowed for the successful operation of SWRO in an NF-SWRO hybrid pilot plant at high permeate recovery, e.g., 80% recovery at an applied pressure of 65 bars, and producing high purity water in one single stage SWRO. The NF seawater feed pretreatment also allowed for the successful operation of MSF pilot plant without its scaling at high temperature of 120°C and without addition of antiscalant or acid or antifoam in the following hybrid combinations of : NF-MSF and NF-$SWRO_{reject}$-MSF, where in the first and second cases the NF permeate and the SWRO reject from an NF-SWRO unit constituted the make-up to the MSF pilot plant. Main emphasis in this article is on the long term operation performance of those NF-seawater desalination hybrid systems.

SOME MAJOR PROBLEMS IN SEAWATER DESALINATION

As indicated in Section 1 and discussed in detail in earlier publication [1-4], the seawater is characterized by having high concentrations of (1) hardness ions of $SO_4^=$, HCO_3^-, Ca^{++} and Mg^{++}, (2) TDS, (3) Turbidity and microorganism. In seawater desalination processes, the hardness ions give rise to scale formation problem, while specially in the SWRO process high TDS means high osmotic pressure requiring an increase in applied pressure to overcome it. This leads to an increase in energy waste in form of pressure as seawater TDS is increased. The presence of turbidity and microorganisms in the feed leads to membrane fouling problems. To overcome those problems and in order to minimize their effect on seawater desalination, the seawater feed to desalination plant is pretreated to produce a certain quality feed. This is summarized in Table 1. Presence of hardness ions in feed to SWRO or Thermal plants requires removal of those ions or inhibition of their precipitation by addition of antiscalant and by the operation at correct operating conditions. The high concentration of salts in seawater requires, when possible, the lowering of TDS which results in lowering of SWRO feed osmotic pressure and, therefore, also the lowering of process energy followed by an increase in both permeate flow and recovery ratio. This is also beneficial to thermal desalination process since lowering of TDS reduces the concentration of hardness ions. Obviously, removal of turbidity and microorganisms diminishes the chance of membrane fouling.

Both the high degree of hardness and high TDS place limits on product water recovery, while depending on the process the presence of large turbidity, if not removed, tends to degrade plant performance. In the past, it was demonstrated that use of beach-well effectively removed turbidity and improved SWRO plant performance. Use of antiscalants proved effective in preventing scale formation but failed to increase significantly water recovery in both the membrane and the thermal processes. Also, the coagulation-filtration process is employed in the removal of fine particles. This process, however, does not remove the very fine particles or ions with sizes of less than 1 to 2 μm. For removal from seawater of particles with sizes less than 1 μm, microfiltration (MF), and UF have been used for separation of particle having sizes above 0.08 and 0.01, respectively [5,6,7]. Other membranes that allow for fine particle separation are the RO and NF processes. The RO process deals with separation of ionic size particles in the range of 0.001μ or less. The NF Membrane falls in-between the RO and UF separation range, and is suited for the separation of particle sizes in the range of 0.01μ to 0.001μ. In addition to the rejection of neutral particles according to their sizes, as is the case with the MF and UF membranes, the NF rejection of inorganic matter is achieved by their electrostatic interaction with the negatively charged membrane [8]. Moreover, the degree of rejection by the NF membrane is lesser for mono-valent ions, such as Cl^-, Na^+, than that for the divalent $SO_4^=$ and Ca^{++}.

The above ion selectivity allowed for the use of NF in the removal of hardness from low salinity water. It has been applied in softening of brackish water and drinking water, especially to meet the various Drinking Water Acts, water softening, removal of color, turbidity, removal of dissolved organic which are precursors to disinfection by-products (THM) [9-13]. The NF has been used in other applications to treat salt solution and landfill Leachate [14], demineralization of whey, removal of sulfate from seawater to be injected in off-shore oil well reservoirs [15-17], oil water separation, etc. The use of NF membrane as part of a combined NF-seawater desalination, to pretreat feed to seawater desalination plants in order to remove hardness, to lower TDS, to remove turbidity, has been used by SWCC, for the first time, in the pretreatment of feed to SWRO and make-up to MSF pilot plant units in the hybridization process of NF-SWRO, NF-MSF or NF-SWRO$_{reject}$-MSF [1-4]. With those processes, significant improvement in desalination processes was achieved. The long term operation effect on performance of those hybrid system is presented in the following sections.

EXPERIMENTAL

All experimental work was done on pilot plants scale (capacity 20m^3/d). A schematic flow diagram of the NF-SWRO pilot plant is given in Figure 1, while Figures 2 shows the integration of NF-SWRO with an MSF pilot plant distiller comprising 2 and 4 stages of heat rejection and recovery, respectively. Moreover this last arrangement allows for utilization of the seawater from MSF heat rejection section as the feed to the NF unit during winter season. The NF-SWRO, the SWRO, and MSF pilot plant set-ups were described in earlier work [1-4, 5,18]. The NF unit consists of a high pressure pump and five NF modules each containing two commercial NF spiral wound membrane elements (size 4"x40"). The feed is supplied to the first two modules, arranged in parallel, and the reject of each is fed to its following module which is connected to it in series. Reject from the latter two modules constitutes the feed for the final fifth module. The SWRO unit is made of a high pressure pump followed by six SWRO modules, each contains one commercial spiral wound membrane element (size 2.5"x40"), all arranged in series as shown in Figure 1. After its filtration **without coagulation,** the filtrate was passed to the NF membrane under pressure, initially of about 18 bars. This was followed by passing the product from the NF unit to the SWRO unit, or alternatively by passing the NF permeate or SWRO reject from an NF-SWRO pilot plant, to the MSF unit as shown in Figure 2. Detail of experimental procedure was given in earlier publications [2-4].

RESULTS AND DISCUSSION

NF-Trials

Table 2 lists the concentration of the various seawater ions in Gulf seawater before and after the NF treatment along with their percent salt rejection. At an applied NF feed pressure of 18 bars, the concentration of the hardness ions of Ca^{++}, Mg^{++}, $SO_4^{=}$ and HCO_3^{-} in NF permeate was 93 ppm, 193 ppm, 206 ppm and 46 ppm, respectively, compared to their concentration in seawater of : 481 ppm, 1608 ppm 3200 ppm and 128 ppm. Their average salt rejection were 80.7%, 87.7% 93.3% and. 63.3%. Total hardness was reduced by 86.5%. In addition to the reduction of hardness ions by the NF pretreatment, the Cl^- ions were also reduced from 22,780 ppm in seawater feed to an average of about 16,692 ppm in NF permeate or a reduction of about 26.7% with similar reduction for the Na^+ and K^+ ions. The net effect of this reduction by the NF treatment in Cl^-, Na^+ and K^+ ions together with the reduction in hardness ions caused a reduction in TDS from 44,046 ppm in seawater to an average of 27,720 ppm for the NF pretreated feed, for a reduction of 37.3%. The pH of the feed of 8.2 was also reduced to an average of 7.85 in the NF permeate. Raising the NF feed pressure to 22 bars reduced further the Ca^{++}, Mg^{++}, $SO_4^=$ and HCO_3^- concentration in the filtrate thereby increasing their salt rejection (Table 2). Moreover, reduction in seawater hardness and TDS, the latter by up to 63%, was achieved when the NF feed pressure was raised to 31 bars, although hardness reduction was less than in the previous case, at $p = 22$ bar, Table 2.

Long Term NF Operation

Figure 3 shows the actual and normalized NF flow of feed, permeate and product recovery, their conductivity and operating conditions which are plotted vs operation time. At an applied feed pressure of about 20 bars, the product conductivity remained steady at about 41,000 μs/cm, while product water recovery, depending on feed, was about 40 to 45%. Increasing the NF applied pressure to 31 bars resulted in further reduction of both conductivity to above 24,600μs/cm and TDS to about 16,400 ppm, Table 2. The normalized NF product flow fluctuated at about 13 l/min at the start of the operation, to about 11 l/min after 5000 hours of operation time, Figure 3. The seawater filtrate SDI was about 4.3, while the SDI of NF permeate was less than 1. The differential pressure across the NF membrane (ΔP) remained steady at 15 psi ($\approx$ 1bar).

Figure 4 illustrates the NF permeate flow vs operation time, for about 9700 hours of operation. The data in Figure 4b are fully normalized for feed: flow, temperature and pressure, while data in Figure 4a are normalized only for temperature effect. Figure 4a shows that during the cold seasons, operation hours 6000 to 9000 hours, adjustment of feed pressure allowed for raising the feed flow by off-setting the decline in flow due to the seasonal lowering of feed temperature. Full normalization of the data, however, shows that the decline in flow occurred after the cleaning of the NF membranes by a commercial phosphate - based type detergent, DMCA-14/BIZ, made by Cheyma Inc., Monterial, Canada. Use of various cleaning and flushing procedures failed to improve the permeate flow to its level prior to cleaning.

Operation at higher pressure of 31 bars instead of 22 bars, however, increased the permeate flow to its level before membrane cleaning (Figure 4a). However, after cleaning the NF permeate flow remained nearly steady at its level after the cleaning (Figure 4). Prior to this cleaning the membrane retention coefficient (MRC) calculated from Qt/Qi was about 80%, where Qt and Qi are the quantity of permeate flow at time t = 5000 hour and initial time over the first 100 hours.

In the NF membrane process, permeation of the NF permeate through the membrane occurs by two means, either by passage through the fine pores or by the RO permeation process. In both cases the permeate flow is dependent on the applied feed pressure, where up to the membrane flux limitation, the flow increases as the pressure increases. This is illustrated in Figure 5a, where both the permeate flow and recovery increased while permeate TDS decreased as the applied pressure is increased. As shown in Figure 5b, more specifically, the observed increase in permeate flow and recovery is due to the net driving pressure (Pnet). As illustrated by equation given in Figure 5b, a good portion of the applied pressure is lost in overcoming the osmotic pressure (π). For example, at the applied pressure of 37.9 bars, the Pnet, the net driving pressure, is only 12.6 bars for a loss in the applied pressure of 25.3 bars (Figure 5b).

NF-SWRO Trials

During the early operation, 0.0 to 2200 hours at the applied pressure of 56 kg/cm^2 and feed temperature of 33 ± 1 °C, the conductivity of the NF product, which constituted the feed to the SWRO unit in the NF-SWRO hybrid system, was 41000 µs/cm. The SWRO permeate flow and recovery ratio were maintained steady at 5 l/min and about 50%, respectively. This is illustrated in Figure 6, which also shows the SWRO permeate flow, product recovery and conductivity plotted vs operation pressure. During the final phase of SWRO operation, because of a drop in NF permeate conductivity to about 25000 µs/cm, the same above SWRO permeate and recovery ratio were maintained at an applied pressure of only 40 bars as shown in Figure 6. Because of the low conductivity of the NF feed it was possible to operate the unit at 40 bars. Operation at the normally applied pressure of 56 bars increased both the permeate flow and permeate recovery each by about 40%, Figure 6. Most important, the SWRO membranes maintained, a steady high performance, which did not decline with operation time when operation was done at same operating conditions.

The effect of applied pressure on SWRO permeate flow, recovery and conductivity are illustrated in Figure 7, which for reasons of comparison shows also the same for the conventional operation of same SWRO membranes under identical conditions but without the NF pretreatment. Passage of the NF permeate to SWRO unit under pressure gave satisfying results with ΔP remaining steady and constant at 2 bars during the entire operation. As shown in Figure 7, because of the low hardness of SWRO feed (see Table 2 for ions conc. at 31 bar) it is possible to obtain a recovery of up to 80% when the pressure is raised to about 70 bars. This high product recovery was achieved with NF permeate compared to one half this value or less for normally pretreated seawater feed. The product flow (Q_p) and recovery ratio are also increased directly with the applied pressure (Figure 7). The SWRO permeate from the combined NF-SWRO desalination system were much greater than those for the SWRO alone when the two systems are operated at same pressure and temperature conditions. For example, at 40 bars the permeate flow and recovery from the conventional SWRO is 1 l/min and 16.7%, respectively, as compared to a much higher flow and recovery ratio of 4.8 l/min and 48% from the new process of NF-SWRO, i.e., for an increase of 480% in flow and by 3 folds for permeate recovery. Even at the frequently employed pressure of 56 bars (800 psi) the SWRO product flow and recovery ratios for NF-SWRO : SWRO alone are in the ratios of 2.43:1.

Moreover, the quality of the permeate product from SWRO process is 4500 μs/cm at an applied pressure 40 kg/cm^2 and drops to 2300 μs/cm at 60 kg/cm^2 as compared to less than 500 μs/cm for SWRO permeate from the NF-SWRO process obtained from the same membrane at the same pressure range. The SWRO membranes used in this test, Figure 6, are old membranes and the NF pretreatment revives its low performance. This process (NF-SWRO) is expected to extend the life of an otherwise ready to be replaced membranes.

NF-MSF Trials

In this trial NF permeate was used as an MSF make-up at a flow rate of 1.5 m^3/hour replacing normal seawater at concentration of scale forming ions of alkaline and non-alkaline types in the NF feed to the MSF pilot unit as shown in Table 2, while Table 3 shows for comparison these concentrations in the brine recycle stream of the MSF operated with NF or SWRO reject from an NF-SWRO unit as make-up or seawater as make-up (conventional MSF). Also, listed in Table 3 are pH and conductivity values of the brine recycle streams. From this table it can be seen that scaling potentials in the MSF system have been significantly reduced and it was safe to operate the MSF plant with NF make-up for over 2320 hours, or with reject SWRO from the NF-SWRO unit for 1000 hours at high temperature of 120 °C without addition of antiscalant or antifoam chemicals. At the same operating conditions, the concentration of the scale forming ions of Ca^{++}, and $SO_4^{=}$ of 168 and 410 ppm in the NF-MSF case, Table 3A, and 232 and 1020 in the SWRO reject make-up case, Table 3B, are low when compared to 882, and 5830 ppm in the brine recycle stream of conventional MSF. These observations, especially the drastic reduction in $SO_4^{=}$, Ca^{++} and Mg^{++}, are encouraging to project MSF operation at higher TBT in the range of 120 °C to 160 °C. Thus improving plant production and hence water cost. Operation of MSF plants at higher temperature should increase the gain output ratio (GOR) in $Kg_{product}/Kg_{steam}$ and the performance ratio (PR) in $Kg_{product}/1000$ Kj, while decreasing the energy consumption in Kj/Kg product. Finally, the MSF plant operation on NF make-up remained steady with operation time.

CONCLUSION AND RECOMMENDATION

The NF membrane treatment of noncoagulated dual media filtered seawater feed to desalination plants removes from it (1) very fine turbidity, (2) residual bacteria, (3) scale forming hardness ions, in some cases by up to 98% and (4) lowers its TDS, depending on operation conditions by more than 60%. With this NF feed treatment the otherwise complex conventional seawater desalination process, are simplified since the effects on seawater desalination by the above four factors, which constitute the major problems in seawater desalination by the conventional processes, are eliminated. Feeding of the said NF product to desalination plants, whether based on the thermal or the membrane processes, not only allows for their operation with less or no chemicals normally used in the conventional process (i.e., antiscalants, and in case of MSF also antifoam) and by raising significantly their permeate and distillate recovery ratios to 70% and 80%, respectively, but also by lowering their energy consumption with the ultimate benefit of lowering potable water production cost. The combination of NF with MSF process makes it possible to operate MSF plants on NF-product or $SWRO_{reject}$ from NF-SWRO unit at high distillation temperature of 120 °C to 160 °C with high distillate recovery, and again without chemical addition or at reduced level thereof. Similarly, the NF-SWRO process makes it feasible to produce high purity permeate from a single stage SWRO process without the need for a second desalination stage. Also, this process improves significantly the quality of permeate from an otherwise low performance SWRO membranes. In short, it can be concluded that operation of seawater desalination plants when combined with this new NF membrane pretreatment is superior in performance to their operation without the NF pretreatment. Further, work is required in improving the NF membrane performance at an applied high pressure of 35-40 bars. Definitely, the process should be demonstrated by its application to demonstration and commercial seawater desalination plants.

REFERENCE

1. Hassan, A. M., Al-Sofi M. AK., Al-Amoudi A. S., Jamaluddin A. T. M., Dalvi A. G. I., Kither N. M., Mustafa G. M. and Al-Tisan, A New Approach to Membrane and Thermal Seawater Desalination Processes using Nanofiltration Membranes, A Paper presented at IDA, Madrid, Oct. 6-9, 1997.

2. Hassan, A. M., Al-Sofi M. AK., Al-Amoudi A. S., Jamaluddin A. T. M., Dalvi A. G. I., Kither N. M., Mustafa G. M. and Al-Tisan, A New Approach to Membrane and Thermal Seawater Desalination Processes using Nanofiltration Membranes, D&WR. The International Desalination & Water Reuse Quarterly, P54, May-June Issues, 1998.

3. Hassan, A. M., Al-Sofi M. AK., Al-Amoudi A. S., Jamaluddin A. T. M., Farooque A. M., Rowaili A., Dalvi A. G. I.,. Kither N. M., Mustafa G. M. and Al-Tisan, A New Approach to Membrane and Thermal Seawater Desalination Processes using Nanofiltration Membranes (Part 1), Paper Presentation at EDS Conference on Membrane in Drinking Water Production, 21-24 Sept., 1998, Amsterdam, the Netherlands.

4. Hassan, A. M., Al-Sofi M. AK., Al-Amoudi A. S., Jamaluddin A. T. M., Farooque A. M., Rowaili A., Dalvi A. G. I., Kither N. M., Mustafa G. M. and Al-Tisan, A New Approach to Membrane and Thermal Seawater Desalination Processes using Nanofiltration Membranes, Progress Report, July, 1998.

5. Hassan, A. M, Abanmay, A., Farooque, A. and Jamaluddin, IDA World Congress, Abu Dhabi, Nov. 18-24 (1995), Proceedings Vol. IV, 131-148.

6. Ebrahim, S., Bau-Hamada, S., M. and Sairafi, A. World Congress, Abu Dhabi, No. 18-24 (1995), Proceedings Vol. VII, 229-240.

7. Taniguchi, K., Onta, K., Okanbi, T., Hirai, M. and Goto, T., IDA World Congress, Abu Dhabi, Nov. 18-24 (1995), Proceedings Vol. II, 135-146.

8. Rautenbach, R., and Groschl, A. Desalination 77 (1990) 73.

9. Bergman, R.A., Desalination, 102 (1995) 11-24.

10. Duran, F.E., and Dunkeiberger, G. W. Desalination, 102 (1995) 27-34.

11. Fu, P., Ruitz, J. H., Lozier, J., Thompsion, K. and Spangenberg, C. Desalination, 102 (1995) 47-56.

12. Schwartz, E.D., and Murphy, 1. L., Desalination, 102 (1995) 63-75.

13. Boonthanon, S., Dharmapa, H. P., Vigneswaran, S. and Ben Aim, Aqua V. 40 (1991).

14. Linde, L., and Johsson, A., Desalination, 103 (1995) 223-232.

15. Aksia Serch Baker, Filtration and Separation, June 1997, p. 451.

16. Marthon Oil Company and DOW, Prevention of Barium Sulfate Scaling, Brochure.

17. Broom, G.P., Squires, R. C., Simpson, M. P. J. and Martin, I., Journal of Membrane Science, V. 87 (1994) 219-230.

18. Al-Sofi M. A. K., Al-Sayed, E. F., Imam M., Mustafa G. M. and Hamada T., IDA World Congress, Abu Dhabi, Nov. 18-24 (1995), Proceedings Vol. III, 191-205.

Table 1: Pretreatment and Quality Requirements of Feed Taken from an Open Sea (Surface) Intake

Problems in Seawater Desalination Due to Seawater Characteristics	**Pretreatment and Quality Requirement of Feed to**	
	SWRO	**Thermal**
High Degree of Hardness of (Ca^{++}, Mg^{++}, SO_4^{2-}, HCO_3^-)	Requires * Removal or * Inhibition of precipitation by addition of antiscalant, and by * Operation at correct conditions	Requires * Removal or * Inhibition of ppt by adding antiscalant * Operation at correct conditions
High TDS	Requires lowering of TDS which * Lowers Waste due to π * Increases Recovery Ratio * Lowers Energy/m^3 * Lowers Cost/m^3	Lowering of TDS is not essential, but it is beneficial by reducing concentration of hardness ions
High Turbidity (TSS, Bacteria, etc.).	Requires complete removal	* Requires partial Removal * Complete removal of turbidity, however, reduces foaming and, therefore, eliminates need for addition to make-up of antifoam

Table 2: Chemical Composition and Physical Properties of Seawater, NF Filtrate, and NF and SWRO rejects at Different NF Feed pressure

Element / Parameter	**Seawater**	**NF Filtrate (5 modules)***						**SWRO Reject**	**NFReject**
	Ion. Conc.	Ion Conc.	Rejection (%)	Ion Con.	Rejection (%)	Ion. Con.	Rejected%	Ion Con.	Ion Con.
NF Feed Pressure (Bar)		18	18	22	22	31	31	31	31
A. Hardness Ca^{++} (ppm)	481	93	80.7	50	89.6	52	89.2	96	701
Mg^{++} (ppm)	1608	193	87.7	96	94.0	143	91.1	253	2200
Total Hardness (ppm)	7800	1049	86.5	520	93.3	720	90.8	1280	10800
SO_4 (ppm)	3200	206	93.3	72	97.8	230	92.8	414	4950
HCO_3^- (ppm)	128	46	63.3	30	76.6	24	81.3	42	133
B. Other Ions Cl^- (ppm)	22780	16,692	26.7	12320	46.3	9640	57.7	19570	29350
Na^+ (ppm)	(12860)	(94261)	26.7	(6904)	46.3	(5442)	57.7		
C. Total Dissolved Solids TDS (ppm)	44046	27,720	37.3	20230	54.1	16400	62.8	30,640	63640
pH	8.2	7.85		7.92		6.38		7.08	7.46
Conductivity (μs/cm)	60,000	40,470		31100		24600		43300	68600

* Module arrangement 2:2:1, each module contains 2 NF elements, arrangement equals two parallel lines each having 5 elements in series

Table 3 : Operation and Performance Parameters of NF-MSF and NF-SWRO $_{reject-}$MSF Desalination Hybrid Systems Vs Conventional Seawater MSF Desalination System

(Operation of MSF unit with NF product or SWRO Reject from NF-SWRO unit was done without addition to make-up of antiscalant or antifoam)

Trials	**Brine Recycle Data***						**Performance Parameters**		
	TBT (°C)	**CA^{++} (ppm)**	**SO$_4^=$ (ppm)**	**M-alkalinity (ppm)**	**Conductivity**	**pH**	**Make-up (m^3/hr)**	**Product (m^3/hr)**	**Recovery ratio (%)**
A. NF-MSF									
With acid	120	160	390	26	59000	8.19	1.5	0.97	65
Without acid**	120	168	410	65	62000	8.63	1.5	0.97	65
B. NF-SWRO $_{reject-}$MSF*									
Without acid	120	232	1020	72	87400	8.50	1.5	0.97	65
C. Seawater MSF									
With acid	120	882	5830	30	92000	7.99	1.5	0.97	65
With acid	90	661	4460	20	74000	7.57	1.5	0.59	39
With acid	120	561	3330	14	61000	7.50	4.0	0.92	23
With acid	90	581	4000	18	66000	7.51	2.1	0.94	45

* Brine recycle flow rate was maintained between 6.5 to 6.8 m^3/h.

** Make-up is *NF* product having Ca^{++} 52, Mg^{++} 143, SO$_4^-$230, M-Alkalinity 24 and TDS 16400 ppm

*** Make-up is *SWRO* reject from *NF-SWRO* unit with composition: Ca^{++}96 Mg^{++} 253, SO$_4^-$ 414, M-Alkalinity 42 and TDS 30640 ppm

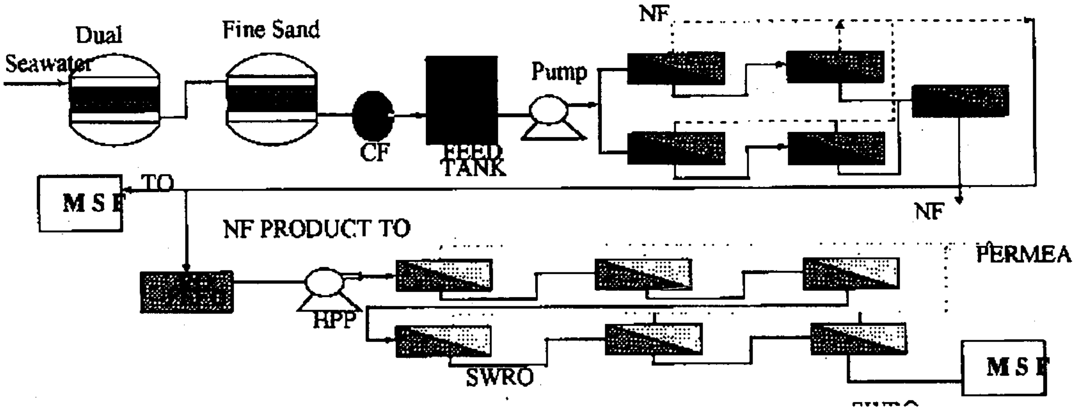

Figure 1. Schematic Flow Diagram of NF-SWRO Desalination Pilot Plant

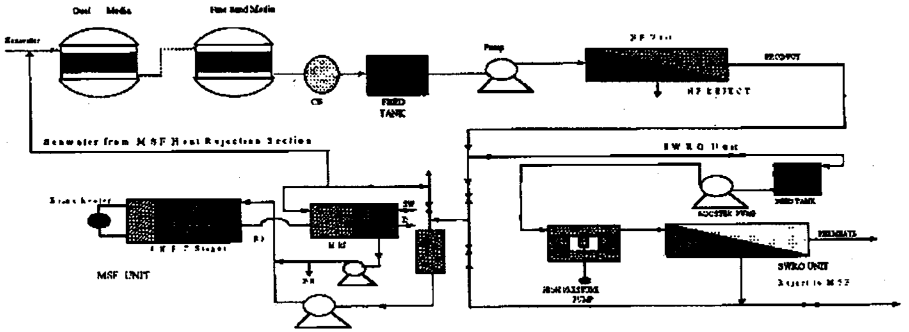

Figure 2: Schematic Flow Diagram of NF, SWRO and MSF Pilot Plants

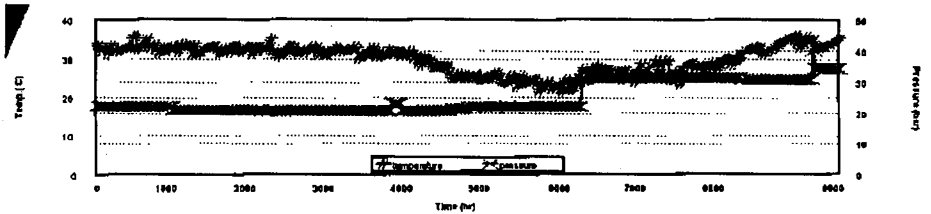

a. Operating Conditions

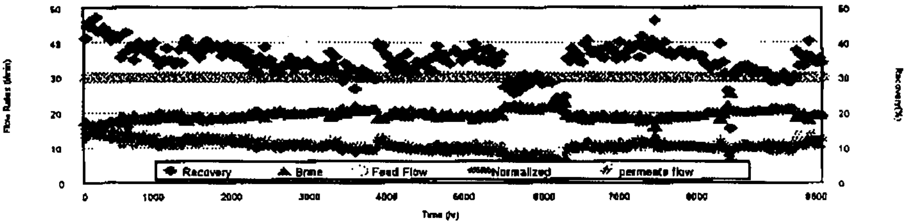

b. Flow Rates

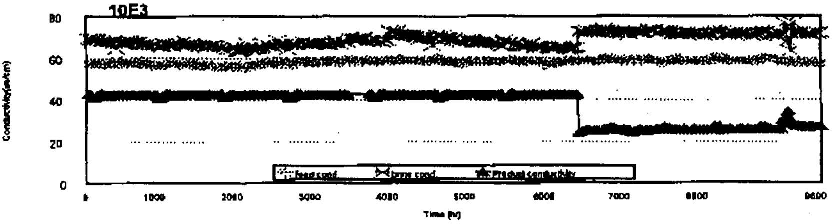

c. NF Product, Brine and Feed Conductivity

Figure 3: a. NF Operating conditions and
b. NF Treated Gulf Seawater Actual and
Normalized Flow Rates and Recovery (%)
c. NF Product, Brine and Feed Conductivity Vs Operation Time

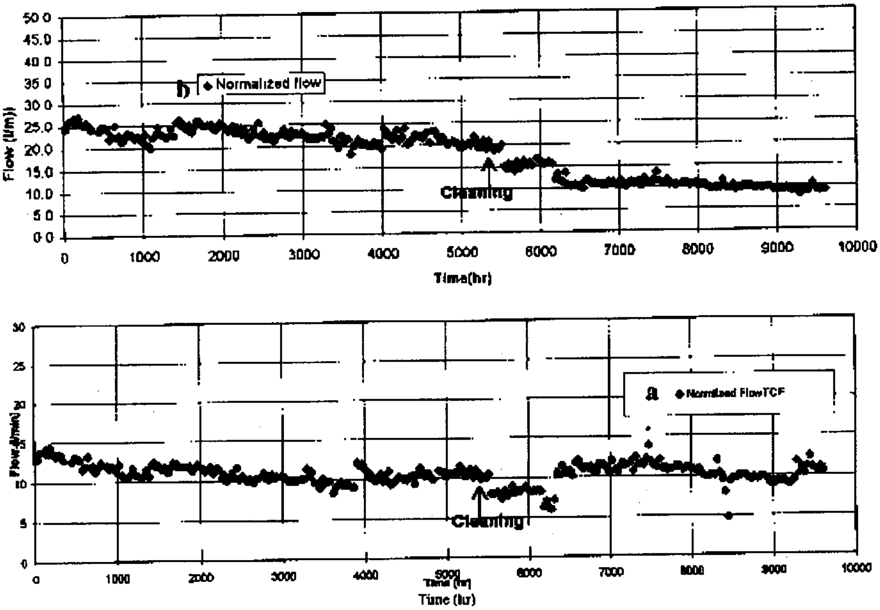

Figure 4: NF Permeate Flow Vs Operation Time

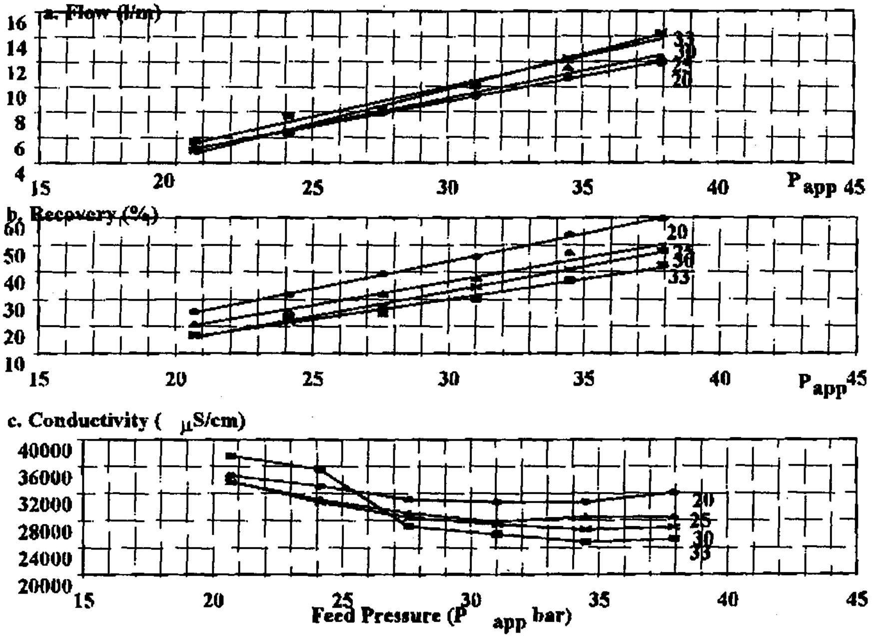

Figure 5a : NF Permeate (a) Flow, (b) Recovery and (c) Conductivity Vs Applied Pressure at Different Feed Flow Rates (l/min)

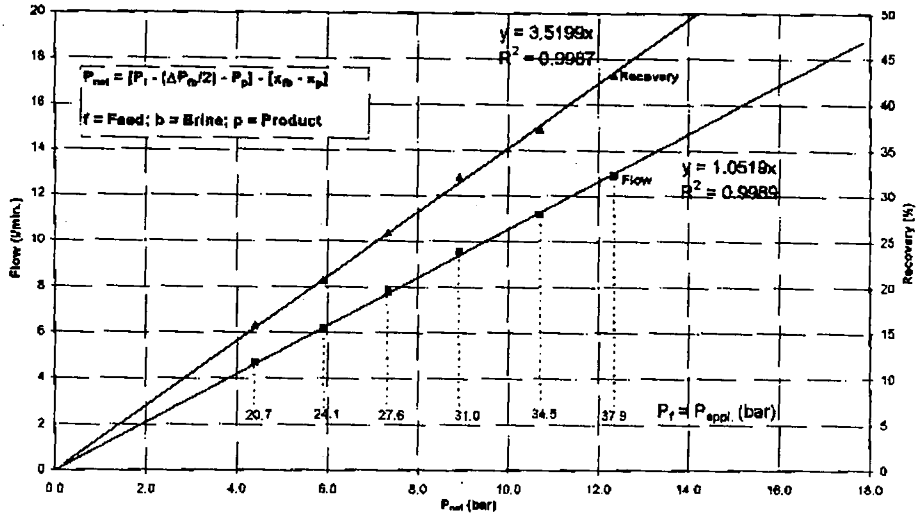

Figure 5b: Effect of Net Driving Pressure (P_{net}) on NF Permeate Flow

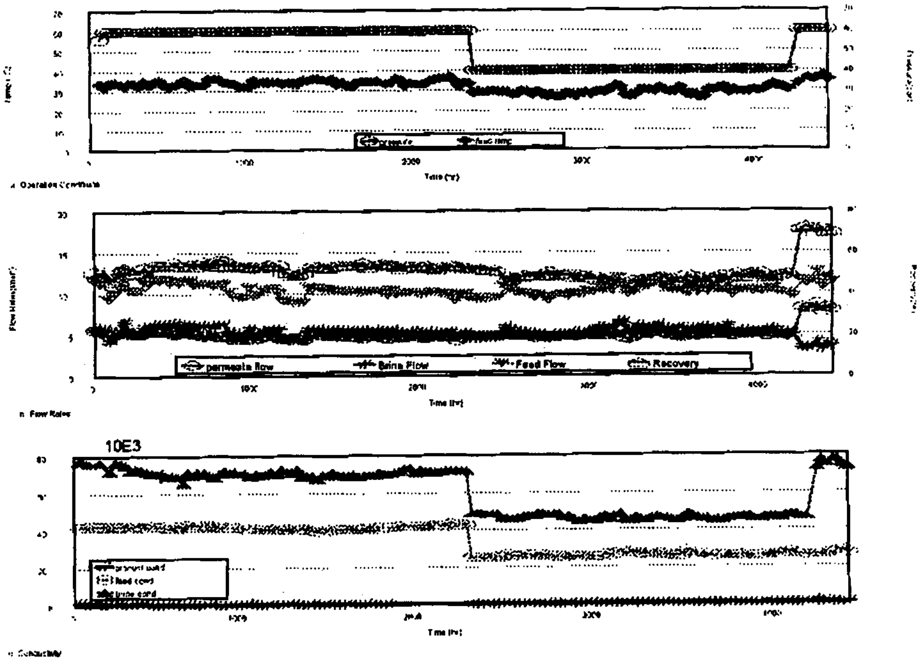

Figure 6: a. SWRO Operation Conditions b. SWRO Flow Rates and Recovery (%) and c. SWRO Conductivity of Feed, Product and Reject in a NF-SWRO Unit Vs Operation Time

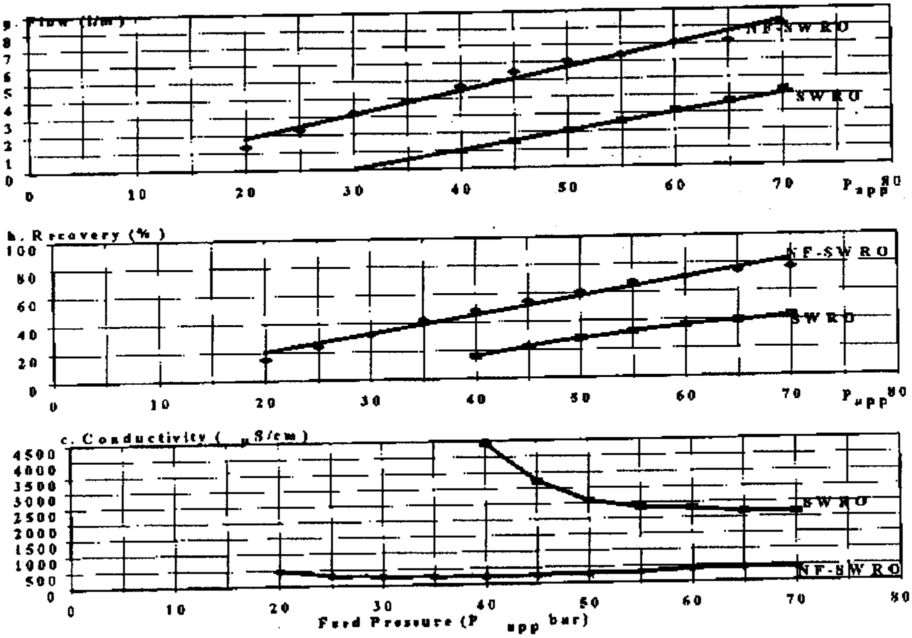

Figure 7: SWRO Permeate (a) Flow (b) Recovery and (c) Conductivity for the New NF-SWRO Process and the Conventional SWRO Vs Applied Pressure

Evaluation of Ultra-Violet Radiation Disinfection on the Bacterial Growth in the SWRO Pilot Plant, Al-Jubail

Hassan Ahmed Munshi, N. Sasikumar,
A.T. Jamaluddin and Kither Mohammed

EVALUATION OF ULTRA-VIOLET RADIATION DISINFECTION ON THE BACTERIAL GROWTH IN THE SWRO PILOT PLANT, AL-JUBAIL

Hassan Ahmed Munshi, N. Sasikumar,
A.T. Jamaluddin, and Kither Mohammed
Research and Development Center
Saline Water Conversion Corporation,
P.O. Box 8328, Al-Jubail 31951,
Kingdom Of Saudi Arabia

ABSTRACT

The present study summarizes findings of an experiment on the evaluation of UV- treatment for bacterial disinfection at SWRO pilot plant at Al-Jubail. Two UV-generation units were installed along the pretreatment line. One before the dual media filter and the second before the micron cartridge filter. The study was carried out at three seawater flow rates: the regular flow operation and two other flow rates below the normal flow. The investigation was carried out at five locations in the plant: raw seawater (RSW), after UV-unit (AUV), after media filter (AMF), after cartridge filter post the second UV-unit (ACF) and the brine (BR). The study showed 90-99% reduction in bacterial counts after UV- treatment as compared to raw seawater at the three flow rates suggesting relatively good performance of the first UV-sterilizing unit. However, an increase in bacterial count was noticed at AMF and ACF. Presumably, the second UV-sterilizing unit has not reduced the bacterial counts in the feed water at this site. Laboratory studies also showed that, incubation of UV-treated samples for 24h resulted in bacterial recovery and aftergrowth. AMF and ACF also registered reduced Total Organic Carbon (TOC), nitrite and phosphate levels in the feed water indicating the presence of a nutrient trap before CF. A decline in phosphate, nitrite and TOC levels were also found in 24h incubated samples indicating that bacteria had used these nutrients. The study suggests that while UV-treatment considerably reduced bacterial counts in the SWRO plant, stagnant condition of the feed water before CF has presumably led to bacterial recovery.

KEY WORDS: Ultra-Violet Radiation, Bacterial After Growth, Reverse Osmosis, Micronutrients

INTRODUCTION

In the last twenty years the use of UV-radiation technology has been developed and applied on a large scale in treatment of waste water and drinking water. The germicidal effects of UV-radiation at wavelength ranging from 227 to 329nm was known as early as 1900 (Barnard & Morgan, 1903). The action spectrum of UV- degermination exhibits a maximum at 270nm wavelength for most of the microorganisms (Gates, 1930). It is now well established that killing of cells by UV-radiation is primarily due to denaturing of deoxyribonucleic acid (DNA) (Block, 1991). The UV absorption by DNA is maximal at 260 nm so the UV-radiation at the 260nm is most effective as a lethal agent. Proteins also absorb UV-radiation, but have a peak at 280 nm. The UV-radiation has already been suggested as one of the successful disinfection practices for water treatment (Gaudy and Gaudy, 1980). In addition to bacteria, phages, viruses and organic micropllutants are also killed or degraded by photochemical wet combustion down to and below detection limits of organic carbon (Armstrong, *et al.* 1966). Therefore UV-sterilization has become a practical solution to safe disinfection of drinking water. Also, usage of medium pressure lamps with small reactors has helped to substantially reduce the capital costs of UV-treatment (Kruithof *et al.*, 1989 a).

The seawater reverse osmosis (SWRO) desalination plants face biofouling problems from bacteria originating from feed seawater. The problems are most evident in SWRO plants using surface seawater as feed. Biofouling leads to decreased SWRO membrane performance and thus affects its successful operation. Once bacteria are permitted through the pretreatment system and reach the RO membrane, they divide and colonize the membrane surface building a biofilm and causing membrane fouling.

Most of the disinfection procedures in SWRO plants can be roughly classified into: (1) chemical disinfections like chlorine, chloramine, copper sulfate, chlorine dioxide, hydrogen peroxide and ozone, (2) physical disinfections such as ultraviolet radiation, ultra sound, X-ray and ionizing radiation. The chemical disinfectants like chlorine and chloramine are widely adopted in pretreatment of SWRO plants. However, control of bacterial growth depends on factors such as chemical concentration, its nature and mode of action, density of the organisms and total suspended solid (TSS) content of feed water (Gaudy and Gaudy, 1980). These factors make it often extremely difficult to attain absolute disinfection processes. In addition, chemical disinfectants like chlorine may be hazardous to health directly or through by-products (Kutty *et al.*, 1991). Chlorine which is a widely used biocide is known to oxidize and degrade the humic substance in the seawater, thus resulting in smaller molecules which are assimilable organic carbon (AOC) (Kruithof *et al.*, 1989 b). The AOC in turn become a good nutrient source to bacteria (Applegate *et al.* , 1989) and under such situations could also result in elevated fast growth of biofilm in the SWRO plant.

On the other hand, UV-treatment offers certain advantages: in a closed system it is safe, it requires only a small space for equipment and it has got immediate germicidal effect (Haruhiko, 1985). However, incorrect application of UV- radiation in the feed water treatment can be unsuccessful (Luckiesh, 1946) and determining the right dosage for a system is therefore essential. The present study was carried out to evaluate the UV-radiation disinfection in an SWRO pilot plant at Al-Jubail.

EXPERIMENTAL

The study was carried out during June-July, 1996, a period known for its high biological activity of the microorganisms in the seawater feed at Al-Jubail (Munshi *et al.*, 1995). Samples were aseptically collected for bacterial growth studies using standard pour plate method (APHA, 1995) from the following points: 1. Surface raw seawater (RSW), 2. Seawater After UV-treatment (AUV), 3. After media filter (AMF).4. After cartridge filter (ACF) following the second UV-treatment., 5.Brine (BR) (Appendix A). Samples were serially diluted and plated using marine agar 2216. Plates were incubated at 30 ^{0}C for 48-72h (Munshi *et al.*, 1994) and the colony numbers were recorded as colony forming units (CFU). Samples were further incubated at 30 ^{o}C for 24 and 48 hours for bacterial aftergrowth studies.

In order to monitor the changes in micronutrients concentrations during the UV-treatment process and their possible effects on the bacterial aftergrowth, TOC and micronutrient measurements were carried out. The samples for Total Organic Carbon (TOC) were collected in sterilized glass bottles. TOC was determined by measuring CO_2 released by catalytic combustion of organic carbon using infrared detector. The sample was acidified and total inorganic carbon (TIC) was purged off prior to the analysis. TOC analysis was carried out using SHIMADZU TOC Analyzer using the Instruction Manual and USEPA Method (1983). The samples were also collected for analyses of phosphate, nitrite and silicate and analysis was carried out following methods of Parsons, *et al.* (1985). pH and conductivity of the samples were recorded using a pH meter (Fisher Scientific Co.) and a conductivity meter (Yellow Springs Inst. Co.).

RESULTS

The viable bacterial counts observed at different feed flow rates of pretreatment and at different locations of the SWRO pilot plant are given in Table 1. At the three flow rates (2, 4 and 7m^3/h) reduction in bacterial counts was observed at AUV as compared to RSW. While RSW showed 1.21x10^3 CFU/ml, AUV and AMF showed 1.37x10^1 CFU/ml and 76.26x10^1 CFU/ml, respectively. BR showed an increase in number of bacterial counts as compared to ACF and AMF except on June 2, 1996 when ACF, AMF and BR showed identical growth. At 4m^3/h and 7m^3/h also an increase in bacterial counts was noticed at AMF and ACF. Therefore, the results showed that UV-treatment has drastically reduced the bacterial growth immediately after the first UV-treatment unit but after the media filter and storage tanks the seawater entering the membrane system showed an increase in bacterial counts.

The percentage of reduction in bacterial counts achieved by the UV-treatment is given in Figure 1. The results showed a 90.59 to 99.99% reduction in bacterial growth after UV-treatment as compared to RSW. Out of the sixteen observations, fourteen showed reduction above 97%. June 11 and July 2, 1996 showed minimum reduction of 90.59 and 94.21% respectively. However, percentage reduction was not related to flow rates. These results demonstrated that the first UV-unit presently employed in the pilot plant before AMF has substantially inactivated the bacteria in the feed seawater at all the flow rates.

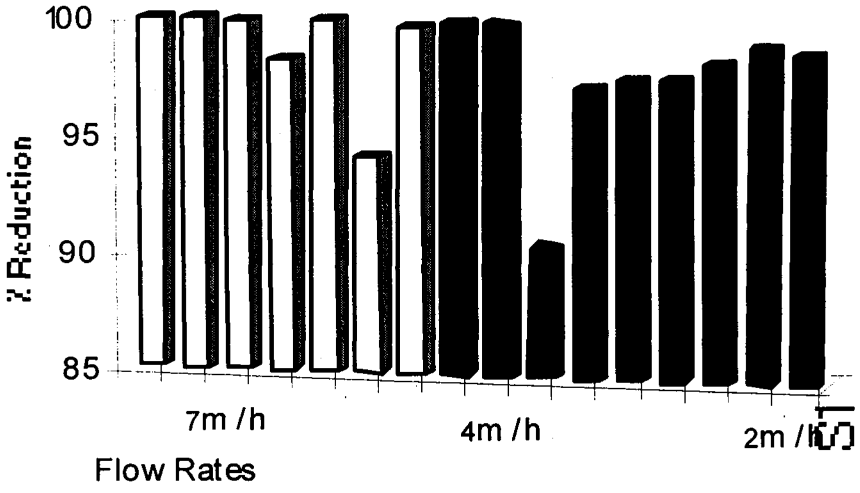

Figure 1. Percentage Reduction in Bacterial Counts After Exposure to UV-Radiation

Table 1. Viable bacterial counts (CFU/ml) in seawater at different flow rates and at different stages of the SWRO pilot plant

Sampling date	**Sampling stage**				
	RSW	**AUV**	**AMF**	**ACF**	**BR**
(2m^3/h Flow rate)					
June 2, 1996	1.47×10^3	1.53×10^1	1.84×10^3	4.60×10^3	1.26×10^3
June 4, 1996	1.00×10^3	0.80×10^1	1.63×10^2	5.12×10^2	7.76×10^3
June 4, 1996	1.17×10^3	1.80×10^1	2.85×10^2	5.46×10^2	1.35×10^3
(4 m^3/h Flow rate)					
June 8, 1996	1.15×10^4	2.51×10^1	1.609×10^2	1.62×10^3	1.39×10^4
June 9, 1996	1.36×10^3	3.08×10^2	3.98×10^2	5.10×10^1	8.06×10^3
June 10, 1996	3.34×10^3	8.94×10^1	2.01×10^2	3.78×10^1	6.77×10^3
June 11, 1996	3.32×10^3	3.12×10^2	5.47×10^2	1.03×10^2	3.15×10^3
June 16, 1996	1.33×10^4	0.40×10^1	5.33×10^3	2.03×10^2	6.77×10^3
June 17, 1996	2.10×10^3	0.60×10^1	5.20×10^2	2.05×10^2	5.95×10^3
(7 m^3/h Flow rate)					
June 30, 1996	1.46×10^4	2.50×10^1	2.18×10^4	1.43×10^4	9.05×10^3
July 2, 1996	3.87×10^3	2.24×10^2	1.35×10^4	3.32×10^2	1.16×10^4
July 6, 1996	4.25×10^3	1.27×10^2	2.57×10^3	6.68×10^3	8.94×10^3
July 7, 1996	5.22×10^3	8.88×10^2	3.28×10^3	1.03×10^3	1.02×10^4
July 8, 1996	5.72×10^3	3.88×10^2	2.70×10^3	2.18×10^3	1.91×10^4
July 9, 1996	1.99×10^4	1.18×10^2	4.76×10^2	3.82×10^3	7.28×10^3
July 10, 1996	1.43×10^4	4.51×10^1	2.99×10^2	2.49×10^5	1.38×10^4

Bacterial after growth at different locations of the SWRO pilot plant after 24 and 48 h incubation times at 30^{0}C are given in appendix B. AUV was similar to RSW at all the three flow rates tested. AMF, ACF and BR also showed similar bacterial growth at the three flow rates suggesting that the bacteria recovered to normal growth after 24 and 48 h, inspite of the UV-treatment. The second UV-sterilization unit at HFRO unit appears to have failed to control bacterial growth.

Conductivity of RSW, AUV and ACF recorded during the study period are given in Table 2. Conductivity values ranged from 59.4 to 60.0 milli seimens/cm at the RSW during the period. A slight elevation (about 1 milli seimens/cm) in conductivity was noticed after 24h incubation time of samples at 30^{0}C. In general, conductivity values were identical at RSW, AUV and ACF. pH values ranged from 8.09 to 8.26 at RSW during the period (Table 2). pH values were similar even after 24h incubation time at 30^{0}C. In general, RSW and AUV showed identical pH but a decrease in pH was found at ACF.

Table 2. Conductivity and pH of seawater at different flow rates and stages of the SWRO pilot plant (24h measurements are given in parenthesis)

Sample source	**Conductivity (milliseimens/cm)**			**pH**		
	2 m^3/h	**4 m^3/h**	**7 m^3/h**	**2 m^3/h**	**4 m^3/h**	**7 m^3/h**
RSW	59.40	59.50	60.00	8.26	8.10	8.9
	(60.40)	(59.40)	(60.00)	(8.15)	(8.17)	(8.13)
AUV	59.40	60.00	60.70	8.16	8.14	8.10
	(61.00)	(60.00)	(60.60)	(8.15)	(8.17)	(8.07)
ACF	ND	59.60	60.20	ND	7.82	8.01
	(59.80)	(59.50)	(60.30)	(7.72)	(7.62)	(7.80)

ND- No Data

TOC values ranged from 0.90 to 2.60mg/l at RSW during the study period (Table 3). A substantial reduction in TOC values were noticed at RSW, AUV and ACF after incubation of samples for 24h at 30^{0}C. In general TOC values were less at AUV as compared to RSW except at 7 m^3/h where TOC values were more at the AUV as compared to RSW. At 2 m^3/h a slight increase in TOC was found. However, at 4 m^3/h, TOC was slightly less at ACF as compared to AUV and at 7 m^3/h all the three sites showed similar TOC values. In general, TOC values declined after UV- treatment and after 24h incubation time at 30^{0}C.

Table 3. Total Organic Carbon (TOC) in seawater at different flow rates and stages of the SWRO pilot plant (24h measurements values are given in parenthesis)

Sample source	**TOC (mg/l) 2 m^3/h**	**TOC (mg/l) 4 m^3/h**	**TOC (mg/l) 7 m^3/h**
RSW	2.60	1.82	0.90
	(1.13)	(0.81)	(0.95)
AUV	1.46	1.59	1.23
	(0.48)	(0.76)	(0.76)
ACF	2.03	0.71	0.80
	(0.33)	(0.53)	(0.72)

Phosphate concentration at RSW ranged from 0.55 to 1.22 μg as PO_4 -P/l during the study period (Table 4). Phosphate values declined at 2 and 4 m^3/h when incubated for 24h at 30^0C. However, at 7 m^3/h the values remained the same even after 24h-incubationat 30^0C. In general phosphate levels were identical at RSW, AUV and ACF. Silicate levels ranged from 3.84 to 18.42 μg SiO_2 - Si/l. There was no considerable change in silicate concentration even after 24h-incubationat 30^0C. At 2 and 4 m^3/h RSW and AUV showed identical silicate levels but slightly high values were found at ACF. At 7 m^3/h a reduction in silicate values was found at AUV and ACF as compared to RSW. Nitrite levels were relatively low and a reduction in nitrite levels were found after 24h incubation time at 30^0C. Elevated nitrite levels were found at AUV. The results showed that phosphate and nitrite levels are reduced after 24h incubation time and silicate levels were similar before and after the incubation.

Table 4. Micronutrients in seawater at different flow rates and at different stages of the SWRO pilot plant (24h measurements values are given in parenthesis)

	Phosphate (μg /l $Po^{3-}{}_4$-P)			Silicate (μg/l SiO_2-Si)			Nitrite (μg/l No_2-N)		
Sample Source	2 m^3/h	4 m^3/h	7 m^3/h	2 m^3/h	4 m^3/h	7 m^3/h	2 m^3/h	4 m^3/h	7 m^3/h
RSW	1.22 (0.14)	1.29 (0.33)	0.55 (0.50)	3.84 (4.50)	4.02 (3.94)	18.42 (15.08)	BDL (BDL)	BDL (BDL)	BDL (BDL)
AUV	1.22 (0.68)	0.64 (0.11)	0.55 (0.75)	3.84 (4.75)	4.69 (4.65)	10.52 (8.77)	3.03 (2.42)	6.06 (BDL)	BDL (BDL)
ACF	ND (0.41)	0.64 (0.22)	0.55 (0.50)	ND (7.0)	6.54 (6.08)	11.84 (6.66)	ND (1.52)	BDL (BDL)	BDL (BDL)

BDL- Below Detection Limit ND- No Data

DISCUSSION

The germicidal effect of UV-radiation is dependent on several factors such as total dissolved solids (TDS), total suspended particles (TSS), conductivity, total organic carbon (TOC), total hardness, sensitivity and type of microorganisms (Gaudy and Gaudy, 1980). The present study showed that UV-treatment has reduced bacterial counts. The number of the viable bacteria count of $1.37X10^1$ at a flow rate of 2 m^3/h (residence time 22.04 secconds) showed a percentage reduction of 98.87 after the UV-treatment. Other flow rates: 4 and $7m^3/h$ (normal operation rate of the plant) (11.02 and 6.29 seconds residence time, respectively) had also achieved 97.24 and 98.88 percentage of reduction respectively. In total, the UV-radiation treatment employed in the pilot plant before MF achieved a high percentage kill of bacteria at the three flow rates.

However, AMF, ACF and Brine samples showed an increase in the bacterial counts suggesting that the second UV-sterilization unit was not successful in controlling bacterial growth. The results showed that the source for increase in bacterial counts at the AMF and ACF appears to be due to recovery of bacteria after UV- treatment. ACF and brine samples showed similar bacterial counts. Gaudy and Gaudy (1980) reported that spore-forming and slowly growing cells are less affected by UV light than vegetative and rapidly growing cells. Since UV acts primarily on DNA, there may be no time for repair mechanisms to be put into effect when cells are rapidly replicating, whereas for less active cells, resistance to UV may be a measure of the operational repair mechanisms. Johnson *et al.*, (1978) have reported that there is increasing evidence that bacterial photoreactivation (recovery after exposure to light) may be a significant concern in UV-disinfection of secondary effluent which is commonly discharged into open receiver systems in the United States. Harris *et al.* (1987) also reported that sunlight penetrating the receiver system may reactivate a significant fraction of the UV-inactivated bacteria. Photoreactivation often repairs much of the damage to the DNA. However, viruses lack the repair enzymes for the photoreactivation processes (Jagger, 1967). Whitby *et al.*, (1984) also reported evidence of reactivation in *fecal streptococci*. Potential photoreactivation of UV-inactivated coliforms in secondary effluent has also been reported. The after growth studies also showed that 24h-incubationtime of UV-treated samples at 30^0C has resulted in normal bacterial counts (of untreated seawater). All samples had similar growth after 24h in spite of the UV-treatment. Therefore, it is reasonable to presume that in the SWRO plant, bacteria after the UV-treatment have received ample time to recover prior to the cartridge filter (CF). It is also possible that 1-2% live bacteria which tolerate UV-treatment could multiply in the storage tanks under favorable conditions such as availability of nutrients. The present study on the 24h-incubationtime of bacteria has shown that bacteria uses phosphate and nitrite. While phosphate concentrations were unaffected by the UV-treatment, an increase in nitrite levels after UV-treatment was noticed. However, at ACF the levels of phosphate and nitrite declined suggesting a nutrient trap prior to ACF, presumably due to consumption by bacteria in the storage tanks where the UV-treated feed water is stored. Nitrite is one source of nitrogen to organisms and only organisms possessing necessary enzymes can utilize nitrite as a source of cellular nitrogen (Gaudy and Gaudy, 1980). Fenchel and Harrison (1976) also showed that after inoculation of bacteria, the concentration of phosphate in the water rapidly decreased and the decrease was related to phosphorus consumption. It was also noticed that if the water was enriched with inorganic nitrogen source, bacterial growth was more rapid. In natural systems, the phosphate is released from bacteria when grazed by ciliates (Johannes, 1965). However, at 7m^3/h AUV and ACF had identical phosphate levels. Therefore at 7m^3/h, increased flow appears to mask the difference between AUV and ACF. The laboratory results also suggested that nutrient consumption takes place during bacterial growth indicating that the observed nutrient consumption prior to ACF is due to bacteria. This showed that determination of micronutrients could be helpful to draw conclusions about the bacterial growth dynamics.

TOC values also showed a slight reduction after UV-treatment except at 7m^3/h. However, a substantial reduction in TOC was found at ACF except at 2m^3/h. Active bacteria exude dissolved organic matter in connection with the decomposition of organic material (Zobell, 1943). In static systems, the process consists of hydrolysis of particulate carbon using extracellular enzymes and later the dissolved organic-substrates are assimilated by the bacteria. The TOC value therefore depends on concentration of substrate, rate of bacterial metabolism including assimilation (Alexander, 1977). Jannasch and Pritchard (1972) showed that substrates at low concentrations were utilized more efficiently in the presence of inert particles such as sand but not in the absence of substrate or when it is present in high concentrations. Apparently the reduction of TOC observed at AUV in the present study is due to physical and chemical change caused by UV-radiation. Li *et al.* (1996) have also stated that UV-treatment can result in decarboxylation of compounds including humic acids. However, further decline in TOC at the ACF appears to be due to consumption by bacteria. Absence of such TOC consumption at 2 m^3/h flow rate (not an operational flow) remains unclear at this point. Results of the laboratory study also showed reduction in TOC levels associated with bacterial growth. More than 50% reduction in TOC was evident after 24h-incubation time.

The results of the present study showed that the significant increase in bacterial count at ACF is due to bacterial recovery. This data are comparable to the result from Al-Birk SWRO plant where the bacterial aftergrowth rates increased after the chlorination point and the aftergrowth rate was substantially high. Applegate *et al.*, (1989) also reported that the chlorine degrade humic acids (HA) into small molecules which are assimilable organic compounds (AOC) and since AOC favor bacterial growth this could result in bacterial aftergrowth. Li *et al.*, (1996) found that there is a slight decay of HA after UV-treatment presumably due to decarboxylation. Egil *et al.* (1991) also stated that UV-treatment of water containing humic substances may cause presence of oxidizing compounds such as single oxygen, hydrogen peroxide and OH-radicals. While details of chemical changes under UV-treatment is not clear at this point, it appears that the initial bacterial kill by the UV-treatment was followed by bacterial recovery down the pretreatment line. Therefore, mode of UV-bactericidal action may resemble chlorine oxidation. It has been observed that even at the same flow rate the percentage kill by the UV-radiation was subject to fluctuations at different sampling dates. This is to be expected because it is known that the efficacy of UV-radiation is affected by the suspended matter in water column. A turbidity increase could cause decline in the percentage of kill.

TECHNO-ECONOMIC ANALYSIS

Techno-economic analysis of UV-radiation showed an approximate cost of 0.73 SR per cubic meter of water (Table V). UV lamps require replacement after each 8000 hours and this appears to be the only maintenance cost for the UV-unit. Chlorination would cost about 0.75 SR per cubic meter of water with relatively high operation and maintenance cost to achieve similar disifection efficiency. The magnitude of bacterial recovery after initial kill of both technologies are comparable.

Table 5 Techno-economic analysis of UV-radiation vs Chlorination

Description	UV-radiation	Chlorine (approx)
Unit Cost	4348.00	2000.00
Operation Cost	Nil	4000.00
Maintenance Cost	3827.00 / Lamp	2000.00
Chemical Cost	Nil	448.00
Total	8175.00	8448.00
Cost / m^3	0.73	0.75
*Bacterial disinfection Efficiency (%)	90 - 99.9	**98.0
**Aftergrowth *(k/h)*	0.19	0.16

*Chlorine cost calculated at 2ppm dosing (hypochlorite 4.00 SR/m^3)
**(Munshi *et al.*, 1995)

CONCLUSIONS

The following conclusions were drawn from the present study..

1. The study showed a reduction of 90-99.9% in bacterial count after the UV-treatment.

2. At all the flow rates, the bacterial counts increased through the pretreatment stage specially at the AMF and ACF suggesting that the second UV-sterilization unit has failed to control bacterial growth. This also indicates bacterial recovery from UV-treatment, prior to ACF.

3. Laboratory studies have shown that bacteria recover from the UV-treatment within 24h.

4. The results of laboratory analysis of TOC and micronutrients suggest that the bacterial growth recovery following UV-treatment resembles chlorination disinfection.
5. The following are the advantages of the UV-radiation for disinfection: 1. Relatively less maintenance cost., 2. Requires less space for equipment., 3. Minimal supervision., 4. Unlike chlorination, UV-radiation does not facilitate corrosion and 5. No phase change in water and no toxic by-products.

In summary, UV-radiation appears to be a potential alternative to chlorination, if it is employed in plant with continuous flow of water. This would considerably minimize the operation and maintenance cost and avoid other plant problems allied with the chlorination, particularly discharge of toxic chlorine by-products such as trihalomethanes into the receiving water. However, the storage of UV-treated water in tanks during its passage through different stages of the plant could permit bacterial reactivation and recovery as evident in the present study. This could eventually affect the plant performance.

RECOMMENDATIONS

1. Since suspended particles could affect the efficiency of UV-radiation treatment, the UV-unit may be installed right before the SWRO membrane section.

2. To increase the performance of UV-radiation disinfection process in the SWRO pilot plant, stagnant conditions of water flow such as storage of water in the tanks may be avoided.

REFERENCES

Alexander, M., 1977, *Advances in Microbial Ecology,* Volume I, Plenum Press, New York.

American Public Health Association, American Water Works Association and Water Pollution Control Federation, 1995, *Standard Methods For The Examination Of Water and Waste Water*, 19th ed. APHA, Washington, D. C.

Armstrong, F.A.J., Williams, P.M., and J.D.H. Strickland, 1966, Photo-oxidation of organic matter in seawater by ultra violet radiation, and analytical other applications, N*ature,* 211, pp.481-483.

Applegate, L.E. Erkenbrecher,C.W. and H.Winters, 1989, New chloramine process to control aftergrowth and biofouling in Permasep^R B-10 RO surface seawater plants, *Desalination*, pp.74, 51.

Barnard, J.E., and H.R. Morgan, 1903, The physical factors in phototherapy, *British Medical Journal*, 2, pp.1269-1271.

Block, S. S., 1991, *Disinfection, Sterilization and Preservation*, Lea and Febiger, Philadelphia.

Egil, T. Gjessing and Torsten Kallquist ,1991, Algal and Chemical Effect of UV- radiation of water containing Humic Substances, *Water Research.*, 25(4), pp.491-494.

Fenchel, T. and P. Harrison, 1976, The significance of bacterial grazing and mineral cycling for the decomposition of particulate detritus. In the *Rule of Terrestrial and Aquatic Organisms in Decomposition Processes.* (ed) J.M.Anderson, Blackwell Scientific, Oxford, pp.285-299.

Gates, F.L., 1930, A study of the bactericidal action of ultraviolet light, the absorption of ultra light by bacteria, *Journal of Genetic Physiology*., 14, pp.31-42.

Gaudy A.F and E.T. Gaudy, 1980, *Microbiology for Environmental Scientists and Engineers*. Mc Garw Hill Book Co., New York, p.73.

Haruhiko, O., 1985, *Ultra Pure Water Production Technology*, Saiwai Shobo Press, Japan.

Harris, D.G., V.D.Adams, D.L.Sorensen and M.S. Curtis, , 1987, Ultraviolet inactivation of selected bacteria and viruses with photoreactivation of the bacteria. *Water Ressearch*, 21 (6), pp.687-692.

Hassan,A.M, Abanmy A.M. Thobiety M., Mani M., Luhibi T., Masudi I., Gherier A., Bakheet L.M and M. Khalid Amri, 1991, Performance Evaluation of SWCC-SWRO Plants - Part II, *Research Activities And Studies, Annual Book of SWCC - R&D Dept*artment, pp.94- 121.

Instruction Manual of SHIMADZU Total Organic Carbon Analyzer Model TOC-500, Part No. 638-90887.

Jaggar, J., 1967, *Introduction to Research in UV Potobiology*, Prentice Hall, Englewood, Cliffs, NJ.

Japanese International Cooperation Agency, 1985, Operation and Maintenance Manual Of Reverse Osmosis Pilot Plant, Jubail, Saudi Arabia.

Jannasch , H.W. and P.H. Pritschard, 1972, The rule of inert particulate matter in the activity of aquatic microorganisms, *Mem. Ist. Ital. Idrobiol. Suppl.*, 29, p.289.

Johnson, G.D., Aldrich, K., Franscis, D.E., Wolf, T. and M. Elliot, 1978, UV disinfection of secondary effluent. In progress in Waste Water Disinfection Technology, *Proceedings of the National Symposium, Cincinnati, Ohio*, pp.108-116.

Johannes, R.E., 1965, Influence of marine protozoa on nutrient regeneration. *Limnology Oceanography*, 10, *p*.434.

Kelner, A., 1949, Effect of visible light on the recovery of Streptomyces grisens condia from ultraviolet irradiation injury, *Proceeding of National Academy* of Science, 35, p.73-79.

Kruithof, J.C., van der Lear, R. C., Hijren, W.A.M., Huhn, P.N.M., Houtepen, F.A.P. and L.A.C. Feij, 1989 a, Ultraviolet disaffection of Carbon Filtered Drinking Water. In *Ozone and UV in the Treatment of Water and Other Liquids*, (Edited by Masshelein, N.), International Ozone Association, Paris, pp. III-3-1-III-3-15.

Kruithof, J.C., Van der Gaag, M.A., and D. Van der Kooy, 1989 b, Effect of ozonation and chlorination on humic substances in water, In *Aquatic Humic Substances* (Edited by Sufflet, I. H. and MacCarthy, P.), Advances in Chemistry Series 219, *American Chemical Society, Washington D. C.* p. 664.

Kutty, P.C., And S. Al-Jarrah, 1991, Disaffection By - Products - Present Status and Future Perspective in Seawater Desalination, *Research Activities And Studies, Annual Book of SWCC - R&D Dept.*, pp.53 - 72.

Li, J.W., Z. Yu, M. Gao, L. Zhang, X. Cai, and F. Chao, 1996, Effect of ultraviolet Irradiation on the characteristics and trihalomethanes formation potential of Humic acids. *Water Research*, 30(2), pp.347-350.

Luckiesh, M., 1946, *Application of Germicidal, Erythermal and Infrared Energy*. Van Nostrand, New York.

Munshi, H., Chandy, J., and I.Al-Tisan, 1994, Effect of incubation, teperature and nutrients on growth potential of marine bacteria (Al-Jubail Seawater), Proceedings of the Second Gulf Water Conference, *Water Science and Technology Association, Manama, Bahrain, 5-9 November*, pp.89-99.

Munshi, H., Al-Tisan, I., Chandy, J., Hamida, A., Chida, K. and H.W. Polland, 1995, *Identification and Disinfection of Marine Microorganisms*: SWCC-Du Pont, First Report of The Joint Technical Team.

Parsons, Y. Maita, and C. M. Lalli, 1985, *A Manual of Chemical and Biological Methods For Seawater Analysis*, Pergamon Press, Oxford.

USEPA, 1983, Method for chemical analysis of water & wastes.

Whitby, G.E, Pallamateer, G., Jook, W.G., Marshalker, J., Huber, D., and K. Flood, 1984, Ultraviolet disinfection of secondary effluent, *Journal of Water. Pollution Control. Federation,* 56, pp.844-850.

Zobell, C.E, 1943, The effect of solid surfaces upon bacterial activity. *Journal. Bacteriology.*, 46, 39.

Appendix A

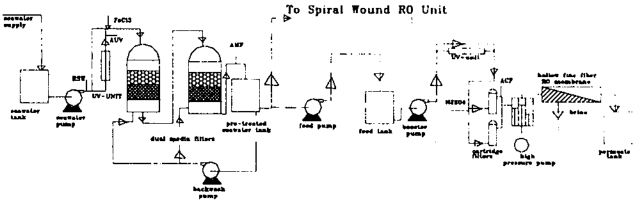

A Schematic Flow Diagram of The SWRO Pilot Plant Consisting of a common pretreatment and UV-Sterilization Unit

Appendix B

24 and 48h bacterial aftergrowth counts (CFU/ml) in seawater at different flow rates and stages of the SWRO pilot plant (48h aftergrowth values are given in parenthesis)

Sampling date	Sampling stage				
	RSW	**AUV**	**AMF**	**ACF**	**BR**
(2 m^3/h Flow rate)					
June 03, 1996	1.88×10^{5}	2.13×10^{4}	6.53×10^{4}	3.36×10^{5}	6.51×10^{4}
[June 04, 1999]	[NA]	[NA]	[NA]	[NA]	[NA]
June 05, 1996	9.66×10^{4}	TNTC	9.26×10^{4}	TNTC	TNTC
[June 06, 1996]	[1.46×10^{5}]	[4.03×10^{5}]	[1.41×10^{5}]	[1.3×10^{5}]	[4.06×10^{5}]
June 04, 1996	2.63×10^{4}	4.10×10^{3}	7.03×10^{5}	1.50×10^{5}	1.20×10^{5}
[June 05, 1999]	[NA]	[NA]	[NA]	[NA]	[NA]
Mean	1.04×10^{5}	1.27×10^{4}	2.86×10^{5}	2.43×10^{5}	9.25×10^{4}
[Mean]	[1.04×10^{5}]	[4.03×10^{5}]	[1.41×10^{5}]	[1.3×10^{5}]	[4.06×10^{5}]
(4 m^3/h Flow rate)					
June 09, 1996	1.24×10^{4}	8.53×10^{3}	1.23×10^{4}	6.68×10^{5}	2.66×10^{5}
[June 10, 1996]	[3.00×10^{6}]	[1.41×10^{5}]	[1.26×10^{5}]	[8.3×10^{5}]	[1.31×10^{5}]
June 10, 1996	3.65×10^{4}	9.80×10^{4}	4.70×10^{4}	3.20×10^{5}	9.96×10
[June 11, 1996]	[1.41×10^{5}]	[2.75×10^{5}]	[1.88×10^{5}]	[3.5×10^{4}]	[9.73×10^{5}]
June 11, 1996	3.07×10^{5}	3.25×10^{5}	5.93×10^{4}	8.70×10^{4}	1.41×10^{5}
[June 12, 1996]	[2.44×10^{5}]	[1.71×10^{6}]	[9.56×10^{4}]	[3.9×10^{5}]	[3.25×10^{5}]
June 12, 1996	5.40×10^{4}	1.31×10^{5}	3.23×10^{4}	3.05×10^{4}	5.65×10^{4}
[June 13, 1996]	[NA]	[NA]	[NA]	[NA]	[NA]

June 17, 1996	7.80x10^{4}	2.43x10^{4}	2.00x10^{5}	3.30x10^{5}	1.42x10^{5}
[June 18, 1996]	[1.57x10^{4}]	[4.70x10^{5}]	[1.26x10^{5}]	[1.7x10^{5}]	[5.20x10^{5}]
June 18, 1996	8.05x10^{4}	4.40x10^{4}	7.10x10^{4}	1.56x10^{5}	1.32x10^{5}
[June 19, 1996]	[7.20x10^{4}]	[4.15x10^{5}]	[1.25x10^{4}]	[1.5x10^{4}]	[3.50x10^{6}]
Mean	1.12x10^{5}	1.26x10^{5}	8.44x10^{4}	3.18x10^{5}	1.67x10^{5}
[Mean]	[6.94x10^{5}]	[6.02x10^{5}]	[1.09x10^{5}]	[2.9x10^{5}]	[1.09x10^{6}]
(7 m^{3}/h Flow rate)					
July 01, 1996	3.04x10^{5}	1.40x10^{6}	4.60x10^{6}	1.32x10^{4}	1.27x10^{5}
[July 01, 1996]	[TNTC]	[5.53x10^{5}]	[5.11x10^{5}]	[TNTC]	[5.33x10^{5}]
July 03, 1996	1.40x10^{5}	6.07x10^{5}	3.96x10^{4}	2.44x10^{5}	8.63x10^{4}
[July 03, 1996]	[NA]	[NA]	[NA]	[NA]	[NA]
July 07, 1996	5.70x10^{3}	1.31x10^{5}	7.55x10^{4}	3.10x10^{5}	2.89x10^{5}
[July 08, 1996]	[1.30x10^{5}]	[1.45x10^{5}]	[2.40x10^{4}]	[4.8x10^{5}]	[5.36x10^{5}]
July 08, 1996	3.00x10^{4}	3.52x10^{5}	3.29x10^{6}	8.00x10^{5}	2.02x10^{5}
[July 09, 1996]	[4.00x10^{5}]	[1.48x10^{5}]	[4.45x10^{5}]	[6.2x10^{4}]	[3.40x10^{5}]
July 09, 1996	1.95x10^{4}	1.66x10^{5}	1.78x10^{4}	1.77x10^{5}	2.10x10^{5}
[July 10, 1996]	[1.05x10^{5}]	[2.05x10^{5}]	[2.00x10^{4}]	[1.3x10^{5}]	[1.35x10^{5}]
July 10, 1996	1.76x10^{5}	2.65x10^{5}	1.07x10^{4}	2.07x10^{5}	1.03x10^{5}
[July 11, 1996]	[NA]	[NA]	[NA]	[NA]	[NA]
Mean	1.12x10^{5}	4.87x10^{5}	1.34x10^{6}	2.92x10^{5}	1.69x10^{5}
[Mean]	[9.16x10^{5}]	[2.62x10^{5}]	[2.04x10^{5}]	[2.2x10^{5}]	[3.86x10^{5}]

Effect of Various Forms of Iron in Recycle Brine on Performance of Scale Control Additives in MSF Desalination Plants

Abdul Ghani I. Dalvi, M.N. Kither Mohammad,
Saad Al-Sulami, K. Sahul and Radwan Al-Rasheed

EFFECT OF VARIOUS FORMS OF IRON IN RECYCLE BRINE ON PERFORMANCE OF SCALE CONTROL ADDITIVES IN MSF DESALINATION PLANTS

Abdul Ghani I. Dalvi, M. N. Kither Mohammad,
Saad Al-Sulami, K. Sahul and Radwan Al-Rasheed
Research and Development Center, Saline Water Conversion Corporation
P. O. Box # 8328, Al-Jubail 31951, Kingdom of Saudi Arabia

ABSTRACT

Scale control additives (SCA) or antiscalants are used in multistage flash desalination plant to prevent fouling problems. Effective dose rates of some of these SCA are found to vary from plant to plant. Efficiency of antiscalants could be influenced by its chemical nature, plant configuration and design, heat transfer rate and its surface and antiscalant reaction with brine constituents. To understand the variation in concentration of SCA and effect of brine constituents on efficiency of SCA, some bench top experiments at 95 °C with brine were conducted using the threshold effect technique. Two SCA, a polyphosphonate based (PPN) and polymaleic acid based (PMA) were used for these evaluations. The effect of Fe^{3+}, Fe^{2+}, Fe_2O_3, $Fe(OH)_3$, and rust on efficiency of SCA was determined.

The threshold effect method which measures the total alkalinity and calcium content of supernant to evaluate efficiency of SCA was found to be an effective technique. Recycled brine constituents and corrosion products, especially Fe and its various chemical forms affect the efficiency of SCA at 2 ppm concentration and at 95 °C in 1.4 times concentrated seawater brine. Various chemical hydrated and hydroxylated forms of Fe present in brine, viz., $Fe^{3+}(H_2O)_6$, $Fe(OH)_3$, Fe^{2+}, Fe_2O_3, rust, etc., all showed detrimental effect on efficiency of SCA. Among all the species of iron, $Fe(OH)_3$, reduced the efficiency of SCA by maximum of 40%.

Among the two antiscalants, PPN showed 10-12% better efficiency in the presence of various iron species compared to PMA under similar bench top experimental conditions. The effect of brine constituents on PMA was more pronounced compared to PPN perhaps due to better complexing ability of the former.

Key words: Antiscalant, Polyphosphonate, Polymaleic acid, Scales, MSF, Iron, Brine

INTRODUCTION

Saline Water Conversion Corporation (SWCC) being the largest desalted water producer in the world, produces about 20% of world production of desalted water and thus is also the biggest consumer of scale control additives (SCA) [1-2]. Scale control additives or antiscalants which are used in multistage flash (MSF) desalination plants to minimize scaling problems, act nonstiochiometery but still cost several million dollars every year. Thus to make SCA consumption more economical and at an optimum level, it would be of great significance to evaluate various parameters that affect the efficiency of scale control additives. It is known that optimum dosages of SCA often differ from plant to plant and location to location [2]. The root causes for such variation has not been understood. However, it appears that the variation in concentrations and/or efficiency of antiscalants could be influenced by its chemical nature, plant configuration and design, heat transfer rate and its surface and antiscalant reaction with brine constituents.

The exact chemical composition of scale control additives is a closely guarded secret of the manufacturer. In this respect, Sham-El-Din and Mohammad carried out physico chemical studies of antiscalant additives in relation to their functional groups [3, 4]. Further, the role or mechanism of antiscalants reactivity is still not clear in spite of their popular use. It is believed that either it alters the crystal morphology preventing scale growth or it may be acting by what is known as the threshold effect or both [5]. Interaction of brine constituents with SCA may be either advantageous to prevent scale formation or may be detrimental to its performance. In seawater some transition metal ions are present in trace concentrations which can preferentially coordinate with these agents thus reducing their efficiencies. However, the conditions inside distillers and condensers vary due to the construction materials used. The generation of oxides of iron, copper and nickel due to corrosion is unavoidable. A variety of species may circulate through the evaporators as corrosion products such as Fe^{2+}, Fe^{3+}, $Fe(OH)_2$, $Fe(OH)_3$, Fe_2O_3 and rust. These ferrous and ferric ions may readily complex with scale control additive agents and thus in turn will reduce the availability of antiscalant for scale control reaction thereby resulting in an increase in SCA consumption. On the other hand $Fe(OH)_2$ and $Fe(OH)_3$ may form good a suspension in saline water, providing nucleation sites for alkaline scale formation thereby accelerating the rate of scaling. It is this property of iron species along with its electrical property in aqueous solution which make Fe^{3+} an effective coagulant in water treatment processes [6]. In short, iron species may affect the efficiency of an antiscalant agent due to their characteristic complexing and coagulant abilities. This paper describes the results of an investigation on possible influences of iron species that may be present in recycle brine on the performance of antiscalants. The major objective of these investigations is to study the effect of main corrosion related species namely Fe^{2+}, Fe^{3+}, $Fe(OH)_2$, $Fe(OH)_3$, Fe_2O_3 and rust on antiscalant efficiency. The study indicates that there is a specific range of iron species that appreciably affect the threshold effectiveness of SCAs. Moreover, comparison of efficiency of various SCA in the presence of different species of iron shows the necessity of choosing the right type of SCA in a highly corroded environment.

EXPERIMENTAL

Reagent

The specification of the reagents used is as follows :

(a) Sodium carbonate (1N) :- 53 gm Na_2CO_3 dissolved in a liter of water

(b) Antiscalant solution (1000 ppm) :- 0.5 gram of each antiscalant was dissolved in 500 ml of deionized water to give 1000 ppm.

(c) Brine

  (i) Chemical used for preparation of brine
  Chemical A - NaCl
  Chemical B - instant ocean salt (commercially available mixture salt with almost all seawater components)

  (ii) In order to prepare brine with concentration of 1.4 time that of seawater, 8.8 gm NaCl and 6.4 gm instant ocean were dissolved in one liter of seawater, M.alkalinity of final solution was 180 ppm.

(d) Brine Constituents

  (i) Fe^{3+} was taken in the form of $FeCl_3$ solution.

  (ii) $Fe(OH)_3$ and $Fe(OH)_2$ were freshly precipitated from solution containing known concentrations of Fe^{3+} and Fe^{2+} ions. Precipitate was then centrifuged and transferred to reaction vessel as a slurry in seawater.

  (iii) Fe_2O_3 used was powdered Analar grade.

  (iv) Rust was collected from some rusted parts of the plant which was further grounded before use.

Apparatus

Figure (1) shows the schematic diagram of set up used for evaluation of performance of the SCA. It consists of three necked round bottom flask of 1 liter capacity fitted with water condenser, thermometer, sampling port and chemical injection port. Heating mantle equipped with stirrer was used to heat up brine the solution. The condenser is connected to a water bath where the temperature of condensing water is maintained at 10 to 15 °C. To create dynamic flashing in the brine at temperature at 95 °C, vacuum is applied using a pump.

Test Conditions

(a)	Test temperature	:	95 °C
(b)	Brine M-Alkalinity	:	180 ppm
(c)	Concentration of antiscalant	:	2 ppm
(d)	Retention time	:	40 minutes maximum

Test Procedure

Brine 500 ml was measured accurately and spiked with 1 ml of antiscalant stock solution in order to make 2 ppm of antiscalant in the final brine solution. The brine was charged to the reaction vessel and was heated to the desired temperature under refluxing. When the solution reached the required temperature, it was refluxed for 15 minutes to reach equilibrium and to observe any possibility of scale formation. Because there was no precipitation in the presence of antiscalant, 7.5 ml of 1 N Na_2CO_3 was added to break the supersaturation point and to form the scale. The moment at which Na_2CO_3 was added, was considered to be time T = 0. Successive samples (30 ml each) were withdrawn from solution at time intervals of 5, 10, 15, 20, 30 and 40 minutes. The samples were filtered through 0.45 micron filter paper and filtrate was analyzed for Ca, Mg and M-Alkalinity. Total alkalinity (M-Alkalinity) as function of time intervals was plotted to get the efficiency of antiscalant (a scaling threshold diagram).

RESULTS AND DISCUSSION

The efficiency of the two antiscalant additives used viz., polyphosphonate based (PPN) and polymaleic acid based (PMA) was determined in the presence and absence of various iron species such as Fe^{3+}, $Fe(OH)_3$, $Fe(OH)_2$ and rust by what is known as the threshold effect. The scaling threshold is defined as the "maximum permissible concentration factor of water samples at fixed temperature before nucleation begins under equilibrium conditions" [5]. Thus scaling threshold diagrams are drawn between concentration factor and temperature. In MSF plants it is the practice to fix both temperature and concentration factors at optimum values to avoid or minimize scaling problems. In the present study, the net total alkalinity (TALK) after super saturation due to the addition of sodium carbonate as function of time (threshold diagram) was taken as a measure of the efficiency of antiscalant. The comparison of the scaling threshold diagram of antiscalant in the presence and absence of chemical constituent of brine leads to the understanding of the behavior of these antiscalants. Figure (2) shows the loss of TALK with time for distilled water (DW), Gulf seawater and brine, with and without antiscalant. One can see that the saturation of Ca^{2+} and CO_3^- in case of DW is lower than seawater and brine indicating that the high salt content in brine significantly increases the saturation of Ca^{2+} and CO_3^- above their solubility product value $Ksp = 4.8 \times 10^{-9}$. The addition of antiscalants PPN and PMA at 2 ppm concentration raised the solubility of Ca^{2+} and CO_3^- by manifold compared to undosed. This property of certain chemical agents in raising the supersaturation determines the scale control performance of SCA. It is commonly referred to as threshold effect or scaling threshold of that agent. The scale control performance of antiscalant agent is affected by the presence of foreign constituents in the brine solution especially various forms of iron. Figure (3) shows the effect of Fe^{3+} on the performance of PPN and PMA. It is clear from the plot of TALK vs time (Fig. 2) that PPN has got a higher scale control property than PMA. Secondly, up to 0.3 ppm of Fe^{3+} concentration, the scale control performance is unaltered under the conditions of a flashing temperature of 95±0.5 °C, a brine concentration factor of 1.4, an antiscalant concentration of 2 ppm and pH = 8.2. However, as the concentration of Fe^{3+} was varied from 0.3 to 5 ppm, a pronounced effect on the performance of antiscalant was seen. Figures (4) and (5) show the effect of varying the concentration of Fe^{3+} on PPN and PMA respectively. It can be seen that the scaling threshold alkalinity gradually dropped as the Fe^{3+} concentration increased. The decrease in alkalinity is more in the case of PMA than PPN. These experimental results could be explained on the basis of the chelation of active center of SCA with Fe^{3+} which is stronger in PMA than in PPN [7].

When Fe^{3+} is added to an aqueous system several hydrated and hydroxylated species coexist in equilibrium with each other. In acidic solution, hydrated species dominate while in alkaline solution, like seawater pH 8.2, the hydroxylated species are predominate. The equilibrium could be written as follows;

$$Fe^{3+}(H_2O)_6 \rightleftharpoons Fe(OH)^{2+} \rightleftharpoons Fe(OH)_2^+ \rightleftharpoons Fe(OH)_3$$

These hydrolyzed species may have a significant influence on the scale control performance of SCA. The PMA which contains $COOH^-$ group, may chelate with Fe^{3+}. The chelation of Fe^{3+} with COO^- form a strong bond in complexes such as Ferric ethylene-diaminetetacetate and Ferric nitriloacetate [7, 8]. With the high possibility of strong bond formation with PMA, the active centers concentration will deplete with net result of reduced scale control performance. However, from Figure (4), it can be seen that even at a concentration of 5 ppm of Fe^{3+}, the scale control performance is still more than 20% which indicates that chelation has a minor effect on SCA performance. Hence other effects such as nucleation site offered by $Fe(OH)_3$ and hydrolyzed chain of ferric ions may be playing a role in retarding scale control performance. In fact as the Fe^{3+} concentration is increased from 1 ppm to 5 ppm the ferric species is extensively hydrolyzed into $Fe(OH)_3$ and polymeric hydrolytic chains [8]. Retardation of scaling threshold could therefore be related to the combined effect of the presence of Fe^{3+}, $Fe(OH)_3$, $Fe(OH)_2^+$, $Fe(OH)^{2+}$, $Fe(OH)_n^{m+}$ species. It is evident from the Figures (4) and (5) that alkalinity is steady up to 0.5 ppm Fe^{3+} after which loss of TALK is very sharp as the Fe^{3+} concentration increases. It appears that the drop in alkalinity is due to the formation of $Fe(OH)_n^{m+}$ and $Fe(OH)_3$ species at higher Fe^{3+} concentration. $Fe(OH)_3$ may disperse in the brine and offer enormous nucleation site for $CaCO_3$ precipitation. This kind of coagulating tendency is more pronounced in ferric species and thus ferric is extensively used as coagulant in water treatment [6, 9]. It can also be seen from the Figures (4) and (5) that TALK beyond 2 ppm remains almost constant which means the scale control performance is unaltered and unaffected by the species. Furthermore, from the figures it can be seen that the effect of Fe^{3+} is very similar in both PMA and PPN except that PPN is slightly less affected than PMA. Table (1), which shows the efficiencies of antiscalant in the presence of 2 ppm of iron species at treatment time of 15 minutes, also leads to the same conclusion. This may be because the -P=0 group in the PPN may not chelate with Fe^{3+} as effectively as COOH in PMA.

The effect of $Fe(OH)_3$ on the efficiency of SCA was studied by adding freshly prepared $Fe(OH)_3$ to brine solution containing SCA. Figures (6) and (7) show the effect of $Fe(OH)_3$ in the presence of PPN and PMA. The two figures also include the performance of the antiscalants in the presence of 1 ppm of Fe^{3+}. It can be seen that 1 ppm Fe^{3+} has almost the same effect as that of 0.6 ppm $Fe(OH)_3$. Further retardation of scale control performance was observed in both PMA and PPN almost to the same extent. The results thus suggest that the nucleation effect rather than chelation plays a significant role in the scale control process.

Highly porous $Fe(OH)_3$ may loose water molecules to form denser Fe_2O_3

and may also offer nucleation sites. Figure (8) shows the loss of TALK with time in the presence of Fe_2O_3. Its effect on retardation was much less in comparison to $Fe(OH)_3$ and Fe^{3+}. The effect of 2 ppm Fe_2O_3 was almost negligible, but 10 ppm it was significant and was almost equal to that of 2 ppm $Fe(OH)_3$. This may be due to the fact that Fe_2O_3 is more compact and may offer fewer nucleation sites with lesser electrical property and surface area than $Fe(OH)_3$.

In actual plant conditions, corroded surfaces offer more nucleation sites as compared to smooth metal surfaces. The outer corroded surface may have metal oxides (rust). Figure (9) shows the effect of rust on SCA performance. The retardation effect by rust is very low at 2 ppm and only at 10 ppm, loss of TALK is appreciably high. However, the extent of retardation is less compared to $Fe(OH)_3$. Once again this is due to the high density of rust, (i.e., higher compactness in comparison to $Fe(OH)_3$) and thus offers less surface area for nucleation.

Corrosion is a process whereby the Fe is oxidized first into Fe^{2+} at seawater pH = 8.2, then Fe^{2+} is further oxidized to Fe^{3+} by O_2. However, in desalination units, O_2 is removed in the deaerator and the O_2 level is brought down to less than 0.02 ppm. Thus, the probability of oxidation of Fe^{2+} to Fe^{3+} is reduced under these conditions and Fe^{2+} may be hydrolyzed to $Fe(OH)_2$ before being oxidized to $Fe(OH)_3$. Thus to study the effect of $Fe(OH)_2$, freshly prepared $Fe(OH)_2$ was used. Figure (10) shows the results of these studies. It can be seen that the loss of TALK in these experiments was less significant, yet similar to that observed in the case of $Fe(OH)_3$.

Summaries of the results obtained on the efficiencies of antiscalants are shown in Table (1). The table gives efficiencies of PMA and PPN in the presence of 2 ppm of various species of iron in brine at 95 °C with a treatment time of 15 minutes. These results indicate that PPN efficiency was less affected by iron species in the brine compared to PMA.

CONCLUSIONS

From the foregoing discussion it is evident that various forms of iron in the recycle brine tend to retard the efficiency of Scale Control Agent (SCA). When 2 ppm of iron species (as ferric) is present in the brine, the performance of PMA was reduced to 37% by Fe^{3+}, 32.3% by $Fe(OH)_3$, 84.1% by Fe_2O_3, 85% by rust and 73.1% by $Fe(OH)_2$, while that of PPN was reduced to 46.4% by Fe^{3+}, 40.5% by $Fe(OH)_3$, 90.6% by Fe_2O_3, 88.1 by rust, and 84.5% by $Fe(OH)_2$.

These conclusions can be elaborated on as follows:

1. The method of adding 1000 ppm Na_2CO_3 to 1.4 times concentrated seawater brine and determining the scaling threshold by measuring total alkalinity in the brine as a test for scale control performance of SCA, was found to yield satisfactory results. It is thus recommended that this method can be adopted for preliminary screening of antiscalants for alkaline scale control.

2. Using the above test under laboratory conditions PPN efficiency was found to be better than PMA antiscalant. PMA efficiency is 88% of PPN (in the absence of iron).

3. In the presence of 0.5 ppm Fe^{3+}, SCA efficiency is reduced to 93% while at 5 ppm Fe^{3+}, it is reduced down to 30%.

4. Ferric hydroxide reduced the efficiency of SCA as compared to Fe^{3+}. At 2 ppm of $Fe(OH)_3$, the efficiency of PPN is 40% and the efficiency of PMA is 32%.

5. Fe_2O_3 and rust showed significant reduction of SCA performance only at 10 ppm concentration.

6. The efficiency of antiscalant was reduced by the presence of brine constituents in the following order :
$Fe(OH)_3 > Fe^{3+} >> Fe(OH)_2 > Fe_2O_3 >$ Rust.

REFERENCES

[1] Al-Sofi M. A. K., Hamada T, and Saad Al-Sulami. (1993), Laboratory Testing of Antiscalant Threshold Effectiveness, 2nd Gulf Water Conf. Bahrain. 66-67.

[2] Al-Zahrani, S. G., Al-Ajlan A. M. and Al-Jardan A. M. (1993), Using Different Types of Antiscalants at the Al-Jubail Power and Desalination Plant in Saudi Arabia, 6th World Congress. Yokohoma, Japan. 421-433.

[3] Sham-El-Din A. M. and Mohammad R. A., (1996) Desalination, 107, 277-290.

[4] Sham-El-Din A. M. and Mohammad R. A., (1997) Desalination, 114, 77-84.

[5] Speigler K. S. and Laird A. D. K. (1980) Principles of Desalination Part B, Academic Press N. Y.

[6] Clifford G. W. (1986) The Hand Book of Chlorination (Ed. II). Van Nostrand, Reinhold NY.

[7] Martell A. E. and Smith R. M. (1974) Critical Stability Constants, Vol. I. Plenium Press NY.

[8] Gustafson R. L. and Martell A. E. (1963) Hydrolytic Tendencies of Iron Aminopolycarboxylate chelate in aqueous solution, Journal of Physics. 6, 576.

[9] Faust, E and Aly O. (1982), Chemistry of Water Treatment, American Public Health Association (APHA), NY.

Table (1) Percent Efficiency of Antiscalant in Presence of 2 ppm Iron Species

Iron Species / Antiscalant	Fe^{3+}	$Fe(OH)_3$	Fe_2O_3	Rust	$Fe(OH)_2$
PMA	37%	32.3%	94.1%	85%	73%
PPN	46.4	40.5	90.6%	88.1%	84.5%

(Treatment Time 15 Minutes)

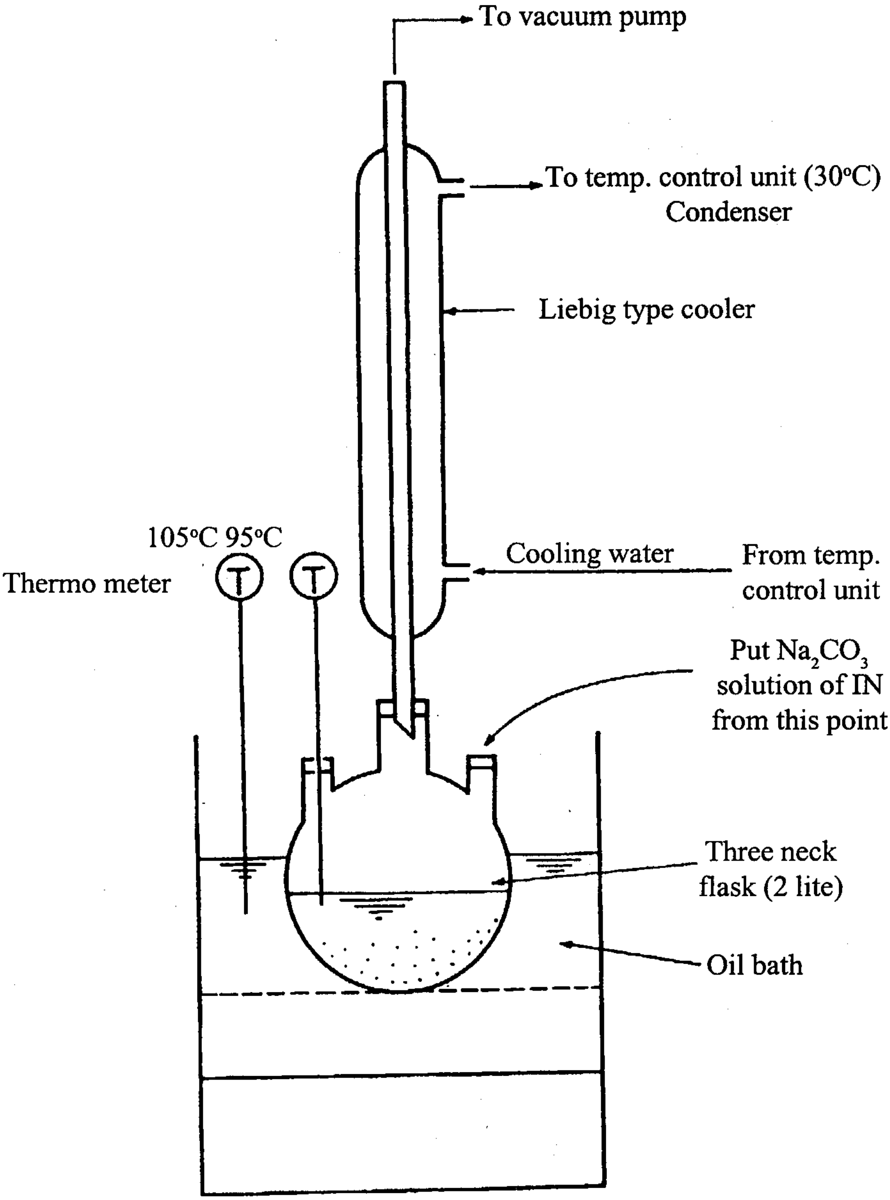

Figure 1: Schematic diagram of experimental set up for determination of scaling threshold of antiscalants

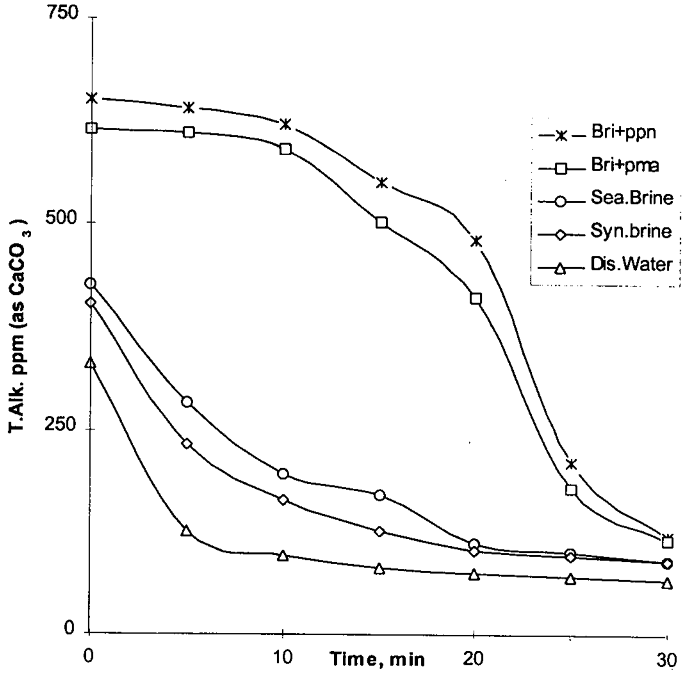

Figure 2: The scaling threshold in Brine with and without scale control additives

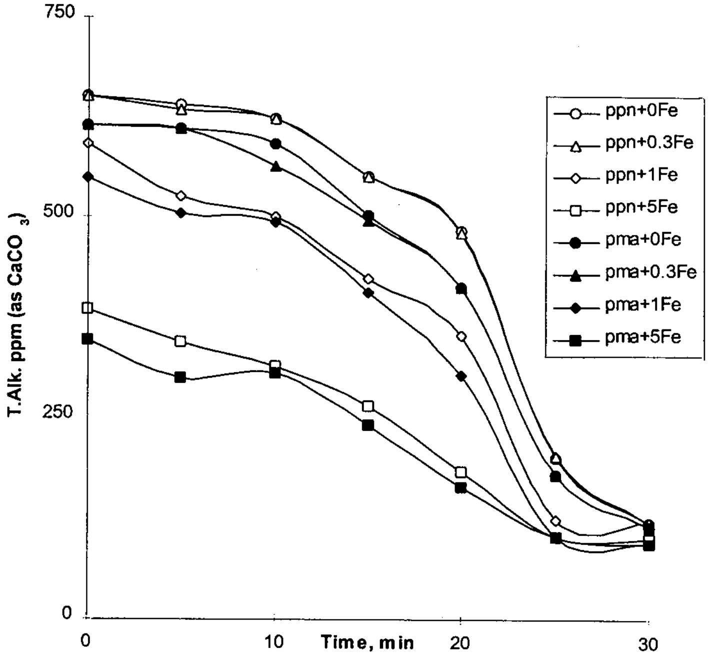

Figure 3: The effect of Fe^{3+} on the performance of PPN and PMA

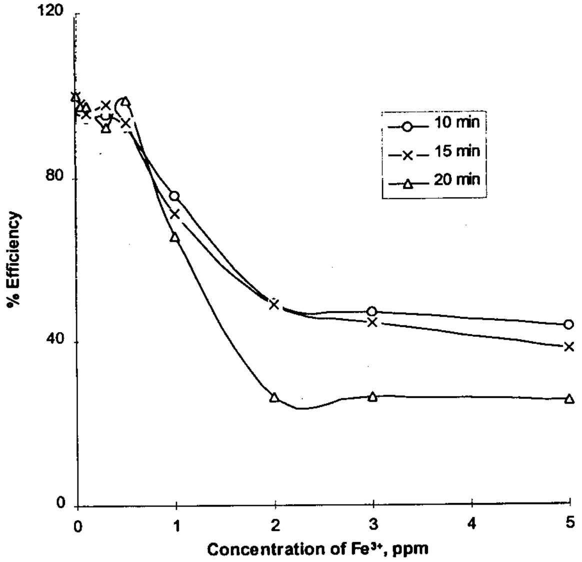

Figure 4: Percent efficiency of PPN in the presence of Fe^{3+} at different time intervals

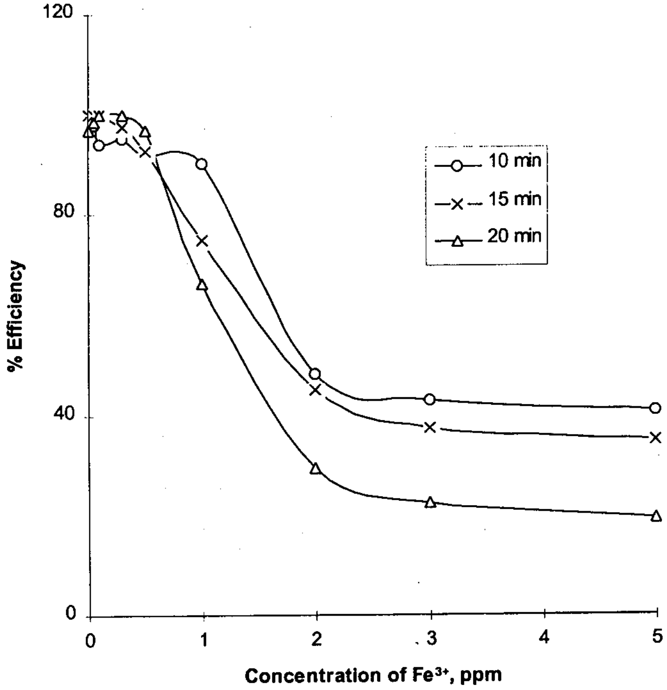

Figure 5: Percent efficiency of PMA in the presence of Fe^{3+} at different time intervals

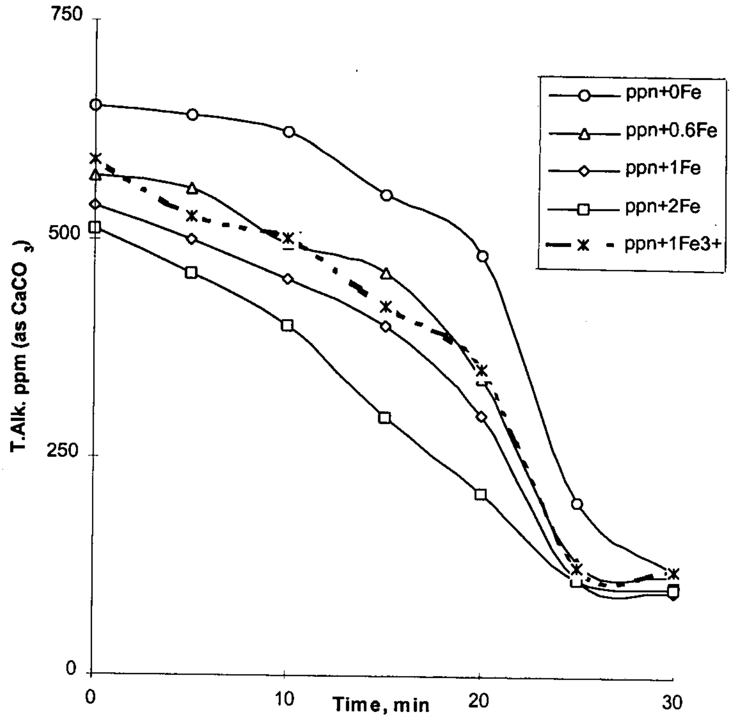

Figure 6: The effect of Fe(OH)$_3$ on the performance of PPN

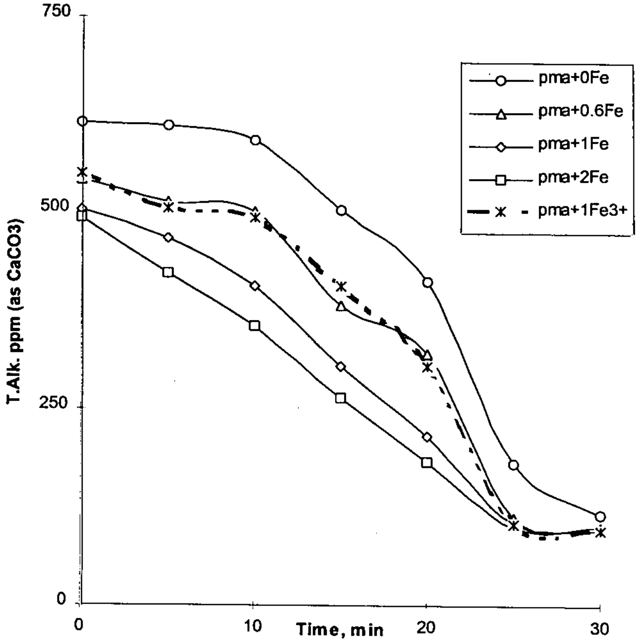

Figure 7: The effect of Fe(OH)$_3$ on the performance of PMA

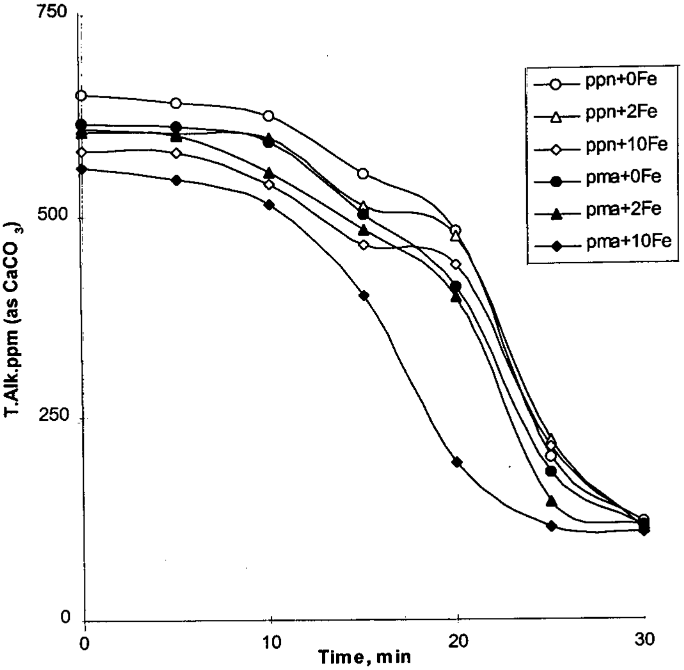

Figure 8: The effect of Fe_2O_3 on the performance of PPN and PMA

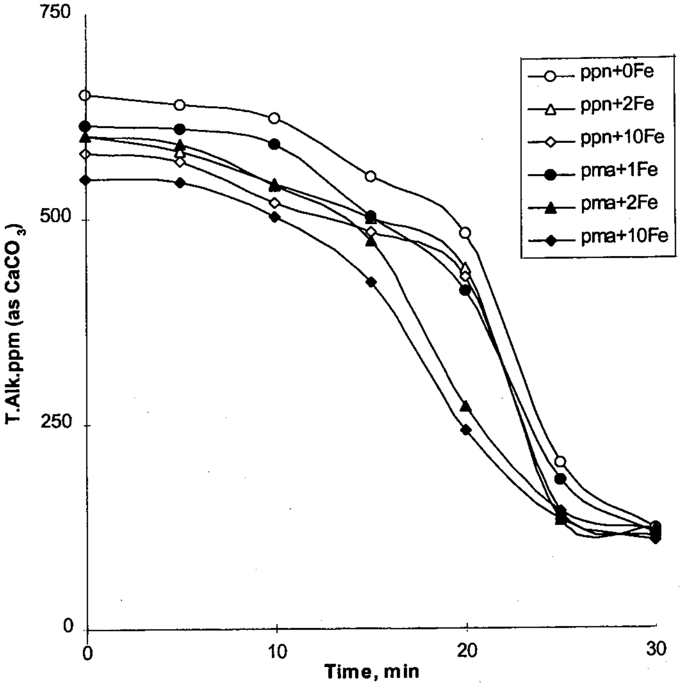

Figure 9: The effect of Rust on the performance of PPN and PMA

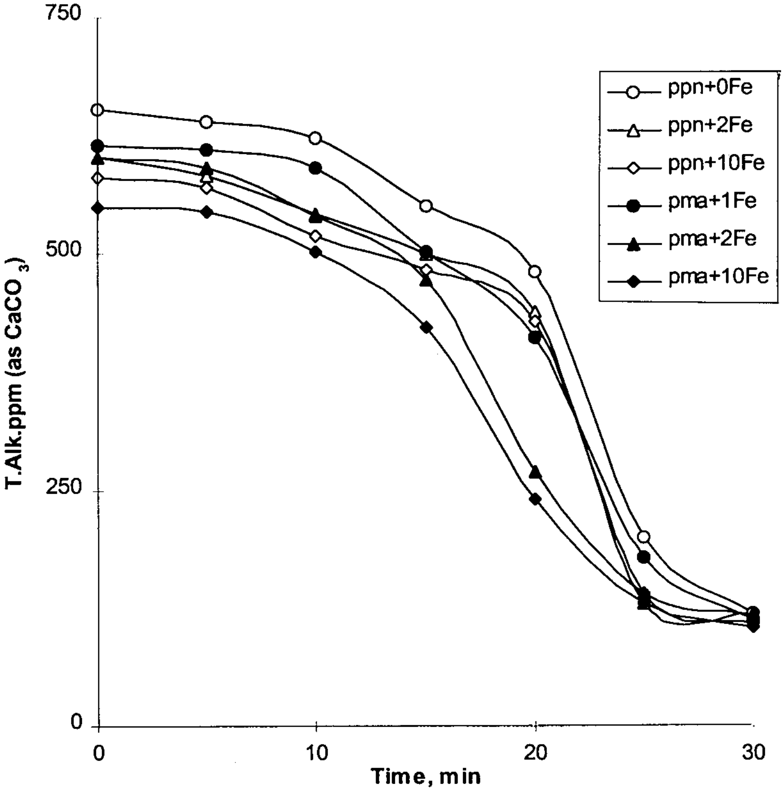

Figure 10: The effect of Fe(OH)$_2$ on the performance of PPN and PMA

The Performance of Different Antiscalants in Mutli-Stage Flash Distillers

Osman A. Hamed, Mohammad AK. Al-Sofi,
Ghulam M. Mustafa and Abdul Ghani Dalvi

THE PERFORMANCE OF DIFFERENT ANTISCALANTS IN MULTI-STAGE FLASH DISTILLERS

Osman A. Hamed, Mohammad AK. Al-Sofi,
Ghulam M. Mustafa, and Abdul Ghani Dalvi
Research & Development Center
P. O. Box- 8328, Al-Jubail, SWCC
Saudi Arabia

ABSTRACT

The Saline Water Conversion Corporation (SWCC) is an internationally recognized authority on scale control in multi-stage flash (MSF) distillers. This international recognition came about as a result of many years of work on this topic. There are publications of SWCC on MSF scaling phenomena over the past couple of decades. During the last decade, there was a monumental growth in SWCC's installed MSF plant capacities. The majority of SWCC MSF distillers were designed to operate with additive scale control method rather than the previously predominant method of carbonate depletion through chemical reaction with acid, e.g., sulfuric or hydrochloric.

The Research and Development Center (RDC) in Al-Jubail has been involved during the last three years in the evaluation of available commercial scale inhibitors. A total of eight tests have been carried out at RDC MSF pilot plant, Jeddah Phases III & IV and Al-Jubail Phase II to evaluate the effectiveness of three antiscalants. These tests by antiscalant types and places are (i) polycarboxylates in Al-Jubail II, RDC pilot plant and Jeddah IV, (ii) polymaleic acid in Jeddah IV and RDC pilot plant and (iii) polyphosphonate in Jeddah III and RDC pilot plant. Moreover, a run of acid operation carried out in the pilot plant is included for comparison.

This paper presents qualitative and quantitative performance results of three different antiscalants as well as acid dosing tests for scale control. The threshold effect of these antiscalants was tested on laboratory scale. On pilot and commercial plants the variation of the fouling factor with time is examined and quantified. The evaluation tests conducted on the commercial plants revealed that all the examined antiscalants were successful in inhibiting alkaline scale formation and improving plant performance at top brine temperature ranging between 105 and 110°C and with respective dosing rates of 1.5 and 3.0 ppm.

Keywords: Desalination, Multistage flash, Alkaline scale, Antiscalants and Fouling Factor.

INTRODUCTION

Control of scale formation on heat transfer surfaces is one of the basic problems in the distillation processes. Formation of scale on heat transfer surfaces impedes the rate of heat transfer. The main scale forming constituents of sea water are calcium, magnesium, carbonate, bicarbonate and sulfate. On heating, bicarbonate will yield carbonate which can precipitate with calcium if the saturation limit is exceeded. As a result magnesium hydroxide will also form. In practice, the formation of alkaline scales are controlled by either lowering the pH through bicarbonate depletion or by threshold additive chelation through special chemicals called threshold agents[1]. Conversely, $CaSO_4$ formation is primarily controlled, so far in commercial plants, by operating at top brine temperature (TBT) that are lower than its appreciable precipitation limits, i.e., TBT < 120 °C in view of the raised salt concentration in MSF brine streams.

Mixtures of sodium tripolyphosphate dispersing agent have been used to inhibit alkaline scale deposition in seawater evaporators since the 1950s [2]. The major problem with polyphosphate based inhibitors was found to be its thermal degradation at temperatures above 90°C and the subsequent loss of its threshold effect. This restriction in TBT to 90°C limited the thermal efficiency of evaporator designed for threshold treatment from mid 1950's through 1960's into a good part of 1970's.

Acid dosing was introduced in the 1960s as a means of overcoming the temperature limitations and the poor performance of polyphosphate. As problems associated with acid operation became dominant, the need for high temperature scale control additives to replace acid while giving commensurable performance was felt towards the end of the seventies into the eighties (1970 & 1980s) [2]. Low molecular weight polymeric/ carboxylic acid and phosphorous base alkaline were developed as high temperature additives. It has become a common belief that these chemicals distort the lattice structure and minimize the rate of growth of the alkaline scales. Polyphosphonate "phosphorous base alkaline group" does not hydrolyze as easily as the polyphosphate group due to the greater stability of the c-p bond in phosphonates as compared with the p-o bond in phosphates.

The dosing rate of antiscalant is one of the most important operating parameters. Under dosing leads to scale formation while overdosing is believed to enhance sludge formation [3]. It is thus essential to establish an optimum dose rate. Although a number of chemical reagents have been used to minimize or prevent the formation of alkaline scales [4], no commonly accepted method for avoiding the formation of scales due to calcium sulfate salts at high temperatures and brine concentrations in large commercial MSF plants is available. The only commercialized approach so far, i.e., currently used to prevent the formation of calcium sulfate; is to operate the plant below the solubility limits of calcium sulfate. Yet the known ones are by sulfate depletion or reaction removal of calcium and/or sulfate content of the seawater make-up. Most recent promising approach was addressed last couple of years in international and regional conferences and is expected to be addressed in this conference. In the recent work, membrane nanofiltration has been successfully used in almost total sulfate depletion [5-7].

Saline Water Conversion Corporation (SWCC) has been actively involved in the inhibition of scale formation in order to improve the performance of its distillers. A direct comparison on the performance characteristics and economics of a number of additives tested on the MSF distillers of Al-Jubail phase I has been reported [8,9]. SWCC also conducted optimization of scale control additive dose levels at different top brine temperatures in Al-Khobar II and Al-Jubail II desalination plants[10]. Moreover, the performances of polymaleic acid (PMA) and polyphosphonate (PPN) antiscalants at Al-Jubail phase II desalination plant were verified[11]. Gained operational experiences on Al Khobar Phase II plant with only one acid cleaning during the period 1982-1992 was presented in detail by Al-Sofi, et al.,[12].

BASIC APPROACH

This paper reports the results of the evaluation tests of scale control additives performed by Al-Jubail Research and Development Center during the last three years. Testing of scale inhibitors characteristics and effectiveness has been carried out at three levels: laboratory, pilot plant and finally testing on commercial plants. At the laboratory level the threshold effect of different antiscalants was first tested on a bench scale equipment. At the pilot plant level the effectiveness of polymaleic and polycarboxylic acids was tested [13]. The MSF pilot plant is of 20 ton per day capacity and its schematic diagram is shown in Figure 1. It consists of a brine heater, four heat recovery and two heat rejection stages. The plant is also equipped with external deaerator as well as decarbonator (for TBT of 120 °C acid operation) and on-line ball cleaning facilities. At the commercial levels, tests were conducted in Jeddah III and IV also Al-Jubail II to evaluate the performance of polycarboxylic acid, polymaleic acid and polyphosphonate as scale control additives. Design characteristics and parameters of tests carried out in these commercial plants are summarized in Table 1.

Table 1: Design Characteristics and Test Parameters of the Commercial Plants

S. No.	**Design & Test Parameters**	**Jeddah IV Unit 19**	**Jeddah IV Unit 15**	**Jeddah III Unit 10**	**Jubail II Unit 8**
1	Top brine temperature	110	110	108	105
2	Concentration ratio (RB)	1.4	1.3 - 1.32	1.4	1.4
3	Antiscalant dose rate, ppm	1.8	2	3	1.5
4	Ball cleaning , times/week	2	2	14	21
5	No. of ball cycles/ per shift	9	9	3	10
6	Ball to tube ratio	0.4	0.4	0.75	0.3
7	Production, MIGD	5	5	5	5.75
8	Number of stages	24	24	16	22
9	Gain output ratio (GOR)	7	7	7	9.0
10	Flash range, °C	72	72	70	69
11	Design fouling factor BH (m^2K/kW)	0.395	0.395	0.325	0.2
	HRS (m^2K/kW)	0.176	0.176	0.178	0.15

RB = Recycle Brine, BH = Brine Heater, HRS = Heat Rejection Section

RESULTS AND DISCUSSION

LABORATORY TESTS

Antiscalants have two principal effects: threshold and crystal distortion. Threshold effect is responsible for preventing scale initiation and inhibiting or slowing down the deposition of soft scale consisting mainly of calcium carbonate and magnesium hydroxide. Crystal distortion effect is responsible for suppressing the adhering ability of scale. Antiscalant addition results in the distortion of scale crystals into spheroid structures which have less contact surface than a flat shaped untreated scale crystal hence less adherence ability to metals. Spheroid shaped particles tend to rotate around their own axis while moving with the liquid stream along pipe axis. This combined, i.e., revolution as well as traversial motion results in a radial force that causes the particle to migrate towards the pipe center leaving particles free pipe wall.

The threshold characteristics of three different antiscalants were examined. These were a modified blend of polyphosphonates (PPN-M), polymeric maleic acid (PMA) and polymeric carboxylic acid (PCA). The method of confirming the threshold effect was performed through the addition of a certain quantity of inhibitor in a supersaturated brine solution. The ability of the scale inhibitor to prevent the deposition of scale was checked by observing the change of M-alkalinity with time. The threshold effect of the three examined antiscalants was carried out in laboratory at a constant 2 ppm dosing rate and at two different temperatures of 95 and 110°C. The change of M-alkalinity as $CaCO_3$ (ppm) with time in minutes is shown in Figures 2 and 3. Both figures show that the alkalinity of the supersaturated solution with no scale inhibitor (blank), which can be considered as a reference state, decreased rapidly with time. At 10 minutes time the alkalinity dropped to 140 ppm at 95 °C and 80 ppm at 110 °C.

Figures 2 and 3 also reveal that all scale inhibitors have the ability to prevent the deposition of scale when they contact supersaturated brine solution but their effects decrease with the increase in retention time. Modified polyphosphonate and polymaleic acid were found to exhibit the highest threshold effect compared to polycarboxylic acid especially at conditions of 95 °C with a retention time boundary of 20 minutes and 110°C with retention time boundary of 10 minutes. All scale inhibitors lost their threshold effect within 30 minutes at 90 °C and 15 minutes at 110 °C under the above laboratory conditions.

PILOT PLANT TESTS

Two different antiscalants PCA and PMA were tested on the RDC MSF pilot plant. Tests were conducted with TBT range of 110-112 °C, concentration ratio of 1.38 -1.4, antiscalant dose rate of 2 ppm and cyclic ball cleaning. The increase of fouling factor in the brine heater with time was calculated to demonstrate the thermal effectiveness of antiscalants. Figure 4 shows the time dependence of the fouling factors. It shows that both antiscalants are quite effective in their performance and maintaining fouling factors well below the design values. Small variance is seen where the slope of PCA line is slightly less than that of PMA and where PMA starts at a lower value than PCA, yet after 700 hours they are almost the same. Results of visual inspection conducted before and after these tests revealed that there was a very thin layer of soft sludge on the tubes. The increase of the fouling factor in the brine heater (R_D, m^2 K/kW) with time (t, hours) is quantified. Using a regression analysis the following linear relationships are obtained assuming that the rate of fouling remains constant.

For Polycarboxylic acid, $R_D = 0.00002\,t + 0.0349$ .... (1)
For Polymaleic acid $R_D = 0.00004\,t + 0.0217$ .... (2)

The linearity of fouling factor with time indicates that the rate of increase in fouling factor is very small which is reflected in the low values of the time coefficients. Assuming the linear behavior of fouling factor, the allowable periods required for the fouling factor to reach design value and before acid cleaning becomes necessary, are 375 and 483 days for polycarboxylic and polymaleic acids, respectively. Based on the experience especially those reported in reference [12] such periods are found to be very short. This could be attributed to the fact that the rate of change in fouling was only linear during those limited duration tests. However, for longer operating periods the asymptotic fouling model could be better representative to the behavior of fouling curve [14]. Moreover, in view of cyclic ball cleaning this asymptotic behavior is expected to follow the saw-tooth trend.

Two additional runs were conducted in the MSF pilot plant distiller operating with a once-through mode rather than the conventional recirculation mode to briefly show the effect of total concentration and alkaline scale forming ions content on heat transfer performance. Figure 5 shows how far polyphosphonate dose rate can be reduced when only seawater of 128 ppm alkalinity is used to flow through the brine heater i.e. once through operation. In this test antiscalant dose rate was reduced down to as low as 0.5 ppm at an elevated TBT of 115°C. Although the quantity of seawater which has to be pretreated in the once-through mode of operation is 2.6 times that of the recycle mode, the required quantity of antiscalant has been reduced down by a factor of two. In essence, the pretreatment cost is halved.

COMMERCIAL PLANT TESTS

Tests were conducted in Jeddah III and IV and Al-Jubail II to evaluate the performance of polycarboxylic and polymaleic acids and polyphosphonate as antiscalant agents. In these tests pre, interim and post trial visual inspections were conducted as frequent as was deemed essential and as production schedules could have allowed. During each test relevant flow rates, temperatures and pressures were monitored. Calculations were then made to determine the heat transfer characteristics induced by each examined antiscalant. Design characteristics and test parameters of the four tested commercial units are summarized in Table 1.

Results of the performance evaluation of polycarboxylic acid at Jeddah IV unit 15 commercial plant are shown in Figure 6. The fouling factors of both the brine heater and heat recovery section are well below the design values which indicates that the distiller was working satisfactorily. Analytical results of pH values, M-alkalinity, turbidity, chlorine and total dissolved solid indicate that the unit was working smoothly with no abnormal behavior. Analysis for residual antiscalant in the samples taken before flashing shows that the antiscalant was active throughout the brine recycle passage. The assumed linear regression analysis reveals that the allowable operating periods for the brine heater and heat recovery sections, before acid cleaning becomes essential are 403 (compared to 375 days in the pilot test) and 867 days, respectively, while dosing 2.0 ppm of PCA at a TBT of 110°C.

Results of the performance of polymaleic acid at Jeddah IV unit 19 commercial plant are shown in Figure 7. Trends of fouling factors in heat recovery and heat input (i.e., the brine heater) sections show an increase with time but remain below their respective design fouling factors. The rates of increase of fouling factor for this unit (as well as unit 15 discussed in the above paragraph) are very low indicating minimum depositions inside the brine heater and heat recovery tubes. These findings are supported by the interim and post trial inspections of brine heater and the first three stages of the recovery section which show that tubes were in good clean condition. These results are found to support the validity of the asymptotic behavior of scale buildup. Post inspection at the end of this trial run showed that demister fouling in the first stage had blocked all the pads. In the next two stages, demisters were less fouled compared to the first stage and the scale was also soft. These results are found to support the proposed asymptotic growth behavior in Jeddah tests.

Results of performance of polyphosphonate at Jeddah III unit 10 commercial plant are shown in Figure 8. The fouling factor of heat recovery section remained at almost a constant value during the whole period of the test which indicates negligible deterioration in its thermal performance. This was confirmed by the visual inspection which revealed that only a very thin layer of scale had been deposited in the first stage and a dusting of scale inside the tubes of the second stage was apparent. The GOR remained virtually unchanged throughout the trial period. The fouling factor of the brine heater was increased from 0.05 to 0.1 m^2K/kW during 2100 hours which was well below the design value of 0.325 m^2K/kW. Post trial visual inspection of the brine heater revealed that there was no evidence of excessive sludge and only a thin layer of scale was observed on the tubes inner surfaces. The demister pads in the first three stages showed some depositions, similar in degree to that experienced under normal operation. The assumed linear regression analysis predicts that it will take 4.37 and 3.2 years for the fouling factors of the brine heater and heat recovery sections to reach the design fouling factors at a dose rate of 3 ppm and a TBT of 108°C.

Evaluation tests were performed in Al-Jubail II to demonstrate the effectiveness of polycarboxylic acid at a TBT of 105 °C. The test results are depicted in Figure 9 which shows slight increase of fouling factor with time. The distiller was also inspected before and after test trial. The post trial inspection revealed that no sludge was found in tubes of brine heater and heat recovery section. The demister pads were found in good and clean condition. Thus both the calculated test results and visual inspection confirmed that the tested antiscalant is highly effective in controlling scale formation and its deposition thereafter. The linear regression analysis revealed that it will take 415 days for the fouling factor of the brine heater to reach the design value.

CONCLUSIONS

1. Literature search revealed that one of SWCC's main achievements in controlling alkaline scale formation in commercial MSF distillers was successful operation at low antiscalant dose rates.

2. The threshold laboratory tests revealed that modified polyphosphonate and polymaleic acid inhibitors are having higher threshold effects compared to polycarboxylic acid. All scale inhibitors lost their threshold effectiveness within 30 minutes at 90°C and 15 minutes at 110°C during laboratory testing.

3. MSF pilot plant distiller tests revealed that the rate of rise in fouling factors for PCA & PMA are quite comparable. Another test in this pilot plant indicated the effect of concentration of total and alkaline scale forming ions, in allowing operation at drastically reduced antiscalant dose rate and increased TBT of 115°C. Last test conducted in the pilot plant revealed the effect of alkaline scale forming ions

of bicarbonate origin through reaction with acid, in allowing operation at a reduced brine recycle flow rate hence lowered tube velocity through the brine heater from 2.34 meters per second down to 1.8 meters per second at TBT of 110°C (as shown in Figure 5).

4. Evaluation tests on polyphosphonate, also polymaleic and polycarboxylate polymers performed in Jeddah and polycarboxylate polymer in Al-Jubail desalination plant showed that these antiscalants are very effective and successful in controlling scale formation at a TBT range of 105 and 110°C and with dose rate in the range of 1.5 and 3.0 ppm. The fouling factors of brine heater and heat recovery section suppressed by the three antiscalants were always well below the design values. The linear regression analyses of the tests results reveal that the allowable operating periods for the brine heater and heat recovery sections before acid cleaning is required, are generally more than a year. These findings were confirmed by post trial visual inspection which revealed in all cases that brine heater and heat recovery tubes were normally maintained in clean conditions.

REFERENCES

[1] Shams El Din, A.M., and R.A. Mohammed, 1994, "Brine and scale chemistry in MSF distillers". *Desalination*, 99, pp. 73-111.

[2] Finan, M.A., S. Smith, C.K. Evans, and J.W.H. Muir, 1989, "Belgard EV-15 year's experience in scale control". *Proceedings of the fourth world congress on desalination and water reuse*, pp. 341-357.

[3] Al-Sofi, M.A., S. Khalaf, and A. Al-Omran, 1989, "Practical experience in scale control". *Desalination*, 73, pp. 313-325.

[4] Nada, N., 1986, "Comparison of cost of three MSF desalination plants using different chemical treatment". *Topics in Desalination (No. 20)*, SWCC, pp. 36-55.

[5] Hassan, A. M., M. AK. Al-Sofi, A. Al-Amoudi, A. T. M. Jamaluddin, N. K. Mohammad, G. M. Mustafa, and I. Al-Tisan, 1997, "A new approach to membrane and thermal seawater desalination using nanofiltration membranes". Presented at IDA of the international conference, Madrid, Spain.

[6] Hassan, A. M., M. AK. Al-Sofi, A. Al-Amoudi, A. T. M. Jamaluddin, N. K. Mohammad, G. M. Mustafa, and I. Al-Tisan, Part 1 & 2, May-June & Aug.-Sept. 1998, "A new approach to membrane and thermal seawater desalination using nanofiltration membranes". Desalination & Water Reuse, Vol. 8/1&2, pp. 53-59.

[7] Al-Sofi, M. AK., G. M. Mustafa, A. M. Hassan, A. G. I. Dalvi, and M. N. M. Kither, 1998, "Nanofiltration products (NFP) or NF-$SWRO_{reject}$ NF-ROR as make up to MSF". Membrane conference, Amsterdam, Holland.

[8] Al-Mudaiheem, A. M. A., and Szostack, R.M., "Evaluation of chemical additives for scale control in MSF evaporators". *Topics in Desalination (No. 8)*, SWCC, 1986.

[9] Nada, N., 1986, "Evaluation of various additives at Al-Jubail Phase I during reliability trials". *Topics in Desalination (No. 13)*, SWCC.

[10] Al-Sofi, M. AK., M. A. Al-Hussain, and S. Al-Zahrani, 1987, "Additive scale control optimization and operation modes". *Desalination*, 66 pp. 11-32.

[11] Al-Zahrani, S., A. M. Al-Ajlan, and A. M. Al-Jardan, 1993, "Using different types of antiscalants at the Al-Jubail power and desalination plant in Saudi Arabia". *Proceedings of IDA and WRPC World Conference on desalination and water treatment*, Yokohama, Japan,. 1, pp. 421-431.

[12] Al-Sofi, M.AK., M. A. Al-Hussain, A. A. Al-Omran. and K. M. Farran, 1994, "A full decade of operating experience on Al-Khobar II multistage flash (MSF) evaporators (1982-1992)". *Desalination*,.96 pp. 313-323.

[13] Al-Sofi, M. AK., E. F. El-Sayed, M. Imam, G. M. Mustafa, T. Hamada, Y. Tanaka, S. Haseba, and T. Goto, 1995, "Heat transfer measurements as a criterion for performance evaluation of scale inhibitor in MSF plants". Seventh IDA international conferences, UAE.

[14] Malik, A., and F. A. Aleem, 1994, "Scale formation and fouling problems and their predicted reflection on the performance of desalination plants in Saudi Arabia". *Desalination*, 96, pp. 409-419.

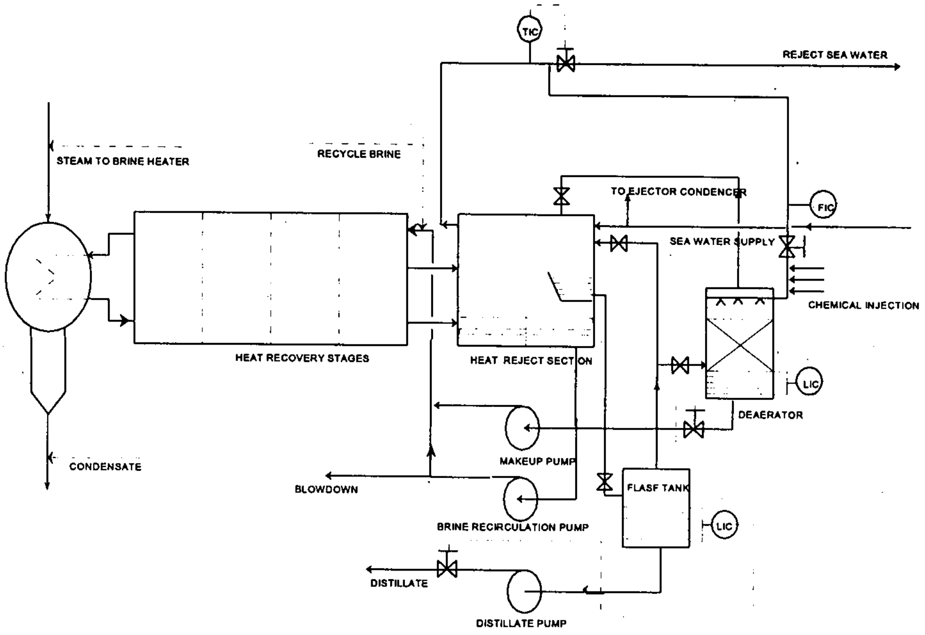

Figure 1. Schematic Diagram of the Pilot MSF Plant

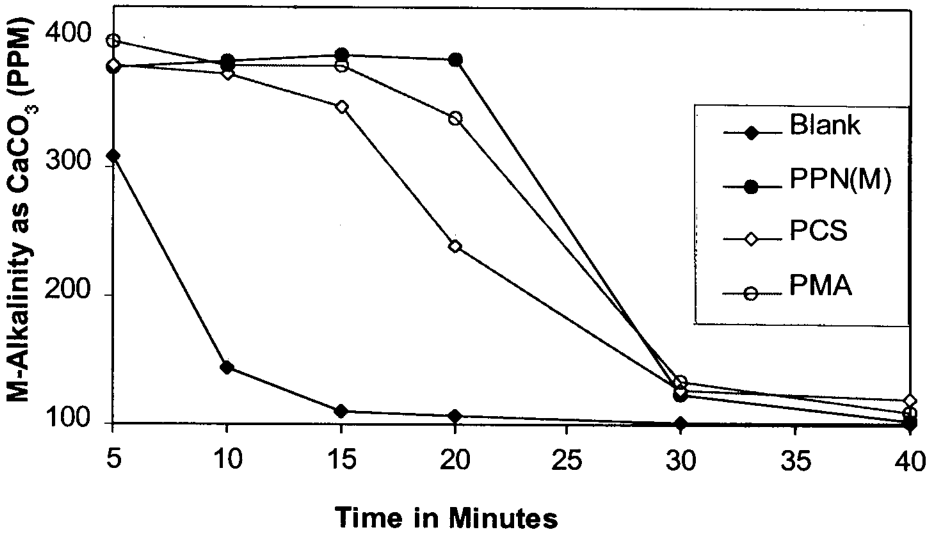

Figure 2. Laboratory Test of Various Antiscalants for their Threshold Effect at 95°C & 2 ppm Concentration

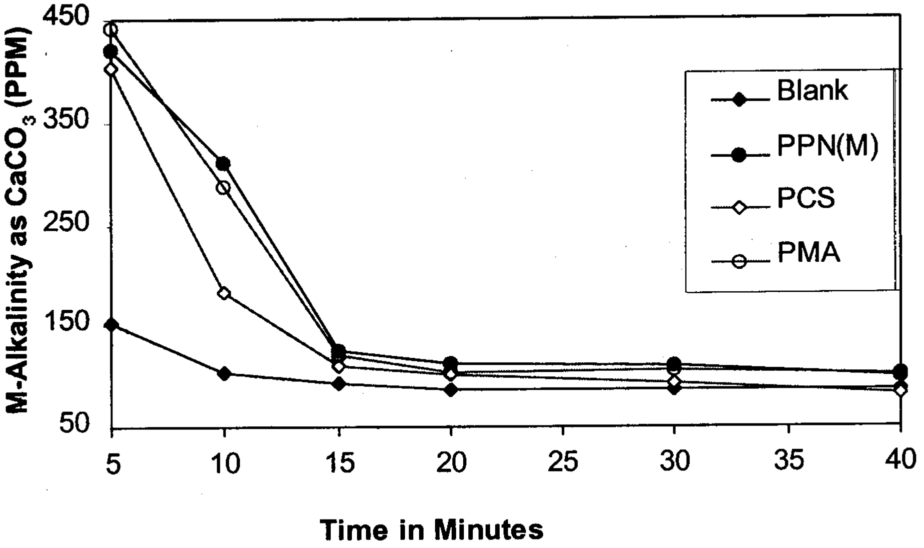

Figure 3. Laboratory Test of Various Antiscalants for their Threshold Effect at 110°C & 2 ppm Concentration

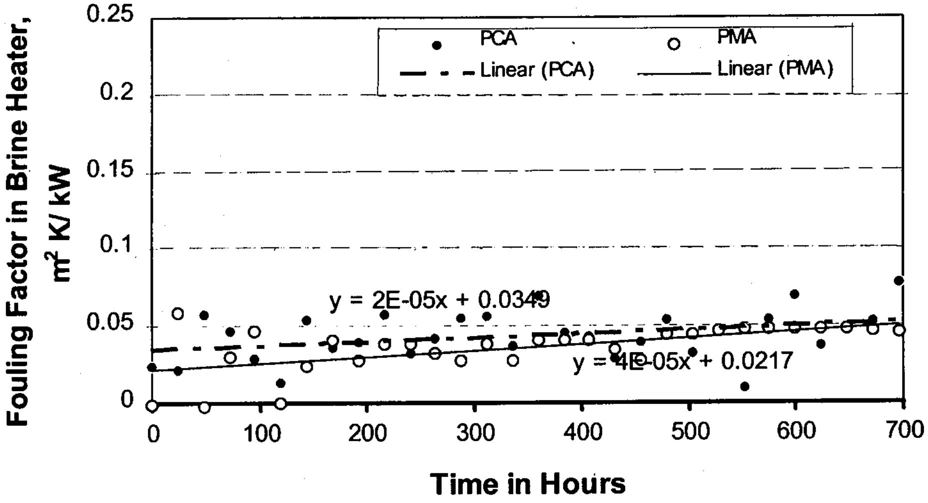

Figure 4. Pilot Plant Tests of Polycarboxylic & Polymaleic Acids at 112 °C and 2 ppm

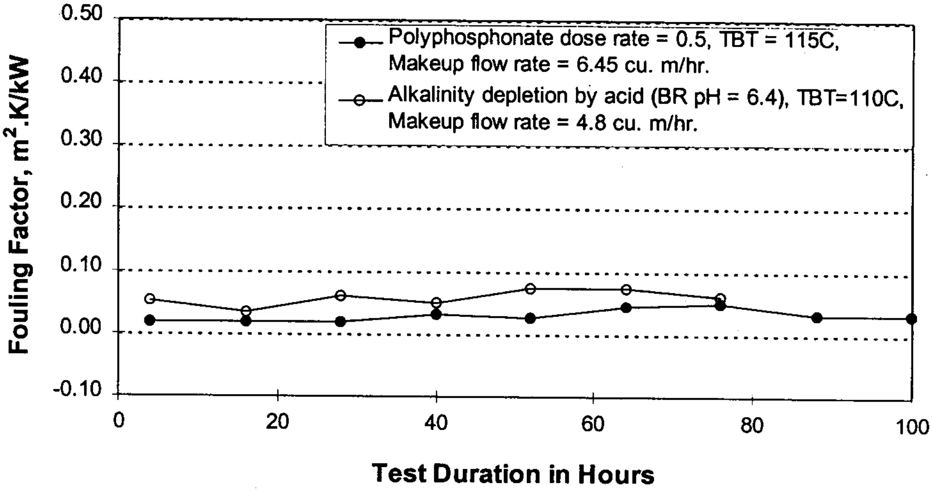

Figure 5. Once-Through Operation in Pilot Plant

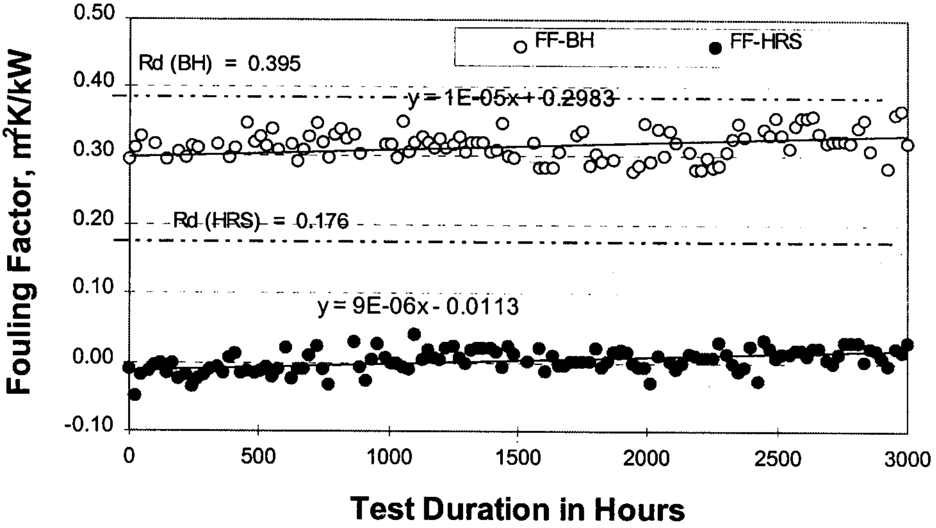

Figure 6. Test of Polycarboxylic Acid in Jeddah IV Unit # 15 at 110 °C and 2.0 ppm

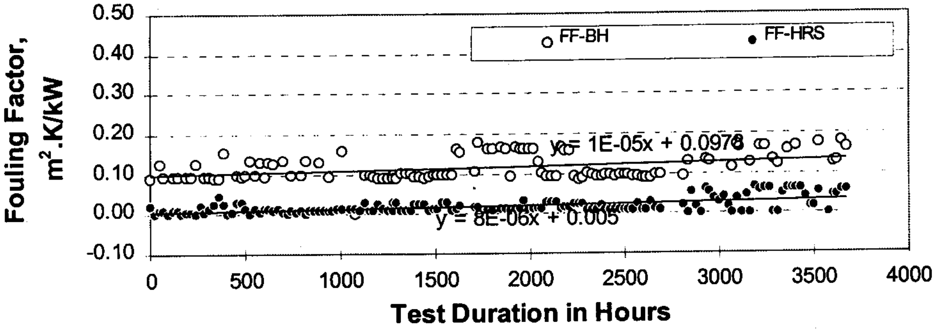

Figure 7.Test of Polymaleic Acid in Jeddah IV Unit # 19 at 110 oC and 1.8 ppm

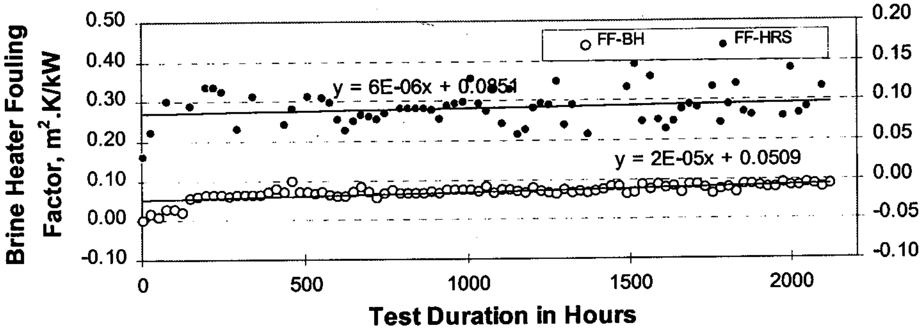

Figure 8. Test of Polyphosphonate in Jeddah III Unit # 10 at 108 °C and 3 ppm

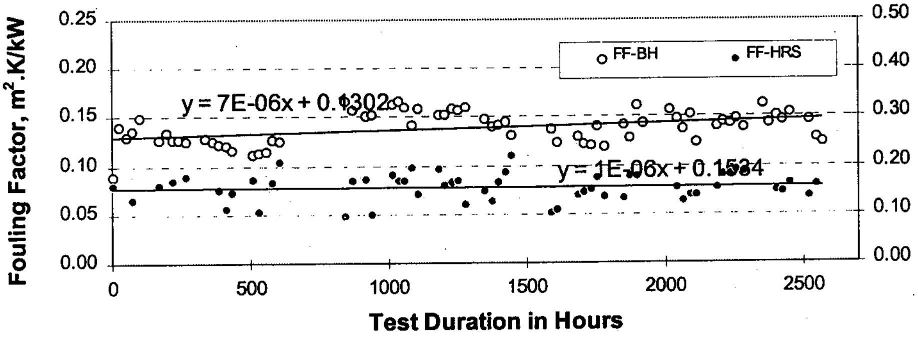

Figure 9. Test of Polycarboxylic Acid in Al-Jubail II Unit # 8 at 105 °C and 1.5 ppm

Investigating Intake System Effectiveness with Emphasis on Self-Jetting Well-Point (SJWP) Beachwell System

A.M. Hassan, A.T.M. Jamaluddin and Ali Rowaili,
Ellen Abart and Robert Lovo

INVESTIGATING INTAKE SYSTEM EFFECTIVENESS WITH EMPHASIS ON SELF-JETTING WELL-POINT (SJWP) BEACHWELL SYSTEM

A. M. Hassan, A.T.M. Jamaluddin and Ali Rowaili
Research and Development Center
Saline Water Conversion Corporation (SWCC)
Al Jubail, Saudi Arabia

Ellen Abart and Robert Lovo
United States Bureau of Reclamation (USBR)
Denver, U.S.A.

ABSTRACT

A well-designed subsurface SWRO intake not only yields good quality feed that requires none or minimum of pretreatment, but also when used instead of surface type intake results in a significant saving in plant capital investment and in cost of plant O&M. An SJWP subsurface intake system was tested at SWCC Al-Jubail site, onshore, at high-tide seawater line and mid-tide point at depths of 3.5 m, 3.5 m, and 4.5 m, respectively. The project objective is to investigate the suitability of this relatively new subsurface SJWP as an intake for some SWRO plants. The best SDI values with an average of $SDI_{ave} = 2.9$, which compares reasonably well with $SDI_{ave} = 2.6 \pm 0.2$ for conventionally pretreated surface seawater feed, were obtained when the well-points were fixed at sea mid-tide point at depth of 4.5 m. The filtrate TDS, total hardness and pH values were lesser than those of seawater indicating mixing of seawater with underground or surface water. At zero incubation time, bacteria count was in the range of $5x10^2$ to $4x10^3$ colony forming units (CFU), but high aftergrowth rates and short bacteria generation time were observed in the SJWP feed after 24 and 72 hours of incubation. Based on SDI measurements, as well as on other physical and chemical measurements, a good quality SWRO feed can be derived from subsurface well-point beachwells located on a clean non-polluted site, which is expected to diminish the high aftergrowth rate and short generation time of bacteria found in the present case. Accurate information on this point can be established by testing the effect on SWRO membrane performance of feed derived from SJWP beachwell located on a clean non-polluted site which is to be conducted under Part 2 of this program.

1. INTRODUCTION

To avoid membrane fouling, which leads to degradation in SWRO plant performance, feed to SWRO plants is pretreated to remove from it all potential membrane foulants, ideally leaving only the dissolved solids in the feed. To a large extent, the success of SWRO plant operation is dependent on the feed quality and the feed pretreatment. An ideal pretreatment is designed to cause a minimum or no membrane fouling at the lowest possible cost. This not only results in longer membrane life but also improves the overall plant efficiency and reduces the cost of fresh water production. The degree and type of pretreatment required are dependent on the raw seawater quality, in particular its content of suspended solids, debris, biological and organic matters, pollutants, residual heavy metals, etc. However, the water quality, is very much dependent on type of **intake** used in SWRO plants.

The design and selection of seawater intake system are very crucial not only to the optimization of both the pretreatment, and the overall plant performance but also to lowering of cost of water production. A fault in intake design and/or intake site selection could make it difficult, if not impossible, for the pretreatment and the SWRO plant as a whole to function properly. On the other hand, a proper intake system that yields high quality feed requires minimum pretreatment. A good example, **a well-designed seawell or beachwell** type intake produces high quality water that requires no further pretreatment. The natural filtration of feed through the porous subsoil strata cleans the feed from nearly all contaminants normally present in feed taken from an open sea. In addition to low oxygen content, the feed is characterized by its constant physical and chemical properties; also unlike surface feed it is unlikely to be affected by changes in weather or sea conditions. In this case, the seawater intake feed can be supplied directly to the membrane system (only with the addition of the necessary antiscalant), thus avoiding the coagulation filtration step, the addition of coagulant, coagulant-aid and disinfectant or other chemicals to the feed stream. Moreover, many of the SWRO plant problems associated with feed supplied from an open sea intake, some of which are caused by the added chemicals, can be eliminated by drawing the feed from sea subsurface regions. Most obvious example is the elimination of chlorine. Chlorine when present in the feed could react with organic present in the same feed to form the harmful THM compounds. It could also degrade organic, mainly humic acids, to form assemble organics which serve as nutrients to bacteria leading to their fast multiplication and thus membrane biofouling. Moreover, many of SWRO membranes are oxidized and, therefore, are degraded by chlorine. Other well-designed subsurface type intakes could work equally good as seawell and are likely to produce high quality feed.

By contrast to the minimum or no pretreatment required to treat feed taken from subsurface intakes, an extensive, complex pretreatment with array of equipment, chemicals and chemical dosing systems is required to clean the surface feed from all the contaminants and membrane potential foulants. The complexity in pretreatment is dependent on type, nature and site of intake as well as on quality of feed required by the different membrane system, i.e., hollow fine fiber, spiral wound or plate and frame. All this is in addition to a higher level of dissolved oxygen which leads to the higher growth and multiplication of bacteria and other microorganism attached to the membrane as well as it may lead to a slow membrane oxidation. Moreover, it is well-known that both the expected inherent decline in membrane flux and salt passage are significantly greater when the feed is taken from an open sea than that derived from seawell.

In this paper results obtained from the application of a relatively new subsurface self-jetting well-point intake system are discussed. This work which is done at SWCC RDC, Jubail, is part of a joint R&D program on SWRO between SWCC and USBR.

2. SWRO INTAKE SYSTEM

The various intake systems that are now in use or may be utilized in the future to supply seawater feed to SWRO plants either from an open sea or from subsurface shore sites can be classified into two major intake systems: (a) Surface Intake consisting of: Pipe systems or Open Channel, Canal Lagoon, (b) Subsurface which can be classified into seawell (beachwell), Well-point, seawater gallery with gravel packing, seabed filtration with filter media packing, and Ranney Collector system.

The submerged pipe tends to be the dominant choice when the SWRO plant feed is taken from an open sea. This system is utilized in all SWCC SWRO plants located on the Red Sea shores with capacity (including SWRO plants under construction) of 87 mgd. Depending on coastal line geology and topography, the intake depth varies from one site location to another for SWCC plants on Red Sea shores the intake depth varies from 4 to 19 m [1,2,3]. This arrangement which places the SWRO intake deep in the sea and away from the coastal line allows for the supply of the SWRO plant with a relatively better quality feed than that obtained from an open channel intake. The open channel intake is rarely used to supply feed to SWRO plants. This type of intake is more suited to deliver feed to MSF plants where, unlike SWRO plants, no extensive feed pretreatment is required.

Seawells are the most used intakes among the subsurface systems. It is employed in many parts of the world to supply feed to a relatively large number of SWRO plants. All the SWRO plants in Malta, capacity 31 mgd, utilize beachwell intake at well depth of about 50 to 60 m [4]. Many of the SWRO plants in Canary Islands [5] as well as in UAE [6,7] and Caribbean Islands are supplied seawater feed from beachwells. Other examples of beachwells and wells with high salinity water TDS > 12000 ppm are described in literature [8,9,10]. Another form of seawell is the seawell infiltration system which bas been reported only for two cases at the Island of Lanzarote, Canary Islands [13]. Seawells or beachwells are drilled onshore at varying depth below the sea floor. The design and construction of seawells are similar to those of artesian wells of same dimension. Central part of the well double casing is perforated with large number of slots of about 0.3 to 0.5 mm for the interior casing as compared to about 0.7 mm for the exterior one. The depth of the well is determined by the soil geology, soil permeability and the quality of water desired from the well. Water quality tends to vary from one subsoil stratum to another. Seawell water turbidity and SDI are about 1 NTU and less than 2, respectively, as compared to a much higher values for surface feed turbidity of up to 20 NTU and SDI values of up to 6.7 or above. The high quality feed expected from seawell and other subsurface intakes constitutes their major advantage over other surface type intakes. This situation not only eliminates the pretreatment process but also leads, as mentioned earlier to lowering in plant capital cost by up to 25% and plant operation cost by up to 15% [12]. The improvement in the quality of seawater derived from wells has also a great influence on plant availability which could exceed 95% and product water recovery ratio reaching 45% [5].

Although feed with constant chemical composition and physical properties is derived from seawells its composition is not necessarily the same as that of seawater. The composition of feed derived from a well or subsurface intake is always influenced by the composition of the subsoil strata from which the seawater flows into the well. Thus, the selection of both site and depth of subsurface intakes are to be thoroughly investigated in advance of well construction by drilling of bore holes at various locations to establish the site suitability for subsurface intake construction and to make sure that the intake can supply high quality feed to SWRO plants at constant feed flow without water depletion.

Directional drilling now allows for drilling of seawells in a horizontal position which has the advantage of increasing the flow from such seawells. A new porous polyethylene well pipe that is now available since 1995 is reported to require no additional external media packing for long-term operation as that required with conventional seawells. The polyethylene pipe porous structure acts as both well screen and packing media. This product is claimed to make the horizontal drilling of wells under the seafloor feasible and economical for the first time [13].

The subsurface intake systems of: seawater gallery with gravel packing, seabed filtration with filter media packing and the Ranney Collectors have one feature in common in that in these cases feed water is collected through a number of horizontally laid PVC screen pipes at certain depth in the subsoil strata. Seabed and gallery filtration systems are similar in design and construction except for their packing system. Instead of crushed stone packing used in the seawater gallery, filter media packing material is used in the seabed filtration system. This way the seabed filtration system functions as both seawater gallery and sand filter giving it the advantage for use in SWRO intakes over the seawater gallery intake system. The three subsurface intake systems of seawater gallery, seabed filtration and Ranney Collectors appear to be promising, and good candidates for SWRO plant intakes with the advantage of possibly supplying greater quantity of feed than that taken from a single seawell, nevertheless, they have not been reported in literature as a feed source to SWRO plants. They are discussed in literature only as a possibility for SWRO intakes. For more information on those subsurface intakes see reference [14].

The well-point beachwell system tested here as a SWRO intake is shown in Figure 1. The well-point itself is similar in design to the well-point system used in ground dewatering, mainly in the coastal areas where water table is high (Figure 2). However, this system offers a finer degree of water filtration than that delivered by the well-points ground dewatering. The well-points are constructed in a fashion similar to that of seawell construction although the well-points are much smaller in diameter. Central part of the double casing is perforated with large number of very fine slots (less than 0.5 mm) in the interior casing. Outer casing consists of a screen normally with media packing in-between the two screens.

The well-point intake system combines features from both the beachwell and the other subsurface intake systems. Like the beachwell intake, the well-points are vertically jetted but at several points on or off shore at shallower depth than that of seawells. Like the subsurface intake of seawater gallery, seabed filtration and Ranney Collector, the well-point system collects the feed from many screen pipes which are vertically laid in the subsoil as opposed to their horizontal burial in the latter three systems. The well-point system, however, differs from all other subsurfaces intake systems in that it can be easily self-jetted at site without major construction as required by other subsurface intake systems. The system, as the name indicates, is self-jetting, the one and same pump used to pump feed to SWRO plant is also used to jet the well-points to the desired underground depth. Unlike other intake systems, which once constructed remain fixed to the site, the well-points can be easily moved for use at other sites.

The well-point intake system has been used by the US Army as a quick SWRO intake system for providing water for mobile SWRO plants in remote areas. The system has been in continuous operation in Port Hueneme, California and San Nicholas Island, USA, since 1993 [13, 15].

3. EXPERIMENTAL

3.1 Site Selection and Bore Holes Drilling

Because of its proximity to SWCC R&D Center, a coastal area about 100m north of Al-Jubail MSF plant intake, was selected as project site. A local company [16] was contracted to drill three onshore test bore holes at about 30m away from the sealine, 30m apart and each at depth of about 10 to 11m. Subsoil samples were collected from the surface (i.e., depth of zero) also from 3, 6 and 9m below ground level. The samples were analyzed by the contractor at his laboratories.

3.2 The Self-Jetting Well-Point Beachwell Intake

The SJWP system used in this investigation (Figure 1) consists of two well-points of 1.5" diameter and 3' in length, followed by three 316 stainless steel risers, each of 1.5" in diameter and 3' in length. The risers are connected to a common header of PVC pipe terminating at the pump. A control valve controls the water flowing through the system.

The beachwells were constructed at the selected site by using the same pump in jetting the well-points slowly through the subsoil to the desired depth, 3-5m, without encountering any difficulties. The well-points were slowly driven in the porous ground by pumping the water at low pressure through its central pipe. The water flowing out (from inside the well-point) fluidize the porous soil around it and allows for the drilling of a shallow beachwell to the desired depth below the sea floor. Based on core sample analytical results, (see section 4.1) it was possible to drive the well-point to a depth of 4.5m without difficulty. Once the well was drilled the system was put into service (using the same pump in reverse). This way, naturally filtered water through the sand layers starts to flow into the beachwell and well-points from which it was continuously pumped. To allow for good formation of the beachwells 15 to 20 minutes were required per jetting of each well-point. Trial tests were made at three location at the selected site where test bore holes were made: onshore at well-point depth of 3.5m, at high-tide seawater line at depth of 3.5m and at mid-tide seawater line at well-point depth of 4.5 m.

3.3 Water Quality Analyses

Various chemical, physical and biological analyses were made according to standard procedures for various samples collected at each of the three site locations. Main emphasis was on the measurement of beachwell filtrate: temperature, pH, conductivity and SDI. Complete chemical and biological analyses were carried out on selected samples. Analyses of residue collected on SDI filter paper were also performed by the scanning electron microscope (SEM) and the energy dispersive X-ray (EDX) method. Prior to bacteria count in CFU/ml each of the samples was incubated at 30°C for different periods of 0, 24, 72 and 96 hours, after culturing on marine agar by the pour plate method for 96 hours, at 30°C.

4. RESULTS AND DISCUSSION

4.1 Soil Structure Analysis

Results of soil analysis done by the contractor at his laboratories showed that the upper subsoil layer at a depth of about 7m consists of sand with silt and in some cases extends to a depth of 9m [16]. Below the sand-silt layer, there was a layer of a very weak lime stone moderately weathered and closely fractured.

4.2 Water Quality Criteria. for Well-point Beachwells

When the saline water is intended for use as feed to a SWRO plant it must meet certain quality requirements. The feed with the highest possible quality standard is a seawater that does not contain any impurities e.g., bacteria and other microorganisms and suspended solids including colloidal matter, organic carbon, that may cause harm to the membrane or other SWRO process components. For certain membranes the case of no chlorine or no oxygen in the feed is also a rigid requirement. Use of the disinfectant and coagulant chemicals which are essential to the pretreatment of surface seawater feed may have an adverse, damaging side effect on the membrane. Dissolved oxygen when present in the feed is also a process variable. It may lead to a slow but progressive damage to the membrane in addition to its influence on speeding up bacteria growth and multiplication which may give rise to membrane biofouling. The ideal feed case is rarely realized in practice, especially if the feed is derived from surface type intake, although quality of feed from a well-designed seawell or subsurface intakes or membrane treated feed could approach this idealized situation. In this investigation the quality of feed derived from the well-point beachwell at Al-Jubail site was evaluated as a possible feed for a SWRO plant mainly by measuring the feed SDI, pH, TDS, biocount and measurements of other relevant chemical and physical parameters.

Tables 1 and 2 list, respectively, the chemical and biological analyses parameters measured for samples collected at the same site. For reasons of comparison the chemical composition of surface seawater is also included in Table 1. Depths are measured below ground level at the location. The SDI values for the filtrate collected at different sites are plotted versus operation time in Figure 3.

4.2. 1 Well-Point Filtrate Chemical and Physical Properties

The best SDI values with an average SDI_{ave} of 2.9 were obtained when the well-points were fixed at mid-tide seawater site at a depth of 4.5 m. This value compares reasonably well with the average SDI_{ave} values of about 2.6±0.2 obtained from SDI measurements made on conventionally pretreated feed derived from an open sea at Al-Jubail. The pretreatment consisted of coagulation with $FeCl_3$ and dual media filtration [17]. Filtrate water conductivity ranged between 18,880 to 26,800 μs/cm at the onshore site and rose to over 40,000 to 49,000 μs/cm at the other two site locations at the hightide and mid-tide water lines. In all cases the conductivity of filtrate from the well-point beachwells is lower than that of surface seawater of about 60,000 μs/cm. Total hardness, is also less in beachwell water than that in seawater. Variation in pH with site location was noticed and in all cases it ranged between 7.1 to 7.9 and was less than the seawater pH of 8.2. Total organic carbon (TOC) of 1.2 to 2 ppm is of the same order, as in seawater of $TOC \leq 2$ ppm. Temperature of filtrate collected from the well-point beachwell also differs from one site location to another. The lower pH, hardness and conductivity values of filtrate samples than those of seawater indicate seepage of surface water or the mixing of ground water with seawater at these three site locations, with a greater mixing ratio of surface water to seawater at the onshore site. This also tends to be true for seawell water from Kuwait beachwell drilled to a depth of 30m where the water TDS and pH are about 38,850 ppm and 7.7, respectively [18].

The H_2S water smell, which was noticeable when the water samples were taken from onshore site, disappeared when the well-points site was shifted toward the sea and was fixed at lower subsoil level of about 1m and 2m at the high-tide line site and mid-tide site, respectively. The presence of H_2S smell in the well-point beachwell filtrate indicates the presence of unaerobic sulfur reducing bacteria in the water at onshore underground at depth of 3.5m. It also indicates lack of sufficient oxygen in that water.

As was established from EDX spectrum the main residues collected on the SDI filter paper are dried seawater salts and ions, mainly Na^+, Cl^-, Mg^{++}, Ca^{++}, S^+ and K^+, most of which disappeared from the EDX spectrum upon washing gently the filter paper with deionized water. From the EDX analysis it appears that no major residue or total suspended solids (TSS) matter are present in the water derived from well-point beachwell at depth of 4.5m below mid-tide sea floor. This, however, does not rule out the presence in the well-point beachwell filtrate of soluble elements such as humic acid and other soluble organics which serve as nutrients to bacteria.

4.2.2 Well-Point Filtrate - Biological Properties

At zero hour of incubation, bacterial count in CFU/ml in filtrate from well-point beachwell and surface seawater are similar in number. At the zero hour, the bacteria count was about $1.8x10^3$ CFU/ml to $4.04x10^3$ CFU/ml in surface seawater and about $5.0x10^2$ CFU/ml to $3.79x10^3$ CFU/ml in subsurface water (Table 2). (Strangely enough and unexpectedly, these numbers compare favorably well with $1.2x10^3$ to $1.3x10^3$ T. count (CFU/ml) in water derived from two beachwells drilled at depth of 30m near the beach in Doha, Kuwait [18]! However, they (bacteria) are not necessarily the same type or possess the same properties, mainly in their ability to attach themselves to membrane surfaces. At 24 and 72 hour aftergrowth, however, the bacteria aftergrowth were faster in filtrate from beachwell than their aftergrowth in surface seawater. This is evidenced by the time in hours required for the bacteria generation (gt) to double in number, Table 2.

In the case of subsurface water where samples were collected from onshore beachwell it is noticed that only 0.207 hour is required for the bacteria to double its population after 72 hours of incubation as compared to more than twice this time of 0.484 hours when the sample is collected from surface seawater and 0.226 hours for subsurface water samples collected from beachwells located at the mid-tide point. The latter value increased to 0.235 hours after 96 hours of incubation indicating the possibility of decreasing nutrients in the sample, as shown in Table 2. This situation, indicates that bacteria aftergrowth is proceeding at a faster rate in subsurface water obtain from this site than in open seawater. Moreover, it indicates the availability of sufficient nutrients in the present subsurface water which partially originates from the accumulated organic seawater residues, e.g., humic acid and is partially due to the residues present in the surface water seeping from the surrounding areas. The data suggest the possibility of a polluted site, which was established to be the case after through survey of the site. Surface and some waste water was seeping to the site from neighboring grounds. A better quality feed with SDI ≤ 2, containing low bacterial count and presumably having low level of nutrients can be obtained by the selection of a non-polluted site.

5. CONCLUSION

From the above discussion it can be concluded that based on SDI, as well as on other physical, chemical and biological measurements (Tables 1 and 2, also Figure 3) a good SWRO quality water with low TSS content can be derived from subsurface well-point beachwell. The high aftergrowth rate and short generation time of bacteria found in the feed may be attributed to the site itself, which was found to be polluted by the seepage of surface and waste water. Changing the site to a clean non-polluted site could alleviate this effect and may result in good quality feed to SWRO plants and in consequence to good plant performance. To a certain degree, however, this should depend on type of bacteria and nutrients found in SJWP beachwell feed and the bacteria ability to condition and to attach themselves to membrane surface. These conditions are essential for the formation of biofilm [19]. Accurate information on this point can be established by testing the effect on SWRO plant performance of feed derived from SJWP beachwell located on a properly selected clean non-polluted site. This work is to be conducted soon.

6. RECOMMENDATION

From the trial tests made with this subsurface SJWP beachwell intake good quality water with an $SDI_{ave} = 2.9$ was obtained but high aftergrowth rates and short generation time of bacteria may be expected to give rise to a decline in SWRO plant performance. This latter factor can be corrected by the selection of a clean non-polluted site. Moreover, the experiment done so far was exploratory in nature and it is, therefore, recommended: (1) to conduct further experiments on a clean non-polluted site; (2) to work on optimization of the SJWP beachwell intake by improvement of yield and filtrate quality; (3) to determine design criteria for small to medium size SWRO plants; and (4) to perform process technoeconomic analysis. These recommendation were accepted by SWCC and a future evaluation of the system is under way.

7. REFERENCES

1. Hassan, A. M., Abanmy, A.M., Al-Thobiety, M, Thomas, M., Al-Luhibi, T., Al-Masudi, I., Al-Gherier, A. A., Bakheet, L. M., Amri, M. M. I., Khalid, A. and Al- Hydaibi, M. Performance Evaluation of SWCC SWRO Plants Part II. Presented at IDA World Conference on Desalination and Water Reuse, August 25-29, 1991.

2. Hassan, A. M., Al-Jarrah, S., Al-Luhibi, T., Al-Hamdan, A., Bakheet, L. M. and Al-Amri, M. M. I. Performance Evaluation of SWCC SWRO Plants. Published in Desalination, 74, 1989 pp 37-51.

3. Nada, N, Yanaga, Y., Serizawa, and Tanaka, K., Design Features of the Largest SWRO in the World. Proceeding IDA World Congress on "Desalination and Water Science", Abu Dhabi, Nov. 18-24, 1993. Vol. V pp 3-16.

4. Lamendola, M. and Tua, A., The International Desalination and Water Reuse, May/June (1995) 18-22.

5. DuPont Permasep Products, Pamphlet, When the Modern World Embraces an Ancient Paradise, Permasep Permeators Help Canary Islands Meet New Demand for Fresh water, 8/91.

6. Schierach, M. SWRO Plant in Fujairah, UAE. Proceeding IDA World Congress on "Desalination and Water Science", Abu Dhabi, Nov. 18-24, 1995. Vol. III, pp 99-108.

7. Hydrotechnik, Salzburg, Austria, the 9000 m^3/d SWRO Desalination Plant in Fujairah, UAE, 1991.

8. Heyden. W., Desalination 52 (1985) 189-199.

9. Al-Arrayedh, M. I., Ericsson, B. and Yoshioka, H., Reverse Osmosis Desalination Ras Abu Jarjur, State of Bahrain - Two years operation experience for the 46,000 m^3/day RO Plant, Proceedings of the Third World Congress on Desalination and Water Re-use. Vol. 1/2 (1987) p 197-230, also Desalination, 64(1987) 65-82.

10. Al-Arrayedh, M. I., Ericsson, B., and Ohtani, M., Construction and operation of 46,000 m^3/day Reverse osmosis Desalination Plant, Ras Abu Jarjur, Bahrain, Desalination 55 (1985) 319-342.

11. Redondo, Jorge A. and Frauk, K. W. T. F., Pamphlat., 1991 DOW Europe, Systems in Filmtec Membranes Seawater Applications with Filmtec RO Membranes, 10 Years of Desalination Experience:

    (a) Case Study of 3000 m^3/d Plants Lanzarote and

    (b) Case study of 5000 m^3/d SWRO Plant Inalsai.

12. Soo-Hoo, R., Parametric Study of SWRO Desalting Plants, Report Prepared for U. S. Department of Interior, USBR, Contract # 14349001 - 1486, Jan, 1983.

13. Kuepper, T., A Proposal to SWCC for the Development of a Sub-floor Seawater Intake Structure System (SWISS) for Reverse Osmosis Desalination Plants, 1993, The Naval Facilities Engineering Service Center, 560 Center Drive, Port Hueneme, CA 93043-4328.

14. Hassan, A. M., Jamaluddin A. T. M., Al-Rowaili, A., Abart, E. and Lovo, R., "Investigation Intake System Effectiveness", Final report, Project APP 93013, SWCC, RDC, May, 1997.

15. Lovo, R., Pacific Research Group, 162 Fraser Lane Venfurd, Ca 93001, Beach Well Intake Structure, a Lecture as Part of SWCC/USBR Seminar on the Same Subject.

16. Fugro-Suhami, Nearshore Soil Borings, SWCC Desalination Plant, Al-Jubail, Saudi Arabia, Report submitted to SWCC R&D Center, December 7, 1997.

17. Hassan, A. M., Abanmy A., Farooque, A. M., Jamaluddin, A. T. M., Al-Amoudi, A. and Mani T., Optimization of SMRO Pretreatment - Part I: SDI measurement, Proceeding IDA World Congress on "Desalination and Water Science", Abu Dhabi, Nov. 18-24, 1993. Vol, V pp 115-129.

18. Bou-Hamad, S., Abdel Jawad, M., Al-Tabtabaei, M. and Al-Shammari, S., The 3rd Gulf Water Conference, Muscat, Oman, 8-13/3/1997.

19. Winters, H., Biofouling History and How it Affects Desalination Plants, Proceeding IDA World Congress on "Desalination and Water Science", Abu Dhabi, Nov. 18-24, 1995. Vol. I, p 255-264.

Table 1: Chemical Composition of Well-point Beach Well Water Samples From On-Shore, High-Tide and Mid-Tide Test Areas

Parameters		**Seawater**	**On-Shore**	**High-Tide**	**Mid-Tide**
Temperature °C			25	24	23.5
pH		8.2	7.5	7.62	7.3
Conductivity at 25 =°C	(µS/CM)	60000	1900	40100	41000
T.D.S. at 105 °C	(ppm)	46900		31289	31430
Total Hadness (as CaCO3)	(ppm)	6738		5250	5850
Calcium as Ca^{++}	(ppm)	519		480	480
Magnesium as Mg^{++}	(ppm)	1326		984	1130
Sodium as Na^{+}	(ppm)	12860		7888	9000
Potassium as K^{+}	(ppm)	450		344	392
Sulfate as SO4^{-}	(ppm)	3265		5400	5514
Chlorides as Cl^{-}	(ppm)	23000		13650	16661
TOC	(ppm)	2		1.2	2

Table 2: Bacterial Count (CFU/ml) and generation time in hours/double generation, (hrs/2g) in Well point water at two different locations: on-shore and at mid-tide seawater line

Sample	**0h**	**24 h**		**72 h**		**Locations**
	CFU/ml	**CFU/ml**	**hrs/2g**	**CFU/ml**	**hrs/2g**	
Raw seawater	1.8x10^{3}	1.1x10^{5}	0.404406	5.6x10^{4}	0.483831	Onshore
Well water	1.3x10^{3}	3.3x10^{5}	0.300394	4.0x10^{6}	0.20708	
Raw seawater	4.04x10^{3}					Mid-tide point
Well water	3.79x10^{3}					
Raw seawater						
Well water	5.9x10^{2}	4.86x10^{5}	0.247727	9.3x10^{5}	0.225892	Mid-tide point

Generation time = t x 0.693/ (Ln Nt - LnNo) : Where: t = time; Nt = Bacterial count at time t hrs; No Bacterial count at zero hrs

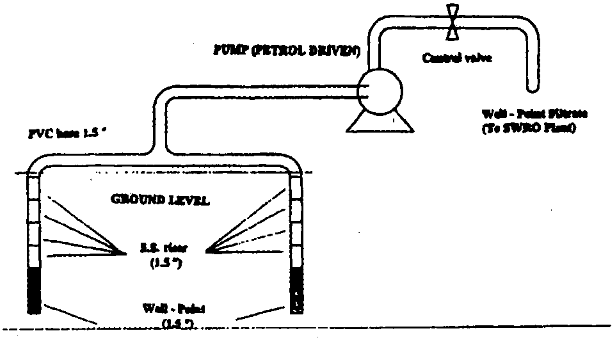

Fig. 1: Two Well-Point Beach Well Layout

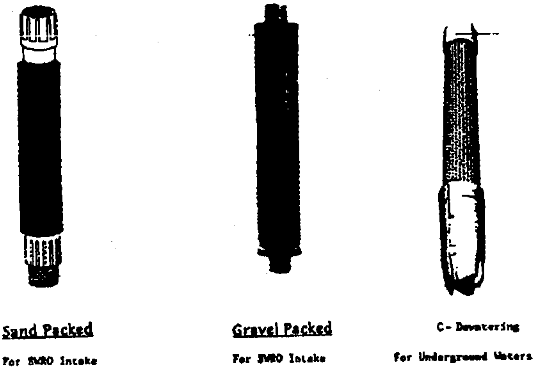

Fig. 2: Fine Water Filtering Well-Points

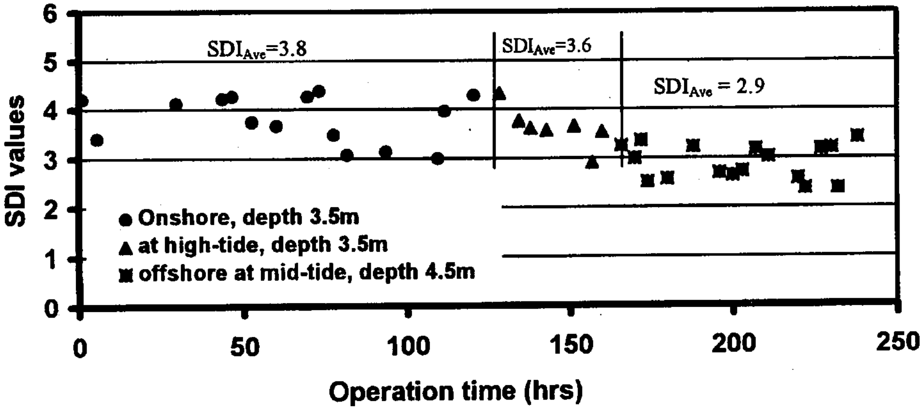

Fig. 3: Quality of water at different well-point depth as well as different locations onshore and offshore

CORROSION BEHAVIOR OF STEELS IN GULF SEAWATER ENVIRONMENT

Anees U. Malik, Shahreer Ahmad and **Ismaeel Andijani**
SWCC, R&D Center, Al-Jubail

Saleh Al-Fouzan
Al-Jubail Desalination Plant

ABSTRACT

Due to the aggressive environment prevailing in and around the Gulf seacoast, the materials of construction are subjected to corrosion of varying degree. There are many factors influencing the initiation of one or several corrosion processes. These factors include nature of material, surface finish, temperature, humidity, wind directions, rainfall, etc. Steels are the predominant constructional materials in seashore structures including desalination plants which are subjected to general or localized corrosion of varying degree. A complete systematic information regarding corrosivity of materials in Gulf seawater is lacking. Keeping in view the importance of the corrosion data of materials particularly steels in Gulf seawater, a systematic study on this subject had been initiated in 1990 and was completed in 1996. This paper provides the results of this study concerning the corrosion behavior of steels, in Gulf seawater. The steels include carbon steels, stainless steels and super stainless steels (austenitic, ferritic and duplex). The study encompasses the factors influencing general, pitting and crevice corrosion of materials. The effects of TDS in general and chloride concentration in particular and degree of chlorination have been discussed in detail. The role of dominant alloy addition on the corrosion behavior of steels has been emphasized.

Weight loss and electrochemical techniques have been employed in determining the corrosion rates of materials. Potentiodynamic polarisation technique has been used to evaluate parameters related to localized corrosion. Both exposure and accelerated tests have been carried out to study crevice corrosion attack. Effect of surface finish on crevice attack has been investigated in detail. Rank orders of corrosion rates of steels under different conditions have been presented and their importance concerning materials selection in desalination plants is discussed.

Keywords: Pitting, Crevice Corrosion, Stainless Steel, Breakdown Potential, Pitting Potential, PRE_N and Chlorination

INTRODUCTION

Steels are the most extensively used structural materials in industry. Mild steel is the most versatile general purpose material due to its good mechanical strength, easy fabricability, formability, weldability, abundance and low cost. In corrosive enrionments, mild steel structures can be protected by coating and / or cathodic protection. However, in more severe or aggressive environments such as marine or seawater, mild steel may not withstand and austentic stainless steels such as 304 and 316 have round applications as construction materials. The excellent corrosion resistance, good mechanical properties and reasonable cost are the contributing factors for their application as outstanding structural material. In seawater process industries which also include desalination plants, 316 type alloys have been formidable material for construction of evaporators, distiller pipes, pumps valves and condensers. These alloy are the most dependable structural materials under dynamic or flow conditions and virtually show no corrosion even on very long exposures. However, these alloys are subject to localized corrosion in presence of chloride ions and under static or stagnant conditions. The pitting of 316 L stainless steel is often encountered in desalination plant and appears to be the most effective factor responsible for corrosion failure in plants. The pits also provide active crevices for a formidable corrosion attack. In most cases, pitting is precursor of crevice corrosion and there are obvious similarities between crevice and pitting corrosion mechanisms. High chromium containing Ni-base alloys (Cr-Ni-Mo) were used as possible replacement for stainless steels to combat localized corrosion. However, the prohibitive cost of Ni-base alloys has severely restricted their application. Based on the fact that Cr and Mo has synergic effect in enhancing the pitting resistance of steel in seawater, 6% Mo containing stainless steels so called high alloy stainless steels were introduced in sixties and the following decades. The application of conventional and high alloy stainless steels in marine environment have been dealt in a number of review and articles [1-6].

Electrochemical techniques have been the principal tool for characterizing pitting and crevice corrosion. The pitting potential, Epit is a fundamental parameter in evaluating the susceptibility of different materials in different environment to localized corrosion [7]. Some authors [8,9] asserted that due to similarities between crevice and pitting corrosion mechanisms, it would be more appropriate to refer to localized corrosion by a new parameter called breakdown potential, Eb, which is defined as potential where pitting or crevice corrosion or both will initiate or propagate.

Temperature and velocity are the two important factors influencing the corrosion of SS superaustenitic and Ni- and Co- base alloys in seawater [8]. Electrochemical studies explicitly demonstrated the effect of increased temperature in facilitating premature breakdown of passive film on all materials. The effect of high velocity impinging flow was to further shift the passivity breakdown potential to active values but not necessarily to result in greater depth of attack. In general, increase in temperature caused a decrease in pitting potential and an increase in corrosion rate and pitting tendency [10, 11]. However, at a certain temperature, the decrease in Dissolved Oxygen (DO) level could result in reversal of the process.

The Cr, Mo and N contents of the alloy greatly influence their pitting and crevice corrosion behavior. The synergic effect of Cr and Mo in resisting pitting was first shown by Lorenz and Madwar [12] in 1969 and was further investigated by Herbsleb [13] in 1982 who also considered nitrogen. The pitting resistance equivalent, PRE_N is represented by the equation

$$PRE_N = \%\ Cr + 3.3\ \%\ Mo + 16\%\ N$$

A PRE_N above 38 is supposed to provide resistance to marine corrosion. Crevice corrosion of highly alloyed SS ($PRE_N > 40$) exposed to seawater, once initiated can propagate at temperature far lower than the initiation temperature. Repassivation properties of the material are thus important with respect to material selection and control.

This paper incorporates the results of various studies concerning with the corrosion behavior of conventional and high alloy stainless steels in Gulf seawater. A number of studies carried out in recent years signified the importance of PRE_N in assessing the ability of alloy to resist to pitting. Interesting yet useful relationship have been shown between PRE_N and several corrosion parameters such as pitting potential, Epit, pitting induction time, ti, corrosion rate (CR), etc., [13]. Alloy addition such as Mn appeared to negate the resistance to pitting [14].

Chlorination of seawater is the normal practice to destroy microorganism or microbiological growth, the residual chlorine influences significantly on the corrosion behavior of materials. The results of a number of studies concerning with pitting and crevice corrosion tendencies of conventional and high alloy steels in chlorinated seawater are reported in literature [15, 16]. High alloy stainless steels appear to have good resistance to residual chlorine. In such study [17] it has been shown that besides 254 SMO which did not corrode in seawater (25,000 to50,000 ppm Cl^- and 0-10 ppm residual chlorine) all other alloys developed crevice and suffered some degree of corrosion.

Critical crevice temperature and critical crevice index (CCI) have been used for measuring crevice corrosion tendencies of superaustenetic and duplex steels in chlorinated seawater [18] Critical Crevice Temperature (CCT) was found to be in the same range. No significant difference in CCT for metal-metal and metal-gasket crevices was found. Even the Ni-base alloys which were supposed to have formidable resistance against crevice attack in seawater have been found to be vulnerable. Creviced Ni-Cr-Mo-Fe alloys (alloy 625 and C 276) immersed in two different types of seawater were found to contain concentrated amounts of dissolved Ni^{2+}, Cr^{3+}, Mo^{3+} and Fe^{2+} in crevices showing that both the alloys undergone crevice corrosion [19].

EXPERIMENTAL

15 different commercial grade stainless steels, viz., 304L, 316L, 317L, 904L, 17-4PH, 254 SMO, 654SMO, HMO 1925, HMO 3127, 20Cb3, Remanit 4565, Remanit 4575, Monit 44635, Martensitic 410 and Duplex 2205 were used during the studies. Table 1 lists the composition of the alloys.

Aqueous chloride solutions of varying chloride concentration, seawater (Arabian Gulf seawater) and chlorinated seawater were used during the experiments. The composition of the seawater is given in Table 2. The chlorinated seawater was prepared by dozing with sodium hypochlorite and the residual chlorine was measured by HACH DREL/IC portable kit. For potentiodynamic polarisation studies, circular specimens of ~15 mm diameter and 3-5 mm thickness were machined from the sheet and were abraded sequentially on 180, 320 and 600 grit SiC papers. Rectangular coupons of the size 10 x 20 x 3-5 mm were cut from the sheet and surface furnished at 0. 12 μm rms were used for open circuit potential measurements.

Experimental details of crevice corrosion measurements and potentiodynamic polarisation and cyclic polarisation experiments carried out in this study are described in previous publications [2, 7, 10, 13].

Open Cricuit Corrosion Potential (OCP) of alloys was measured in normal and chlorinated seawater. The residual chlorine was monitored everyday. A special cell was designed and fabricated in the laboratory. Two multiples chart records of 6 and 3 pens were electrically connected to the specimens. The change in voltage against SCE as reference was plotted vs time. Every day the data were transferred into the computer and combined graph was drawn to study the change in potential for each of the alloys.

Accelerated Tests

Salt spray tests were carried out in Salt Spray fog Chamber following ASTM B17-73. Test coupons of 12 cm^2 were cut from the sheet and abroded to 180 grit SiC paper. Accelerated testing for resistance to crevice corrosion initiation was also carried out. The crevice corrosion assembly consisting of the specimen (rod or sheet form) attached with Teflon crevice former was mounted in epoxy former to provide a crevice free mount. The experimental details of salt spray and crevice corrosion accelerated tests are given in previous papers [7, 20].

RESULTS AND DISCUSSION

Accelerated Tests

The conventional (316 L and 904L) and high alloy stainless steels (SMO 254 and 654 hMo 1925 and 3127, 20 Cb3, Remanit 4565 and 4575, Monit 44635) were subject to salt-salt fog environment in a salt spray fog chamber for testing under accelerated conditions. Results of 3024 and 5000 hours exposure tests indicate very low weight losses corresponding to corrosion rates in the range of 0.001-0.005 mpy. This leads to a foregoing conclusion that conventional and high alloy stainless steels are resistant to general corrosion under severest environments.

A study of the potentiodynamic polarisation curves for the high alloy stainless steels in seawater indicate that little or no corrosion current was noticed on chloride additions showing thereby the outstanding resistance of these steels towards chloride. For getting measurable corrosion current, polarisation experiments involving most aggressive conditions were carried out. In these experiments, such conditions were produced by bringing down the pH to low values (0-3) plus addition of NACl solution at 50°C. Critical corrosion current value representing as active peak height (APH) is taken as the measure of critical crevice solution (CCS). The CCS of the alloy is taken as the value corresponding to APH of 10 $\mu A\ cm^{-2}$. Conventional alloys such as 304L and 316L and high alloy stainless steels such as 3127hMo and 654SMO have low CCS pH values of 0.481 and 0.50, respectively (Fig. 1). These results indicate excellent crevice corrosion resistance of high alloy stainless steels under aggressive conditions. Plots of critical crevice index (CCI = % Cr + 4.1% Mo + 27%N) and CCS pH for conventional and high alloy steels show a liner relationship (Fig. 2) indicating a strong but negative dependence of critical crevice solution aggressivity on Cr, Mo and N content.

Effect of Surface Finish

The surface finish has a considerable influence on the localized corrosion behavior of stainless materials in seawater. Under surface finish conditions of wheel ground, as received, 180 grit SiC ground, 600 grit SiC ground, sand blasting and HNO_3 etching, except 304 L and 316L, none of the alloys corroded to measurable depth of attack at 25°C thus indicating that crevices do not act as sites for corrosion initiation for high alloys stainless steels. Stainless steels 304L and 316L provide small yet measurable crevice corrosion depth. At 50°C, under aforementioned conditions, most of the high alloy steels either do not corrode or corrode surficially. The surficially corroded alloys showed very small crevice corrosion buildup. However, after crevice formers were removed and sample were cleaned, no perceptible depth of attack was found when examined microscopically. This has been attributed to high propagation resistance of the alloy due to the strong passivation of the protective passive film on the metal surface. Therefore, the crevice corrosion initiation of an alloy does not necessarily relate to its propagation rate. Solution immersion tests indicate that alloy SS 304 and 316L show mild attack at 25°C, the attack is more pronounced at 50°C, the former was attacked more severely.

Effect of Temperature

The temperature greatly influences the corrosion behavior of steels in seawater as has been indicated by the values of corrosion parameters from electrochemical studies. Pitting potential of the conventional and high alloy steels measured in the temperature range of 25-90°C indicate a shift to more active values up to the temperature of 65°C.

Above 65°C, Epit becomes constant. The constance in the Epit values has been attributed to the decrease in dissolved oxygen level due to increase in temperature. This factor plays more prominent role at higher temperature (> 65°C). A liner relationship (Arrhenuis plot) exists between logarithm of corrosion rate and reciprocal of absolute temperature (Fig. 3). The slop of line provides activation energy for the process in the temperature range of 25°C to 90°C. In general, with same exposure time, the severity of corrosion attack increases with increases in temperature.

Effect of Chloride Concentration

The effect of chloride concentration on corrosion rates of stainless at 50°C as studied by electrochemical liner polarisation resistance technique indicate that the corrosion rates do not follow a regular pattern but in majority of the alloys, the corrosion rate increase with increasing chloride content.

Whilst the corrosion rates of conventional stainless steels such as 304L, 316L and 317L in seawater are higher than in aqueous chloride solutions containing up to 5000 ppm chloride, the high alloy steels in general appear to have slightly lower corrosion rates in seawater (Fig. 4). The lower corrosion rates in seawater have been attributed to the formation of a stable biofilm which acts as a barrier against corrosion.

The pitting potential, Epit which is a measure of pitting tendency of a material under specific environment show a significant active shift with increasing chloride contents. Due to the formation of a strong and more resistance passive oxide film, the high alloy steels have much higher pitting potential than conventional stainless steels. This is further manifested by the strong dependence of Epit on PRE_N, the pitting resistance equivalent. Alloys having greater PRE_N have lower tendency to pitting, requiring much higher potential (Epit) to initiate pitting in the alloys. Two separate liner relationships exist for conventional and high alloy stainless steels.

Effect of Chlorination

Results from potentiodynamic cyclic polarisation studies carried out on conventional and high alloys stainless steels under chlorined and normal conditions indicate that the breakdown potential, Eb is lowered on chlorination (Table 3). The lower Eb values indicate more chances of breakdown of passive film easily and early start of pitting and crevice corrosion. Low decrease in E_b was observed for 3127 hMO, 1925 hMo, Remanit 4565 and 654 SMO. Therefore, these alloys have less chances of crevice and pitting corrosion in seawater and chlorinated seawater. SS 316L and 317 at 25°C can suffer from general as well as crevice and pitting corrosion due to low E_b and high I_{max} values. Plots of E_b vs PRE_N for high alloy SS show that the alloys having PRE_N values of 30 or above are quite resistant to chlorinated seawater (Fig. 5).

The open circuit potential of the alloys increases with increase in residual chlorine at 25°C. Whilst E_b values of superstainless steels at different levels of residual chlorine are much higher than conventional stainless steels, the open circuit potential values of superstainless steels markedly lower than the conventional stainless steels.

Open Circuit Corrosion Potential (OCP) Measurement

Results from OCP measurements can be very well analyzed from corrosion potential vs time plots. These plots indicate 4 distinct stages:

(i) Increase of potential in the noble direction resulting from thickening or healing of the passive film.
(ii) Constancy in corrosion potential although at time fluctuations in active direction characteristic of local breakdown of passivity may be observed.
(iii) Steep or gradual fall in corrosion potential from the passive region representing pit initiation stage.
(iv) Corrosion potential sustains low values during propagation stage.

The OCP vs time plots provide information about induction time for pit or, crevice initiation, t_i, which is indicated by a constancy in potential. Due to the presence of a strong passive film, high alloy stainless steels have much larger induction time than the conventional steels. In high alloy stainless steels induction time increases with increasing PREN whereas with conventional stainless steels an opposite effect is found. The latter behavior indicates that conventional steels are susceptible to pitting in much shorter time and pitting behavior is greatly influenced by low Cr + Mo t_i contents. This behavior is also manifested by two separate liner plots of Epit vs ti [Fig.6] obtained for the two categories of alloys indicating strong dependence of Cr + Mo contents on the pitting behavior of the alloys.

CONCLUSION

(i) The corrosion rates of conventional austenitic steels and high alloy stainless steels in seawater, under static conditions and at 25°C and 50°C, as determined from immersion and salt spray tests, are extremely low (0.001 - 0.005 mpy). The corrosion rates as determined from electrochemical polarisation technique are low (0.01 - 0.1 mpy) but are about one order of magnitude higher than from immersion tests. This has been attributed to the time lag for stabilisation of protective oxide film.

(ii) High alloy SS when creviced in seawater at 25 and 50°C, show very small corrosion build up but no perceptible depth of attack indicating absence of propagation stage during crevice attack.

(iii) In the temperature range of 25-65°C, a linear relationship exists between logarithmic of corrosion rate and reciprocal of absolute temperature (Arrhenius plot).

(iv) Pitting potential, Epit shows a significant active shift with active chloride contents. Due to the formation of strong and more resistance passive oxide film, the high alloy stainless steel have much higher Epit than conventional high stainless steels.

(v) With the exception of 3127hMo, all other alloys show lowering in breakdown potential, E_b on chlorination. A low shift in E_b indicates a lesser vulnerability of the alloy towards crevice and pitting corrosion in seawater.

vi) Pitting Resistance Equivalent, PRE_N, appears to be a function of Epit, ti, E_b and CSPH. In general, two separate relationships exist for conventional (304, 316, 317, 904) and high alloy SS (254 and 654 SMO, hMO 1925 and 3127, Duplex 2205, etc.).

(vii) For seawater applications, conventional and high alloy SS can be used without risk of localized corrosion in crevice and deposit free systems. However, for crevice forming system, only high alloy SS appear to be satisfactory materials for seawater applications including desalination plants.

REFERENCES

1. Hassan, M. A., and Malik, A. U. (1989), Desalination, **74,** 157-170

2. Malik, A. U., Siddiqui, N. A., and Andijani, I. N., (1994) Desalination, **97**, 189-97.

3. Tuthills, A. H., et al. (1995) The suitability of 6% Mo Austenitic SS for Desalination plant Services, Proc. IDA World Conference on Desalination and Water Science, Abu Dhabi, November 18-24, Vol. VII p. 412.

4. Todd. B., (1977) Materials for Seawater System, Chemistry and Industry, July 2, 14-22.

5. Oldfield, J. W., and Todd, B., (1995) A Review of Materials and Corrosion Desalination - Key Factors for Plant Reliability - Award Winning Treatise. IDA World Congress on Desalination and Water Science, Abu Dhabi, November 18-24.

6. Oldfield, J. W., and Todd, B., (1996) Desalination, **108,** 27-36.

7. Malik, A. U., et al. (1992) Corrosion Science, **33,** 51.

8. Neville, A. and Hodkiess, T., (1996) Corrosion Science, **38**, 927-956.

9. Salvago, G., and Fumagalli, (1996) Corrosion, **52,** 760-767.

10. Malik, A. U., and AI-Fozan, S., (1 994) Desalination, **97,** 199-212.

11. Al-Ghamdi, A. M., Nusair, Y. H., Cocks, F. H., (1996) Corrosion Behavior of Selected Metals in Arabian Gulf Seawater, Proceeding of the 7th Middle East Corrosion Conference Bahrain pp 475-486.

12. Lomz, K., and Mesawar, G., (1 969) Thyssen Forschung, **1(3),** 93.

13. Malik, A. U., et al. (1995) Desalination 97, 171-187.

13. Herbsleb, G., (1982) Werkstoffe and Korrosion, **33,** 334.

14. Jargelius - Patterson, R. F. A., (1998) Corrosion, **54,** 162-167.

15. Wallen B., and Henrikson, S., (1989) Werkstoffe und Korrosion, **40,** 602-615.

16. Oldfield J. W., (1995) Corrosion Initiation and Propagation of Ni-Base Alloys in Seawater Applications, Corrosion '95 paper 266 NACE.

17. Boah, J. K. and Frazer, P. (1996) Localized Corrosion Tendencies of Piping Materials used in Chlorinated Seawater, Proceeding of the 7th Middle East Corrosion Conference, Bahrain, p 409.

18. Steinsmo, U., et al., (1997) Corrosion, **53,** 26-32.

19. McCafferty, E., et al. (1997) Corrosion, **53,** 755-761.

20. Malik, A. U., et al., (1995) Corrosion Science, 37, 1521-1535.

Table 1: Composition of Stainless Steels

UNS No.	Alloys	Product	Fe	Cr	Mo	Ni	C	Cu	Mn	Others
S30403	304L	-	Balance	18	-	10	0.03	0.2	1	0.45P, 0.02S, 1.0si
S31603	316L	-	Balance	16	3	11	0.02	0.2	1	0.045P, 0.02S, 1.0SI
S31703	317L	-	Balance	18	3	13	0.02	0.2	2	0.045P, 0.02S, 1.0si
N08904	904L	AVESTA	Balance	20	5	24.5	0.02	1	1.5	0.045P, 0.02S
S31254	SMO 254	AVESTA	Balance	20	6	18	0.02	0.7	-	0.2N, 0.002Si
S32654	SMO 654	AVESTA	Balance	25	7	22	0.015	0.4	0.5	0.5N
N08925	hMO 1925	VDM	Balance	21	6	25	0.01	0.9	0.9	0.2N, 0.002Si
N0828	hMo 3127	VDM	Balance	27	6.5	32	0.02	1	2	0.003S, Nb, Pb
-	Remanit 4565	THYSSEN	Balance	22-25	4-6	16-18	0.02	0.1	5	0.5N, 0.003Si, 0.1Nb
S44635	Monit 44635	AVESTA	Balance	25	4	4	0.025	0.2	0.4	0.035N, Ti, Nb, Pb, Si
-	Remanit 4575	THYSSEN	Balance	27-29	2-3	3-4.5	0.01	-	0.1	0.025N, Ti, Pb, Si, Nb
S31803	Duplex 2205	AVESTA	Balance	22	3	6	0.02	0.2	1.5	0.15, 0.6 (Cb+Ta)
S41000	410	-	Balance	13	-	-	-	-	1	0.04P, 0.035S, 1Si
S17400	17-4PH	ARMCO	Balance	16	-	4.5	0.07	4	1	0.3Cb, 0.04P, 1Si
N08020	20Cb3	CARPEN-TER	Balance	19	2	33	0.02	3	0.4	0.4Si, 5Cb+ Ta

Table 2: Gulf Seawater Composition, pH 8.2

Ions		Concentration mg/L
Calcium	Ca^{++}	508
Magnesium	Mg^{++}	1,618
Sodium	Na^{+}	13,440
Potassium	K^{+}	483
Strontium	Sr^{++}	17
Bicarbonate	HCO_3^{-}	176
Chloride	Cl^{-}	24,090
Sulphate	SO_4^{--}	3,384
Bromide	Br^{-}	83
Fluoride	F^{-}	1
Total Dissolved Solids	TDS	43,800

Table 3: Breakdown Potential (E_b) of Stainless Steels in Gulf Seawater at 25°C

S.No.	Alloys	E_b (mV) Normal Seawater	E_b (mV) Chlorinated (0.20-0.25 ppm)
1	316-L	228	197
2	317-L	524	300
3	904-L	1016	905
4	3127hM$_o$	950	905
5	1925hM$_o$	968	989
6	254SMO	918	911
7	Duplex-2205	1010	1003
8	Remanit 4565	1039	952
9	654 SMO	1001	948

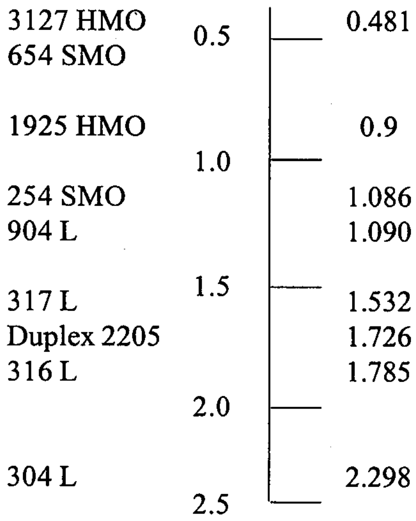

Figure 1 Predicted ranking of conventional and high alloy stainless steels.

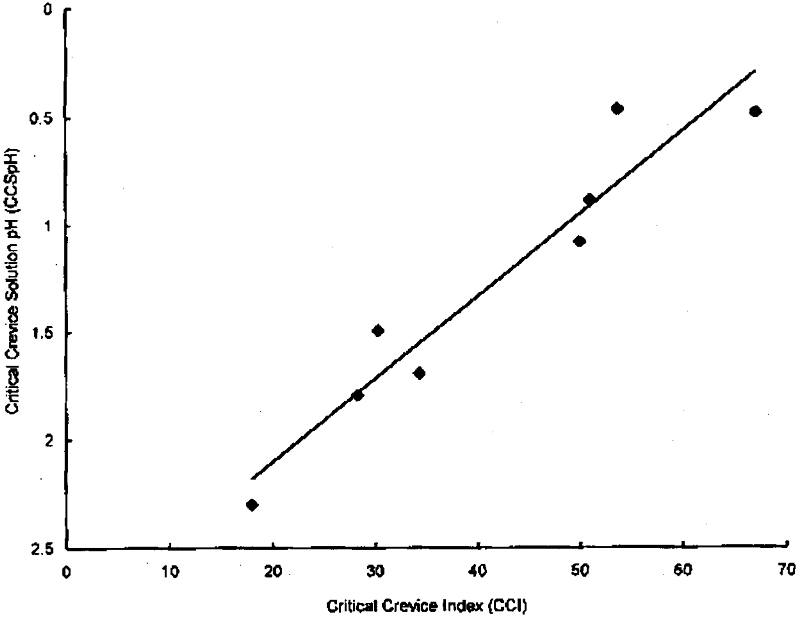

Figure 2 Plots of Critical Crevice Index (CCI) vs Critical Crevice Corrosion pH(CCSpH)

pH (CCSpH)

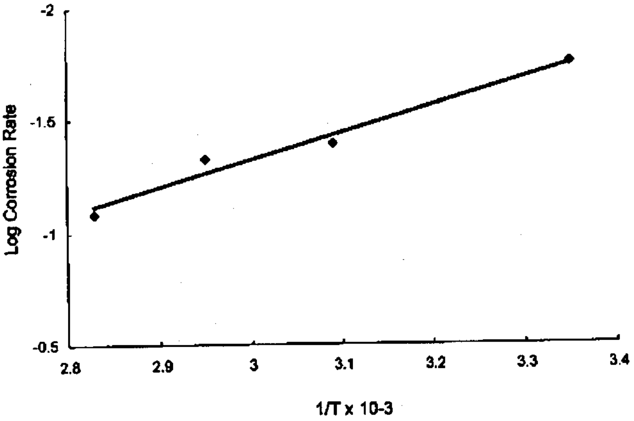

Figure 3 Effect of temperature on corrosion rate of SS316L - Arrhenius Plot.

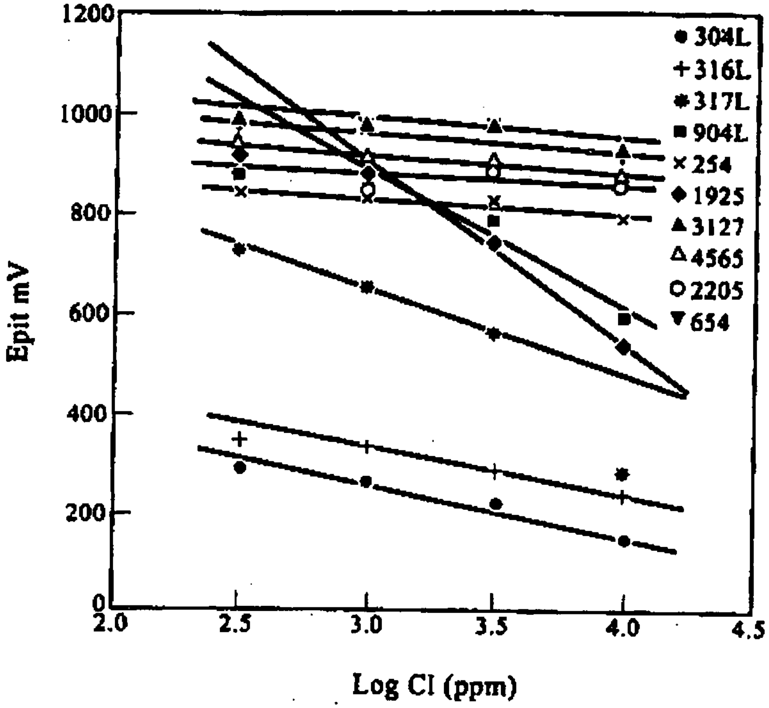

Figure 4 Plots of pitting potential E_{pit} vs Log [Cl^-] for different steels in chloride containing aqueous solutions

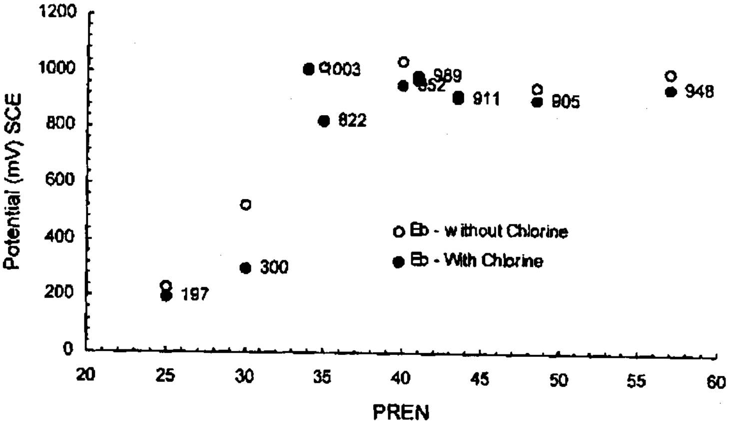

Figure 5 Graph showing variation in break down potential E_b with PRE_N values with and without chlorination (0.2 ppm) at 25°C

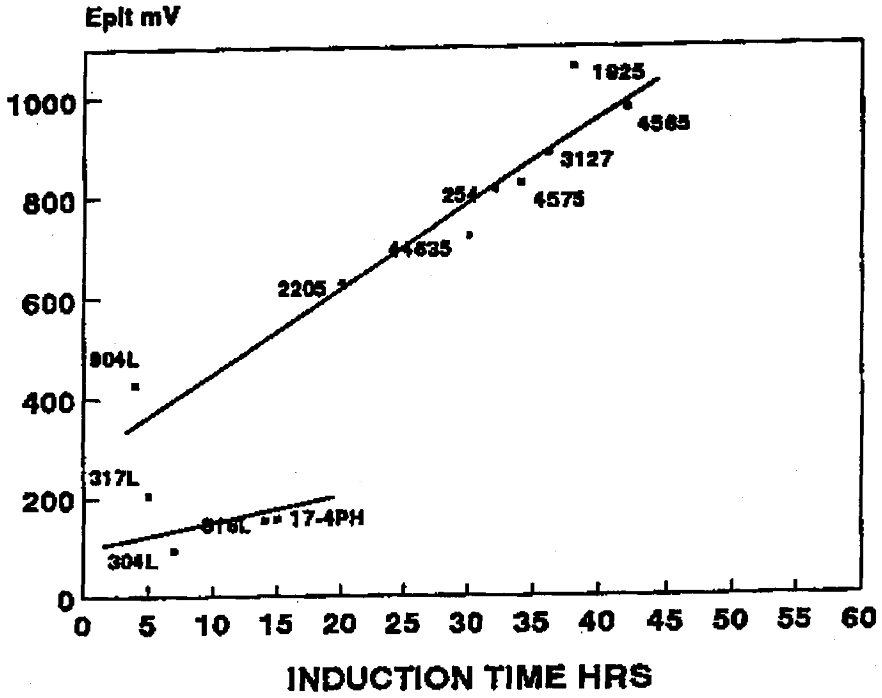

Figure 6 Plot of induction time. t_i and pitting potential, $E_{pit.}$ Two seperate linear plots represent conventional and high alloy stainless steels, respectively.

Vapor-Side Corrosion Monitoring in Al-Khafji Desalination Plant

Nausha Asrar, Anees U. Malik, Shahreer Ahmed,
Madeeh Al-Khalidi and Khalid Al-Moaili

VAPOR-SIDE CORROSION MONITORING IN AL-KHAFJI DESALINATION PLANT

Nausha Asrar, Anees U. Malik and Shahreer Ahmed
R&D Center, SWCC, P.O. Box: 8328
Al-Jubail - 31951, Saudi Arabia

Madeeh Al-Khalidi and Khalid Al-Moaili
Al-Khafji Desalination Plant, SWCC
Al-Khafji, Saudi Arabia

ABSTRACT

The corrosion problem in vapor side is aggravated due to uncertainties in concentrations of oxygen, carbondioxide and other non-condensable gases. In such a situation, vapor-side corrosion could be a limiting factor in a MSF plant life, if not studied properly. This paper presents the results of a vapor-side corrosion monitoring study carried out at Al-Khafji desalination plant. Corrosion behavior of 70/30 Cu-Ni alloy, carbon steel and AISI-316 have been studied in vents and in the vapor-side of evaporator for about 9000 hours. Corrosion rates have been determined by weight loss method. The corrosion products have been analyzed by Energy Dispersive X-ray Analyzer (EDAX).

Analyses of the experimental data indicate that in addition to O_2, H_2S evolved during flashing of seawater has reacted more with Cu-Ni alloy as compared to carbon- and Stainless steels. Contrary to other reported works, ammonia and bromine, have not been found in corrosion products. Explanations for comparatively higher corrosion of alloys exposed to the vapors of early (1-3) and middle (11-13) stages of MSF plant have been given with experimental results. Stainless steel 316L has been found as the most resistant alloy to vapor-side corrosion in all stages of distiller.

Keywords : Vapor-side Corrosion, Non-condensable Gases, MSF Plant, Seawater, Oxygen Ingress.

INTRODUCTION

SWCC manages seawater desalination plants with a total capacity of 520 MIGD of potable water to meet the drinking water requirements of 70% population of the Kingdom. Some new plants are under construction to increase the capacity to 800 MIGD [1]. Failures of components may result in unscheduled shutdown of the plant and consequently in the reduced production of water.

Multistage flash (MSF) evaporation and reverse osmosis (RO) are the two main techniques used for producing potable water from seawater. The former is predominantly employed for the production of desalinated water. An MSF plant is much more prone to corrosion due to its operation at higher temperatures. Corrosion monitoring of the component/material in an operating desalination plant is a profoundly important task because it provides a wealth of information about the condition of plant in terms of construction materials, components and operational parameters. All these information can be useful in evaluating the performance and behavior of materials and efficiency of the plant.

In MSF plants, the corrosion of construction materials in flash chamber and water boxes due to flashing brines has been studied by several investigators [2-7]. However, the major problem in both acid and additive MSF plant is vapor-side corrosion. While in acid dosed plants, almost all the CO_2 is removed by the decarbonator, CO_2 is present along with O_2 as non-condensable gases in additive treatment plants. Other gases like H_2S, NH_3, Br_2 and Cl_2 may also present in significant concentrations and could be responsible for corrosion attack.

Oldfield and Todd [8] studied vapor side corrosion in an MSF plant. It was concluded that in acid dosed plants and probably also in additive plants the vapor-side corrosion is caused primarily by the presence of oxygen, this was coming not from the deaerated brine but from air-in-leakage into the plant. The results of studies on the corrosion behavior of stainless steels were reported [5]. In air ejector system of an MSF plant using 316L and 904L steel pipes, while 316L failed by SCC, the latter grade appeared to be quite resistant to corrosion. Failure of SS 316L steel was attributed to the presence of Br_2 in vent gases [9]. Lee, Oldfield and Todd [10] reported failure of 316L components in the venting system of MSF in Qatar due to bromine. The presence of ammonia in seawater above the normal background level is necessary for this to occur. After 25 years of operation, Abu Dhabi desalination plant experiences corrosion problems in its 23 large distillation units [11]. Substantial copper oxide deposits were found in the distillate product during the start up of the distiller following long and/or short shut down. The deterioration of the protective oxide film appeared to be the main cause of the problem which could be solved by improving the efficiency of the deaerator and the venting system. In another case [12], a group of 24 MSF distillers experienced failure of tubes in the first few high temperature stages after 50,000 to 100,000 hours of operation. It was concluded that the problem of tube failure was due to the presence of pockets of CO_2 gas near the tube, which redissolves in distillate to form an aggressive solution. The installation of an auxiliary vent to reduce the size of the gas pocket allowed a significant increase in distillater pH and reduction in dissolved copper.

Keeping in view the importance of vapor side corrosion in MSF plants, a monitoring study was carried out at Al-Khafji plant. This paper presents the results of that study.

SWCC Al-Khafji Phase II MSF desalination plant was commissioned in 1985. It has a designed capacity of producing 22727 m^3/d (5 MIGD). There are 2 desal units (# 100 and #200), each unit has 22 stages. In this plant seawater make-up is not treated with chemicals for scavenging of oxygen.

EXPERIMENTAL

Coupons of carbon steel, AISI 316L SS and 70 Cu/30 Ni were fixed above the demisters in the flash chamber # 1, 4, 10, 14 and 18 of unit # 100. Coupon of the aforementioned materials were also fixed with the help of retractable coupon holders, in the vent lines of stage # 3, 8, 13, 17 and 22 of unit #100. The arrangement of coupons in vent line and flash chambers of Al-Khafji plant unit #100 is shown schematically in fig. 1.

Coupons fixed in the vapor phase inside the flash chambers were taken out after 9,000 hrs, while coupons fixed in vent lines were taken out after 2,000 or 4,000 hrs of exposure. Weight loss coupon technique was used for corrosion rate measurements following ASTM G 90 [13].

RESULTS AND DISCUSSION

As shown in fig. 2 in evaporator, weight losses shown by Cu/Ni alloy and SS316L are by and large same in all the stages. In vent lines (Fig. 3), weight loss decreases steeply from stage #3 reaching a minimum at #8 and then increases showing a maximum at #13. Also these figures show that the weight losses of SS 316L specimens are much higher (about one magnitude) in vent lines than that in flash chambers although the magnitude of the weight loss is quite low. In case of vapor side corrosion of cupronickel exposed in vent line and flash chambers, weight losses after 2,000 hrs in vent line are more or less same as in flash chambers after 9000 hrs. Tables 1 and 2 indicate that in vent line Cu-Ni alloy corrode much faster than in flash chambers. Table 1 shows that corrosion rates of mild steel are highest in stage #3 (4 MPY). In comparison, corrosion rates of cupronickel are about one magnitude lower to carbon steel. The corrosion rates of AISI 316L in vent line are extremely low at all the stages and are at least one order of magnitude lower than cupronickel alloy.

Figures 4A to 5A show some typical scanning electron microgrpahs of cross-section of mild steel coupons exposed for 9,000 hrs in different stages of flash chambers. All the microstructures have a common feature that the scales are copious and adherent. The inner scales are generally separated from alloy interface. The energy profiles obtained by EDAX for the exposed alloy indicate the presence of Fe and O in the outer layers and that of chloride in the inner layers in all stages (Fig. 5B). In some cases presence of Al, Si and S is also indicated. Chloride is invariably concentrated at the alloy/scale interface.

Figures 6A shows a photograph of carbon steel, 316L SS and 70/30 Cu-Ni alloy, respectively, exposed to vapor in evaporator #100. Heavy corrosion is observed in carbon steel specimen. After removal of scale pitting can be seen on the surface of alloys (Fig. 6B), the pitting is more extensive in later stages. No or very little corrosion is observed on 316L specimen. Figure 7A shows a photograph of cupronickel alloy specimens exposed to non-condensable gas in the vent line for 2,000 hrs, appreciable corrosion is found on the specimens. Fig. 7B shows a photograph of carbon steel exposed for the same period. Heavy corrosion product formation is noticed in all the stages.

Table-2 provides corrosion rate values of all the three alloys exposed to non condensable gases in flash chambers. The corrosion rates for carbon steels are higher in stages # 10 onwards than those observed in the initial 4 stages. Corrosion rates of cupronickel are highest in stage # 1 (0.1 MPY) and lowest in stage # 18 (0.007 MPY). These corrosion rates are much below the accepted limit. Corrosion rates of AISI 316L in all stages are extremely low (0.001 to 0.002 MPY) showing virtually no corrosion occurring in flash chambers by non condensable gases.

It appears that a decrease or increase in corrosion rates is directly related to build up of non condensable gases in vents and subsequent cascading. As the non condensable gases concentration increases corrosion rates are also increased. With cascading, corrosion rate goes down but increases again from stage to stage as non condensable gases concentration builds up. In early stages, corrosion rates are high due to elevated temperatures and high concentration of corrosive gases in the vapor phase.

In flash chambers, the weight losses progressively increase due to vapor phase attack up to stage #10 when it becomes constant. In mild steel, the weight losses in flash chambers are much higher (about one order of magnitude) than vent line. In flash chambers, the vapor phase is mainly consisted of moisture and non condensable corrosive gases. This provides favorable conditions for rust formation and could be the reason for high corrosion rates in flash chambers. In vent lines, mild steel is attacked by non condensable gases but not so aggressively as in flash chambers.

Considering, vapor-side corrosion of cupronickel 70/30 exposed in vent line and flash chambers, the corrosion rates in vent line are much higher than in flash chambers. In vent lines, the cupronickel alloy is attacked much more severely due to the presence of predominantly corrosive gases. In flash chambers, there is predominant concentration of water vapors and relatively low concentrations of non condensable gases and in consequence, attack is not so severe. The corrosion rates of stainless steel 316L in vents are extremely low (0.04-0.07 MPY) but still one order of magnitude higher than flash chambers (0.001-0.002 MPY). In either case, the corrosion rates are not alarmingly significant and the 316 L can be safely used in vent lines.

An interesting feature of the corrosion products from the carbon steel specimen exposed to non condensable gases in flash chambers or vent lines is that, sulfur is invariably present though in small concentrations. Copper and bromine are present in smaller but in perceptible concentrations and only in the corrosion products of steel coupons exposed in vent lines. Sulfur and bromine are undoubtedly originated from un-condensed gases but there is no plausible explanation for the existence of copper in the scales or corrosion products of the carbon steel coupons.

Considering the corrosion behavior of materials in vent line and evaporator at different stages. The shape of the weight loss vs. no. of stages curves can be explained broadly as follows:

(i) Steep increase in weight loss (or corrosion rates) is due to breaking up or spalling of scales when fresh alloy surface comes into contact with gases.

(ii) Decrease in weight loss could be due to progressive formation of adherent protective scales.

(iii) Presence of plateau (no change in weight) could be due to the formation of protective scales.

CONCLUSIONS

(i) Corrosion rates of cupronickel and stainless steel 316 L exposed to non condensable gases in vent lines are much higher than those exposed in flash chambers.

(ii) Corrosion rates of carbon steel exposed to non condensable gases in flash chambers are higher than those in the vent lines. Higher corrosion rates are attributed to the severe rusting of carbon steel in presence of moisture and oxygen.

(iii) Stainless steels 316L in general show very little or no corrosion either in vent line or flash chambers.

(iv) Cracking of otherwise compact and adhered scales on mild steel exposed to non-condensable gases in the flash chambers has been attributed to the presence of chloride at the metal matrix/oxide scale interface.

(v) Sulfur is invariably present in the corrosion products of Cu-Ni exposed in vent line.

(vi) High corrosion rates of cupronickel in vent line are attributed to the presence of sulfur in non-condensable gases.

(vii) A maxima in corrosion rates has been generally found in the middle stages # 10-14 in all the alloys. This could be explained on the basis of combined effect of temperature and air in-leakage providing most favorable conditions for corrosion at these stages.

REFERENCES

[1] Annual Report, SWCC, 1994.

[2] Cigna, R., L. Guiliani, G. Gusmani, 1985, "Continuous Corrosion Monitoring in Desalination Plants", Desalination, Vol. 55, p. 219.

[3] Oldfield, J. W. and B. Todd, 1979, "Corrosion Considerations in Selecting Metals for Flash Chambers", Desalination, Vol. 31, p. 365.

[4] Hodgkiess, T., W. T. Hanbury, and M. H. Hejazian, 1983, "Corrosion Tests of Range of Materials in Three MSF Plants", Desalination, Vol. 4, p. 223.

[5] Nordin, S., 1983, "Studies on Stainless steels for Services in Desalination Plants", Desalination, Vol. 4, p. 255.

[6] Saricimen, H., et. al., 1990, "Performance of Austenitic Stainless Steels in MSF Desalination Plant Flash Chamber in Arabian Gulf" Desalination, Vol. 78, p. 327.

[7] Narain, S. and H. Sami, Asad, 1992, "Corrosion Problems in Low-Temperature Desalination Units", Materials Performance, Vol. 31 (4), p. 64.

[8] Oldfield, J. W. and B. Todd, 1987, "Vapor Side Corrosion in MSF Plants", Desalination, Vol. 66, p. 171.

[9] Oldfield, J. W. and B. Todd., 1981, "Corrosion Problems Caused by Bromine Formation in MSF Desalination Plants", Desalination, Vol. 38, pp. 233-245.

[10] Lee, W. S. W., J. W. Oldfield, and B. Todd, 1983, "Corrosion Problems Caused by Bromine Formation in Additive Dosed MSF Desalination Plants", Desalination, Vol. 44, pp. 209-221.

[11] Al Sum, E. A., et. al., 1994, Vapor Side Corrosion of Copper Based Condenser Tubes of the MSF Desalination Plants of Abu-Dhabi, Desalination, Vol. 97, pp. 109-119.

[12] McGregor, I. D. and S. Karim, 1995, "Tube Corrosion in High Stages of MSF Distillers", Proc. IDA World Congress, Abu Dhabi, Nov. 18-24, pp. 307-310.

[13] Standard Practice for Preparing, Cleaning and Evaluating Corrosion Test - ASTM GI-90.

[14] Fontana, Mars G. "Corrosion Engineering" 3rd Ed. 1987 Singapore. McGraw Hill p. 14.

Table 1: Corrosion of Cu-Ni, Carbon Steel and Stainless Steel 316L in Vent Lines of MSF Desalination Plant, Unit # 100.

S. No.	**Distiller Stage # (Cascading)**	**Exposure Period (h)**	**Corrosion Rate (MPY)**		
			70-30 Cu-Ni	**SS 316L**	**Carbon Steel**
1	3 (1-3)	2000	0.41	0.06	3.97
		4000	0.42	0.05	5.55
2	8 (4-8)	2000	0.07	0.06	0.46
		4000	0.05	0.04	1.02
3	13 (9-13)	2000	0.1	0.07	1.95
		4000	0.06	0.07	1.74
4	17 (14-17)	2000	0.04	0.06	0.42
		4000	0.01	0.02	0.99
5	22 (18-22)	2000	0.08	0.04	0.87
		4000	0.12	0.02	0.96

Table 2: Corrosion of Cu-Ni, Stainless Steel 316 L and Carbon Steel in the Flash chambers of MSF Desalination Plant, Unit # 100.

S. No.	**Distiller Stage #**	**Exposure Period (h)**	**Corrosion Rate (MPY)**		
			70-30 Cu-Ni	**SS 316L**	**Carbon Steel**
1	1	9000	0.1	0.001	1.80
2	4	9000	0.05	0.001	1.72
3	10	9000	0.02	0.002	2.41
4	14	9000	0.01	0.002	2.40
5	18	9000	0.007	0.001	2.36

VAPOR PHASE CORROSION MONITORING

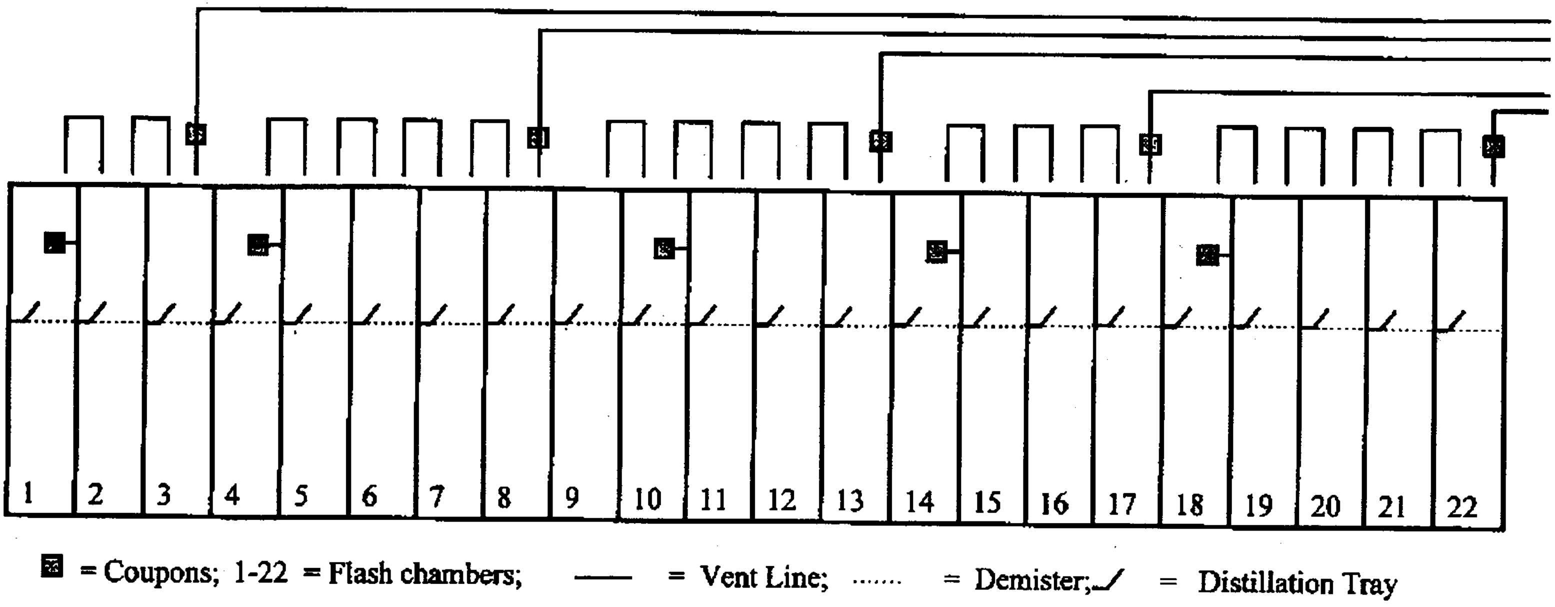

Figure 1: Location of the coupons in vent line and chambers of MSF distiller

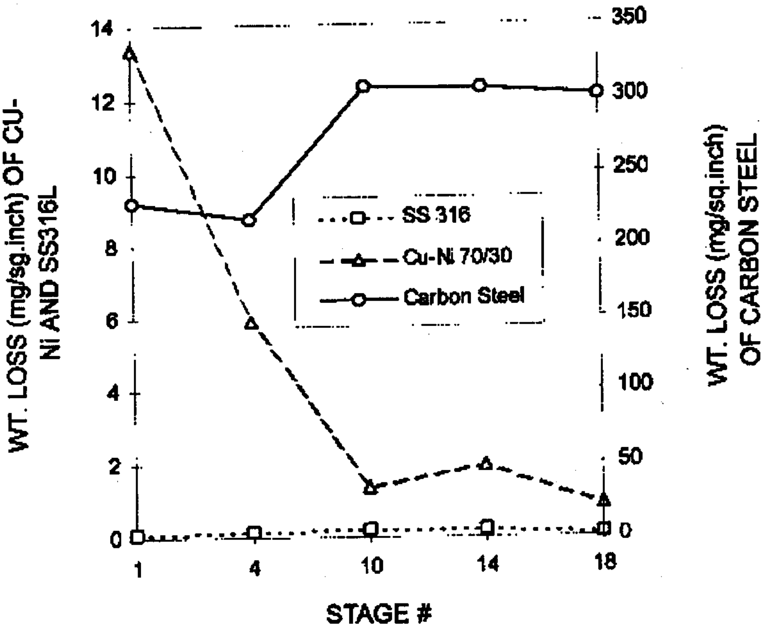

Figure 2: Vapor-side corrosion of different materials exposed for 9000 hrs. in flash chambers of MSF plant

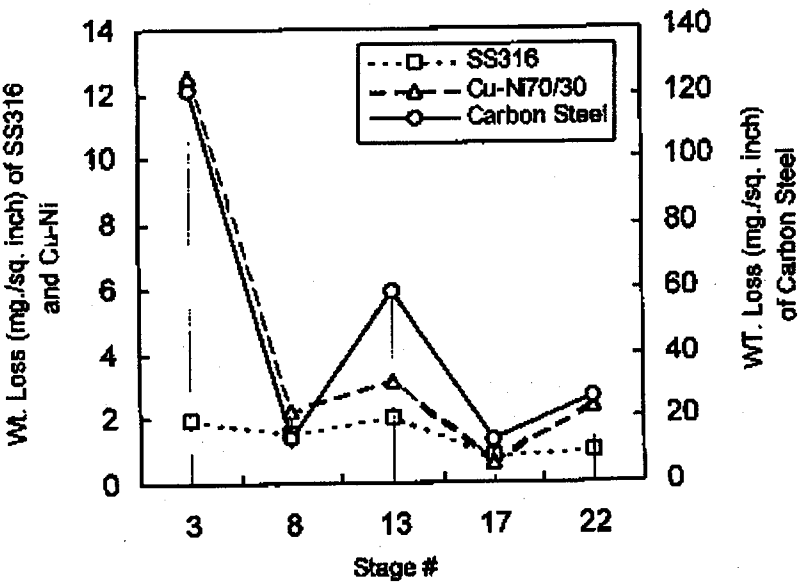

Figure 3: Vapor-side corrosion of different materials exposed for 2000 hrs. in vent line of MSF plant

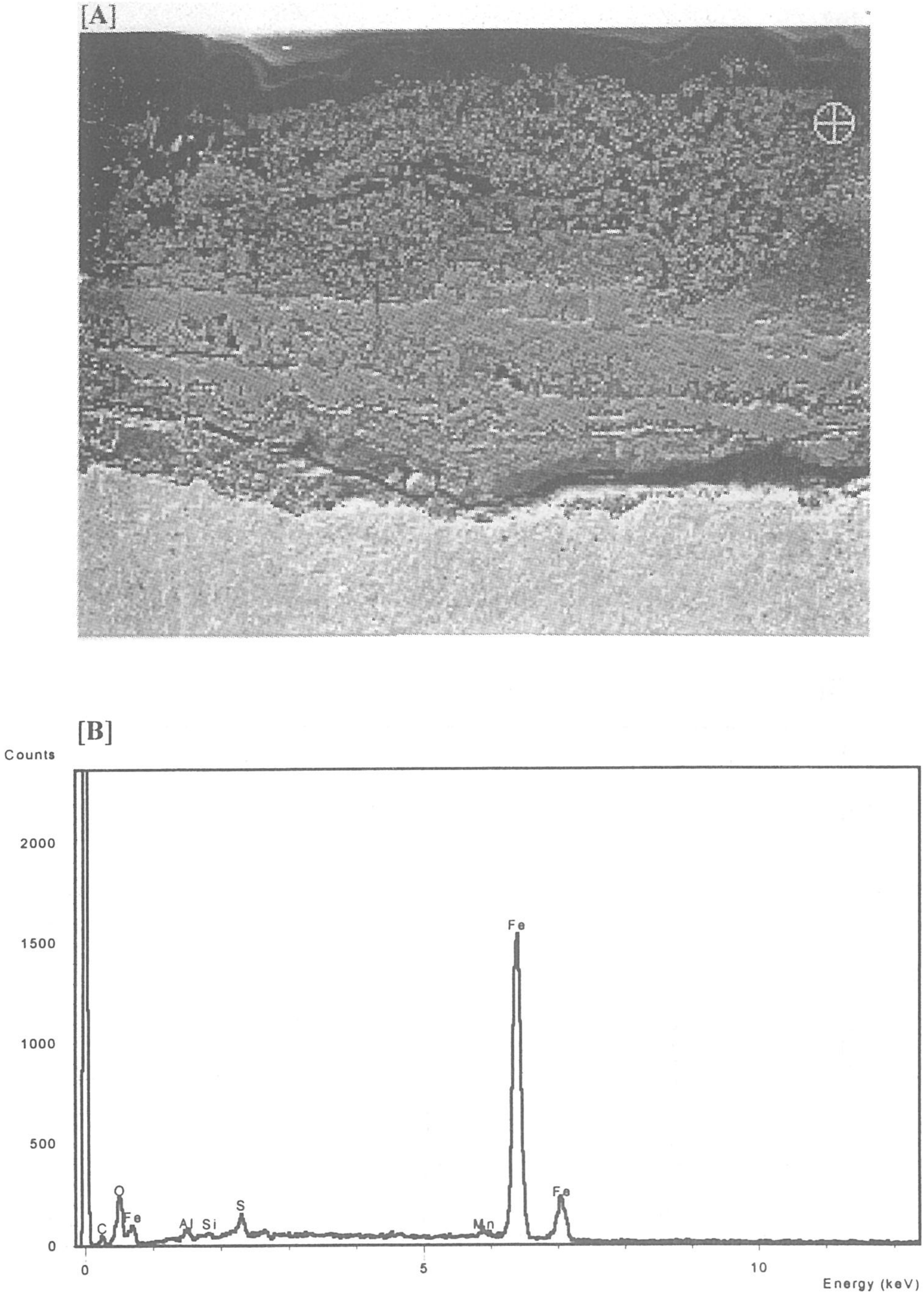

Figure 4. [A] SEM micrograph and [B] EDAX results showing the elemental distribution in the oxide scales formed on carbon steel coupon, exposed for 9000 hrs. in stage #1 of MSF plant

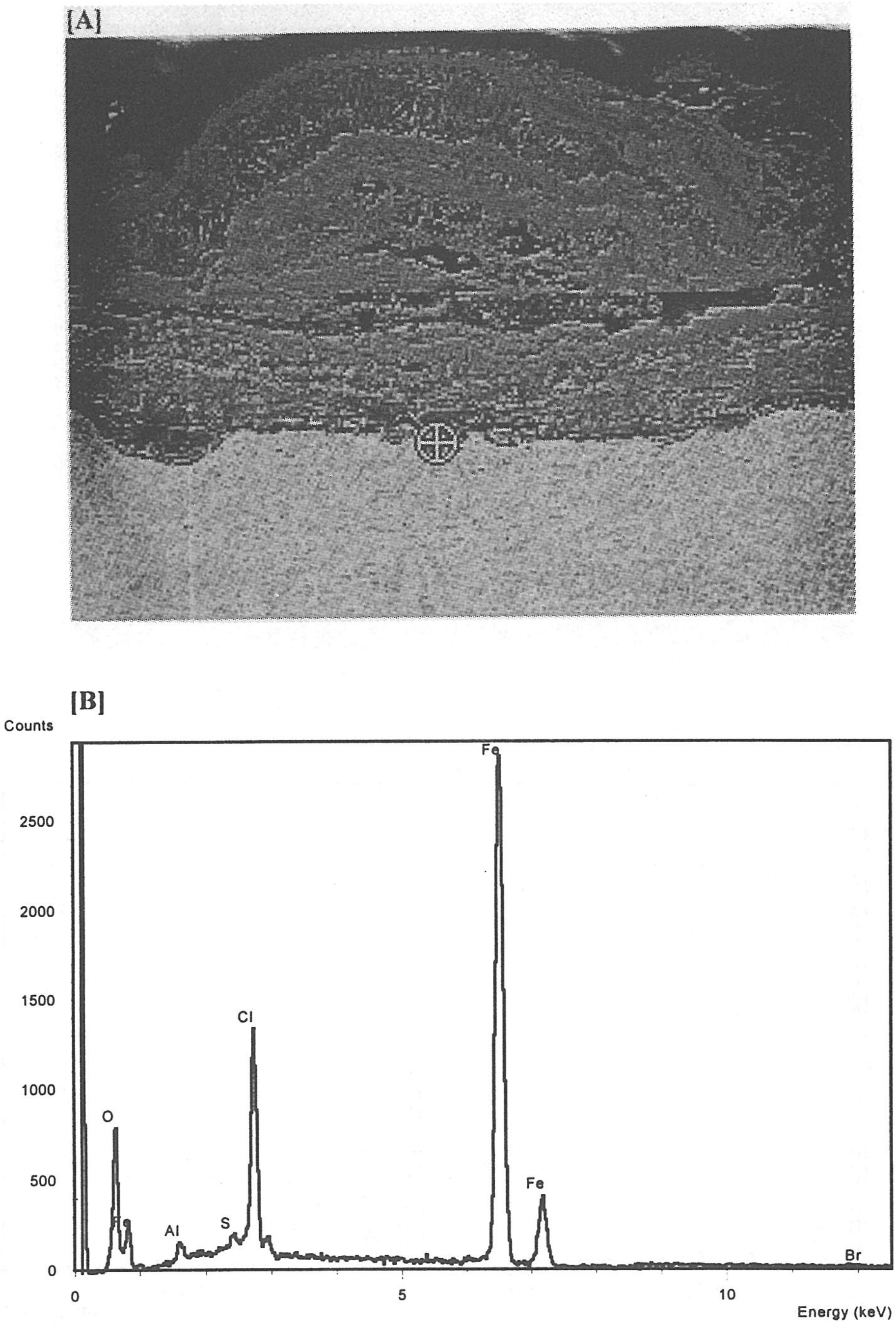

Figure 5. [A] SEM micrograph and [B] EDAX results showing the elemental distribution in the oxide scales formed on carbon steel coupons, exposed in MSF stage #4, for 9000 hrs.

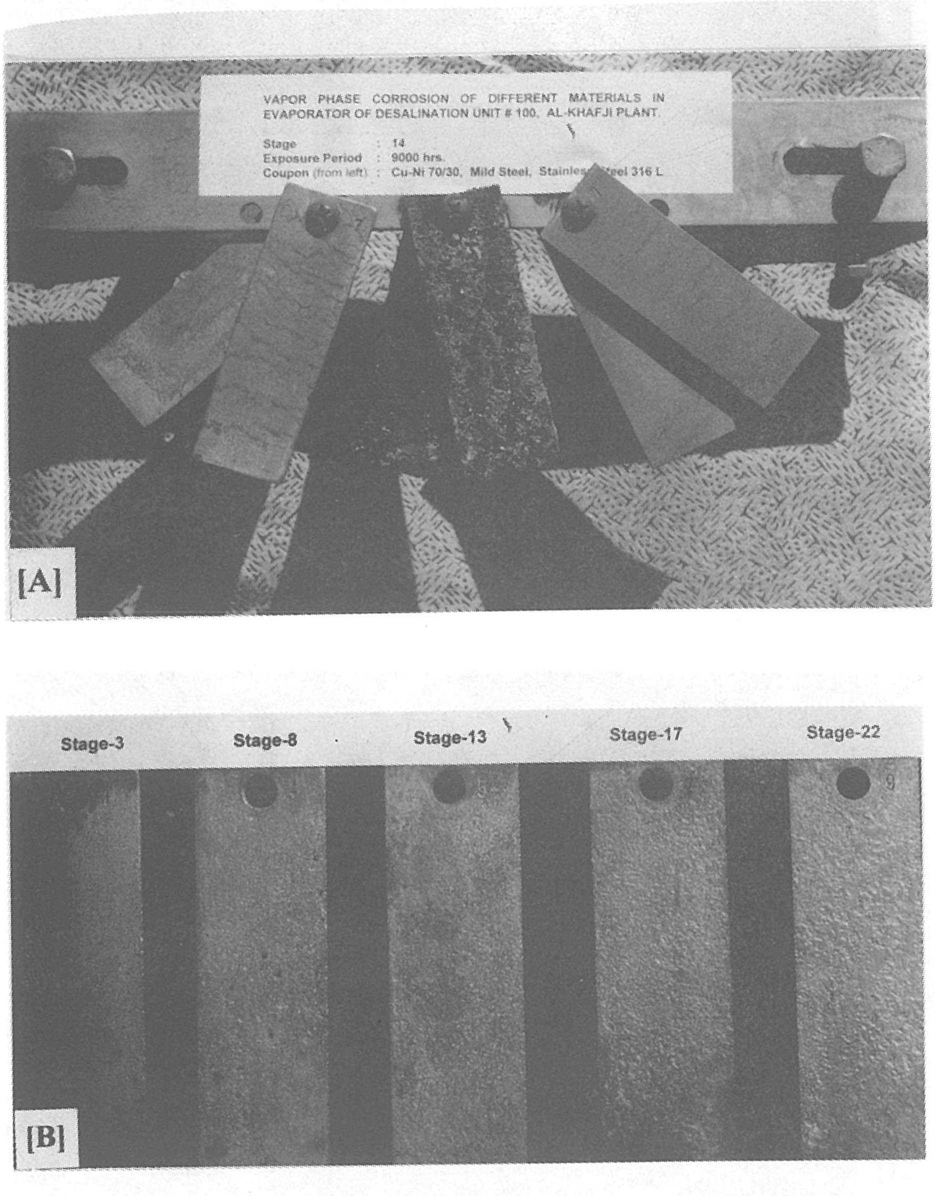

Figure 6. Surface condition of the coupons [A] left to right Cu/Ni alloy, carbon steel and stainless steel 316L, exposed for 9000 hrs. in stage#4 [B] carbon steel coupons exposed for 9000 hrs. in different stages of MSF desalination plant

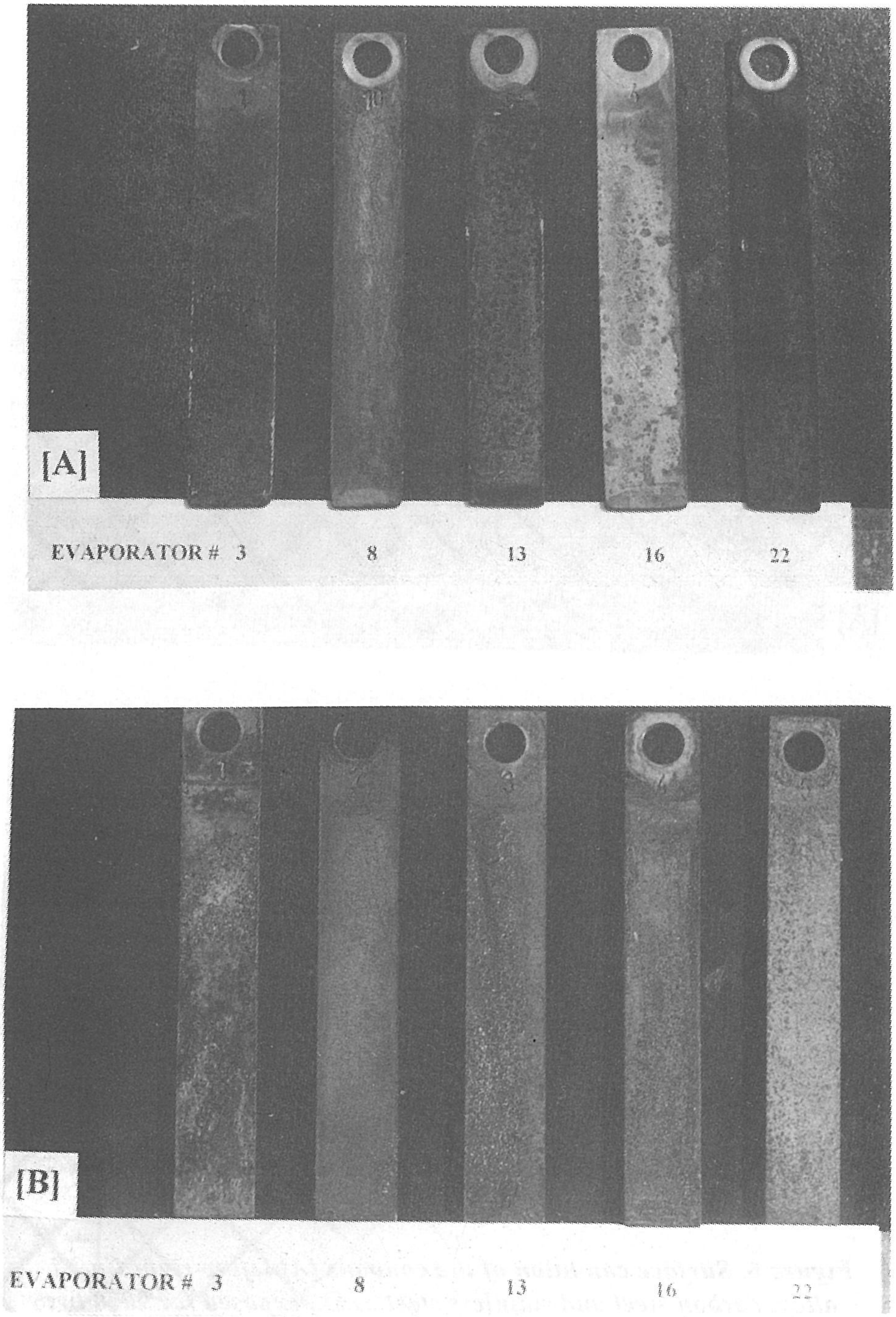

Figure 7 Surface condition of the coupons [A] Cu/Ni 70/30 [B] carbon steel coupons exposed for 4000 hrs. in vent line of different stages of MSF desalination plant

Studies on the Stress Corrosion Cracking Behavior of Few Alloys Used in the Desalination Plants

T.L. Prackash and A.U. Malik

STUDIES ON THE STRESS CORROSION CRACKING BEHAVIOR OF FEW ALLOYS USED IN THE DESALINATION PLANTS

T.L. Prakash and A.U. Malik
SWCC, Research Center,
P.O. Box 8328, Al-Jubail - 31951
Kingdom of Saudi Arabia

ABSTRACT

This paper describes a study on the Stress Corrosion Cracking (SCC) behavior of alloys resulting from the synergistic action of corrodents such as chlorides, oxidants and H_2S. In the this study, the threshold stresses for SCC have been determined for few generic alloys namely, mild steel, 316L, 317L, 430 and Monel 400 used in the desalination plants. The standard Proof Rings and U-Bend samples in NACE and SHELL solutions containing H_2S are used for the purpose. Electrochemical polarization measurements were performed on these alloys in the specified environments to study the effect of electrochemical potential on the intergranular SCC. Structural analysis were conducted by Scanning Electron Microscopy supplemented by Energy Dispersive Spectroscopy. The test results showed that the intergranular and intragranular SCC fracture of mild steel and alloy 430 in H_2S environment occurs only in the limited potential environment, whereas, the alloys viz, 316L and 317L are immune to SCC under the condition of test performed. The alloy Monel 400 was found however susceptible to SCC in presence of H_2S which may be present in some part of desalination plants due to pollution of seawater.

Keywords: Stress Corrosion Cracking; Threshold Stress; Electrochemical Polarization: Sulfide Ion; Passive Film.

INTRODUCTION

Many engineering alloys when in contact with aqueous solutions such as seawater inherently containing number of dissolved ionic species are normally susceptible to corrosion. Chlorides being one of the major constituents of the sea water, its effect on the corrosion of material is of significant concern for the reliability of alloys. Corrosion of alloys under the influence of stresses in service could accelerate and lead to environmentally assisted cracking known as Stress Corrosion Cracking (SCC). Catastrophic failures have occurred due to SCC resulting in loss of life and expensive repairs. There are several types of SCC which include hydrogen embrittlement, sulfide stress cracking and so forth.

In the past, it was thought by several investigators that SCC of a given alloy occurs only in limited range of specific environments [1]. Subsequently, the above notion was diluted when it was found that SCC occurs in wide range of environments [2,3] containing more than one ionic species in solution that act as corrodents. The synergistic action of corrodents namely, Cl_2, CO-CO_2, caustic solutions containing H_2S (elemental Sulfur in solution) etc. have an immense effect on SCC of materials.

The carbon steels are prone to SCC in carbonate, bicarbonate, acetate, phosphate, etc. environment and are identified as main reason of cracking [4]. The low alloy steels are affected by SCC in oxygenated water at high temperature [2], alkaline chloride such as $NaCl$- $Ca(OH)_2$ [5] and anhydrous ammonia- methanol solutions containing chloride [6]. The J-55 and N-80 steels have shown SCC in chloride solution containing H_2S [7]. Similar observation was also made in AISI 1075 steel [8].

In austenitic stainless steels, SCC was well-known since three decades. The cracking was mainly due to chloride (which were neutral at high temperature, acid at low temperature) and hydroxide solutions [9]. Thiosulphate environments of weld sensitized stainless steels have shown SSC [10]. In the duplex stainless steel SSC is severe at 160 °C in 25% NaCl containing H_2S and also in aerated brine solutions [11].

The nickel base alloys viz., C-276 and alloy 825 were susceptible to SSC in HCl oxidizing solution containing S. In chloride containing solution the SSC has been observed at temperatures above 204 °C [11]. The copper base alloys are subjected to SCC in environments like ammonia, sulfur dioxide, organic complexing solution like acetates and tartrates, copper sulfate solution, etc. [12].

Threshold Stress for SCC

As the name implies the threshold stress is the stress below which no SCC occurs. The main purpose of determining the threshold stress for SCC is to establish a ranking order under given condition of metal environment combination, heat treatment microstructure, type of stressing and its magnitude. An exact threshold stress for a given condition is difficult to define. However, the relative ranking seems quite obvious.

The material which shows highest SCC resistance for a given environment may show susceptibility to SCC when it is heat treated to different microstructure. For example, threshold stress in SCC of carbon and low alloy steels was found to be influenced by heat treatment when it is studied using 5% NaCl - 0.5% Acetic acid solution containing 3000 ppm of H_2S [13]. The heat treatment carried out gave untempered martensite in the structure which is attacked by H_2S and resulted in low threshold stress values for cracking. The result of series of test in Drop Evaporation Test on highly alloyed stainless steel and duplex stainless steels as indicated by their threshold stress values [14], the highly alloyed stainless steels such as 654 SMO (UNS S 32654) was most resistant to SCC than the duplex stainless steels viz., 2205 (UNS S 31803).

The purpose of the present investigation was two fold: 1) To study the SCC behavior of few generic alloys used in the desalination plants resulting from synergistic action of corrodents such as chlorides, oxidants and H_2S and to determine the threshold stresses for SCC. 2) To assess the effect of electrochemical potential on the alloy passivity to corrodent species by performing the electrochemical polarization measurements in the specified environments.

EXPERIMENTAL DETAILS

The materials selected for this study were mild steel (MS), AISI 316L, 317L and 430 stainless steels and Monel 400. The chemical composition of these alloys are shown in Table 1.

Stress Corrosion Cracking Tests

Round and flat tensile samples were machined from the rod / sheet material stocks. All the materials selected were of mill finished commercial grades. The tests were carried out in Cortest Proof Rings (15] with corrosion testing environment chamber. An hour meter and H_2S gas manifold were used to measure the time of failure of specimen and H_2S gas monitoring during test respectively.

The media employed for the tests were i) NACE solution (having composition 5% NaCl + 0.5% CH_3COOH) prepared from distilled water and continuously bubbled with H_2S to maintain H_2S saturation in solution. ii) SHELL solution (having composition 0.5% CH_3COOH) prepared from distilled water and continuously bubbled with H_2S to maintain H_2S saturation as in i).

The samples were tested in ambient temperature with the Cortest Proof Ring at 70, 80, 85 and 90% of their respective 0.2% yield stress (YS) with the help of loading nut and calibration charts. During the tests H_2S was continuously bubbled in the solution. The time to rupture of the samples were recorded. The samples those have crossed 500 hours without rupture were withdrawn from the test. During the test samples were periodically withdrawn for examination of any initiation of cracks or corrosion pit development.

Electrochemical Tests

The electrochemical polarization techniques were performed to measure the absolute corrosion rates. Tafel plots were generated for this purpose on samples by polarizing the specimen about 300 mV anodically (positive-going potential) and cathodically (negative-going potential) from the corrosion potential, E_{corr}. The potential is stepped in staircase waveform. The resulting current is plotted on a logarithmic scale. The corrosion current I_{corr} is obtained from Tafel plot by extrapolating the linear portion of the curve to E_{corr}. The corrosion rate was calculated from the I_{corr}.

Experiments were carried out on the samples using EG&G model 273 Potentiostat with Softcorr Corrosion Software M342. A saturated calomel electrode was used as reference electrode. Graphite electrodes were used as auxiliary electrodes. Button samples of 14 mm dia and 2 mm thick were machined from rod/ sheet stock of the respective material. They were polished at one side to 600 # grade paper. The media employed in the electrochemical tests are i) NACE solution ii) Natural seawater iii) Natural seawater containing varied amounts of sulfide ion concentration obtained by dissolving known quantities of sodium disulfide crystal iv) SHELL solution and v) SHELL solution containing known amount of sulfide ion concentration.

RESULTS AND DISCUSSION

The results of the SCC tests are shown in Fig 1 & 2 . The results revealed that the SCC occurred more readily in MS samples in NACE solution and SHELL solution saturated with H_2S at stress ranges of 70, 80, 85 and 90% YS. The alloys 430 and Monel 400 are also found susceptible to SCC only when they are stressed to 90% YS in NACE solution containing H_2S. The alloys 316L and 317L were found immune to SCC in all the condition of tests in NACE or SHELL solutions containing H_2S.

The fracture of SCC tested samples of MS and alloy 430 were analyzed in Scanning Electron Microscopy (SEM). The fractures revealed intergranular as well as intragranular mode of crack propagation (Fig. 3 & 4). Branching of secondary cracks from the primary cracks, which is typical of SCC failure mode were noticed. The Energy Dispersive Spectrum obtained during SEM fractography at fracture crack tips containing corrosion products showed sulfur rich regions (Fig 3b & 4b). This also confirm the onset of SCC due to sulfide stress cracking.

The threshold stress for MS in NACE and SHELL solution is 75% YS, whereas it is 85% for 430 and Monel 400 alloys in NACE solution. Such threshold stress was not found to exist for the same alloy in SHELL solution at all the stress levels. The alloys 316L and 317L, however, did not show any threshold limits upto 90% YS either in NACE or SHELL solutions containing H_2S. It is possible that threshold stress might be greater than the YS of these materials. MS has shown greater susceptibility to SCC in the tested medium when compared to other alloys.

Sulfides play a dominant role in the structural steels particularly in their resistance to sulfide stress cracking. The water present would obviously assist a corrosion mechanism. The reaction will be of the type

$$H_2S + Fe \rightarrow FeS + 2\,H$$

The nascent hydrogen is then expected to embritle the alloy. The presence of chloride all the more aggravate corrosion leading to early failure of steel. The instances of sulfide stress cracking of stainless steels have been reported [16] wherein failure of specimens have been promoted in high chloride environment (>25% NaCl) at elevated temperature and pressure saturated with H_2S. The chloride content used in some of the test being 5% , it is conceivable that the stainless steel of type 316L and 317L are less likely to be affected by H_2S as evidenced in the experiment. The effect of H_2S in SHELL solution suggest that except MS, other alloys were immune to SCC. MS was found prone to SCC > 75% YS. The synergistic effect of chloride in presence of oxidant (CH_3COOH) and H_2S to promote SCC in alloys 430 and Monel 400 at stresses > 85% YS was clearly demonstrated as seen from the results of NACE solution experiment (Fig. 1).

The data obtained from electrochemical polarization studies are shown in Table 2 & 3. The results obtained from NACE solution and natural seawater containing 0.1M of sulfide indicated that alloys 316L and 317L showed higher passive current densities relative to the Monel 400. The passive current density in natural seawater solution for alloy 430 with 0.1M sulfide was lowest which can be attributed to the development of a stable passive film over the surface of the alloy.

The electrochemical data from the SHELL solution revealed that lowest passive current densities for 317L alloy in 0.1M sulfide solution, while the highest was observed for alloy Monel 400 except MS. In general, for all the alloys studied, high sulfide content moved the corrosion potential to active direction thus enhancing localized corrosion. Lowest passive current densities exhibited by alloys 316L and 317L indicated that they are least susceptible to corrosion in presence of sulfide.

From the results of electrochemical tests it is seen that the synergistic effect of chloride and sulfide on the corrosion behavior were prominent particularly for alloys 316L and 317L. For alloys 430 and Monel 400 such effect were not noticed. However, under the influence of stress as noticed from the SCC test results, the trend was reverse. It is plausible that the passive films formed over the alloy 430 and Monel 400 were less stable and get disrupted easily, leading to SCC.

CONCLUSIONS

The following conclusions are drawn on the basis of investigations carried out.

i) In solutions containing sulfide, the chlorides demonstrated the synergistic effect to promote SCC in alloys 430 and Monel 400 at stress levels > 85% YS.

ii) Alloys 316L and 317L were found SCC resistant under all conditions of the tests performed.

iii) Alloys 316L and 317L had shown higher passive current densities relative to the other alloys in presence of specified oxidant, chloride and sulfide ionic species. Under the influence of stress, they were least susceptible to corrosion.

iv) MS was found prone to SCC at stress levels > 75% YS in solutions containing specified amounts of sulfide, chloride and oxidants.

v) Sulfide ion displaces the corrosion potential in active direction thereby increasing the risk for localized corrosion for all the alloys studied.

REFERENCES

1 Staehle, R.W., A.J.Forty and D. Van Rooyen (Eds.), 1969, "Fundamental aspects of stress corrosion cracking", NACE publication, Houston, TX, pp 40-95.

2 Congleton, J.,. T.Shoji and R.N.Parkin, 1985, Corrosion Sci., 25, p 633.

3 Gangloff, R.P., and M.B.Ives (Eds.),1990, "Environment assisted cracking of metals", NACE publication, Houston, TX.

4 Brown, A., J.T.Harrison and R. Walkin, 1969, "Stress corrosion cracking and hydrogen embritlement of iron base alloys", in Ref 1. p 663.

5 Parkin, R.N., M.Elices, V. Sanchez and L.Cabellaro, 1982, Corr. Sci., 22, p 379.

6 Zheng, W., R.C.Newman and R.P..M.Proctor, 1985, Ref 2, p 555.

7 Kerns, G.E., in B.J.Moniz, and W.I.Pollock (Eds.),1986, Proc. Ind. Corr., NACE publication, Houston, TX, pp 353-365.

8 Hudgins, C.M., R.L.McGlasson and W.Rosborough, 1966, Corrosion, 22, p 238.

9 Newman, R.C., and A.Mehta, 1990, Ref. 3, p-489.

10 Issac, H.S., B.Vyas and M.N.Kendig, 1982, Corrosion, 38, p 100.

11 Place, M.C. Jr., R.D.Mack Jr. and P.R.Rhodes, 1991, Metal Performance., December, pp 56-58.

12 Pinchback, T.R., S.P.Clough and L.A.Heldt, 1976, Corrosion, 32, p 469.

13 Snape, E,, 1968, Corrosion, 24, p 261.

14 Arnvig, P.E., and W.Waieleskawa, Acom., 1993, Avesta Sheffield publication, 2, pp 1-7.

15 Sedric, J.A.,ý and B.C.Syrett (Eds.), 1990, "SCC Test methods", 1990, NACE publication, Houston, TX, p 369.

16 Asphahani, A.I., in. R.N.Tuttle and R.D.Kane (Eds.), 1969, "Corr-in oil gas production", NACE publication, Houston, TX, p 369.

Table 1 Chemical Composition of Alloys

S. No.	**Alloy**	**UNS No.**	**Composition (%)**								**Others**
			Fe	**Cr**	**Mo**	**Ni**	**C**	**Cu**	**Mn**	**Si**	
1	Mild Steel	J2503	Bal	0.5 Max	0.2 Max	0.5 Max	0.25 Max	0.3 Max	1.2 Max	0.6	0.04P,0.04S
2	316L	S31603	Bal	16.0	3.0	11.0	0.02	0.2	1.0	1.0	0.04P,0.02S
3	317L	S31703	Bal.	18.5	3.2	13.5	0.02	-	1.0	-	0.08 N
4	430	S43000	Bal.	18.0	-	-	0.12	-	1.0	1.0	0.04P,0.03S
5	Monel 400	N4000	2.5	-	-	66.5	0.3	Bal.	-	0.5	0.024S

Table 2 Potentiostatic Polarization data from NACE Solution and Natural Seawater (NSW).

S.No.	**Material**	**Electrolyte**	**E corr (mv)**	**I corr (μA/cm²)**	**CR (mpy)**
1	316L	i) NACE Solution	-59.6	1.53	0.67
		ii) NSW	-216	0.32	0.13
		iii) NSW + 0.064 M Sulfide	-348	0.31	0.137
		iv) NSW + 0.1 M Sulfide	-389	24.64	10.84
2	317L	i) NACE Solution	-212	0.58	0.26
		ii) NSW	-261	0.31	0.13
		iii) NSW + 0.064 M Sulfide	-383	0.39	0.17
		iv) NSW + 0.1 M Sulfide	-392	15.72	8.17
3	430	i) NACE Solution	-332	0.47	0.21
		ii) NSW	-65	0.16	0.06
		iii) NSW + 0.064 M Sulfide	-480	16.72	7.35
		iv) NSW + 0.1 M Sulfide	-503	1.62	7.12
4	Monel 400	i) NACE Solution	-207	9.53	3.7
		ii) NSW	-244	8.85	3.45
		iii) NSW + 0.064 M Sulfide	-315	1.61	0.63
		iv) NSW + 0.1 M Sulfide	-601	7.98	3.11

Table 3 Potentiostatic Polarization data from SHELL Solution

S. No.	Material	Electrolyte	E corr (mv)	I corr (μA/cm²)	CR (mpy)
1	Mild Steel	i) SHELL Solution ii) SHELL Solution+0.1 M Sulfide	-705 -715	57.88 37.71	25.46 16.59
2	316L	i) SHELL Solution ii) SHELL Solution+0.1 M Sulfide	-100 -72	1.31 4.81	0.57 2.11
3	317L	i) SHELL Solution ii) SHELL Solution+0.1 M Sulfide	-62 -125	0.34 3.87	0.15 1.7
4	430	i) SHELL Solution ii) SHELL Solution+0.1 M Sulfide	-150 -215	0.93 1.6	0.41 0.7
5	Monel 400	i) SHELL Solution ii) SHELL Solution+0.1 M Sulfide	-492 -450	9.96 11.89	3.88 4.64

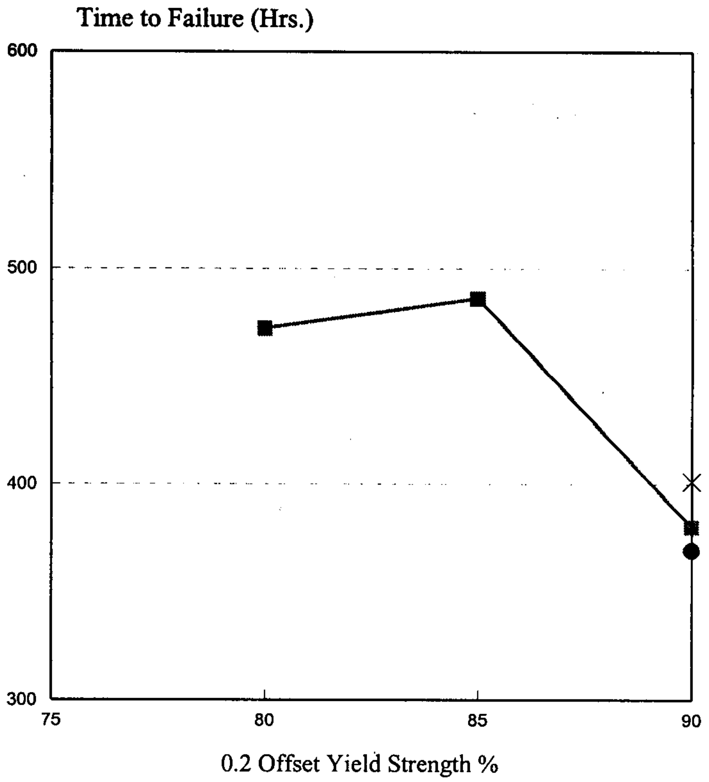

Fig SCC of alloys in NACE Soln. Containing Hydrogren Sulfide

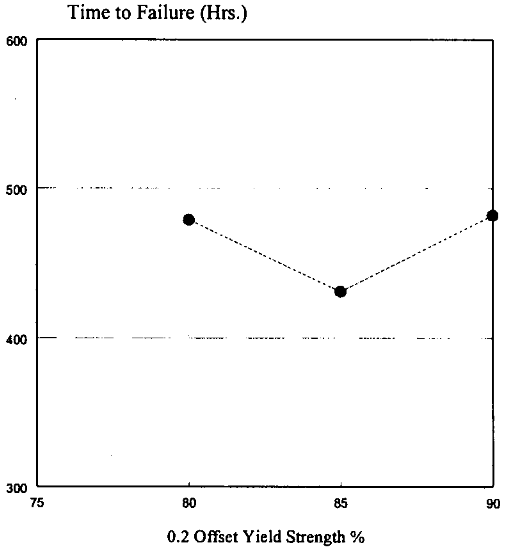

Fig.2 SCC of Alloys in SHELL Solution Containing Hydrogen Sulfide

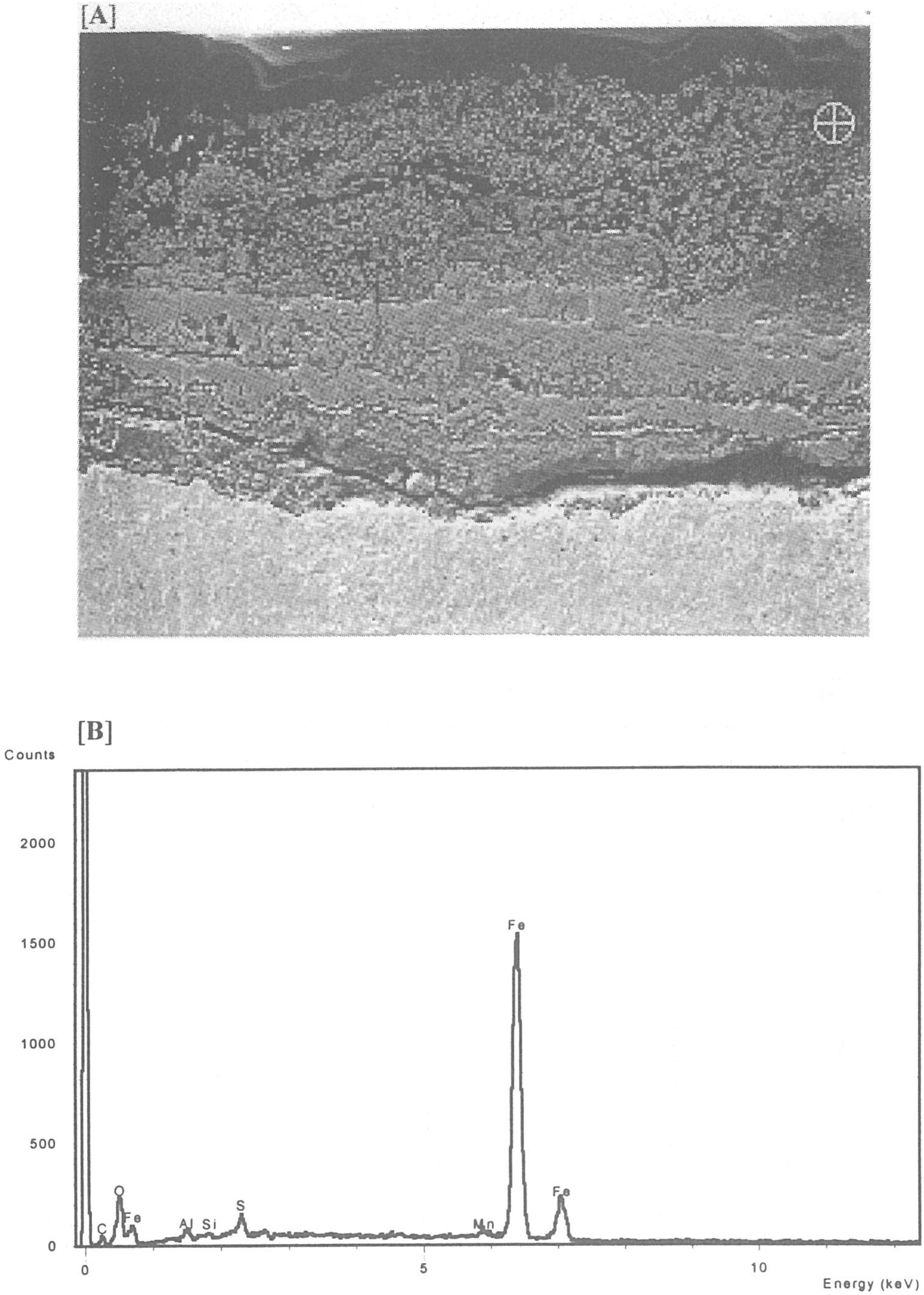

Figure 4. [A] SEM micrograph and [B] EDAX results showing the elemental distribution in the oxide scales formed on carbon steel coupon, exposed for 9000 hrs. in stage #1 of MSF plant

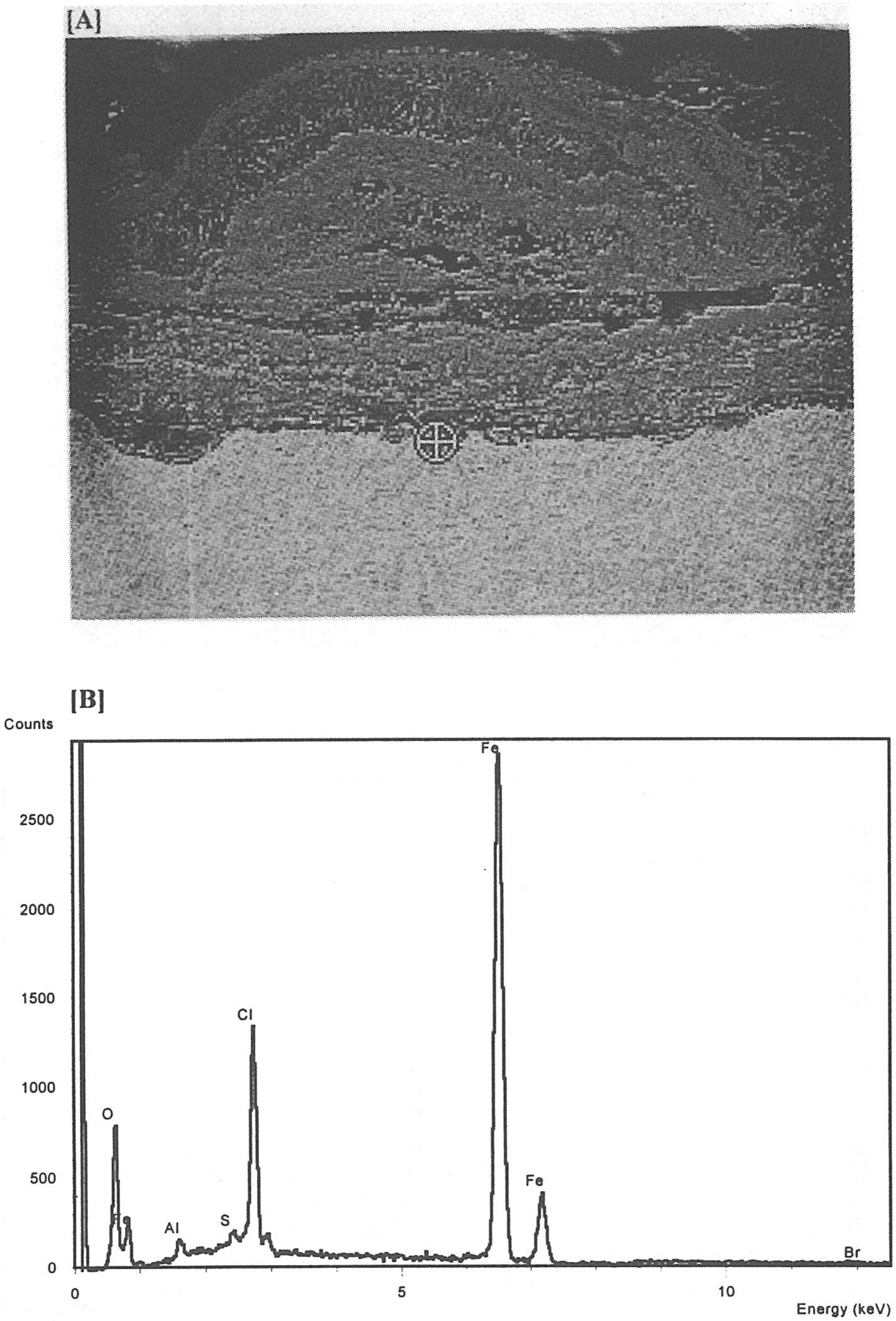

Figure 5. [A] SEM micrograph and [B] EDAX results showing the elemental distribution in the oxide scales formed on carbon steel coupons, exposed in MSF stage #4, for 9000 hrs.

Studies on Corrosion of Carbon Steel in Deaerated Saline Solutions in Presence of Scale Inhibitor

Ismaeel Andijani and S. Turgoose

STUDIES ON CORROSION OF CARBON STEEL IN DEAERATED SALINE SOLUTIONS IN PRESENCE OF SCALE INHIBITOR

Ismaeel Andijani[1] and S. Turgoose[2]
[1] SWCC, RDC
P.O. Box 8134, Al-Jubail 31951
[2] Corrosion Protection Centre, UMIST
Manchester, M60 1QD
UK

ABSTRACT

An investigation has been carried out to evaluate the corrosion behaviour of carbon steel in deaerated 1.0 M NaCl solutions and artificial seawater at pH ranges of 3 to 8.5 and temperatures up to 80°C under static conditions, using the polarization resistance technique. The effect of scale inhibitor addition on the corrosion rates has also been studied.

It has been found that the polarization resistance of carbon steel in deaerated solutions is generally high. With increasing pH, the polarization resistance increases, and is highest at 25°C and lowest at 80°C.

In long-run measurements, for 50°C at pH 8.5 the corrosion rates gave lower values compared to short-run measurements under the same conditions. This reduction in the corrosion rate is due to the formation of a protective hydroxide film on the metal surface, which restrict access of H_2O to the surface.

The results obtained with addition of 20 ppm phosphonobutanetri- carboxylic-acid scale-inhibitor at 50°C at pH 8.5, showed that there was no effect on the R_P values.

Key words: Carbon Steel, Desalination, Dissolve oxygen, Corrosion rate, Inhibitor, Polarization,

INTRODUCTION

Production of water by desalination of seawater is the prime source of drinking or potable water in the Arabian Gulf Countries. Multi Stage Flash evaporation (MSF) is the main process used for production of desalinated water. Carbon steel and wide variety of materials of diverse properties are used in MSF plants. A seawater desalination plant offers numerous corrosion problems due to its process conditions, including factors such as temperature and pH, and operation in relatively aggressive environments consisting of deaerated seawater, seawater-air and salt-air aerosols, corrosive gases, slow moving or stagnant liquids or deposit forming liquids [1]. To control the scale formation, acid treatment and anti-scale additive are used in desalination plants. To reduce the corrosion rates, removal of oxygen from the seawater by physical and chemical methods is used.

Therefore, mechanistic studies are required, which can provide experimental data and good understanding of the corrosion behaviour of metallic materials in these environments.

Some studies involving the use of a range of materials have been carried out under actual service conditions in desalination plants [2-6]and in laboratory conditions [7,8] using seawater and deaerated seawater at temperatures up to 90°C with different ranges of pH.

This work is concerned with the electrochemical study of carbon steel corrosion in deaerated 1.0 M NaCl solution and artificial seawater with and without addition of 20 ppm phosphonobutanetri- carboxylic-acid scale-inhibitor at different pH and temperatures under static conditions.

EXPERIMENTAL PROCEDURE

Specimens used in the polarization resistance measurements were cut from a mild steel cylindrical rod of 0.785 cm^2 cross section area. The electrodes were approximately 1.5 cm long, covered with adhesive lined hot shrink tube for 50° and 80°C test solution to prevent water entering between electrode and araldite resin, due to expansion of the resin with heat, and consequently to avoid crevice corrosion. A conducting wire was spot welded to each piece of metal; then the wires were insulated with PVC tubes of 6 mm in diameter in order to avoid electrical contact between the wires and the electrolyte, and to hold the electrode during the test. The electrodes were then mounted in araldite setting resin. The specimens were prepared by polishing with a 600 grit SiC abrasive paper, then rinsed with distilled water and dried in a stream of air. The corrosive media are 1.0 M NaCl solution, prepared by dissolved 58.5g of NaCl salt in 1dm^3 distilled water, and artificial seawater. The pH of solutions was adjusted to different range values from pH 8.5 to pH 3.0 with dilute HCl and NaOH solutions. Phosphonobutanetricarboxylic-acid scale-inhibitor, PBTC, with commercial name of BAYHIBIT,

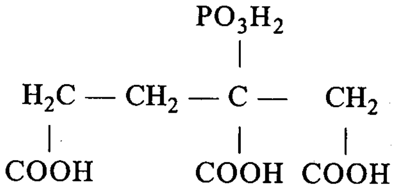

$$\begin{array}{ccccccc} & & & & \mathrm{PO_3H_2} & & \\ & & & & | & & \\ \mathrm{H_2C} & — & \mathrm{CH_2} & — & \mathrm{C} & — & \mathrm{CH_2} \\ | & & & & | & & | \\ \mathrm{COOH} & & & & \mathrm{COOH} & & \mathrm{COOH} \end{array}$$

was added to the test solutions. Deaeration was achieved by continuous purging N_2 gas (oxygen free) through the sealed test cell.

Polarisation resistance data were obtained using a standard three-electrode arrangement in 1 litre of deaerated test solution, in conjunction with an EG&G model 273 potentiostat/galvanostat and a chart recorder. A saturated calomel electrode and platinum electrode was used as reference and counter electrodes, respectively. The current-potential curve of carbon steel electrode in deaerated solution with and without scale-inhibitor was measured in the region of ±10 mV around E_{corr} under static condition. The slope, DE/DI, at the corrosion potential, is defined as polarisation resistance (R_P). The corrosion current density is $I_{corr} = B / R_P$ where B is the Tafel slopes determined from the E vs. $\log_{10}$ I plot. The measurements were repeated at three different temperatures, 25, 50 and 80°C. Before starting the experiments, the specimens were left in the test solution for about 1 hour to attain a steady state which was shown by a constant potential. The scan rate of applied potential was 0.25 mV/sec.

The short run measurements were carried out by successively adjusting the pH and measuring corrosion rate on the same electrode. The entire experiment took only a few hours. The long run measurements were carried out by taking readings at different time intervals at fixed temperature over 24 hours. The pH was monitored over this period.

EXPERIMENTAL RESULTS

Figure 1 shows the results of polarization resistance measurements of carbon steel in deaerated 1.0 M NaCl solution at temperatures of 25, 50 and 80°C and over a pH range of 8.5 to 3.0.

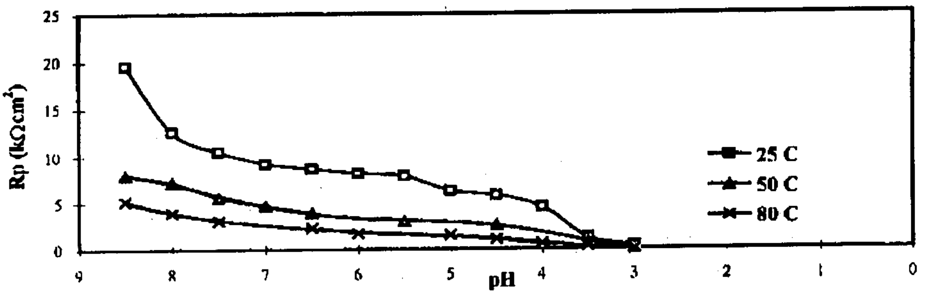

Fig.1 Polarization resistance measurements of carbon steel with pH in deaerated 1 M NaCl solution

At 25°C, the results indicate high R_P values in the neutral pH range and which then decrease with decrease in the pH values, while corrosion potential increases with decrease in the pH. Same phenomena observed at 50 and 80°C as summarised in tables (1,2,3).

Table (1) Short-run Measurements Results of Carbon Steel in Deaerated 1 M NaCl Solution at 25°C

	pH						
	8.5	8.0	7.5	7.0	6.5	6.0	3.5
E_{corr}, (mV)	-785	-780	-777	-775	-772	-770	-750
R_P, (kΩ.cm^2)	19.6	12.6	10.5	9.2	8.7	8.2	1.2
I_{corr}(μA/cm^2)	1.27	1.98	2.38	2.71	2.87	3.05	20.8
CR (mm/y)	0.013	0.02	0.024	0.027	0.029	0.031	0.21

Table (2) Short-run Measurements Results of Carbon Steel in Deaerated 1 M NaCl Solution at 50°C.

	pH						
	8.5	8.0	7.5	7.0	6.5	6.0	3.5
E_{corr}, (mV)	-810	-800	-787	-780	-774	-770	-745
R_P,(kΩ.cm^2)	8.0	7.2	5.6	4.7	3.9	_	0.78
I_{corr}(μA/cm^2)	3.12	3.47	4.46	5.32	5.41	_	31.8
CR (mm/y)	0.031	0.035	0.045	0.053	0.064	_	0.32

Table (3) Short-run Measurements Results of Carbon Steel in Deaerated 1 M NaCl Solution at 80°C.

	pH						
	8.5	8.0	7.5	7.0	6.5	6.0	3.5
$E_{corr,}$(mV)	-830	-810	-803	-798	-794	-790	-740
$R_{P,}$(kΩ.cm^2)	5.2	3.9	3.1	_	2.3	1.7	0.3
I_{corr}(μA/cm^2)	4.81	6.4	8.06	_	10.87	14.71	83.3
CR(mm/y)	0.048	0.064	0.081	_	0.11	0.15	0.83

Table 4 shows the results of polarization resistance measurements with time of carbon steel in deaerated 1 M NaCl solution at 50°C and pH 8.5.

Table (4) Long-run measurements results of carbon steel in deaerated 1.0 M NaCl solution at 50 ^{0} C and pH 8.5.

Time, hr	1	2	3	4	21	22	23	24
I(μA/cm^2)	3.62	3.33	3.2	3	2.58	2.56	2.43	2.4
E(mV)	-797							-818

The tables indicate that the Icorr values decreases with time and the Ecorr shifted to more negative value. Figure 2 shows the Tafel Plot of carbon steel in deaerated 1.0 M NaCl at 50 C and pH 8.5 under static conditions. The experiments were carried out at two different time intervals e.g., 1 hr and 24 hrs.

Fig. 2 Potentiodynamic polarization curves of carbon steel in deaerated 1 M NaCl at different immersion interval

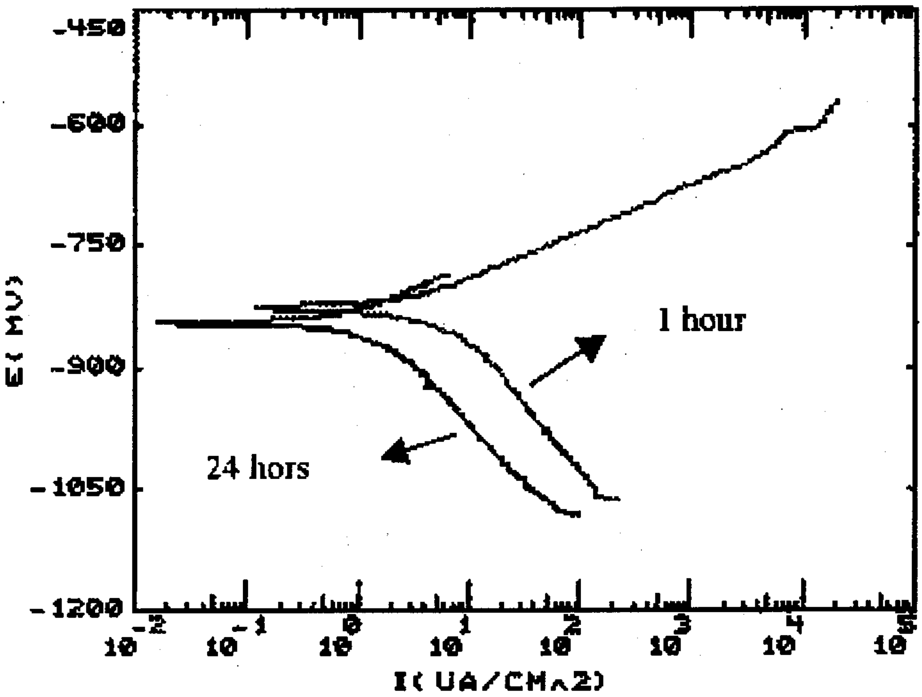

Figure 3 shows the results of polarization resistance measurements with time of carbon steel in deaerated 1.0 M NaCl solution and artificial seawater with and without addition of scale-inhibitor at 50°C and pH 8.5. The objective of this experiment is to distinguish, in terms of corrosion current of steel, between NaCl solution and artificial seawater and between inhibited seawater and uninhibited seawater in long term tests.

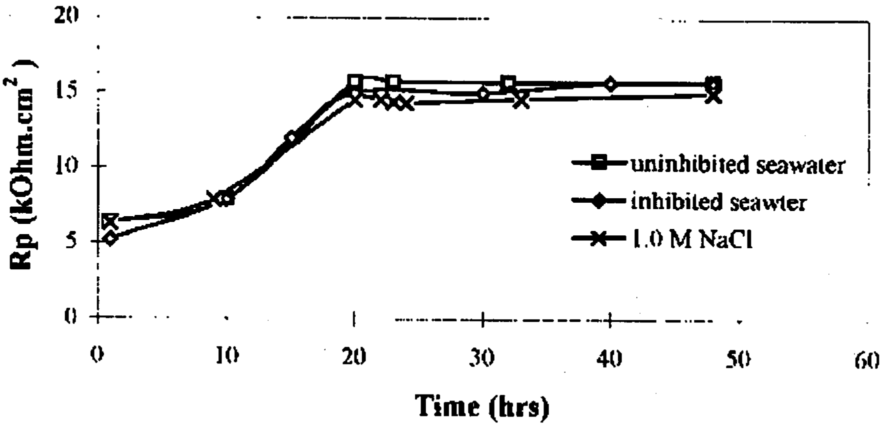

Fig. 3. Polarization resistance measurements of carbon steel with time in deaerated solution

DISCUSSION

The mixed potential theory was derived originally to explain experimental electrochemical laboratory measurements. The useful of E-log I diagrams is that they combine thermodynamics and kinetics to form a whole picture: the potential axis is the thermodynamic factor and the current axis is the kinetic factor. Obviously, the rate of corrosion of steel in deaerated solution is controlled by such factors as:

(i) the anodic polarization line of steel.

(ii) the cathodic polarization line of water reduction in the neutral and slightly alkaline solution.

(iii) the cathodic polarisation line of hydrogen reduction in the acidic solution.

Since water reduction is the only cathodic reaction in the deaerated neutral solution therefore, the corrosion rate depends on how rapidly H_2O diffuses to the metal surface through the barrier of oxide film and on diffusion of Fe^{2+} out through the film. Thus any change in temperature, bulk concentration and disturbance of the oxide film will affect the reaction rate.

Within the acid region of the solution the oxide film is dissolved, the steel surface is in direct contact with the aqueous solution and hence the increased rate of reaction is due to the higher rate of hydrogen evolution. Increasing hydrogen ion concentration in the neutral and slightly alkaline solution i.e., 8.5 - 6.5 the equilibrium potential of the hydrogen electrode becomes more noble, according to this relation $E_{H/H}{}^{+} = 0.0 - 0.059pH$, although $I_{oH/H2O}$ remain constant, hence $E_{H/H}{}^{+} - E_{Fe/Fe}{}^{2+}$ becomes larger and the resulting corrosion current increases. Graphically this may be represented in Evans diagram as shown in Fig. 4

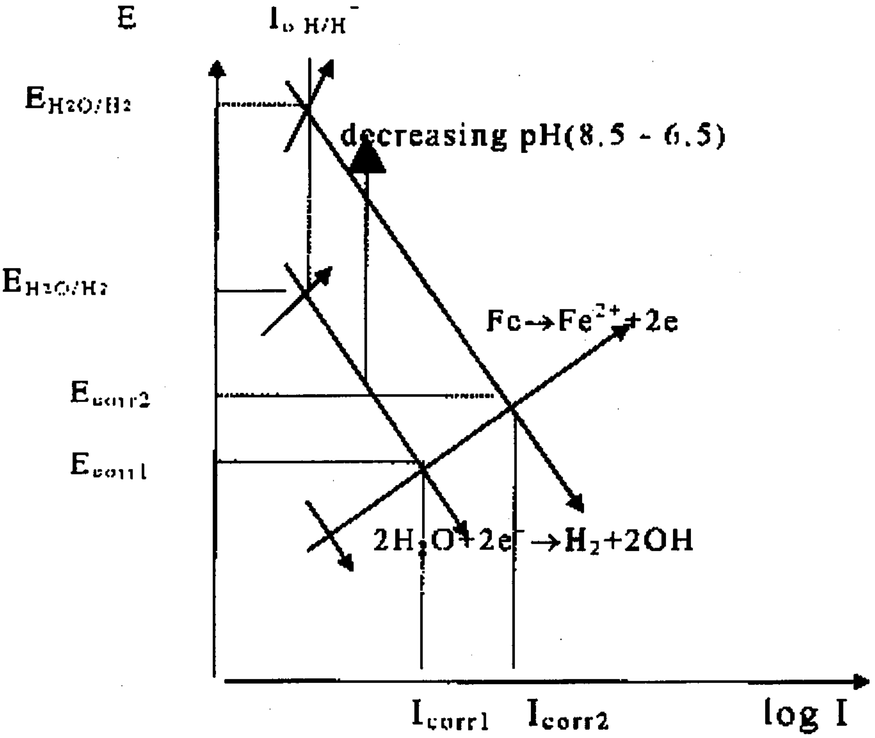

Fig. 4 Evans diagram for pH range of 8.5 and 6.5 for carbon steel in deaerated 1 M NaCl solution at 50°C.

This explains why the corrosion rate of carbon steel in deaerated NaCl solution increases with decreases in pH at neutral and slightly alkaline solution and also E_{corr} shifts to more positive values. When the solution become more acidic, the equilibrium potential of the hydrogen electrode becomes more noble and the exchange current density of hydrogen on steel, $I_{oH/H}{}^{+}$ on Fe, increases and hence the corrosion rates increases compared to neutral solution. Schematically:

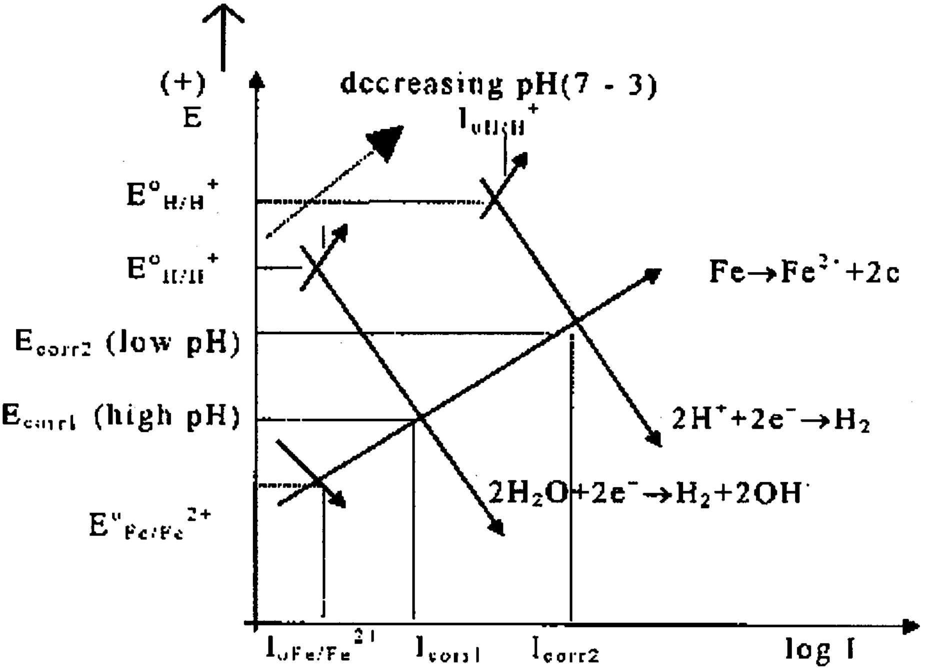

Fig.5 Evans diagram for pH range of 7 and 3 for carbon steel in deaerated 1 M NaCl solution at 50°C.

This explains why the corrosion current of steel in deaerated NaCl solution at 25°C (Table 1) was increased slowly at pH 8.5 to pH 6.0 (1.27 to 3.05 $\mu A/cm^2$) where at pH 6.0 to pH 3.5 the corrosion current was increased drastically (3.05 to 20.8 $\mu A/cm^2$). At increased temperature, 50 and 80°C, the velocity of corrosion reaction is greater than at 25°C due to $I_{oFe/Fe}{}^{2+}$ increasing at elevated temperatures. However, the relationship between exchange current, $I_{oFe/Fe}{}^{2+}$, and temperature is given by [9]

$$I_{oFe/Fe}{}^{2+} = n.F.f.c^n .\alpha. \frac{N_s}{N_o} \exp\left[\frac{-\Delta G}{RT}\right]$$

where:

n = number of electron.

F = Faraday constant.

f = the frequency of thermal vibrations, ~ 10^{12} Hz, which determine frequency with which atoms exchange thermal energy.

c^n = the concentration of solvating species in the environment and n the number of solvating molecules associated with each cation.

α = the proportion of atoms on a metal surface located at link site, 10^{-3}, it depends on whether the metal is annealed or coldworked.

N_s/N_o = the number of moles of metal per unit area of surface, where N_s is the number of metal atoms per unit area of surface (typically $\sim 2\times10^{13}$ atoms/mm^2) and N_o is the number of atoms/mole (Avogadro,s number, $\sim6\times10^{23}$ atoms/mole).

ΔG = electrochemical activation energy.

R = perfect gas constant.

T = absolute temperature.

Increasing the temperature of the solution will increase $I_{O\ M/M^{n+}}$ of both electrodes, hydrogen reduction reaction and iron oxidation reaction and hence corrosion rate increases.

Increase in temperature also affects the reversible equilibrium potential, $E^O_{M/M^{n+}}$ of both electrodes. The relationship between temperature and reversible equilibrium potential is given by

$$\Delta G^O = n\ F\ E^O$$

$$\Delta G^O = -\ R\ T\ \ln K_{eq}$$

$$E^O = -\ \frac{RT \ln K_{eq}}{nF}$$

With increasing temperature, the reversible equilibrium potential becomes more negative.

Figure (6) shows the temperature influence on the polarisation curves of carbon steel in deaerated 1.0 M NaCl solution at pH 8.5. As the temperature increases from 25 to 80^O C, the E_{CORR} shifts to more negative values and I_{CORR} increases.

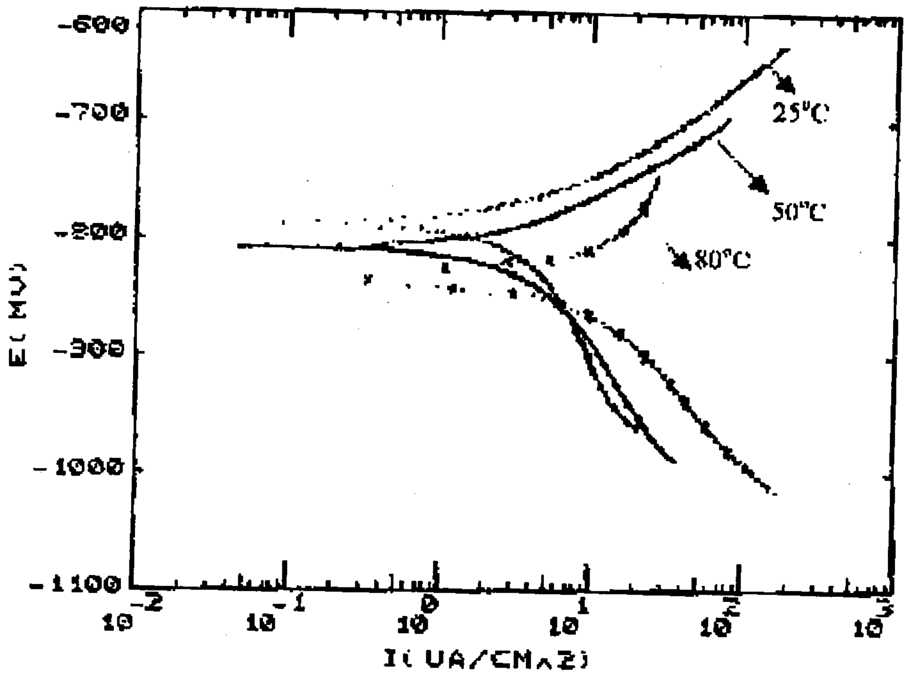

Figure 6. Potentiodynamic polarisation curves of carbonsteel in deaerated 1.0 M NaCl solution at pH 8.5 and different temperature under static condition

Thus increased rate of reaction at increased temperatures from 25 to 80°C is due to the kinetic change of anodic and cathodic reactions. E_{CORR} in general had more negative value at 80°C compare to 50°C and 25°C. at pH 8.5.

Graphically this may be represented in Evans diagram as shown in Fig. 7

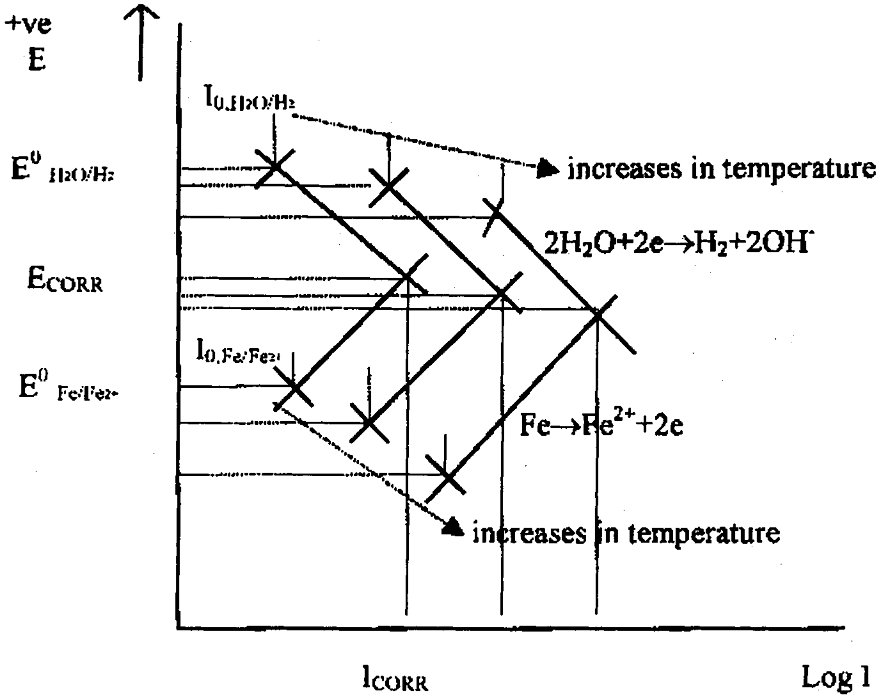

Fig. 7 Evans diagram for carbon steel at temperature 25, 50 and 80°C in deaerated 1.0 M NaCl solution at pH 8.5 under static condition.

This diagram illustrates the effect of increase in temperature on the anodic and cathodic partial reaction. With increase in temperature, $I_{0,Fe/Fe2+}$ increases and $E^0{}_{Fe/Fe2+}$ becomes more negative, the resulting anodic curve shifts to down right. Similarly, the cathodic curve, with increase in temperature also shifts to down right. Hence, the resulting corrosion current increases and E_{CORR} becomes more negative.

Deaerated Seawater

The results of corrosion behaviour of steel in seawater showed no significance difference compared to NaCl solution in same condition as shown in figure 3. Usually seawater has tendency to form adherent scale deposit on the metal surface at elevated temperature that isolates the metal from the seawater and hence corrosion decreases. But no such case occurred here.

Effect of Addition of Scale-inhibitor

Addition of scale-inhibitor basically is to distort the crystals of the scale-forming material at elevated temperature. The experimental results (figure 8) indicated that the influence of scale-inhibitor on the corrosion rates of the steel was mostly on the cathodic reaction. Decrease of the pH of the solution and consequent corrosion current increase when scale-inhibitor was added to the solution with the increase in E_{corr} means that the corrosion rate is under cathodic control, because when the pH was adjusted to the initial value, the corrosion current was almost the same as without inhibitor. Thus, addition of phosphonobutanetricarboxylic-acid scale-inhibitor at constant pH has almost no effect on the corrosion rates.

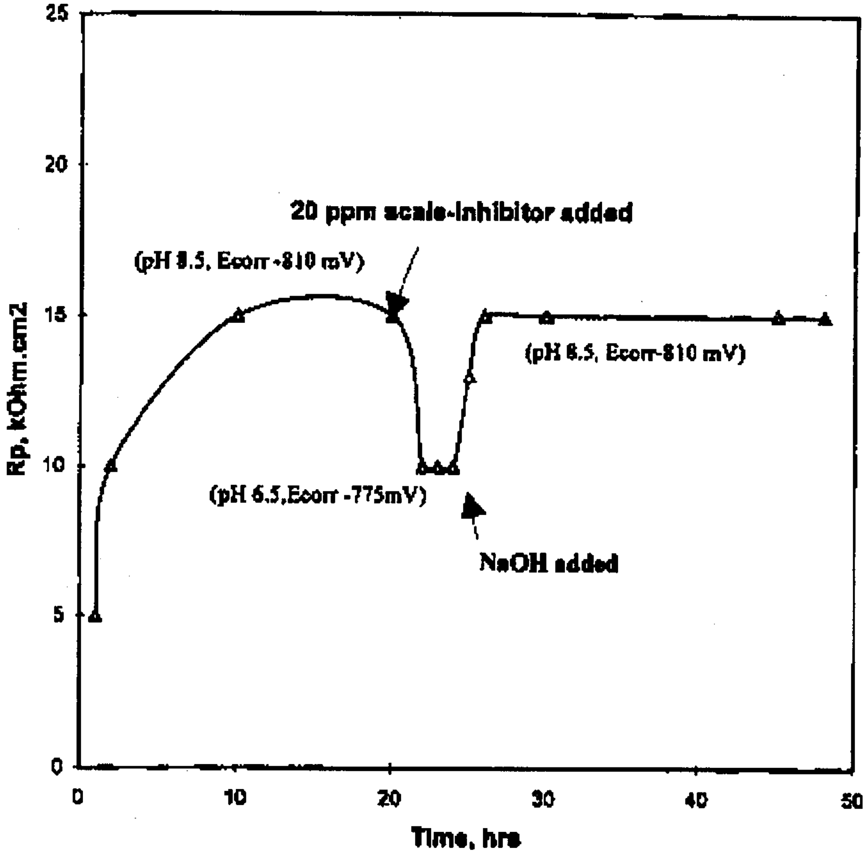

Fig. 8 The addition effect of scale-inhibitor on the corrosion behaviour of carbon steel in deaerated solution at pH 8.5 and 50°C.

Long-run Test

The results of these tests have confirmed that the corrosion rates of carbon steel tend to reduce in seawater and NaCl environments at 50 °C and pH 8.5. This has been explained on the basis of formation of a protective hydroxide film as represented by the following electrochemical reactions: Under deaerated condition, the anodic reaction is represented as follows:

$Fe \rightarrow Fe^{2+} + 2e$ (1)

The cathodic reaction at neutral pH is

$2H_2O + 2e \rightarrow H_2 + 2OH^-$ (2)

Fe^{2+} hydrolysis to form $Fe(OH)_2$

$Fe^{2+} + 2H_2O \rightarrow Fe(OH)_2 + 2H^+$ (3)

Under deaerated condition, the corrosion product, $Fe(OH)_2$ formed on metal surface increases with time but it also impedes the cathodic reaction (2) resulting in lowering of the current density. When sufficient amount of the deposit is formed on the steel surface, the current subsequently becomes constant.

From the Tafel Plot of carbon steel in deaerated 1.0 M NaCl at 50°C and pH 8.5 under static conditions, the study of the cathodic curves indicates that Icorr shifts towards left (to low current value) at 24 hrs and Ecorr is also shifted to less noble value. This behaviour can be represented by Evans diagram:

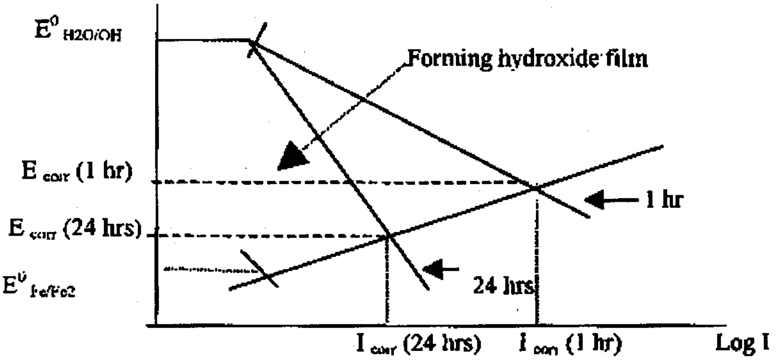

Fig 9 Evans diagram at different immersion interval of carbon steel in deaerated 1 M NaCl solution at 50°C and pH 8.5.

The diagram shows clearly the shifting of I_{corr} to lower value with increase in time. Thus after 24 hrs there will be more formation of $Fe(OH)_2$ than that after 1 hr and this will result in lower value of I_{corr}.

CONCLUSIONS

In the present study, the corrosion behaviour of carbon steel in deaerated 1 M NaCl solution and artificial seawater were studied by polarisation resistance measurements, the following characteristics were found:

- The corrosion rates were very low at 25°C and neutral pH.
- With decrease in pH the corrosion rates increase and the corrosion potential increase [more noble].
- With increase in temperatures [25° to 80°C] the corrosion rates increase [$(0.024\ mm/y)_{pH7.5}$ to $(0.081\ mm/y)_{pH\ 7.5}$] and the corrosion potential decreases (less noble).
- In the neutral and slightly alkaline solution, H_2O diffusion to the metal surface through the barrier of oxide film is the rate determining. While in the acidic solution, the oxide film is dissolved, the rate of hydrogen evolution alone determines the reaction rate.
- The addition of phosphonobutanetricarboxylic-acid scale-inhibitor has no significant effect on the corrosion rates.
- In long-run measurements, at 50°C and pH 8.5, the corrosion rates gave lower values compared to short-run measurements at the same conditions. This reduction in the corrosion rate is due to the formation of a protective hydroxide film on the metal surface which restrict access of H_2O to the surface

REFERENCES

1. A.U. Malik and P.C. Mayan Kutty, Desalination, 97 (1994) 171-187.

2. T. Hodgkiess, W.T. Hanbury and M.H. Hejazian, Desalination, 44 (1983) 223-232.

3. F.C. Wood and Y.N. Wu, Desalination, 30 (1979) 347-358.

4. K. Harding and D.A. Bridle, Desalination, 28 (1979) 84-108.

5. Schrieber, C.F., Coley, F.H., Mat. Perform., No.7, 15 (1976) 47-54.

6. Heitz, E., Manner, R., Werkstoffe and Korrosion, 29 (1978) 783-791.

7. J. Sakuma, T. Takagi, S. Yamada and Y. Kibe, Desalination, 14 (1974) 189-196.

8. T. Hodgkiess, W.T. Hanbury, M. Arndt and N. Eid, Desalination, 31 (1979) 399-410.

9. M. Stern and A. L. Geary, J. Electrochem. Soc., Vol. 104 (1957) 56.

المراجع

{1} أحمد عبدالقادر المهندس، "الماء ثروة الحاضر وأمل المستقبل" المجلة العربية، العدد الثالث عشر، محرم 1419هـ الموافق ليونيو 1998م، الرياض، المملكة العربية السعودية.

{2} سامر مخيمر وخالد حجازى، "أزمة المياه في المنطقة العربية، الحقائق والبدائل الممكنة"، سلسلة عالم المعرفة 209، المجلس الوطنى للثقافة والفنون والآداب، ذى الحجة 1416هـ الموافق لمايو 1996م، الكويت، دولة الكويت.

{3} جميل العلوى ومحمد عبدالرزاق، "الماء بشبه الجزيرة العربية - صعوبات وتطلعات"، الماء بالعالم العربي، مطبعة جامعة هارفرد، 1994م، الولايات المتحدة الأمريكية.

{4} محمد بن عبدالكريم الصوفي " تحديات المستقبل " محاضر المؤتمر العالمي السادس للتحلية وإعادة إستخدام الماء ، 1993م ، يوكوهاما ، اليابان .

الأولى إلى الثانية العاشرة ، كما هو مبين عمودياً بالجدول (ك) ، ثم تحديد فئات المستخدمين بدءً بالفئة المعفاة التى تمثل الفئة التى ليس بوسعها إستخدام الماء إلا بالنزر اليسير أى أن العائلة المكونة من خمسة أفراد والتي لا يصل إستخدام الفرد بهذه العائلة من الماء ما يصل إلى 66 لتر يومياً. فإذا ما وجدت مثل هذه العائلة بحواضر الخليج فهي جديرة ومستحقة للإعفاء الكامل من دفع كلف الماء الذى يصل إلى دار هذه العائلة. وبهذا يتم تعريف هذه الفئة على أنها الفئة المعفاة. أما الفئات الباقية فيقترح أن تدفع الكلف تصاعدياً. إذ لماذا وكيف يمكن تبرير إستفادة الفئات المتقدمة ؟ إى فئات تتجاوز شرائحها الدنيا الحد الأعلى للشرائح السابقة فكيف يمكن أن تتمتع هذه الفئات بميزات الدعم ما دامت ستطلب الماء بكميات متزايدة ؟ هذا ويمكن تبني آلية شرائح سلمية مماثلة للماء للأغراض الصناعية وكذلك الكهرباء مع تحديد سعات متدرجة ، كما إقترح بهذا الطرح لسعات شرائح الماء للإستخدام الحضرى، حيث جاءت الكميات باللتر ومضاعفاته كالآلاف والملايين وذلك لأسباب لا مجال للخوض بها هنا عدى أن مجرد ذكر كلمة ألف كأداة للترشيد سيكون لها إيحاء نفسي وحتى ذكر مئات اللترات هو خير من ذكر أجزاء المتر المكعب.

هذا ولقد جاء بالجدول (ك) تصنيف للشرائح (سعات الإستخدام) والفئات ضمن ثلاث مجموعات تبين طبيعة الإستخدام فالمجموعة الأولى هي لقوام حياة الفرد والمجموعة الثانية للإستجابة للضرورات الحياتية أما المجموعة الثالثة فهي لضمان الرفاه الإجتماعي { 4 } .

و يمكن أن تصل هذه المراجعة وإستنادا إلى ما تقدم إلى إستنتاجين هامين هما ضرورة إيجاد نظام تعرفة يراعى مصلحة الجهات المنتجة وقبل ذلك تلك المستخدمة لهذه المرافق الحيوية. وكذلك الفصل بين الجهات ذات الأهداف المتباينة . حتى يمكن وضع سياسات متوازنة عادلة ومنصفة بمجالات المحافظة على الثروات وحمايتها من الإسراف . ويمكن أن تتحقق هذه الآمال متى ما وجد الجهاز المتكامل الذى يتولى إدارة المدخلات وذلك لتحقيق :

الإستخدام الأمثل للموارد والطاقة معاً.

الجدول (ك). الحدود الكمية لشرائح إستخدام الماء والتعرفة المقابلة لها (حسب الفئات المستخدمة).

طبيعة				قوام الحياة			الضرورات الحياتية			الرفاه الاجتماعي		
الإستخدام	الشرائح	التعرفة المقترحة فلس بحريني لكل ألف لتر	الفئات الكميات بآلاف اللترات شهرياً للأسرة	أ	ب	ج	د	هـ	و	ز	ح	ط
	الأولى	صفر	10	✓	✗	✗	✗	✗	✗	✗	✗	✗
	الثانية	5	10	✗	✓	✗	✗	✗	✗	✗	✗	✗
	الثالثة	15	20	✗	✓	✓	✗	✗	✗	✗	✗	✗
	الرابعة	25	30	✗	✓	✓	✓	✗	✗	✗	✗	✗
	الخامسة	50	40	✗	✓	✓	✓	✓	✗	✗	✗	✗
	السادسة	100	50	✗	✗	✓	✓	✓	✓	✓	✗	✗
	السابعة	200	70	✗	✗	✗	✓	✓	✓	✓	✓	✗
	الثامنة	300	90	✗	✗	✗	✗	✓	✓	✓	✓	✗
	التاسعة	400	110	✗	✗	✗	✗	✗	✓	✓	✓	✓
	العاشرة	500	140	✗	✗	✗	✗	✗	✗	✓	✓	✓
	الحادية عشر	600	170	✗	✗	✗	✗	✗	✗	✗	✓	✓
	الثانية عشر	900	مفتوحة	✗	✗	✗	✗	✗	✗	✗	✗	✓

(✓) إستعملت إشارة الصحيح للتعبيرعن إمكانية تطبيق التعرفات ضمن الكميات المحددة حسب الفئات.

(✗) إستعملت إشارة خطأ للدلالة على عدم تمتع الفئات ذات الإستخدام الأعلى من ميزات الفئات ذات الإستخدام الأدنى وذلك بتحديد الكميات والتعرفة وهو المبين بالتظليل.

فالمراد طرحه هنا أسلوب أطلق عليه سلمية شرائح التعرفة. ويبين الجدول (ك) المراد بهذه السلمية. أى أن يتم التعامل مع كميات الطلب لا على أساس شرائح ثابتة من الألف إلى الطاء بل تحديد الفئات على أساس كميات الطلب حسب تزايدها. فالمقترح وضع نمط للشرائح من

نظـرة مستقبلية

هذا ولقد دلت هذه المراجعة التحليلية الحد من تولي جهاز ما إدارة إنتاج الزيت الخام (المدخلات) وكذلك التكرير والتصنيع (المخرجات). وقد يعزى الإسراف فى إستغلال، أي إستنزاف مكامن الغاز الطبيعي ، عند التوجه لتشجيع إنتاج صناعي مثل فصل معدن عن مادته الخام. رغم أنه قد يكون معروفا من الناحية التقنية أن عملية الفصل هذه تتطلب قدرا كبيرا من الكهرباء الذي لا يمكن توفيره إلا باستغلال متسارع لمكامن الغاز. أي أن يندرج الوضع تحت المقولة التى تشير إلى توحد المصالح (إذ يقال : المصلحة وحدة أو شيل من ذا وحط على ذا).

مستقبل الترشيد

ولما كانت المراجعة قد أتت على الإنتاج الصناعي للمّاء أى الإستعذاب فإنه من الضرورة بمكان بيان أن الغرض الأساس للإستعذاب هو الإستخدام الحضري وقدراً يسيراً للصناعة. وعند الحديث عن الكميات فإنه يلزم إيضاح حقيقة هامة هى أن مجمل إحتياجات الإستخدام الحضري والصناعي لا تصل إلى مستوى ربع الإستخدامات بغالب المجتمعات وحتى معظم دول المنطقة. وقد يثير ذلك تساؤلا هو: لماذا كل هذا العويل والصياح عن الترشيد بمجتمعات دول المنطقة والمنصب على الحواضر وحياة الإنسان اليومية؟ وللرد على هذا التساؤل يمكن بيان حقيقة أن الخدمات التي يتطلبها إيصال الماء الصالح للإستخدام الآدمى ومن ثم جمع ماء الصرف وإستصلاحه يتطلب كثيراً من المال والأجهزة الآلية والإدارية. وتبعاً لذلك فإن حملات الترشيد قد إنصبت حتى الآن على رأس الإنسان فى حياته اليومية. ومما سبق يتبين ضرورة ذلك ولكن دون ترك الحبل على الغارب . لذا فمن الضرورة بمكان إيجاد أسلوب أكثر آلية وإنصافاً للمنتج والمستخدم لتحديد تعرفة الماء بلا ضرر ولا ضرار كما هو مبين بالجدول (ك).

العجز وأن هذا التراجع سيكون أكثر وضوحاً متى ما نفذت الخطط التى تضعها هذه الدول خلال العقد القادم.

مواطن القوة والضعف

ويندرج كثير مما سبق على الموارد الطبعية الأخرى بهذه المنطقة. لذا فالحاجة ماسة جداً إلى تسليط الضوء كى تتجه سياسات المنطقة نحو التوازن أملا بالوصول إلى الإستخدام الأمثل للموارد والطاقة. وعليه يمكن القول أن الوصول إلى وضع مقبول يتطلب قرارات حاسمة قد تؤثر على البنى والهياكل المؤسسية لكافة القطاعات الإنتاجية والمستخدمة لموارد الطبيعة فالمرجو أن تتجه المنطقة نحو الإستخدام الأمثل للموارد والطاقة. وقد يتطلب ذلك مراجعة شاملة للأوضاع بما سيحقق نوعاً من التوازن بالمستقبل ومن أهم ما يستحق البحث والدراسة كما أسلف وضع البنى والهياكل الإنتاجية والقطاعات المستخدمة للموارد والطاقة. فلقد حققت الأجهزة الإدارية بدول المنطقة إنجازات هائلة عبر العقدين الماضيين على طريق التنمية. ورغم كل إيجابيات المرحلة السابقة فإن النمو السريع والمضطرد لهذه الأجهزة قد أدى إلى حدوث تشابكات إدارية قد تصبح مع مرور الوقت عوائق فى طريق التنمية عبر العقود القادمة.

لذا لزم مراجعة مواطن الضعف التى قد تقف عقبة كأداء على درب مسيرة الخير. ولكى تكون أهداف هذه المراجعة واضحة فقد تم تحديد أساس لها. أى التحديد الواضح للأنشطة الحياتية للمجتمع البشرى أياً كان وأين ما كان فى هذا الزمان. ثم تحديد المدخلات الضرورية لكل واحدة من هذه الأنشطة. ولقد تبين أن المدخلات الأساس لجمل هذه الأنشطة هى الأخرى تشتمل على أربع مدخلات أساس أولها الماء وثانيها المواد الخام ثم النفط ورابعها الكهرباء.

وبهذا يمكن تحديد المدخل الأساس لكل واحدة من الأنشطة ثم تحديد مخرجاتها ويظهر الترابط الوثيق بين المدخل (والذى أشير إليه بالمدخل الأساس) وذلك النشاط الذى يقابله ، ودون أن يعنى ذلك الترابط الوثيق عدم وجود صلات أو متطلبات للانشطة الأخرى من المدخلات غير المقابلة لها. وبالمقابل فإن الصلة وثيقة جداً وذات صفة توحدية بين الأنشطة والمخرجات التى تقابلها .

الجدول (ح). توقعات عام 2000 بدول بشبه الجزيزة العربية لموارد الماء المتجدد مقارنة بالإحتياجات.

التسلسل	الدول	الموارد المتجددة كم 3 سنويا {1}	الإحتياجات كم 3 سنويا {3}	النسبة المئوية %
1	قطر	0.304	0.334	110
2	الكويت	0.508	0.640	136
3	البحرين	0.157	0.260	159
4	الإمارات	1.05	2.23	212
5	اليمن	1.5	3.6	240
6	عمان	0.345	1.417	411

الجدول (ط). توقعات عام 2010 لدول بشبه الجزيرة العربية لموارد الماء المتجدد مقارنة بالإحتياجات (3)

التسلسل	الدول	الموارد المتجددة كم 3 سنويا	الموارد المتجددة المضافة كم 3 سنويا	الإحتياجات كم 3 سنويا	النسبة المئوية %	النسبة المئوية المعدلة % (4)
1	قطر	0.259	0.052	0.388	149	125
2	الكويت	0.534	0.053	0.771	144	131
3	البحرين	0.194	0.019	0.315	162	148
4	الإمارات	1.097	0.110	2.456	224	203
5	اليمن	1.517	(5)	4.572	301	301
6	عمان	0.906	0.077	1.585	442	366

(3) إنظر المرجع {3} ، (4) عدلت التوقعات حسب الخطط المعلنة للتحلية والمعالجة.

(5) لا يعرف عن توسع ملحوظ بالمعالجة أو التحلية.

وهكذا يأتي الجدول (ط) ليبرز وضع غير مطمئن. فليس بين دول الجزيرة العربية دولة واحدة ستحقق فائضاً حتى إذا ما تم تنفيذ كل الخطط المعلنة والمتوقعة لزيادة الكميات المستصلحة والمستعذبة كما هو مشار إليه بالجدول (ط) حسب ما أورد المرجع (وبعد التعديل). فدول شبه الجزيرة العربية وحتى اليمن (التي وصفت بالسعيد تاريخيا لمائه وزرعه) سيعاني بالقرن القادم من عجز مائي. إلا أن الجدول (ط) يبين أن هناك تراجعاً بمستوى

مستقبل الوضع المائي بالعالم العربي

وتأكيداً على حراجة الوضع بغالب الدول العربية وخاصة دول شبه الجزيرة العربية، فالجداول السابقة تبين ما يتوقع أن يصل إليه الوضع المائى مع نهاية هذا القرن. ويظهر بأن الوضع سيكون حرجاً بدولتين من دول آسيا العربية الواقعة إلى شمال شبه جزيرة العرب وهما حسب حراجة الوضع الأردن والعراق التى يتجاوز بهما السحب على الكميات المتجددة بنسبة 45% و 11% وبذات الترتيب السابق. في حين أن فلسطين لا يزال سحبها دون الكميات المتجددة (راجع الجداول السابقة). ورغم ذلك فوضع فلسطين له خصوصيته بما يعانى منه أهلها من ظروف قاسية فى ظل الإحتلال.

هذا وتتمتع دولتان من دول الشمال هما الوحيدتان بآسيا العربية التى تتمتع بوضع مائى آمن إذ لا تسحب أي من لبنان وسوريا (راجع الجدول ب) سوى 31.5% و 23.5% من الكميات المتجددة وعلى الترتيب. أما الدول العربية الأفريقية المطلة على البحرين الأحمر والمتوسط، فإن أوضاعها المائية لا تبدوا حرجة سوى وضع ليبيا (والذى قد يكون محدود الحراجة لوجود مخزون جوفى هائل تحت رمال صحرائه)، حيث يتجاوز السحب بما يصل إلى 40% من الكيمات المتجددة (راجع الجدول ج).

وبعد هذا وذاك تأتى دول بشبه جزيزة العرب والتى تتقدمها دولة قطر عند وضع قريب من التوازن. أى عند 110% للسحب مقارنة بالكميات المتجددة بمافيها الإستعذاب. وتقع باقي دول شبه الجزيرة بما فيها اليمن ضمن مستويات السحب التى تتجاوز الكميات المتجددة بنسب أعلى. فخمس دول يتراوح سحبها بين 136% إلى 411%. ونظراً لحراجة هذا الوضع، فقد أعد الجدول (ط) حسب المراجع التى توقعت الوضع بنهاية العقد الأول من القرن القادم. ولأهمية هذه التوقعات، فقد تم تحليلها وتعديلها بما يتفق والزيادات المتوقعة بالكميات المستصلحة والمستعذبة خلال ما يصل إلى عقدين هما الأخير من هذا القرن والأول من القرن القادم فالمرجع الذى إعتمدت عليه المراجعة كان قد صدر بمطلع هذا العقد لا نهايته (تقريباً أى وقت إجراء المراجعة عام 1998).

حالات خاصة

ويمكن الآن الإنتقال إلى أوضاع خاصة إذ يبين الجدول (ز) ترتيب خمس دول ترتيباً تنازلياً أى من الأعلى إلى الأدنى. فالنرويج التى سبق ذكرها تسحب ما يقل عن عشر العشر 0.48% من الكميات المتجددة. ثم يأتى الجدول بذكر كندا من حيث أنها ذات كميات متجددة هائلة. وتليها الولايات المتحدة ذات السحب الهائل كماً. رغم أن هذا الكم الهائل من السحب لايصل إلى خمس الكميات المتجددة. وبعد هذه الدول الثلاث يرد بهذا الجدول ذكر إثنتين من الدول العربية أولها جمهورية مصر العربية. إذ (جاء بواحدة من الدراسات التى إعتمدت هذه المراجعة عليها بأنها) تقف عند مستوى قريب دون التوازن أي أنها تسحب حوالى 95% من مواردها المتجددة. وقد يدعو هذا الإقتراب من التوازن إلى ترجيح ضعف المرجع أو أن الحساب قد تم لما يسحب و لم يجرى حساب ما يعاد إلى مجرى النيل وهو أمر قد يكون مقبولاً في ظل غياب الإستصلاح اللازم للماء المعاد. ويلى مصر بهذا الجدول دولة البحرين بصفتها تمثل الدولة التى تناظر كندا ذات الكميات الكبرى فالبحرين هى ذات صغرى الكميات وكذلك الإحتياجات بين الدول التى تمت مراجعتها. ويجدر بالذكر هنا أن المرجع الذى إعتمد بهذه المراجعة وبعد تعديل أرقامه بما يتفق والزيادة الإنتاجية قد أبقى البحرين بموقع الصغرى رغم إدخال الإستعذاب أى الإنتاج الصناعى للماء كجزء من الكميات المتجددة.

الجدول (ز). الدول ذات الأوضاع الخاصة من حيث موارد الماء المتجدد مقارنة بالإحتياجات.

التسلسل	الدول	الموراد المتجددة كم 3 سنويا	الإحتياجات	النسبة	خصوصية الوضع
1	النرويج	413	2.00	0.48	النسبة الدنيا للسحب
2	كندا	2901	42.20	1.45	كبرى كميات التجدد
3	الولايات المتحدة	2478	467.00	18.85	المستوى الأعلى
4	مصر	74.05	70.50	95.21	للسحب
5	البحرين	0.157	0.250	159	أقرب الدول إلى التوازن
					صغرى كميات التجدد
					والإحتياجات
					النسبة العليا للسحب

هذا وإن وضع دول صناعية أخرى حسب ما هو مبين بالجدول (هـ) فإن الحد الأدنى لسحبها يقل عن عشر العشر، إذ تسحب النرويج 0.48% فقط من كميات الماء المتجددة. ويقل عن السدس كحد أعلى حيث تسحب هولندا 16.08%.

الجدول (هـ). موارد الماء المتجدد مقارنة بالإحتياجات بدول صناعية أخرى.

التسلسل	الدول	الموارد المتجددة كم 3 سنويا	الإحتياجات كم 3 سنويا	النسبة المئوية %
1	النرويج	413	2.0	0.48
2	النمسا	90	3.13	3.48
3	إستراليا	343	17.8	5.18
4	سويسرا	50	3.2	6.4
5	الدنمارك	13	1.46	11.23
6	هولندا	90	14.47	16.08

كذلك فإن الدول الواردة بالجدول (و) وهى التى إشير إليها بأنها بإتجاه تنموى صاعد فهى الأخرى تسحب أدناها ما يقل عن السدس (15.18%) وهو الوضع بجمهورية المكسيك وأعلاها يقل عن الثلث (32.78%) وهو الوضع بجمهورية باكستان الإسلامية. وتشير الجداول الثلاث إلى إحدى المسلمات بوضوح هام وهو حقيقة أن الماء هو الركن الأساس فى بناء المجتمعات. إذ أن جميع الدول التى وردت بهذه الجداول الثلاث (د & هـ & و) هى دول لا تسحب إلا بحدود الثلث من الموارد المتجددة.

الجدول (و). موارد الماء المتجدد مقارنة باحتياجات بعض الدول النامية.

التسلسل	الدول	الموارد المتجددة كم 3 سنويا	الإحتياجات كم 3 سنويا	النسبة المئوية %
1	المكسيك	357	54.2	15.18
2	الهند	2085	380	18.23
3	جنوب أفريقيا	50	9.2	18.4
4	الباكستان	1547	153.4	32.78

الجدول (ج). عدد من الدول ذات العجز المحدود والهائل بموارد الماء المتجدد مقارنة بالإحتياجات.

التسلسل	الدول	الموارد المتجددة كم 3 سنويا	الإحتياجات كم 3 سنويا	النسبة المئوية %	مستوى العجز
1	العراق (2)	42.56	47.33	111	محدود
2	قطر (3)	0.259	0.334	129	محدود
3	الكويت (3)	0.508	0.640	136	متوسط
4	ليبيا (2)	3.98	5.58	140	"
5	الأردن (2)	0.88	1.28	145	"
6	البحرين (3)	0.157	0.250	159	مرتفع
7	الإمارات (3)	1.05	2.23	212	حرج
8	اليمن (3)	1.5	3.6	240	حرج
9	عمان (3)	0.345	1.417	411	حرج جداً

(2) إنظر المرجع {2} ، (3) إنظر المرجع {3}.

ويبين الجدول (د) وضع الدول الصناعية الكبرى. أما الجدول (هـ) فإنه يبين وضع دول صناعية أخرى. يليه الجدول (و) الذى يصور الوضع بدول يمكن أن تعتبر ذات توجهات تنموية صاعدة. ومما يسترعى الإنتباه أن الدول الصناعية الكبرى تقع ضمن مستوى الربع (25.6%) تقريبا، عند مقارنة الكميات المتجددة بمستوى السحب. وما يستحق تسليط الضوء فعلاً هو وضع واحدة من هذه الدول فكندا لا تسحب إلا ما يزيد على العشر (1.45%) تقريبا.

الجدول (د). موارد الماء المتجدد مقارنة بالإحتياجات بدول الصناعية الكبرى.

التسلسل	الدول	الموارد المتجددة كم 3 سنويا	الإحتياجات كم 3 سنويا	النسبة المئوية %
1	كندا	2901	42.2	1.45
2	الولايات المتحدة	2478	467.0	18.85
3	اليابان	547	107.8	19.71
4	بريطانيا	120	8.35	23.63
5	ألمانيا	161	41.22	25.60

ذات الوفر الهائل، أما الجدول (ب) فبه عرض للدول ذات الوفر الكبير وحتى مستوى التوازن تقريباً، أما الجدول (ج) فيرد به الدول ذات العجز المائي. ويمكن للمراجع أن يرى أن الجدول (أ)يحوي كثيراً من الدول الصناعية وعدد من الدول الصاعدة للنمو بشكل فاعل ومؤثر بموازين القوى على مستوى العالم.

الجدول (أ). عدد من الدول ذات الوفر الهائل بموارد الماء المتجدد مقارنة بالإحتياجات (1).

التسلسل	الدولة	الموارد المتجددة كم 3 سنويا	الإحتياجات كم 3 سنويا	النسبة المئوية %	مستوى الوفر
1	النرويج	413	2.00	0.48	هائل
2	كندا	2901	42.20	1.45	"
3	النمسا	90	3.13	3.48	"
4	إستراليا	343	17.80	5.18	"
5	سويسرا	50	3.20	6.40	"
6	الدنمارك	13	1.46	11.23	عالي جداً
7	المكسيك	357	54.20	15.18	" "
8	الهند	2085	380	18.23	" "
9	جنوب أفريقيا	50	9.2	18.40	" "
10	الولايات المتحدة	2478	467.0	18.85	" "
11	اليابان	547	107.8	19.71	" "

(1) إنظر المرجع {1}.

الجدول (ب). عدد من الدول ذات الوفر الكبير أو المحدود بموارد الماء المتجدد مقارنة بالإحتياجات.

التسلسل	الدول	الموارد المتجددة كم 3 سنويا	الإحتياجات كم 3 سنويا	النسبة المئوية %	مستوى الوفر
1	سوريا (2)	60.1	14.10	23.46	مرتفع
2	بريطانيا (1)	120	28.35	23.60	"
3	المغرب (2)	28	6.98	24.93	"
4	ألمانيا (1)	161	41.22	25.60	"
5	لبنان (2)	4.6	1.45	31.52	"
6	الباكستان (1)	468	153.4	32.78	"
7	الجزائر (2)	17.30	6.10	35.26	"
8	تونس (2)	4.54	2.91	64.10	متوسط
9	فلسطين (1)	2.15	1.90	88.37	محدود
10	السودان (2)	24.30	21.50	88.48	محدود
11	مصر (2)	74.05	70.50	95.21	محدود جداً

(1) إنظر المرجع {1}، (2) إنظر المرجع {2}.

الإستخدام الأمثل للموارد والطاقة

محمد بن عبدالكريم الصوفي

جمعية علوم وتقنية المياه – ص. ب : 20018 دولة البحرين

تمهيد

يقول المولى جلت قدرته "وجعلنا من الماء كل شيء حي".

لقد إرتبط حياة الإنسان على وجه الأرض إرتباطاً وثيقاً بالماء فلقد قامت الحضارات وبدء التمدين بالظهور فى حياة الإنسان الأول على الأرض حيث وجد الماء. كما ولقد كان لوجود الماء الجارى والموصل إلى ممرات مفتوحة على ضفاف الأنهار وحتى مصابها، وكذلك المواقع الساحلية ذات الينابيع العذبة دور بحياة الإنسان. بالإضافة لكونه مصدر الحياه فلقد إستخدم الإنسان المجرى المائى كمصدر غذاء ووسيلة إنتقال سهلة. إضافة إلى الماء فلقد إعتمدت الحضارات منذ ظهروها وتناميها على توفر الموارد الطبعية الأخرى مثل المواد الخام اللازمة للحياة المتمدينة كمواد البناء والوقود إضافة إلى المحاصيل الزراعية والثروة الحيوانية التى تعتمد على الماء أيضا.

وتهدف هذه الورقة إلى تسليط الضوء على الوضع المائى لعدد كبير من دول العالم كبيرها وصغيرها، غنيها وفقيرها، الباردة والحارة، الصناعية والنامية. وذلك لبيان الحاجة الماسة لإتخاذ قرارت حاسمة إذ سيتم التركيز بهذا العرض على الماء كمدخل نحو بلورة نظرة مستقبلية للاستخدام الأمثل للموارد والطاقة. فالواجب بهذه المرحلة وبدول المنطقة خاصة إتخاذ قرارات حاسمة لتحقيق الحفاظ على الموارد بصفة عامة والماء بصفة خاصة.

الوضع العام

تستعرض هذه الورقة الوضع المائى لعدد كبير من دول العالم عبر عدد من الجداول، إذ يرد بالجدول (أ) عرض لكميات الماء المتجدد ومقارنتها بالإحتياجات ونسبتها المئوية للدول

الاستخدام الأمثل للموارد والطاقة

محمد بن عبدالكريم الصوفي

أوراق
مركز الأبحاث

قد إستخدم واحد لمدة خمس سنوات بمحطة جدة . أما الثاني فقد استخدم لمدة سنتين بمحطة جدة أيضاً .

وكانت نتائج التجربة الأولى كما يلي: اللزوجة الجوهرية للعينة الأولى التي عرضت للأكسدة تساوي 0.3 بينما اللزوجة الجوهرية للعينة الثانية والتي عرضت للتميؤ تساوي 1.24 وهي نفس اللزوجة الجوهرية للمرجع . ما يدل على أن العينة الأولى قد تأكسدت وبهذا نقص الوزن الجزيئى للبوليمر مؤديا إلى انخفاض في عامل اللزوجة بمقدار 0.94 ولكن لم يطرأ تغير في درجة أستلة العينة الثانية إذ بقيت كما هي عليه بالمرجع والتي تساوي 59,96 % أي أن العينة التي تعرضت للتميؤ لم تتغير لزوجتها الجوهرية قد بقيت كما هي, بينما درجة أستلة العينة التي تعرضت إلى رقم هيدروجين عالي إنخفضت إلى 58.58% مما يدل على أن جزء من مجموعة الاستيل قد إنفصلت عن سلسلة البوليمر.

وأما نتائج التجربة الثانية للأغشية التجارية التي إستخدمت بمحطات التناضح العكسي بجدة فقد كان مقياس قوة الشد تساوي 32غرام للغشاء الأول الذي إستخدم لمدة خمس سنوات بينما كانت تساوي 69غرام للغشاء الثاني والذي إستخدم لمدة سنتين ، ولكنها كانت دون قوة الشد للمرجع والتي تساوي 132غرام . ومن هذا يتبين أن كلا الغشائين المستخدمين قد تعرضا للأكسدة ولكن أولهما قد تأثر بدرجة أكبر من تأثير الغشاء الثاني, بينما حدث لكلاهما تغيير طفيف في درجة الاستلة إذ أن درجة الأستلة للغشاء الأول كانت تساوي 59.23% وللغشاء الثاني كانت 56.55% ومقارنتهما بـ 59.96% للمرجع . ومن هذه النتائج يتبين أن كلاهما قد تعرض للتميؤ ولكن الغشاء الثاني بدرجة أكبر .

دراسة وتحليل أغشية أسيتات السليلوز والمستخدمة في محطات التناضح العكسي

محمد فاروق, أحمد العمودى ونوماتا

مركز الأبحاث والتطوير – المؤسسة العامة لتحلية مياه المالحة – المملكة العربية السعودية

تلخيص

هناك عاملان أساسيان يؤثران كيميائيا على غشاء بوليمر أسيتات السليولوز وهما عاملا الأكسدة والتميؤ (Hydrolysis). وتتم عملية الأكسدة بتعريض البوليمر لأحد عوامل الأكسدة كالكلورين مما يؤدي إلى تجزأ البوليمر ونقص في وزنه الجزيئي ,وأما التميؤ فيتم حين يتعرض البوليمر إلى رقم هيدروجين عالي (يزيد على PH= 10) حيث يتم فصل الأسيتات عن سلسلة البوليمر المتعلقة به . ويمكن تحديد أثر الأكسدة بطريقة مباشرة وذلك بقياس الوزن الجزيئي بإحدى الطرق المستعملة لهذا الغرض كاللزوجة الجوهرية (Intrinsic viscosity) أو بطريقة غير مباشرة كقياس قوة الشد (Tensile Strength) والتي بدورها تزداد قيمة بازدياد الوزن الجزيئي وبالعكس . ويتم تحديد عامل التميؤ عن طريق قياس تركيز مجموعة الأسيتات بالبوليمر وذلك باستعمال المعايرة (Titration) أو بقياس الطيف (UV spectroscopy). وفي هذا البحث تم قياس أثر الأكسدة على الوزن الجزيئي باستعمال تحديد عامل اللزوجة الجوهرية وقياس قوة الشد . وقد حددت مدى فصل مجموعة الأسيتات عن سلسلة البوليمر باستعمال طريقة المعايرة .

ولدراسة أثر الأكسدة والتميؤ على أداء البوليمر أسيتات السليولوز فقد أجريت تجربتان: التجربة الأولى تشمل ثلاث عينات أغشية جديدة لم تستخدم من قبل في التشغيل وقد تمت هذه التجربة تحت ظروف اختبارية مختلفة وذلك بتعرض الغشاء الأول إلى تركيز عالي من الكلورين لأكسدته , ولتميؤ الغشاء تم إختباره بمياه بحر على رقم هيدروجين عالي PH =9,9 وأستعمل الغشاء يغي الثالث كمرجع (Control) دون تعريضه لأي معالجة . وفي التجربة الثانية تم قياس أداء غشائين إستخدما في عملية التحلية بطريقة التناضح العكسي . إذ

دراسة وتحليل أغشية أسيتات السليلولوز والمستخدمة في محطات التناضح العكسي

محمد فاروق، أحمد العمودي ونوماتا

واحدة بدلا من مرحلتين كما هي الحالة باستعمال الطرق التقليدية ويعمل الباحثون حالياً إلى تطوير هذه الطريقة المستجدة ونقل هذه التقنية من مستواها التجريبية (pilot Plant)، إلى مستوى الإنتاج العالمي وذلك لزيادة إنتاج الماء من المحطات القائمة بإضافة وحدات النابو إليها أو بدمجها مستقلاً كجزء أساسي مع المحطات الجديدة المصممة لتحلية مياه البحر.

ومما لاشك فيه أن نجاح وتطوير هذه الطريقة سيمثل تقدماً ملحوظاً لعمليات تحلية ماء البحر كما وستكون مساهمة كبيرة من المؤسسة العامة لتحلية المياه المالحة في تقدم تقنية تحلية المياه بما فيه نفع ليس للملكة العربية السعودية صاحبة الفكرة والتقنية فحسب بل لكافة المجتمعات التي تحتاج إلى تحلية المياه لقوام حياتها.

وختاماً فكما هو معروف عالمياً فتقدم الأمم إقتصادياً وتقنياً يأتي على الدوام مقترناً بدعمها المعنوي والمادي للأنشطة البحثية التي تؤدي إلى التطوير. وفي هذه الحالة والتي تعمل على رفع إنتاج الماء العذب من محطات التحلية وخفض تكلفة الإنتاج خصوصاً وأن الماء عنصر أساسي للحياة والاقتصاد فالدعم المعنوي والمالي لمجالات البحث والتطوير هما أمران اساسيان لنجاح وتعميم أي عمل من هذه الأعمال ومنها هذه الطريقة والتي تدعمها المؤسسة العامة لتحلية المياه المالحة مالياً ومعنوياً.

وعلى الله التوفيق.
العبود الأغشية

ولقد توصل فريق من الباحثين بمركز الأبحاث والتطوير التابع للمؤسسة العامة لتحلية المياه المالحة بالجبيل إلى أسلوب جديد لتحلية مياه البحر وذلك بمعالجتها أوليًا بأغشية النانو الدقيقة جداً قبل إرسالها إلى أجهزة التحلية التقليدية سواء العاملة بالطرق الحرارية أو التناضح العكسي.

وبهذه الطريقة الجديدة تغلب الباحثون على معظم المشاكل التي تعاني منها تحلية مياه البحر بالطرق التقليدية، إذ تم خفض نسبة ملوحة مياه التغذية (البحر) بحوالي 50% وأما المواد العسرة فتزال إلى حد يفوق في بعض الحالات مثل الكبريتات بنسبة تصل إلى 98%. وبهذه الطريقة ايضاً تم إزالة جميع المواد العالقة والبكتيريا مما يسهل عملية تحلية مياه البحر مع تزايد نسبة إنتاج الماء العذب من المحطات التي تعمل بالطرق التقليدية مثل التناضح العكسي إلى الضعف تقريباً بعد إضافة النابو. ويعني ذلك الوصول إلى نسبة إستخلاص الماء العذب من مياه البحر بطريقة التناضح العكسي إلى حوالي 70% أو أكثر. ونتيجة لذلك فان هذه الطريقة (بدمج النابو مع إحدى الطرق التقليدية لتحلية مياه البحر) تقلل إستهلاك الطاقة وكلفة إنتاج الماء العذب مثلاً زحين إستعمال طريقة التناضح العكسي مقرونة بالنابو بحوالي 30%.

ولقد تم تشغيل وحدة تقطير وميضي تجريبية ذات سعة 20 متر مكعب باليوم على درجة حرارة عالية (120 م) بهذه الطريقة لإنتاج نسبة عالية من الماء وذلك بدون إستعمال المواد الكيميائية (مثل مضاد التكلس والمضاد الرغوي) اللازمة للطرق التقليدية، حيث أن الطرق التقليدية لوحدها بدون إستخدام النابو لتتطلب كميات من المواد الكيميائية وخاصة الحامض لبلوغ الحد الحراري الأعلى إلى 120 م). وبهذه الطريقة أيضاً أصبح ممكنا تشغيل نظام تحلية ثلاثي المراحل يضم المعالجة الأولية بأغشية النابو متبوعاً بتحلية ماء البحر بوحدات التناضح العكسي ومن ثم إرسال رجيعها (أي رجيع وحدة التناضح العكسي) والذي على نسبة متدنية من أيونات العسر إلى وحدات التقطير الوميضي. وبهذه النظام الثلاثي يمكن إستخلاص ما يصل إلى 90% من منتج النابو كمياه عذبه.

علاوة على لمزايا السالفة الذكر فان الطريقة الجديدة تقلل من الحاجة إلى المواد الكيميائية المستعملة حالياً مع الطرق تحلية مياه البحر التقليدية مما يخفف تأثير عمليات التحلية على البيئة البحرية. كما وأصبح ممكناً تحلية مياه البحر حسب الطريقة الجديدة بمرحلة تناضح عكسي

أسلوب جديد لتحلية مياه البحر بطريقة مزدوجة باستعمال أغشية النانو مع أحد طرق التحلية التقليدية

عطا محمد حسن ، محمد عبد الكريم الصوفي ، أحمد العمودي ، أبو طاهر جمال الدين ، محمد فاروق ، على الرويلي ، عبدالغني إسحاق دلفي ، محمد خضر ، غلام مصطفى ، إبراهيم التيسان

مركز الأبحاث والتطوير

المؤسسة العامة لتحلية المياه المالحة – الجبيل – السعودية

الخلاصة

أصبحت مياه البحر المحلاة تشكل مصدرا رئيسياً لمياه الشرب بالمملكة العربية السعودية ودول الخليج العربي وكذلك بكثير من الجزر التي بها عجز بالمصادر الطبيعية للماء. وفي الآونة الأخيرة إرتفع إنتاج دول مجلس التعاون إرتفاعاً ملحوظاً ليصل إلى حوالي 45% من الإنتاج العالمي.

وبالرغم من إنتشار هذه الطريقة لاستخلاص ماء الشرب من مياه البحر إلا أنها لا زالت تعد باهظة التكاليف إذا ما قورنت بسواها مثل طرق تحلية المياه الملوحة. والسبب في ذلك يعود إلى خواص ماء البحر إذ أنه عالي الملوحة ومواد العسر المسببة للترسبات الكلسية (التكلس). كما يحوي الكثير من الكائنات الحية والمواد العالقة الدقيقة وغير الدقيقة وقد تضامر هذه العوامل سلباً لتؤثر بشكل ملحوظ على إنتاج المياه العذبة. كما وأن وجود هذه العناصر يتطلب معالجة أولية عالية التكاليف. وكذلك إضافة مواد كيميائية لمنع التكلس أو لتخثير ما بالماء من شوائب عالقة. وبالرغم من كل هذه العمليات فان نسبة استخلاص الماء العذب من مياه الخليج 35%.

ولهذه الأسباب فإن هذه العمليات تحتاج إلى قدر وافر من الطاقة وخاصة الكهربائية، مما يؤدي إلى إرتفاع كلفة الإنتاج.

أسلوب جديد لتحلية مياه البحر بطريقة مزدوجة باستعمال أغشية النانو مع أحد طرق التحلية التقليدية

عطا محمد حسن، محمد عبدالكريم الصوفي، أحمد العمودي، أبو طاهر جمال الدين، محمد فاروق، علي الرويلي، عبدالغني إسحاق دلفي، محمد خضر، غالم مصطفى، إبراهيم التيسان

تأثير الأنواع المختلفة من أيونات وأملاح الحديد الموجودة في المحلول المحلي الدوار في محطات التبخير الوميضي على كفاءة مواد منع الترسب

عبد الغني دلوي، محمد خضر، سعد السلمي، ك. شاهول و رضوان الرشيد
مركز الأبحاث والتطوير المؤسسة العامة لتحلية المياه المالحة
ص . ب 8328 الجبيل 32951 المملكة العربية السعودية

خلاصة

تستخدم مواد منع الترسب من محطات التحلية بالتبخير الوميضي للحد من تكون رواسب الأملاح على أسطح المحطة المختلفة. تختلف الجرعة الفعالة لهذه المواد من محطة إلى أخرى. تعتمد فعالية مواد الترسب على عدة عوامل منها طبيعية الكيميائية وتصميم المحطة ومعدلات التبادل الحراري ونوعية الأسطح المعدنية المستخدمة والتفاعلات المحتملة لتلك المواد المتواجدة في المحلول المحلي. لفهم بعض نواحي العلاقة بين تركيز مواد منع الترسب والمحلول المتواجدة فيه، تم إجراء مجموعة من التجارب المخبرية باستخدام طريقة التركيز الأدنى عند 95 درجة مئوية. واستخدام لهذا الغرض نوعين من مواد منع الترسب المحتويين أساسا على البولي فوسفونات وحامض بولي ماليك. ولقد تم التركيز على تأثير أيونات الحديد وأكسيده وهيدروكسيده بما في ذلك الصدأ على كفاءة مواد منع الترسب.

هذا ولقد بينت الدراسة مصداقية طريقة التركيز الأدنى بواسطة قياس تراكيز أيونات الكالسيوم و القلوية الكلية كأداة فعالة لتقييم كفاءة مواد منع الترسب. وبينت الدراسة أيضا أن لأيونات الحديد المختلفة ومركباته المحتوية على الأكسجين عند تركيز 2 جزء في المليون و 95 درجة مئوية وتركيز ملحي يعادل 1.4 من تركيز ماء البحر على شاطيء محطة الجبيل. ومن بين الأنواع المختلفة لأيونات الحديد، كان ليهروكسيد الحديديك الأثر الأكبر على خفض كفاءة مواد منع الترسب بنسبة تقارب 40%.

ولقد أوضحت الدراسة أيضا أم كفاءة مواد منع الترسب من نوع البولي فوسفونات أعلى بنسبة 10-12% أي أنها لن تتأثر بالقدر الذي تأثرت به أحماض البولي ميلك وجود الأنواع المختلفة من أيونات الحديد تحت الظروف الموضحة سابقا. ويعتقد بأن التأثير السلبي لأيونات الحديد الموجودة في المحلول المحلي على خفض كفاءة مواد منع الترسب ناتج عن قابلية تلك المواد على تكوين مركبات معقدة مع أيونات الحديد. وكانت هذه القابلية أوضح في حالة البولي فوسفونات عما كانت عليه عند إضافة حامض البولي ماليك.

كلمات دالة : مواد منع الترسب، بولي فوسفونات، حامض البولي ماليك، الترسبات المحلية، الحديد، المحلول المحلي.

تأثير الأنواع المختلفة من أيونات وأمالح الحديد الموجودة في المحلول المحلي الدوار في محطات التبخير الوميضي على كفاءة مواد منع الترسب

عبدالغني دلوي، محمد خضر، سعد السلمي، ك. شاهول، رضوان الرشيد

ويعرض هذا المنشور نتائج اختيار مواد منع الترسب الوارد وذكرها بالفقرة السابقة وكذلك نتائج حقن حامض الكبريتيك. ولقد تم أولا تقييم أداء موانع الترسب على النطاق المعملي ثم بعد ذلك تم تقييم أدائها في الوحدة التجريبية التابعة لمركز الأبحاث والتطوير وتلي ذلك إجراء اختبارات لتقييم الأداء بمحطات التحلية التجارية وذلك بقياس تغيير معامل اعتراض الانتقال الحراري. بينت نتائج اختبارات التقييم في المحطات التجارية أن جميع موانع الترسب تم اختيارها كانت ناجحة إذ لم يطرأ تدني ملموس في أداء هذه وبخاصة أدائها الحراري وبالتالي معدل الإنتاج. كما لم يطرأ تأرجح في متطلبات الطاقة لسخان المحلول المحلي أو المضخات.

تقييم أداء بعض مواد منع الترسب في عمليات التقطير الومضي المتعدد المراحل

عثمان أحمد حمد، محمد عبد الكريم الصوفي، غلام محمد مصطفي و عبد الغني دلفي

مركز الأبحاث والتطوير، ص . ب 8328 الجبيل المؤسسة العامة لتحلية المياه المالحة المملكة العربية السعودية

ملخص

لقد قامت المؤسسة العامة للتحلية المياه المالحة بدراسات عديدة خلال العقدين الماضين للتحكم في تكون الترسبات على أسطح الأنابيب الحرارية في عماليات التقطير الومضي المتعدد المراحل. وقد شهد العقد الماضي زيادة ملحوظة في إنتاجية محطات التقطير الومضي التابعة للمؤسسة العامة لتحلية المياه المالحة. ومعظم هذه المحطات تستخدم موانع الترسب ذات التركيب السلسالي بدلا من استخدام الحوامض كما كان متبعا في السابق.

وقد قام مركز الأبحاث والتطوير بالجبيل التابع للمؤسسة بإجراء دراسات في السنوات الثلاثة الماضية هدفت لتقييم أداء موانع الترسب المتوافرة تجاريا، حيث تم إجراء عدة تجارب في الوحدة التجريبية والتي تعمل بالتقطير الومضي والمتوفرة كجزء من مرافق المركز كما أجريت تجارب أخرى بالوحدات التجارية المنتجة بكل من المرحلتين الثالثة والرابعة بمحطات جدة والمرحلة الثانية بمحطات الجبيل لتقييم كفاءة ثلاثة موانع للترسب، وقد كانت هذه التجارب كما يلي (1) حامض بولو كربكوسيليت في المرحلة الثانية لمحطة الجبيل والمرحلة الرابعة جدة وكذلك الوحدة التجريبية بمركز الأبحاث والتطوير بالجبيل و(2) حامض بولي مليك في المرحلة الرابعة بجدة والوحدة التجريبية و (3) بولو فوسفونات في المرحلة الثالثة بجدة والوحدة التجريبية. إضافة إلى ذلك فقد تم أجريت تجربة بالوحدة التجريبية باستخدام حامض غير عضوي هو حامض الكبريتيك المركز وذلك بغرض مقارنة معدلات التبادل الحراري.

تقييم أداء بعض مواد منع الترسب
في علميات التقطير الومضي المتعدد المراحل

عثمان أحمد حمد، محمد عبدالكريم الصوفي، غالم محمد مصطفى، عبدالغني دلفي

دراسات على سلوكيات تآكل الشروخ الاجهادي لبعض السبائك المستخدمة في محطات التحلية

تي.ال.بركاش و أنيس مالك
المؤسسة العامة لتحلية المياه المالحة، مركز الأبحاث والتطوير
ص.ب.8328 الجبيل 31951
المملكة العربية السعودية

الخلاصة

تستعرض هذه الورقة دراسة لسلوكيات تآكل الشروخ الاجهادي الحاصلة للسبائك من اثر المواد الحافزة التآكلية مثل الكلوريد و المؤكسدات و كبريتيد الهيدروجين .حددت في هذه الدراسة الاجهادات المبدئية لتآكل الشروخ الاجهادي لبعض السبائك المستخدمة في محطات التحلية كحديد الزهر و حديد مقاوم للصدأ 316ال و 317ال و430 و مونيل 400 .ولهذا الغرض استخدمت طوق الاختبار القياسي و عينات محنية على شكل U في محاليل تحتوي على كبريتيد الهيدروجين. استخدمت قياسات الاستقطاب الكهروكيميائية لدراسة أثر الجهد الكهروكيميائى على الانهيار الحبيبي للتآكل الاجهادي. كما تم التحليل الإنشائي باستخدام جهاز المجهر الإلكتروني الماسح. أظهرت نتائج الاختبار أن الانهيار الحبيبي و الانهيار عبر الحبيبات للتآكل الاجهادي لحديد الزهر و سبيكة 430 في أجواء كبريتيد الهيدروجين يحدث فقط في أجواء محتملة محدده في حين أن حديد المقاوم للصدأ 316ال و 317ال يعتبر محصن للتآكل الاجهادي تحت شروط الاختبار المنجزة .كما وجد أن مونيل 400 عرضة للتآكل الاجهادي في وجود كبريتيد الهيدروجين والتي قد تكون موجودة في بعض أجزاء محطات التحلية بسبب تلوث مياه البحر.

كلمات دالة : تآكل الشروخ الاجهادي، الاجهادات المبدئية، الاستقطاب الكهروكيميائى، الطبقة الخاملة، أيون الكبريد.

دراسات على سلوكيات تآكل الشروخ الإجهادي لبعض السبائك المستخدمة في محطات التحلية

تي. إل. بركاش، أنيس مالك

مراقبة تآكل جهة البخار لمحطة تحلية الخفجي

نوشا أسرار و أنيس مالك و شاهرير أحمد
المؤسسة العامة لتحلية المياه المالحة، مركز الأبحاث والتطوير
ص.ب.8328 الجبيل 31951
المملكة العربية السعودية

مديح الخالدي و خالد المعيلي
محطة الخفجي

ملخص

إن عدم التأكد من تركيز الأكسجين و ثاني أكسيد الكربون و الغازات الغير متكثفة تؤدي إلى تفاقم مشاكل التآكل في جهة البخار . في هذه الحالة إذا لم تدرس القضية بدقة ، قد تكون التآكل في جهة البخار عامل محدّد في عمر محطات التحلية بالتبخير الوميضي متعدد المراحل . تستعرض هذه الورقة نتائج دراسة مراقبة التآكل في جهة البخار في محطة تحلية الخفجي . تم دراسة سلوكيات تآكل سبيكة النحاس-النيكل 70\30 و حديد الزهر و حديد مقاوم للصدأ 316 عند فتحة التهوية و جهة البخار للمبخرة لمدة 9000 ساعة . تم حساب معدّل التآكل بطريقة فقدان الوزن . كما تم تحليل نواتج التآكل بمقياس الطاقة المشتتة لأشعة اكس .

أظهرت نتائج التحليل أن سبيكة النحاس-النيكل تفاعلت مع غاز الأكسجين و كبريتيد الهيدروجين بدرجة أكبر من حديد الزهر و حديد مقاوم للصدأ . ولا يوجد الأمونيا و البرومين في نواتج التآكل على عكس ما سجّلت في بعض الدراسات . كما تم شرح أسباب معدّل التآكل المرتفع للسبائك في المراحل الأولى (1-3) و المراحل الوسطى (11-13) لمحطات التحلية بالتبخير الوميضي متعدد المراحل . و بينت النتائج أن حديد مقاوم للصدأ 316 يعتبر أكثر السبائك مقاومة للتآكل في جهة البخار في جميع مراحل المبخرات .

كلمات دالة : تآكل جهة البخار ، الغازات الغير متكثفة ، محطات التحلية بالتبخير الوميضي متعدد المراحل ، ماء البحر ، دخول الأكسجين .

مراقبة تآكل جهة البخار لمحطة تحلية الخفجي

نوشا أسرار، أنيس مالك، شاهرير أحمد

سلوكيات تآكل الفولاذ في أجواء مياه الخليج العربي

أنيس مالك وشاهرير أحمد وإسماعيل أنديجاني

المؤسسة العامة لتحلية المياه المالحة، مركز الأبحاث والتطوير بالجبيل

وصالح الفوزان

محطة التحلية بالجبيل

ملخص

المواد الإنشائية تكون عرضة للتآكل بدرجات مختلفة من خلال تعرضها للأجواء التآكلية المحيطة في ساحل الخليج. وهنالك العديد من العوامل التي تؤثر في بدأ العديد من عمليات التآكل مثل طبيعة المادة ودرجة صقل سطح المعدن و درجة الحرارة الرطوبة و اتجاه الرياح وهطول الأمطار. الخ.

الفولاذ يعتبر من المواد الإنشائية الغالية في الإنشاءات الساحلية مثل محطات التحلية التي للتآكل العام أو التآكل الموضعي بدرجات مختلفة. ومدى درجة تآكل المواد في الخليج تفتقر إلى معلومات منظمة متكاملة. وحيت أن الحصول على معومات التآكل للمواد خاصة الفولاذ في مياه الخليج من الأهمية بمكان فقد بدأ عمل دراسة منظمة في هذه الموضوع في عام 1990 وانتهت في 1996. تبين هذه الورقة النتائج لهذه الدراسة المتعلقة بسلوكيات تآكل الفولاذ في مياه الخليج. يشمل الفولاذ حديد الزهر وحديد مقاوم للصدأ وحديد ممتاز مقاوم للصدأ (الفريتي والأستونيتي و المزدوج). أحاطت الدراسة بالعوامل المؤثرة في التآكل العام وبالتآكل الموضعي للمواد. كما تم مناقشة أثر الأملاح المذابة بصفة عامة وأثر تركيز الكلوريلد بصفة خاصة وأثر درجة الكلورة بإسهاب. وكذلك تم إبراز دور إضافات السبائك على سلوكيات تآكل الفولاذ.

استخدمت الطرق الكهر وكيميائية وفقدان الوزن لحساب معدَل التآكل للمواد. كما تم استخدام طريقة استقطاب الجهد الحركي في تقييم المعالم المتعلقة بالتآكل الموضعي. كما أنجزت اختبارات التعريض واختبارات المتسارعة لدراسة هجوم التآكل الموضعي. أثر درجة صقل سطح المعادن في التآكل الموضعي قد تم بحثها بإسهاب. كما تم عرض الترتيب التصنيفي لمعدلات الفولاذ تحت الشروط المختلفة ومناقشة أهميتها بخصوص انتخاب المواد لمحطات التحلية.

كلمات دالة : النفر، تآكل داخل الشقوق، الفولاذ المقاوم للصدأ، النقر المحتمل، الانهيار المحتمل و الكلورة.

سلوكيات تآكل الفولاذ في أجواء مياه الخليج العربي

أنيس مالك، شاهيرير أحمد، إسماعيل أنديجاني

تقدير تأثير الأشعة فوق البنفسجية المعقم على النمو البكتيري في مياه البحر المغذية للمحطة التجريبية للتناضح العكسي-الجبيل

حسن أحمد منشي _ ن. سامي كومار، أ.ت. جمال الدين، خضر محمد
ص . ب 8328 _ الجبيل 31951 _ المملكة العربية السعودية

ملخص

تكتشف هذه الدراسة عن تقييم الأثر القاتل للأشعة فوق البنفسجية على البكتيريا الموجودة في مياه البحر المغذية للمحطة التجريبية للتناضح العكسي الجبيل استخدمت وحدتين من الأشعة فوق البنفسجية على خط المعالجة الأولية. وأجريت الدراسة عند ثلاث معدلات سريان للمياه المغذية للمحطة : المعدل العادي، وآخر أقل، وثالث أعلى من معدلات تشغيل المحطة. وتمت دراسة خمسة مواقع في المحطة وهي : ماء البحر (RSW)، بعد وحدة الأشعة فوق البنفسجية (AUV)، بعد المرشح الرملي (ASF)، بعد المرشحات الدقيقة (ACF)ومياه الرجيع (BR).

أظهرت الدراسة نسبة قتل 90-99% من البكتيريا الموجودة في مياه البحر بعد المعالجة بالأشعة فوق البنفسجية، وذلك بمقارنتها مع مياه البحر غير المعالجة، وذلك في كل السريان المطبقة في البحث، وهذا يثبت فعالية تعقيم وحدة الأشعة فوق البنفسجية الأولى على الرغم من هذه وجدت زيادة في أعداد البكتيريا في عينات المرشح الرملي والمرشح الدقيق. وقد يكون هذه بسبب عدم التعقيم الكافي لوحدة المعالجة الأشعة البنفسجية للبكتيريا الموجودة في المياه العذبة عند هذه النقطة.

الدراسات المعملية للعينات المعالجة بالأشعة فوق البنفسجية بعد 24 ساعة أظهرت مقدرة البكتيريا المتبقية في المياه المغذية على النمو بعد زوال التأثير المعقم. وسجلت العينات المأخوذة بعد المرشح الرملي وبعد المرشح الدقيق نقص في مستويات الكربون العضوي، النيتريت، والفوسفات في المياه المغذية مما يشير إلى مقداه هذه البكتيريا على استخدام هذه المواد للتغذية والنمو. وبعد فحص نفس العينات بعد 24 ساعة، ظهر انخفاض أكبر في تركيزات الفوسفات، النيتريت و الكربون العضوي. وهذا يؤكد استخدام البكتيريا لهذه المواد.

الدراسة تظهر التأثير الكبير لمعالجة البكتيريا الموجودة في المياه المغذية باستخدام الأشعة فوق البنفسجية، وأن هذه التأثير يقل بسبب تخزين هذه المياه المعالجة في الخزان الموجود قبل المرشح الدقيق، وفيه تستعيد البكتيريا قدرتها على النمو.

تقدير تأثير الأشعة فوق البنفسجية المعقم على النمو البكتيري في مياه البحر المغذية للمحطة التجريبية للتناضح العكسي – الجبيل

حسن أحمد منشي، ن. سامي كومار، أ.ت. جمال الدين، خضر محمد

التناضح العكسي، واختيار جودة هذه المياه ودراسة تأثير الموقع والعمق على جودة كميات المياه المنقاة بواسطة هذه التقنية.

تتميز هذه الطريقة عن سواها بقلة التكاليف وعدم الحاجة إلى حفر آبار عميقة ذات بنية ثابتة إذ أنه من السهل غرس المرشحات في التربة تحت ضغط الماء والذي توفره المضخة المستعملة أيضاً في سحب الماء. كما ويمكن نقلها من مكان إلى آخر بعكس ما هو عليه بمآخذ مياه البحر الأخرى الثابتة بمواقعها. ولاختيار الموقع فقد تمت دراسة جيولوجية لطبقات الموقع وأظهرت نتائج هذه الاختيار الجيولوجي أن الطبقة ما بين سبعة وتسعة أمتار تحتوي على رمل يعلو طبقة من الصخور الكلسية الضعيفة المتفككة. وقد تم اختيار هذه المرشحات الدقيقة الثقوب داخل رمل الشاطئ على عمق يتراوح بين ثلاثة أمتار ونصف وخمسة أمتار على أبعاد متفاوتة شملت الشاطئ الرملي غير المغطى بمياه البحر (ON-SHORE) والنقطة الوسطى بين المد والجزر وكذلك النقطة القصوى التي يصل إليهما الجزر. وكانت أفضل القراءات لمعامل كثافة الطمي (SDI) تساوي 2.93 عند النقطة القصوى للجزر وبعمق أربعة أمتار ونصف المتر تحت سطح البحر، وهي نتيجة خصوصاً إذا ما قورنت بمعدل قيمة معامل كثافة الطمي بعد وحدة التقنية التقليدية والتي تتراوح بين 2.6 0,2

هذا وقد أثبتت الاختبارات أن مجموع المواد الذائبة وعسر وحموضة المياه المنقاة لجميع المواقع الثلاثة كانت أقل مما هو عليه في حالة استعمال مآخذ المياه من سطح البحر المفتوح. ولكن كان هناك رائحة لغاز كبريت الهيدروجين (H2S) للعينات المأخوذة من الشاطئ الرملي على عمق (3.5 متر تحت سطح الشاطئ) ولكنها اختفت من العينات المأخوذة من المواقع الأخرى.

أما بالنسبة لمعدل تكاثر البكتيريا فقد كان عالياً وقد يكون ذلك نتيجة لتلوث الشاطئ. لذا فمن المتوقع الحصول على نتائج جيدة حين استعمال هذه الطريقة على شواطئ غير ملوثه لدراسة أثر أبعاد المرشحات عن بعضها البعض وكيفية توزيعها على الشاطئ وأعماقها داخل التربة وكذلك أثر نوع المواد المستعملة بصناعتها وحجم الثقوب وعددها بهذه المرشحات وحجم المرشح نفسه.

استعمال مرشحات دقيقة من الصلب كمآخذ متنقلة لمياه البحر من آبار سطحية (Well-Point)

عطا محمد حسن ، حسن أبو الطاهر جمال الدين ، علي الرويلي
مركز الأبحاث وتطوير
المؤسسة العامة لتحلية المياه المالحة   الجبيل   السعودية
ابلين ابارت ، روبرت لوفو
مكتب الاستصلاح الأمريكي (USBR) دنفر ، كولورادو   أمريكا

الخلاصة

يعتبر تصميم ونوع مآخذ المياه من أهم العوامل المؤثرة على أداء وحدات المعالجة الأولية والتناضح العكسي الحساسة لنوعية مياه التغذية. ويمكن تضيف مآخذ المياه إلى نوعين الأول يسحب فيها المياه من سطح البحر ومن مسافات وأعماق متفاوتة حسب موقع المحطة والثانية يسحب فيها المياه من آبار حفرت بالقرب من شاطئ البحر وذلك للحصول على نوعية مياه جيدة من حيث قلة المواد العالقة وضعف التكاثر البكتيري بها حيث يعمل الشاطئ على تنقية الماء عبر طبقاته الرملية. كما أن استعمال آبار الشاطئ المصممة على أعماق مختلفة كمآخذ للمياه يقلل التكاليف الثابتة لإنشاء المحطات وكذلك تكاليف التشغيل والصيانة وذلك لعدم الحاجة لبناء منقيات صناعية ذات تكلفة عالية، ويمكن حفر هذه الآبار على أعماق مختلفة تتراوح بين 30 إلى 60 متراً (آبار عميقة). وقد تم تجربتها بنجاح في عدد كبير من المحطات. وهناك طريقة جديدة مبنية على استعمال مرشحات من الصلب غير القابل للصدأ دقيقة الثقوب تغرس على الشاطئ تحت ضغط الماء من التربة حين يكون مستوى الماء فيها مرتفعاً كما هو معمول به تجفيف أرض أساسات المباني. وللاستفادة من هذه التقنية الأخيرة فقد تم اختيار هذه النوعية من مآخذ الماء من آبار غير عميقة على شواطئ الخليج على بعد (100) متر شمال مآخذ مياه محطة الجبيل وذلك لدراسة مدى إمكانية استعمالها كمآخذ للمياه لمحطات

استعمال مرشحات دقيقة من الصلب كمآخذ متنقلة لمياه البحرين من آبار سطحية (Well-Point)

عطا محمد حسن، حسن أبو الطاهر جمال الدين، علي الرويلي

دراسات على تآكل الحديد في محلول ملحي منزوع منه الأكسجين في وجود مانع الترسبات

اسماعيل انديجاني* و س. تورقوس**

*المؤسسة العامة لتحلية المياه المالحة – مركز الأبحاث و التطوير

ص.ب.8163 – الجبيل 31951

**جامعة UMIST مانشستر – بريطانيا

ملخص

تم أجراء بحث لتقييم سلوكية تآكل الحديد في 1 مولار من كلوريد الصوديوم و مياه البحر الصناعي المنزوع منهما الأكسجين عند درجة حموضة تتراوح من 3 إلى 8.5 و درجة حرارة حتى 80 درجة مئوية تحت الظروف الساكنة و باستخدام الطرق الكهروكيميائية. كما تم دراسة أثر إضافة مانع الترسبات على معدل تآكل الحديد.

أظهرت النتائج أن معدل تآكل الحديد منخفض بصفة عامة ويقل مع زيادة درجة الحموضة ويكون في أدنى معدل عند 25 درجة مئوية و أعلى معدل عند 80 درجة مئوية . معدل التآكل عند 50 درجة مئوية و درجة حموضة 8.5 كانت عند أدنى مستوى في قياسات التجارب الطويلة من قياسات التجارب القصيرة و ذلك بسبب تكوين طبقة الهيدروكسيد الحامية مع الزمن على سطح المعدن و التي تعوق وصول جزيئات الماء إلى سطح المعدن . كما بيّنت النتائج أنه لا يوجد أثر على معدل التآكل في وجود 20 جزء من المليون من فوسفونوبيوتان كاربوكسيلك أسيد مانع الترسيب عند 50 درجة مئوية و درجة حموضة 8.5 .

كلمات دالة : حديد الزهر ، الأوكسجين المذاب ، معدل التآكل ، مانع الترسيب ، الاستقطاب .

دراسات على تآكل الحديد في محلول ملحي منزوع منه الأكسجين في وجود مانع الترسب

إسماعيل أنديجاني، س. تورقوس

الإستخدام الأمثل للموارد والطاقة

محمد بن عبدالكريم الصوفي

جمعية علوم وتقنية المياه – ص. ب : 20018 دولة البحرين

ملخص

يقول المولى جلت قدرته "وجعلنا من الماء كل شيء حي".

لقد إرتبط حياة الإنسان على وجه الأرض إرتباطاً وثيقاً بالماء فلقد قامت الحضارات وبدء التمدين بالظهور فى حياة الإنسان الأول على الأرض حيث وجد الماء. كما ولقد كان لوجود الماء الجارى والموصل إلى ممرات مفتوحة على ضفاف الأنهار وحتى مصابها، وكذلك المواقع الساحلية ذات الينابيع العذبة دور بحياة الإنسان. بالإضافة لكونه مصدر الحياه فلقد إستخدم الإنسان المجرى المائى كمصدر غذاء ووسيلة إنتقال سهلة. إضافة إلى الماء فلقد إعتمدت الحضارات منذ ظهورها وتناميها على توفر الموارد الطبيعية الأخرى مثل المواد الخام اللازمة للحياة المتمدينة كمواد البناء والوقود إضافة إلى المحاصيل الزراعية والثروة الحيوانية التى تعتمد على الماء أيضا.

وتهدف هذه الورقة إلى تسليط الضوء على الوضع المائى لعدد كبير من دول العالم كبيرها وصغيرها، غنيها وفقيرها، الباردة والحارة، الصناعية والنامية. وذلك لبيان الحاجة الماسة لإتخاذ قرارت حاسمة إذ سيتم التركيز بهذا العرض على الماء كمدخل نحو بلورة نظرة مستقبلية للاستخدام الأمثل للموارد والطاقة. فالواجب بهذه المرحلة وبدول المنطقة خاصة إتخاذ قرارات حاسمة لتحقيق الحفاظ على الموارد بصفة عامة والماء بصفة خاصة.

الاستخدام الأمثل للموارد والطاقة

محمد بن عبدالكريم الصوفي

الخلاصات

مياه الشرب

المياه العادمة

المياه الزراعية

موار د المياه الجوفية

المياه السطحية

الفهـــــــــرس

تخطيط وإدارة الموارد المائية

فهرس الخلاصات

مؤتمر الخليج الرابع
للمياه

فبراير 13-17 1999
دولة البحرين

الماء في الخليج
وتحديات القرن الحادي والعشرون

وزارة الكهرباء والماء
دولة البحرين

الأمانة العامة
لمجلس التعاون لدول
الخليج العربية

جامعة الخليج
العربي
البحرين

مركز البحرين
للدراسات والبحوث
دولة البحرين

AOAD
ESCWA
EDS
IHP
IAEA
IDA
undp
UNEP
UNESCO
WHO/EMRO

تحرير الدكتور وليد خليل الزباري

أوراق مركز الأبحاث